MABS MONOGRAPH
AIR BLAST INSTRUMENTATION
1943 - 1993

MEASUREMENT TECHNIQUES AND INSTRUMENTATION

August 1995

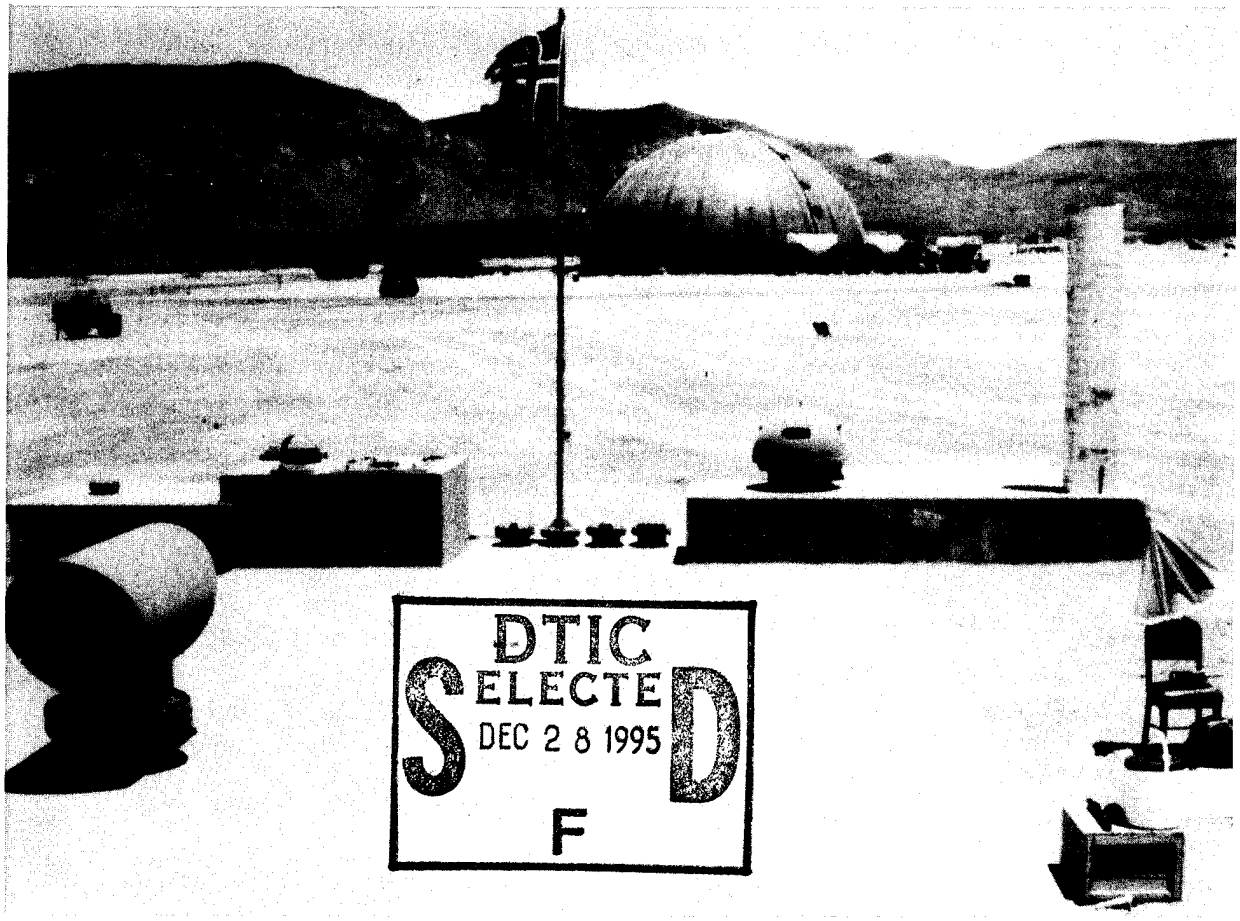

Volume 3 Air Blast Structural Target and Gage Calibration

Published by:
Defense Nuclear Agency
6801 Telegraph Road
Alexandria, VA 22310-3398

Destroy this report when it is no longer needed. Do not return to sender.

PLEASE NOTIFY THE DEFENSE NUCLEAR AGENCY, ATTN: CSTI, 6801 TELEGRAPH ROAD, ALEXANDRIA, VA 22310-3398, IF YOUR ADDRESS IS INCORRECT, IF YOU WISH IT DELETED FROM THE DISTRIBUTION LIST, OR IF THE ADDRESSEE IS NO LONGER EMPLOYED BY YOUR ORGANIZATION.

DNA PRINTING PLANT

DISCLAIMER NOTICE

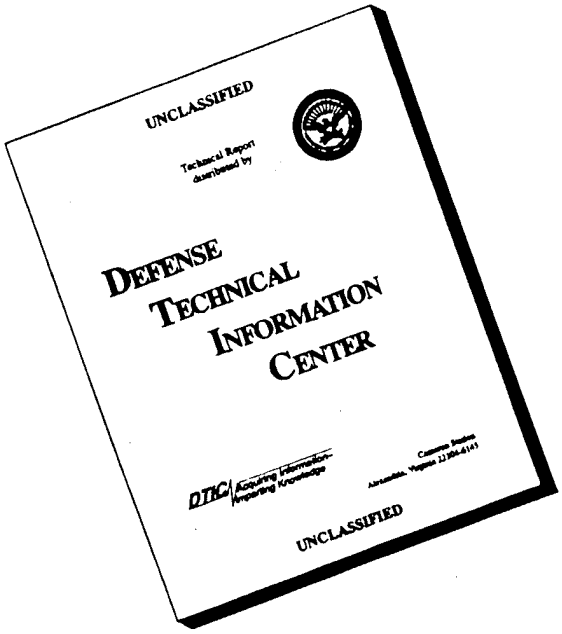

THIS DOCUMENT IS BEST QUALITY AVAILABLE. THE COPY FURNISHED TO DTIC CONTAINED A SIGNIFICANT NUMBER OF PAGES WHICH DO NOT REPRODUCE LEGIBLY.

REPORT DOCUMENTATION PAGE

Form Approved
OMB No. 0704-0188

1. AGENCY USE ONLY (Leave blank)	2. REPORT DATE	3. REPORT TYPE AND DATES COVERED
	950801	Technical 930917 – 940531

4. TITLE AND SUBTITLE
MABS Monograph, Air Blast Instrumentation, 1943 — 1993
Measurement Techniques and Instrumentation
Volume 3—Air Blast Structural Target and Gage Calibration, 1959 — 1993

5. FUNDING NUMBERS
C - DNA 001-92-C-0144
PE - 62715H
PR - AB
TA - HB
WU- DH327450

6. AUTHOR(S)
Ralph E. Reisler, John H. Keefer, and Noel H. Ethridge

7. PERFORMING ORGANIZATION NAME(S) AND ADDRESS(ES)
Applied Research Associates, Inc.
4300 San Mateo Blvd., NE
Suite A220
Albuquerque, NM 87110-1260

8. PERFORMING ORGANIZATION REPORT NUMBER
N/A

9. SPONSORING/MONITORING AGENCY NAME(S) AND ADDRESS(ES)
Defense Nuclear Agency
6801 Telegraph Road
Alexandria, VA 22310-3398
TDTR/Flohr

10. SPONSORING/MONITORING AGENCY REPORT NUMBER
N/A

11. SUPPLEMENTARY NOTES
This work was sponsored by the Defense Nuclear Agency under RDT&E RMC Code B4662D AB HB 00007 5200A AB 25904D.

12a. DISTRIBUTION/AVAILABILITY STATEMENT
Approved for public release; distribution is unlimited.

12b. DISTRIBUTION CODE

13. ABSTRACT *(Maximum 200 words)*

Structural response measurement techniques and instrumentation developed by Military Applications of Blast Simulators (MABS) participating countries for field tests over the period 1943 through 1993 are summarized. Electronic and non-electronic devices deployed on multi-ton nuclear and high-explosive events are presented with calibration techniques. The country and the year the gage was introduced are included with the description. References for each are also provided.

14. SUBJECT TERMS
Calibration, Strain, Acceleration, Pressure, Displacement, Structure, Electronic Gages, Non-Electronic Devices

15. NUMBER OF PAGES
206

16. PRICE CODE

17. SECURITY CLASSIFICATION OF REPORT	18. SECURITY CLASSIFICATION OF THIS PAGE	19. SECURITY CLASSIFICATION OF ABSTRACT	20. LIMITATION OF ABSTRACT
UNCLASSIFIED	UNCLASSIFIED	UNCLASSIFIED	SAR

CLASSIFIED BY:

N/A since Unclassified.

DECLASSIFY ON:

N/A since Unclassified..

PREFACE

This effort was sponsored jointly by the Defense Nuclear Agency (DNA) under contract DNA001-92-C-0144 and the Norwegian Defence Construction Service.

The work was carried out under the direct management of Mr. Mark Flohr of DNA and Mr. Arnfinn Jenssen of Norway.

The Steering Committee of the International Symposium on the Military Applications of Blast Simulation (MABS) recommended that a series of monographs be prepared dealing with topics of interest to all MABS participating countries. The subject matter proposed was (a) a History of MABS; (b) Blast Wave Measurement Techniques and Instrumentation - Passive and Electronic Devices; and (c) Photogrammetric Blast Wave Measurement Techniques.

Blast wave measurement techniques and instrumentation of the participating countries over the past fifty years was to be covered. Three reports came about as a result of the effort under topic (b):

Volume 1 : Air Blast Measurement Techniques and Instrumentation - The Nuclear Era, 1943 to 1963

Volume 2 : Air Blast Measurement Techniques and Instrumentation - The High Explosive Era, 1959 to 1993

Volume 3 : Air Blast Measurement Techniques and Instrumentation - Air Blast Structural Target and Gage Calibration, 1943 to 1993

The photograph on the front cover of this report is the Norwegian structure VALHALL II, exposed to the 4744-ton ANFO shot (8-KT nuclear equivalent), Operation MINOR SCALE, conducted in 1985.

CONVERSION TABLE

Conversion factors for U.S. Customary to metric (SI) units of measurement.

MULTIPLY → TO GET	BY → / ← DIVIDE	TO GET
angstrom	1.000 000 X E -10	meters (m)
atmosphere (normal)	1.013 25 X E +2	kilo pascal (kPa)
bar	1.000 000 X E +2	kilo pascal (kPa)
barn	1.000 000 X E -28	meter^2 (m^2)
British thermal unit (thermochemical)	1.054 350 X E +3	joule (J)
calorie (thermochemical)	4.184 000	joule (J)
cal (thermochemical/cm^2)	4.184 000 X E -2	mega joule/m^2 (MJ/m^2)
curie	3.700 000 X E +1	*giga becquerel (GBq)
degree (angle)	1.745 329 X E -2	radian (rad)
degree Fahrenheit	t_k = (t°f + 459.67)/1.8	degree kelvin (K)
electron volt	1.602 19 X E -19	joule (J)
erg	1.000 000 X E -7	joule (J)
erg/second	1.000 000 X E -7	watt (W)
foot	3.048 000 X E -1	meter (m)
foot-pound-force	1.355 818	joule (J)
gallon (U.S. liquid)	3.785 412 X E -3	meter^3 (m^3)
inch	2.540 000 X E -2	meter (m)
jerk	1.000 000 X E +9	joule (J)
joule/kilogram (J/kg) radiation dose absorbed	1.000 000	Gray (Gy)
kilotons	4.183	terajoules
kip (1000 lbf)	4.448 222 X E +3	newton (N)
kip/inch^2 (ksi)	6.894 757 X E +3	kilo pascal (kPa)
ktap	1.000 000 X E +2	newton-second/m^2 (N-s/m^2)
micron	1.000 000 X E -6	meter (m)
mil	2.540 000 X E -5	meter (m)
mile (international)	1.609 344 X E +3	meter (m)
ounce	2.834 952 X E -2	kilogram (kg)
pound-force (lbs avoirdupois)	4.448 222	newton (N)
pound-force inch	1.129 848 X E -1	newton-meter (N·m)
pound-force/inch	1.751 268 X E +2	newton/meter (N/m)
pound-force/foot^2	4.788 026 X E -2	kilo pascal (kPa)
pound-force/inch^2 (psi)	6.894 757	kilo pascal (kPa)
pound-mass (lbm avoirdupois)	4.535 924 X E -1	kilogram (kg)
pound-mass-foot^2 (moment of inertia)	4.214 011 X E -2	kilogram-meter^2 (kg·m^2)
pound-mass/foot^3	1.601 846 X E +1	kilogram/meter^3 (kg/m^3)
rad (radiation dose absorbed)	1.000 000 X E -2	**Gray (Gy)
roentgen	2.579 760 X E -4	coulomb/kilogram (C/kg)
shake	1.000 000 X E -8	second (s)
slug	1.459 390 X E +1	kilogram (kg)
torr (mm Hg, 0° C)	1.333 22 X E -1	kilo pascal (kPa)

*The becquerel (Bq) is the SI unit of radioactivity; 1 Bq = 1 event/s.
**The Gray (GY) is the SI unit of absorbed radiation.

TABLE OF CONTENTS

TABLE OF CONTENTS (Continued)

TABLE OF CONTENTS (Continued)

TABLE OF CONTENTS (Continued)

FIGURES

FIGURES (Continued)

FIGURES (Continued)

FIGURES (Continued)

TABLES

SECTION 1

INTRODUCTION

The effects of air blast on objects has been of interest to man since the time when explosive devices were first devised. Objects such as structures, both large and small, have been exposed in every major large-scale testing program since the beginning of the nuclear era. In some cases, structures were exposed to unplanned events which historians term as accidents. In any case, researchers from the start sought to gain an understanding of the response of structures to the air blast by way of numerous instrumentation systems and techniques. These systems basically took the form of acceleration, displacement, soil stress, and structural strain. Structures were typically of the form of naval vessels and their components, above-ground structures, sub-surface structures, and vehicles. As time advanced and man's knowledge increased in this area, designs were improved to harden structures to withstand an increasingly greater overpressure.

With every instrument system that has been developed comes the question - how reliable is it to measure the parameter the experimenter is interested in? Calibration thus becomes a necessary and vital procedure. A knowledge of the sensor and its response to forces other than those to which it was designed to measure need to be known. To answer these issues it is important to conduct an extensive static and dynamic calibration in the laboratory before it is deployed in the field. Once installed in the field, the gage should have a forcing function applied and the signal recorded by the recording system, to in essence calibrate the entire system, i.e. the gage, cabling, amplifier, and recorder.

In the pages to follow, the authors-preparers have endeavored to present a description of the many calibration and measuring techniques and instrumentation systems of the MABS participating countries which they have developed or used during the past fifty years to study the response of structures to large explosions (1000 pounds to megatons). As the reader progresses through the report, he will be able to see the tremendous progress which has been made to this end as the developing technology of the scientific community has been applied to this program. Gage response characteristics, for instance, have progressed from rise times in the milliseconds to times of a few microseconds. Intensive work - initiated in the mid-forties - has continued through the end of nuclear atmospheric testing in 1958, later extended to 1963, and into the high-explosive era beginning in 1959 and continuing at the present time.

Innumerable reports have been surveyed in assembling the information presented herein. Descriptive information, figures, and tables from these reports help to describe the systems presented. The country of origin is noted for each system and the year when the system was introduced. The description and comments given relate to the time of the system and not to comments from today's perspective - that will be left to the reader. A reference is provided at the end of each section to indicate the source for further information.

SECTION 2

HISTORY AND SUMMARY OF MEASUREMENTS

With the detonation of the A-bomb in 1945 and the introduction of the nuclear era, blast effects acquired a new and major significance. Destructive overpressures were experienced at greater distances from the detonation, and the long positive phase duration of the blast provided time for targets to respond to dynamic loads. The area of blast damage, when compared to the conventional weapon, had increased by alarming factors and caused the military to become keenly interested in the mechanism of this destruction. In order to understand this and appraise its true potential, experiments would need to be conducted. These experiments would include scaled models, as well as a full scale structure.

The first laboratory for these experiments was the Bikini Atoll in the South Pacific in 1946. Previously, an A-bomb had been detonated on the land (Trinity); in the air (Nagasaki and Hiroshima); and now on the sea (Bikini Atoll). A task force of 42,000 men was assembled for Operation CROSS ROADS and the objective was primarily to determine the effects of the A-bomb upon naval vessels. It would provide answers to such questions as "What effect would an atomic bomb have on a fleet of naval vessels?" and "Is an air burst more lethal than an underwater burst?" It would not, however, answer so directly the questions "To what extent should accepted principles of ship design be altered in future construction?" or "How does one build a blast-resistant structure?" To obtain answers to the latter would require many experiments. Information would have to be developed on the behavior of the blast wave and the pattern it displays when it interacts with a structure. An understanding of the behavior of materials under dynamic loads would be necessary. Gaining such information was needed because it was fundamental to a host of problems that were born with the nuclear explosion era.

Operation CROSS ROADS was the first of a long series of structural response tests, and from the very first experiments it was learned that the loading and target response information sought would come very slowly. Making measurements in an environment electrified by an electromagnetic pulse and bathed in nuclear and thermal radiation was to be a challenge in itself. Finding rugged, reliable gages that would meet these harsh field test requirements was not easy.

It was stated that "since the ships in the Bikini target fleet could not have crews, it was a requirement that the instruments leave some type of permanent record of their responses:

- Ink-records writing on a slow-rotating disk drum.
- Scratch-records with a needle scratching its record on wax-coated disk or drum.
- Magnetic tape recorders.
- Optical recorders.
- Telemetry recording systems, in which pressure data were broadcast by radio transmitters to receivers at convenient locations several miles away.

- Permanent-deformation gages."

There is an axiom in the nuclear weapon testing business which says, "The first time you do an experiment, do everything possible to make it successful. If successful, there will be many subsequent opportunities to refine the results. First-time failures have no future."

In 1951 the second large and fairly complex structures program on a nuclear test was conducted at the Pacific Proving Ground. Dr. Shelton, in his book Reflections of a Nuclear Weaponeer, says "Construction of the Military Test Structures on Operation GREENHOUSE, event EASY, on the large island of Engebi, presented Holmes and Narver (operating contractor) with tasks that were technically unprecedented. The size of the job was not to be measured in the cubic content of brick and mortar, or the lineal feet of steel girders, but in the precision and exactitude of construction and measurements. Further, the types of materials used, and the need to have practically every feature of each of the 26 buildings especially designed and then erected at its proper distance from the 50 KT nuclear detonation, put extraordinary demands on the contractor."

The structures program was organized as program 3 and included numerous projects as shown in Table 1.

Following Operation GREENHOUSE, five more major structures programs were conducted with nuclear weapons before the moratorium on atmospheric testing went into effect. Those operations which included a major structures program are listed in Table 2. A photograph and a diagram of a nuclear structures test layout are presented in Figures 1 and 2. Figures 3 and 4 show test structures before and after a nuclear event.

Use of high explosives for simulating nuclear airblast was initiated in 1959 with the testing of block-built TNT charges of 20 tons. In 1964 a 500-ton TNT block-built charge was detonated for a major structures test. This event was Operation SNOWBALL, which was carried out as a tripartite (British, Canadian, and American) test program at the Suffield Experimental Station, Alberta, Canada (now the Defence Research Establishment). From this beginning have come many large HE tests, some as large as 4000 tons. Ammonium nitrate/fuel oil (ANFO) replaced TNT as the explosive of choice. Presented in Table 3 is a listing of those test operations where structural testing was a major item. In the mid-70s these tests took on the flavor of multi-national participation involving many of the MABS members. A photograph and a diagram of an HE test program are presented in Figures 5 and 6.

Measurements of the response of structures included, at first, blast pressure, acceleration, displacement, strain, and time-of-collapse of structural elements. Experience was gained by the testing organizations and applied to the subsequent tests. Measurements were expanded to include earth pressure and strain, angular velocity, and soil particle velocity. Instruments to make these measurements were developed and improved upon with each successive test. Both passive and active devices were deployed in the field; both oscillograph and magnetic tape recorders were used to record electronic data until they were supplanted by digital recording. A summary of the structural instrumentation is presented in Table 4.

Ref: Shelton, F.H., Reflections of a Nuclear Weaponeer, Shelton Enterprises, Inc., 1988.

Table 1. Organization of an early structures program.

Program 3.0 Structures
3.1 Army Structures:
3.1.1 A multistory composite type building to gain data for defensive structure
3.1.2 Three steel-mill type of buildings
3.1.3 Reinforced concrete shelter
3.1.4 Corrugated
3.2 Navy Structures:
3.2.1 Bomb-proof roof to compare solid and cellular structures
3.2.2 Concrete with panel veneer to test absorption effects of panels
3.2.3 Matchbox type of construction
3.2.4 Precast magazine
3.2.5 Concrete arch to test its response
3.2.6 Precast concrete dome
3.2.7 Reinforced concrete structures
3.3 USAF Structures, 10 Subprojects Designed to Test Atomic Bombs on Enemy Targets:
3.3.1 Key industrial-type building
3.3.2 Industrial building with light crane
3.3.3 Industrial with long spans
3.3.4 Industrial with short spans
3.3.5 Load-bearing wall
3.3.6 Fractionating column to test key components in oil refining target complex
3.3.7 Five log cabins to test incendiary effects
3.3.8 Single-story industrial structures
3.3.9 Girders and bridges
3.3.10 Transformers and switchyards

Table 2. Nuclear test operations having major structural testing.

UNITED STATES

Item	Name	Year	No. of Shots	Location	Height of Burst (ft.)	Type of Burst	Yield Range
1	CROSSROADS	1946	2	Bikini	520/-90	Air, Underwater	23 KT
2	GREENHOUSE	1951	4	Eniwetok	200-300	Tower	47 KT
3	UPSHOT-KNOTHOLE	1953	11	Nevada	100-6020	Tower, Air, Gun	0.2-61 KT
4	TEAPOT	1955	14	Nevada	-67-36, 620	Air, Tower, Underground	1-43 KT
5	PLUMBBOB	1957	25	Nevada		Tower, Rocket Balloon, Underground	0.51-74 KT
6	HARDTACK II	1958	24	Nevada	-848-1500	Balloon, Tower	1.2 T-6 KT
7	STORAX (DOMINIC II)	1962-1963	17	Nevada, Johnston Island Area	Surface, Crater Altitude	Surface, Air, Rocket	Low - Low MT

REF: NOV-209 (Rev. 2), Announced U.S. Nuclear Tests, July 1945 through December 1981, DOE, January 1982.

Figure 1. Photograph of PLUMBOB Priscilla nuclear test for structural testing.

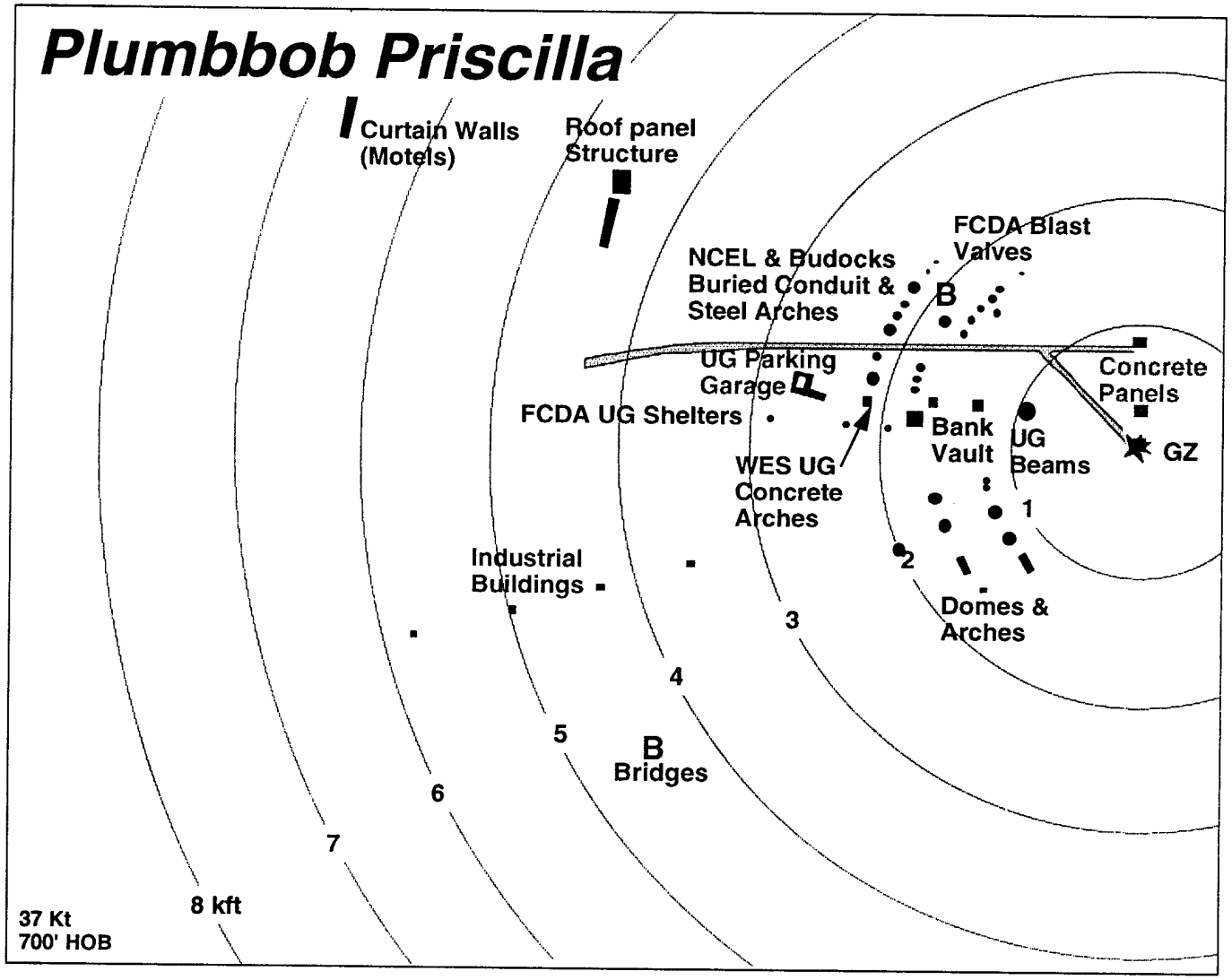

Figure 2. Site layout for a nuclear structural test.

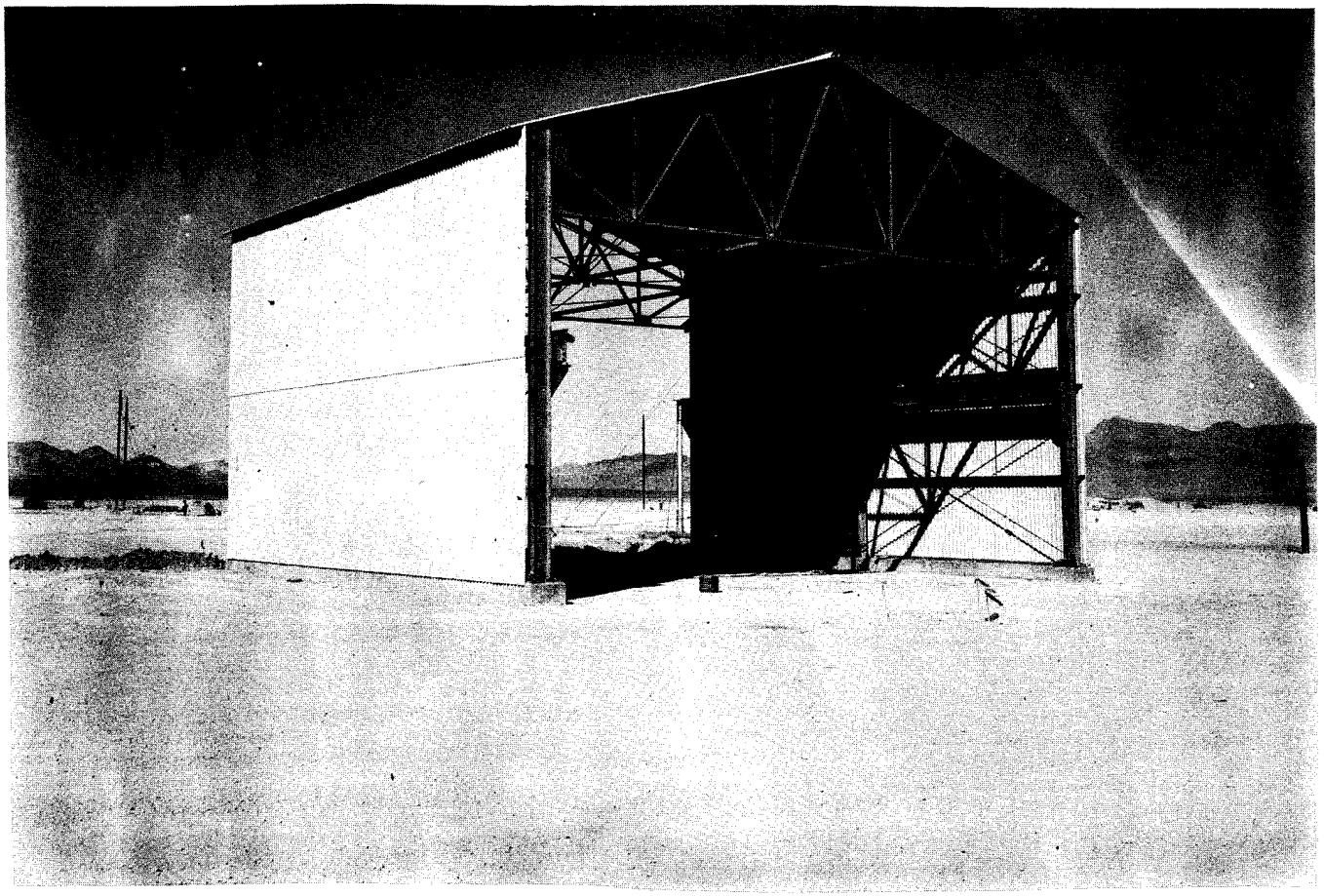

a. Structure before test.

Figure 3. Test structure on a nuclear test.

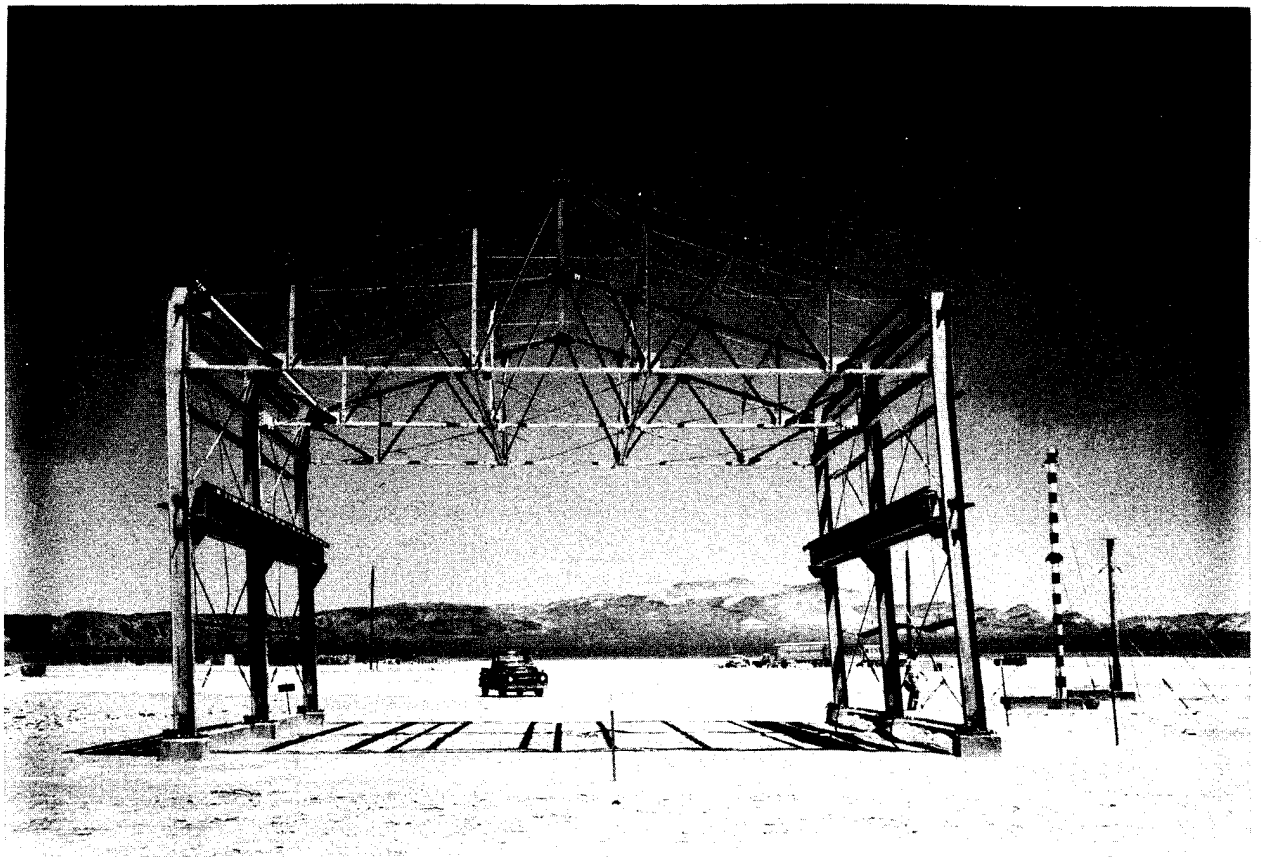

b. Structure after testing.

Figure 3. Test structure on a nuclear test (Continued).

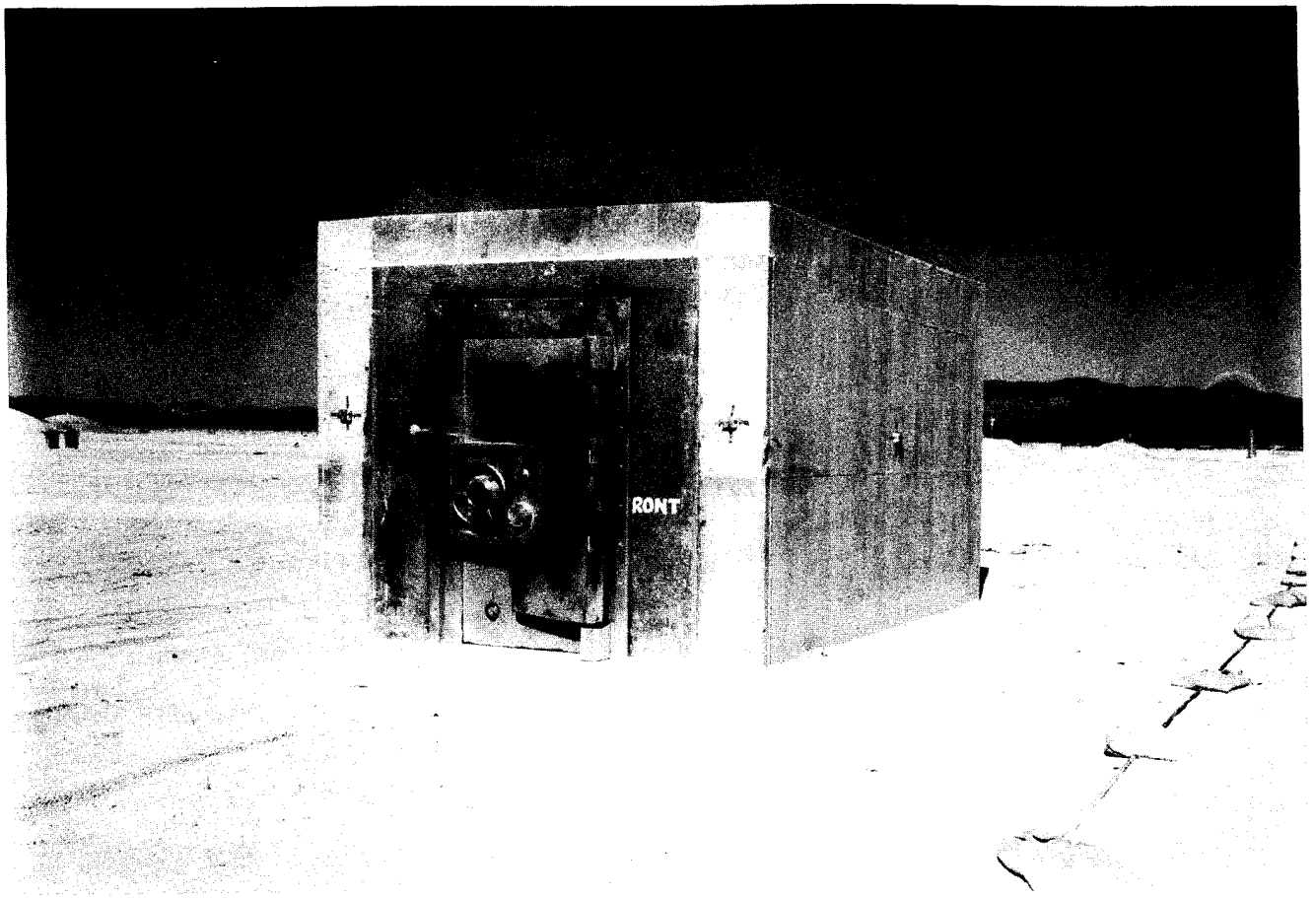

a. Structure before test.

Figure 4. Vault test structure on a nuclear test.

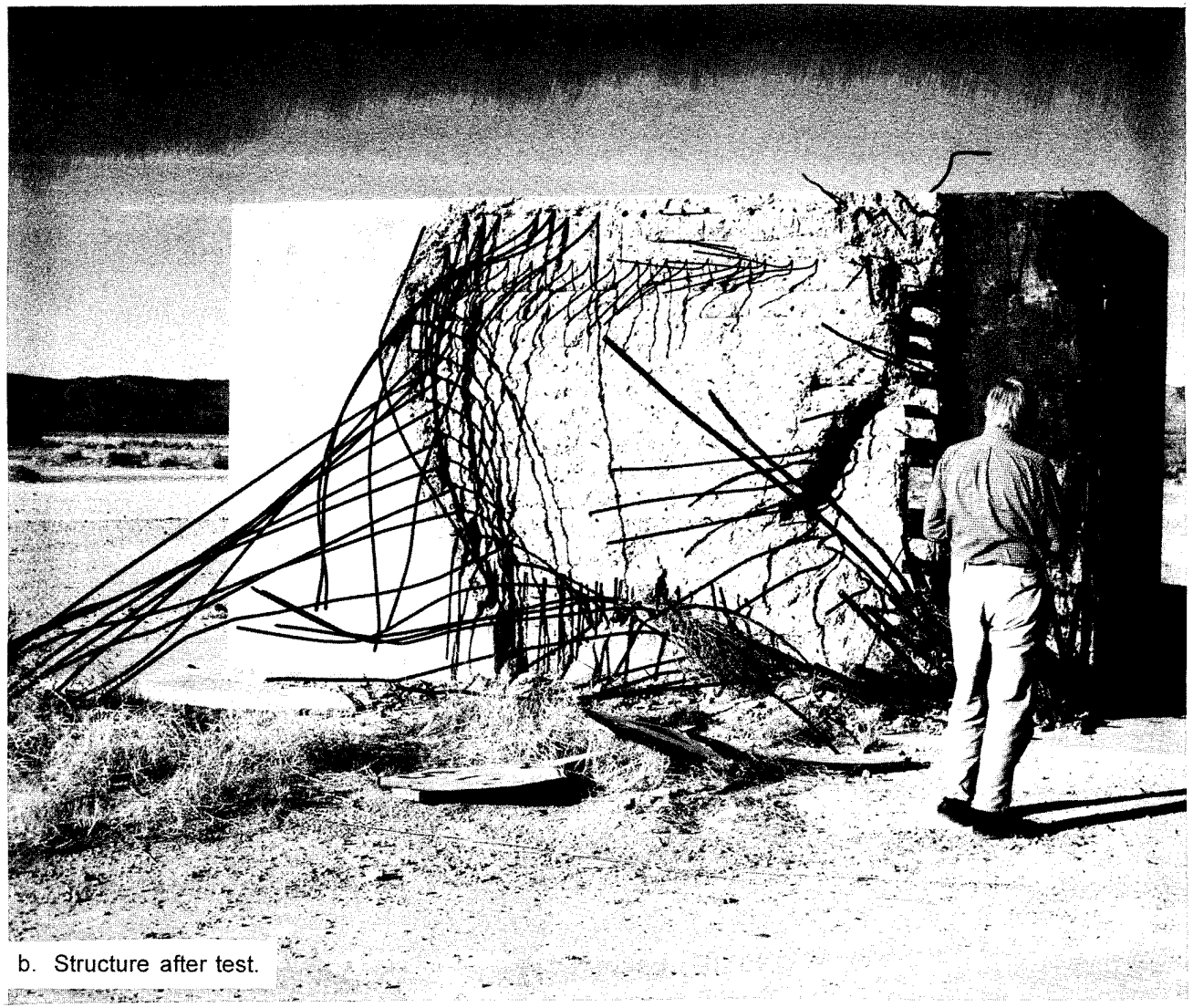

b. Structure after test.

Figure 4. Vault test structure on a nuclear test (Continued).

Table 3. Major structural high-explosive test involvement of the USA.

Item	Operation/Test	Year	Number of Shots	Charge Wt.	Charge Position	Explosive	Location of Test
1	SNOWBALL	1964	1	500T	Surface Hemisphere	TNT-BLK	DRES
2	SAILOR HAT	1965	3	500T	Surface Hemisphere	TNT-BLK	Hawaii
3	PRAIRIE FLAT	1968	1	500T	Surface Sphere	TNT-BLK	DRES
4	DIAL PACK	1970	1	500T	Surface Sphere	TNT	DRES
5	MIXED COMPANY	1972	1	500T	Surface Sphere	TNT	Colorado
6	MILL RACE	1981	1	600T	Surface Hemisphere	ANFO	WSMR
7	DISTANT RUNNER	1981	2	120T	Surface Hemisphere	ANFO	WSMR
8	DIRECT COURSE	1983	1	600T	Tower Sphere	ANFO	WSMR
9	MINOR SCALE	1985	1	4740T	Surface Hemisphere	ANFO	WSMR
10	MISTY PICTURE	1987	1	4685T	Surface Hemisphere	ANFO	WSMR
11	MISERS GOLD	1989	1	2440T	Surface Hemisphere	ANFO	WSMR
12	DISTANT IMAGE	1991	1	2650T	Surface Hemisphere	ANFO	WSMR
13	MINOR UNCLE	1993	1	2500T	Surface Hemisphere	ANFO	WSMR

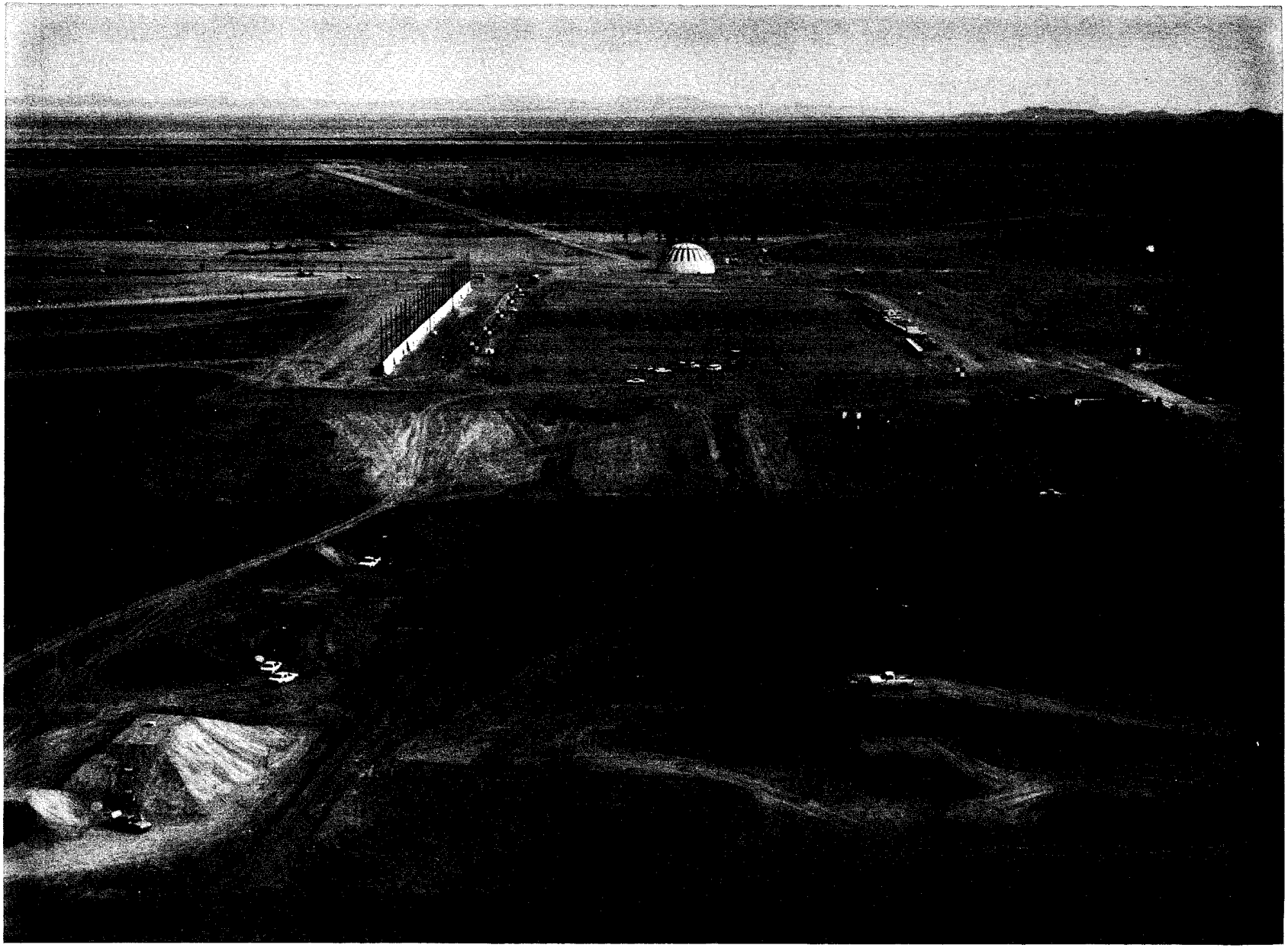

Figure 5. Photograph of a He test site layout.

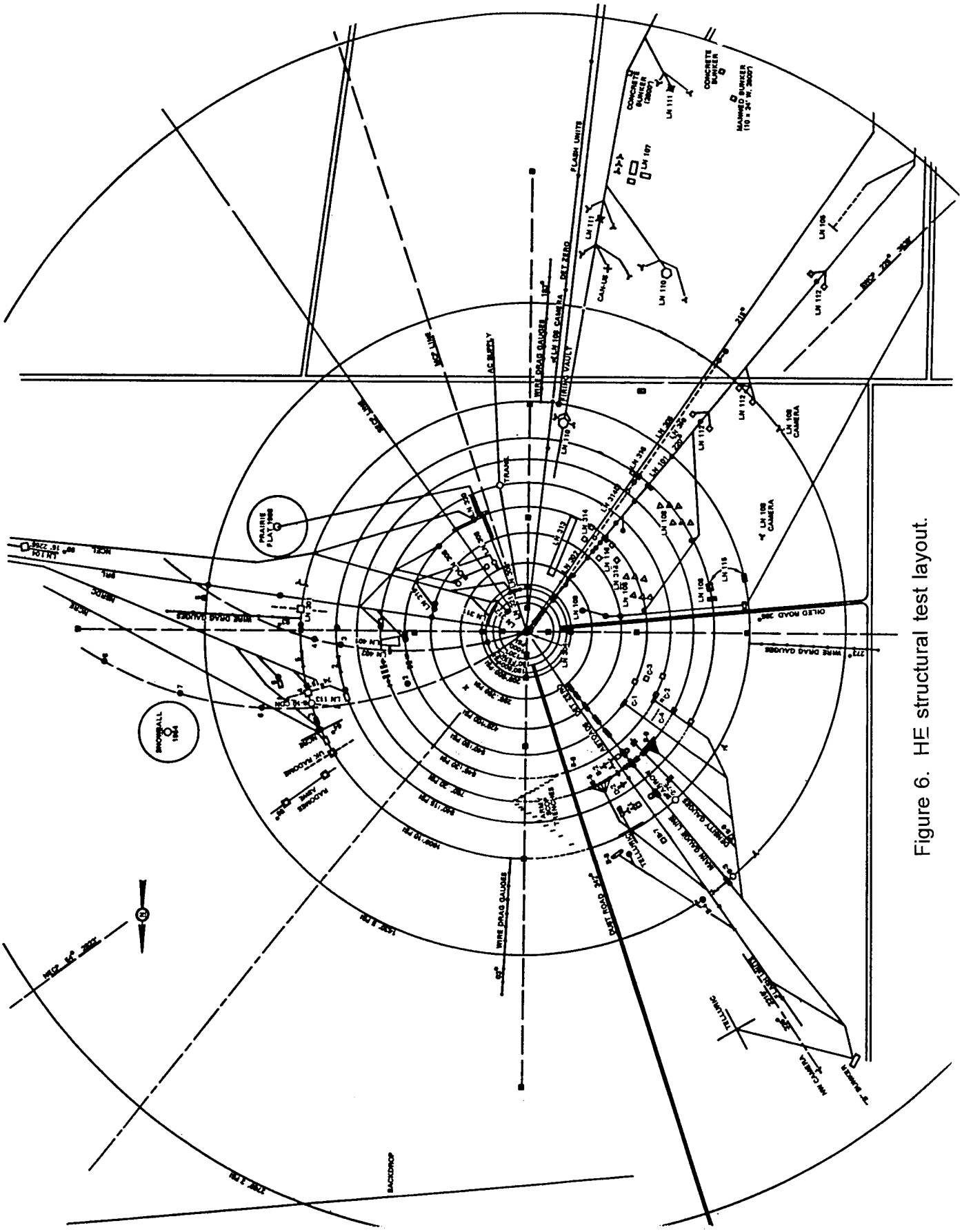

Figure 6. HE structural test layout.

Table 4. Summary of structural instrumentation.

A. Electronic Devices - Nuclear Testing

Gage	Country	Period	Charge Size*
1. Displacement:			
Sandia Rigid Rod	USA	1950	Large
BRL Wire	USA	1953	Large
LVDT Gage	USA	1957	Large
EURO Gage	FRANCE	1957	Large
Seismograph	FRANCE	1957	Large
2. Acceleration:			
Wiancko Gage	USA	1953	Large
EURO Gage	FRANCE	1957	Large
3. Time:			
Sandia Panel-Time-of-Break	USA	1950	Large
Sandia Stimascope	USA	1950	Large
Pressure Switch	USA	1958	Large
Sandia Plexiglas	USA	1962	Large
4. Earth Pressure and Strain:			
Carlson-Wiancko	USA	1953	Large
EURO Earth Pressure	FRANCE	1957	Large
Earth Strain Gage	USA	1957	Large
5. Strain-Structural Members:			
NA Strain Gages	USA	1953	Large
EURO Strain Gages	FRANCE	1957	Large
6. Rate Gyro:			
Giannini	USA	1953	Large

*Medium - 20 to 500 tons
Large - >500 tons

Table 4. Summary of structural instrumentation (Continued).

B. Non-Electronic Devices - Nuclear Testing

Gage	Country	Period	Charge Size*
1. Displacement:			
Peak Recording	USA	1953	Large
Deformeter	FRANCE	1957	Large
Lateral Gage	FRANCE	1957	Large
Recording Pendulum	FRANCE	1957	Large
2. Acceleration and Strain:			
BRL Peak Reading Acceleration	USA	1953	Large
Chocmart	FRANCE	1957	Large
Peak Reading Strain	USA	1953	Large
3. Self-Recording:			
Sandia Combo Displacement	USA	1950	Large
BRL Displacement	USA	1957	Large
ERA Accelerometer	USA	1950	Large
BRL Accelerometer	USA	1957	Large
DOFL Accelerometer	USA	1959	Large
G.L. Martin Strain Gage	USA	1950	Large

*Medium - 20 to 500 tons
Large - >500 tons

Table 4. Summary of structural instrumentation (Continued).

D. Non-Electronic Devices - High Explosive Testing

Gage	Country	Period	Charge Size*
1. Displacement:			
Oak Ridge Peak Gage	USA	1973	Medium - Large
NCEL Deflection Gage	USA	1963	Medium - Large
DRES Spring Mounted Scratch Gage	CANADA	1969	Medium - Large
Boeing Differential Motion Scratch Gage	USA	1969	Medium - Large
Swedish Passive Gage	SWEDEN	1991	Medium - Large
Slope Indicator	USA	1964	Medium - Large
Scratch Peak Gages	USA	1964	Medium - Large
Contact Gages	USA	1964	Medium - Large
TRW Reed Gage	USA	1965	Medium - Large
Boeing Passive Soil-Stress Gage	USA	1968	Medium - Large
2. Pressure:			
UCRL Pin Gage	USA	1965	Medium - Large
UCRL Plastic Gage	USA	1965	Medium - Large
3. Self-Recording Devices:			
WES Displacement Gage	USA	1963	Medium - Large
UED Peak Load Stress Gage	USA	1963	Medium - Large
DRES Mechanical Deflection Gage	CANADA	1967	Medium - Large

*Medium - 20 to 500 tons
Large - >500 tons

Table 4. Summary of structural instrumentation (Continued).

C. Electronic Devices - High Explosive Testing

Gage	Country	Period	Charge Size*
1. Displacement:			
WES Gage	USA	1963	Medium - Large
Spool Gage	USA	1964	Medium - Large
IITRI Coil Gage	USA	1965	Medium - Large
SRI Soil Strain	USA	1960	Medium - Large
Sandia Rack & Pinion	USA	1962	Medium - Large
SRI Inertial	USA	1960	Medium - Large
Commercial:			
Bourns Type 108	USA	60s	Medium - Large
Longfellow LFS12/300-OA5	USA	80s	Medium - Large
SWEMA RLP4104/10	SWEDEN	80s	Medium - Large
2. Acceleration:			
Endevco	USA	1964	Medium - Large
SRI-FMX	USA	1964	Medium - Large
Commercial:			
Cubit Corporation Piezo 2225	USA	60s,80s	Medium - Large
Endevco Piezo 2619	USA	60s,80s	Medium - Large
Endevco Piezo Tri-Axial 2223C	USA	60s,80s	Medium - Large
Statham Strain 4-202	USA	60s,80s	Medium - Large
Sunstrand Strain QA-900, AQ-1000	USA	60s,80s	Medium - Large
Endevco Piezoresistive 2264AMI, 2260, 2261	USA	60s,80s	Medium - Large
Sensor Products Piezoresistive A1	USA	60s,80s	Medium - Large
Kulite Piezoresistive GB-625-250	USA	60s,80s	Medium - Large
Endevco Piezoresistive, 2262, 2264, 7270, 7255	USA	60s,80s	Medium - Large

*Medium - 20 to 500 tons
Large - >500 tons

Table 4. Summary of structural instrumentation (Continued).

C. Electronic Devices - High Explosive Testing (Continued)

Gage	Country	Period	Charge Size*
3. Earth Stress/Strain:			
SRI-FMX	USA	1963	Medium - Large
Sandia Thick Quartz	USA	1965	Medium - Large
UED Spool Stress	USA	1960	Medium - Large
UED Sand Dollar Pancake	USA	1963	Medium - Large
BRL Pancake	USA	1964	Medium - Large
WES-SE Pancake	USA	1964	Medium - Large
IITRI Pancake	USA	1964	Medium - Large
Filpip Gage	USA	1960	Medium - Large
SRI Surface Shear	USA	1961	Medium - Large
Rensselaer Tri-Axial	USA	1964	Medium - Large
Commerical: (Structural Strain)			
BLH Strain 21BLH	USA	60s,80s	Medium - Large
Micro Measurements EA-06-25086-120	USA	60s,80s	Medium - Large
Derifoil Strain	USA	60s,80s	Medium - Large
Micro Measurements CEA-06-250-ON-350 (Soil Stress)	USA	60s,80s	Medium - Large
Kulite Q080	USA	80s	Medium - Large
Kulite VM-750	USA	80s	Medium - Large
4. Pressure (Hydro Region):			
Manganin Gage (HDL-IITRI) (SRI, Sandia)	USA	1963	Medium - Large
Sandia Impedance Mismatch Gage	USA	1963	Medium - Large
IITRI Electrolytic Cell Gage	USA	1964	Medium - Large
SRI Calcium Gage	USA	1964	Medium - Large
BRL Sulphur Gage	USA	1961	Medium - Large
Sandia Thin Quartz Gage	USA	1965	Medium - Large
Commercial Air Pressure:			
Endevco Piezoresistive 8530B	ALL	80s	Medium - Large
Kulite Piezoresistive XT-190	ALL	80s	Medium - Large
Kulite Piezoresistive HSK Series	ALL	80s	Medium - Large

*Medium - 20 to 500 tons
Large - >500 tons

Table 4. Summary of structural instrumentation (Continued).

C. Electronic Devices - High Explosive Testing (Continued)

Gage	Country	Period	Charge Size*
5. Rate Gyro:			
Humprey FG40-0101-1	USA	80s	Medium - Large
6. Time Measurements:			
Slifer Cable	USA	1960	Medium - Large
AFWL Time-of-Stress-Arrival System	USA	1965	Medium - Large
Sandia Shock Wave Detector	USA	1965	Medium - Large
7. Soil Particle Velocity:			
SRI Mark I	USA	1960	Medium - Large
SRI Horizontal Gage	USA	1960	Medium - Large
SRI Mark III Gage	USA	1960	Medium - Large
Sandia DX Gage	USA	1964	Medium - Large
SRI-AFWL Miniature Velocity Gage	USA	1966	Medium - Large
EPCO Velocimeter	USA	1964	Medium - Large
EPCO Faraday Gage	USA	1964	Medium - Large
EPCO Self-Inductance Gage	USA	1964	Medium - Large
CEC Velocity Pickup	USA	1964	Medium - Large
Crescent Velocity Pickup	USA	1965	Medium - Large
DRES Velocity Transducers	CANADA	1970	Medium - Large
Commercial:			
Sparton Southwest 601	CANADA	60s	Medium - Large
Hewlett-Packard LV Syn 6LV4,2	USA/CANADA	60s	Medium - Large

*Medium - 20 to 500 tons
Large - >500 tons

SECTION 3

NON-ELECTRONIC STRUCTURAL - NUCLEAR TESTING

3.1 DISPLACEMENT-SENSITIVE DEVICES.

3.1.1 Peak-Recording Displacement Gages (USA (1953).

In general, peak displacement gages are "gadgets" designed to fit a particular case and are not commercially procured. They have consisted of:

a. telescoping pipes where the displacement is measured by the amount one pipe is pushed into another.

b. scratch gages where a stylus arm is affixed to the moving component of the structure and the displacement is scribed on a metal plate, piece of paper, or on the concrete floor itself.

One such gage is shown in Figure 7 and consisted of an aluminum rod welded to a circular aluminum base and a plate drilled to allow the rod to pass through freely. The rod assembly was attached to the moving member and the plate secured to a stationary reference joint. After the gage was positioned, the rod was painted with black paint. When the rod moved in response to the motion of the structural element, the knife-edge scratched a record of the maximum deflection. Another scratch-type displacement gage is illustrated in Figure 8.

c. A rather unique and inexpensive gage is the "cork" gage. Here the movement between two structural elements is determined by the displacement of corks on a string. One end of the string is attached to one element, the other end to the other element. A spring is included in the string to keep a constant tension. A pointer is affixed to one element to serve as a zero mark. A small dot of paint is placed on the string at the pointer. Two corks are placed on the string, one above and one below the pointer, and pushed against it. When displacement occurs, the maximum positive and negative movement can be measured. Further, any permanent displacement is apparent by the separation of the pointer at the paint on the string (original zero).

Ref: Meszaros, J.J., et al., "Instrumentation of Structures for Air-Blast and Ground-Shock Effects," Project 30.5, WT-1452, 1960.

Meszaros, J.J., et al., "Instrumentation of Structures for Air-Blast and Ground-Shock Effects," Project 3.7, WT-1426, 1959.

Meszaros, J.J. and Randall, J.I., "Structures Instrumentation," Operation UPSHOT-KNOTHOLE, WT-738, 1955.

3.1.2 Deformeter (France) (1957).

Two types of deformeters were developed and deployed for structural response measurements. These deformeters were the door deformeter and the concrete deformeter.

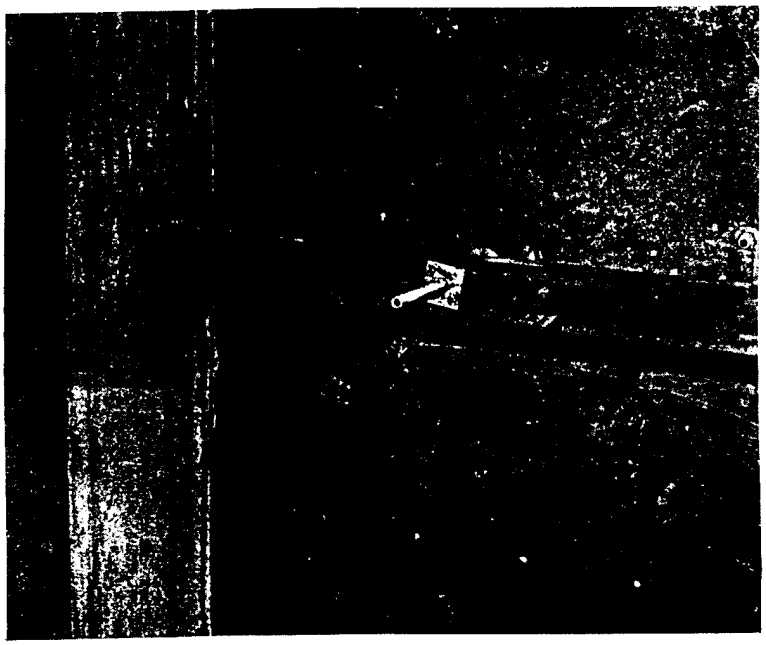

Figure 7. Peak-displacement gage.

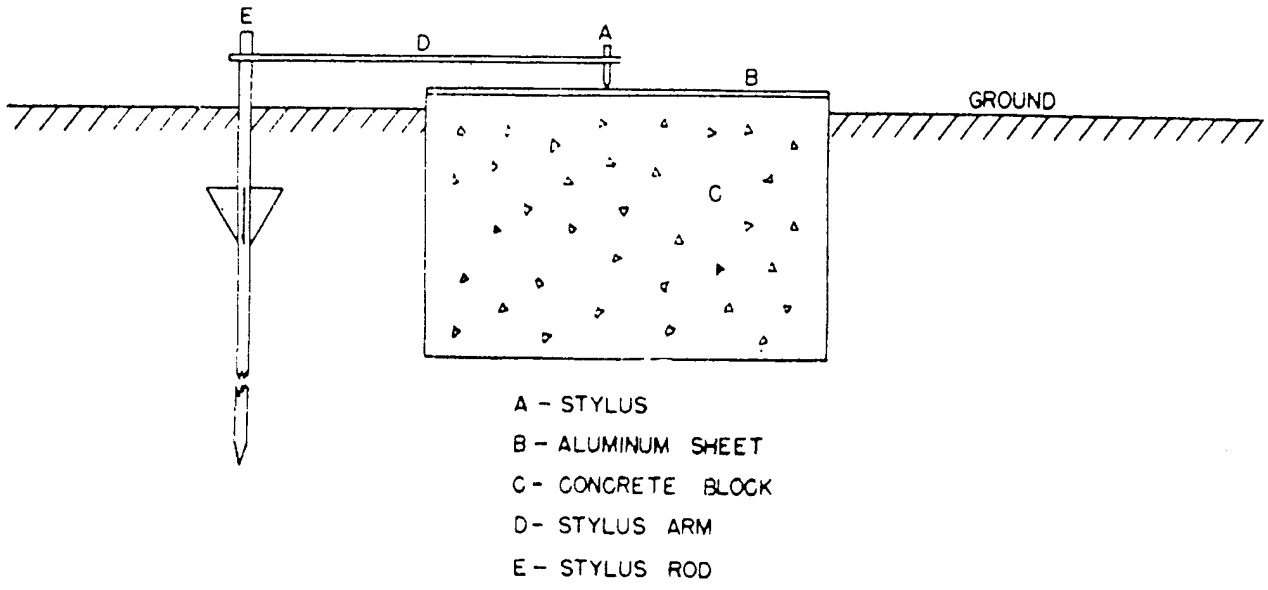

Figure 8. Scratch-type displacement gage.

The door deformeter was designed to measure the inward deformation that results from the impact of the blast on a door. Deflection is measured along the approximate center line of the door where the center line is parallel to the door sill. The deformeter is comprised of a group of five lateral gages, evenly spaced and welded to a bar supported by mounts attached to the vertical posts of the door frame. This is illustrated in Figure 9. A closeup of a lateral gage is shown in Figure 10. By mounting the cross bar in this way, the deformeter is isolated from the effects of deformation of the door frame itself. If the door frame is damaged, a spring absorbs the motion induced and a ball joint allows the gage to remain independent of any warpage of the door frame.

A description of the lateral gage used in the door deformeter is presented in Section 3.1.3.

The concrete deformeter was designed to measure the peak displacement of the walls of a structure or of a ceiling slab. A rod erected vertically, horizontally, or at 45° between walls or floor and ceiling contains a steel punch screwed into one end which penetrates a lead disk in response to the blast forces. The lead disk is supported in a mounting cylinder. The rod or shaft which holds the punch is held in place by two sleeves which are spring-mounted to anchors in the floor or sides of the structure.

The concrete deformeter is shown in Figures 11 and 12.

In case the deflection of the wall should be of magnitude that the thickness of the lead record plate is exceeded, the measurement can still be obtained by observing the scratch marks on the punch. This is made possibe by placing machinists' layout fluid on the punch.

Measurement of the depth of penetration of the lead in the record plate is made by a depth micrometer. The amount of penetration is equivalent to the peak deformation of that point on the slab being tested.

Ref: Meszaros, J.J. and Schmidt, J.G., "Instrumentation of French Underground Shelters," WT-1535, 1961.

3.1.3 Lateral Gage (France) (1957).

The lateral gage was an instrument designed to measure the maximum amplitude of the lateral or vertical displacement of doors in a test structure. A steel punch supported in a mount welded to the door frame is used to penetrate a lead disk. The punch is adjusted before the test so that the point just makes contact with the surface of the lead plate. The other end of the punch is in contact with a steel angle welded to the inside surface of the door. As a result of the displacement of the door, the steel angle forces the punch into the lead disk. The depth of penetration of the punch is measured by a depth micrometer.

The lateral gage is shown in Figure 13.

Ref: Meszaros, J.J. and Schmidt, J.G., "Instrumentation of French Underground Shelters," WT-1535, 1961.

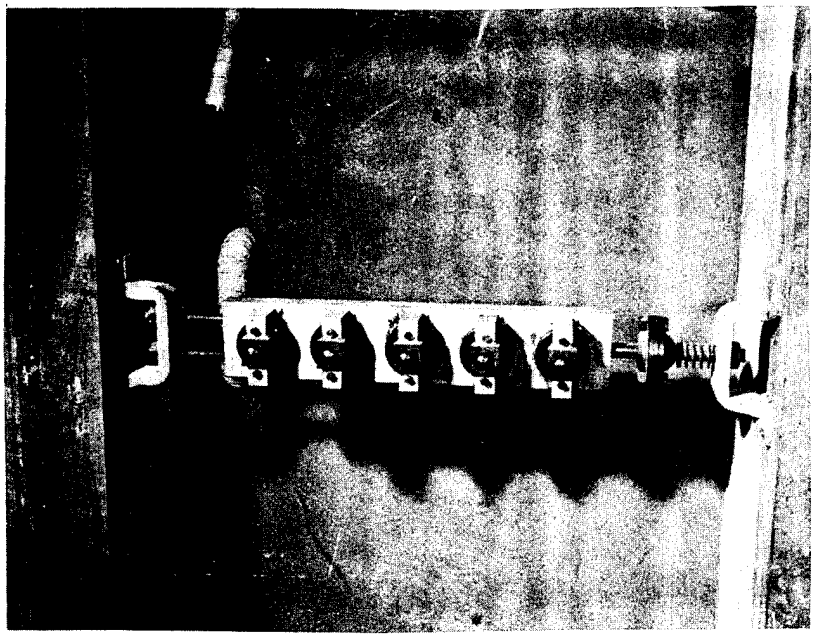

Figure 9. Door deformeter.

Figure 10. Close-up of door deformeter.

Figure 11. Vertical concrete deformeter.

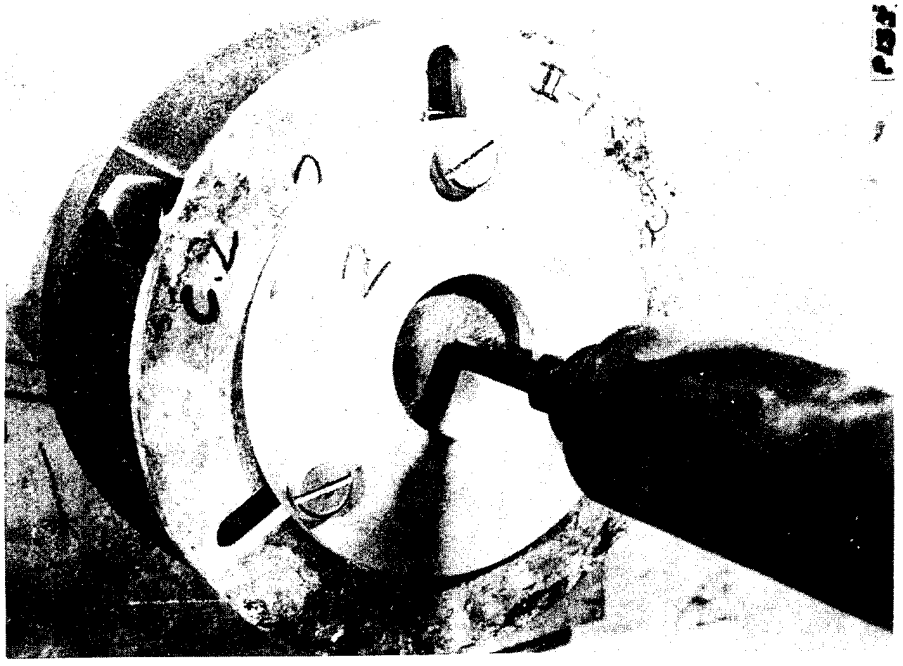

Figure 12. Close-up of punch and record plate, concrete deformeter.

Figure 13. Lateral gage.

3.1.4 Recording Pendulum (France) (1957).

The recording pendulum was designed to measure the lateral motion of the floor of a structure which is exposed to the blast. A heavy cylinder is suspended from the ceiling of the test structure by a steel cable. A piston-like slide located in the bottom of the cylinder is free to move in and out of the pendulum. A pencil inserted in the slide makes contact with a sheet of paper taped to a plate anchored to the floor. The trace scribed by the pencil represents the movement of the floor.

The recording pendulum is shown in Figures 14 and 15.

Ref: Meszaros, J.J. and Schmidt, J.G., "Instrumentation of French Underground Shelters," WT-1535, 1961.

3.2 ACCELERATION AND STRAIN-SENSITIVE DEVICES.

3.2.1 BRL Peak Reading Acceleration (USA) (1953).

The BRL peak reading accelerometer is a simplification of the BRL self-recording accelerometer described in Section 3.3.4 and is shown in Figure 16. A heavy milled block is welded to a 4-inch diameter base-plate and the accelerometer element is attached to the milled block. A small rectangular recording blank is glued to a movable piece secured to the heavier block by screws. After installing the accelerometer element so that its stylus will produce a trace on the recording blank, the piece with the blank attached is moved to obtain a fiducial mark which serves as a reference from which the positive and negative acceleration records are read. The movable piece is then locked into position and the gage is ready for use.

Ref: Meszaros, J.J. and Schmidt, J.G., "Instrumentation of French Underground Shelters," WT-1535, 1961.

3.2.2 Chocmart (France) (1957).

The chocmart is a non-electronic device installed on structures to measure the acceleration which it may experience. The unit is made up of five metal tubes mounted on a metal plate mounted on a metal plate with the opposite end of the tube open. When in use, the mounting plate is bolted to the section of structure of interest. Each tube in the assembly is inclined at angles of 10 to 50 degrees from the perpendicular to the surface of the mounting plate. A steel ball is inserted in each tube; each ball is numbered to match the number on the tube. Each steel ball, in response to the acceleration experienced by the structure, may be ejected from the tube according to the intensity of the pulse. The ball is captured at the end of its travel by a layer of asphalt spread on the floor of the structure.

The chocmart, as installed on a shelter, is shown in Figures 17 and 18.

The trajectory of the ball after it leaves the tube is dependent upon the magnitude of the acceleration forces striking the structure. The distance the ball has traveled, together with the angle of inclination of the tube, and the mass of the ball, enables the magnitude of the acceleration experience by the structure to be calculated.

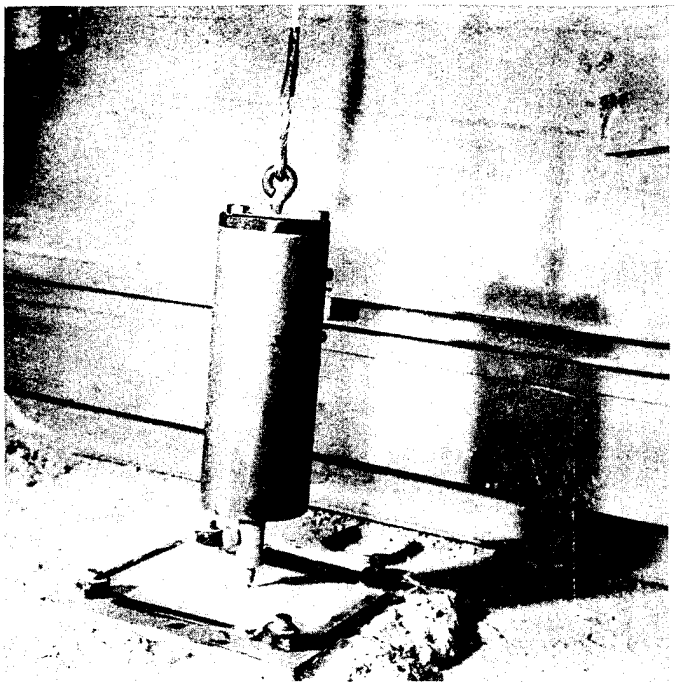

Figure 14. Recording pendulum showing pencil against record player.

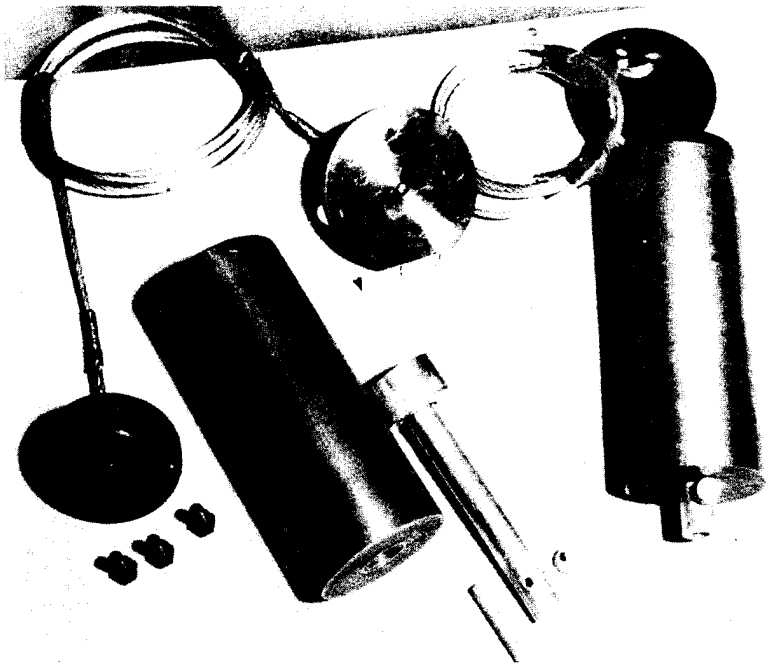

Figure 15. Exploded view of recording pendulum.

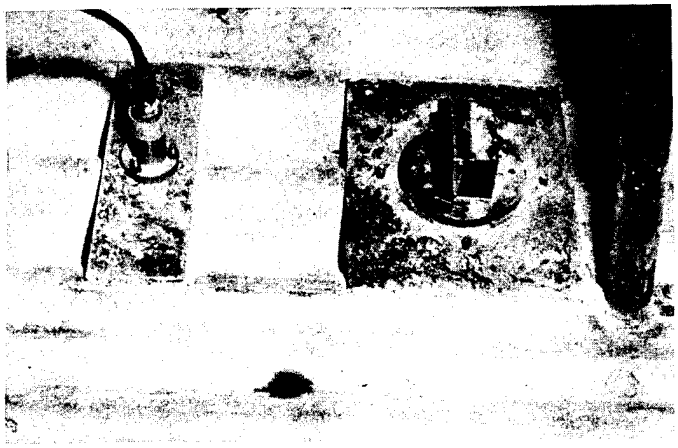

Figure 16. Electronic accelerometer (left) and peak recording accelerometer (right) on floor of test structure.

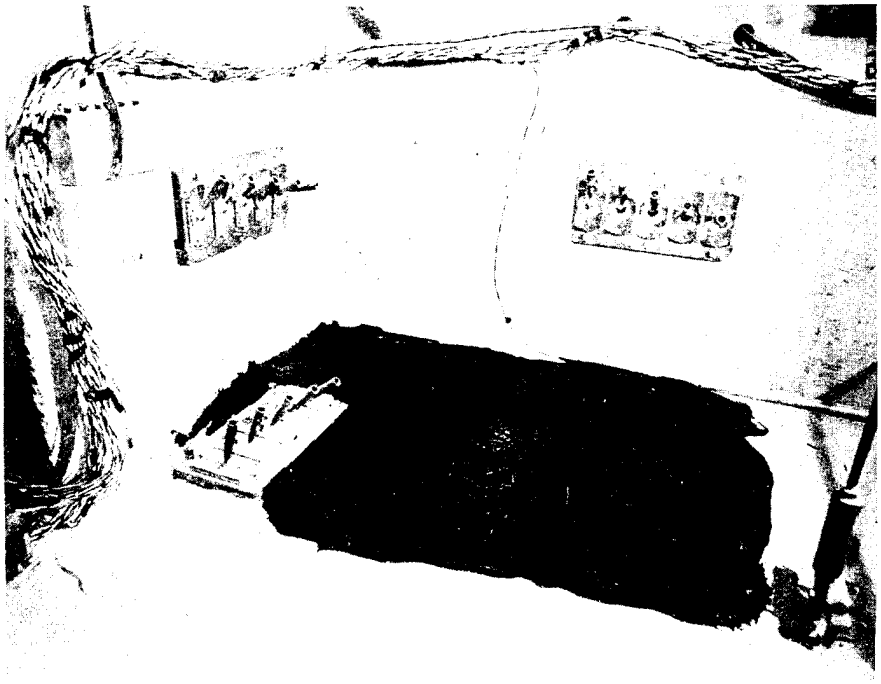

Figure 17. Chocmarts and asphalt layer.

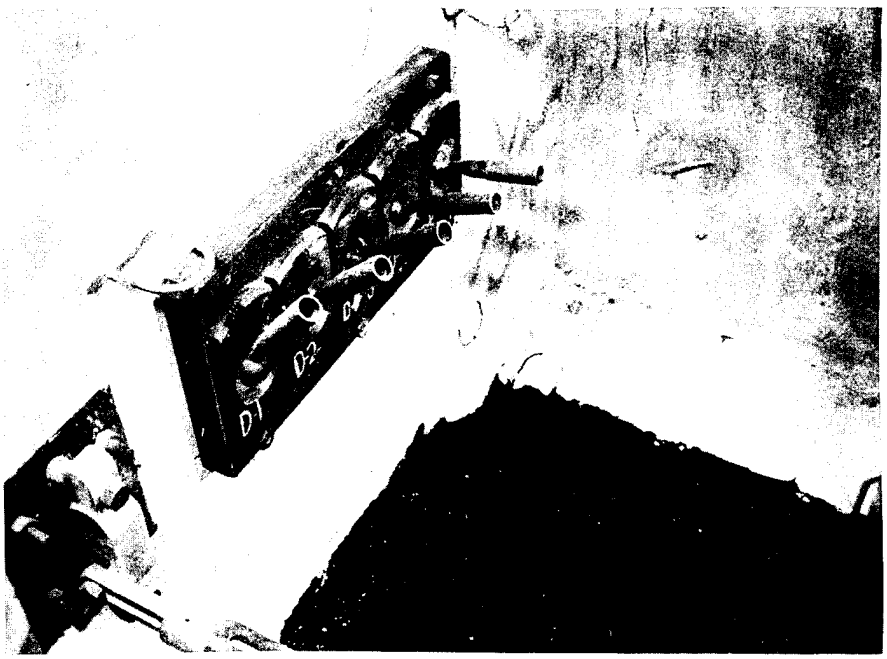

Figure 18. Close-up of chocmart and asphalt layer.

Ref: Meszaros, J.J. and Schmidt, J.G., "Instrumentation of French Underground Shelters," WT-1535, 1961.

3.2.3 Peak Reading Strain Gage (USA) (1953).

The Whittemore strain gage is well suited for the quick measurement of permanent strains in structures or structural components (manufactured by Baldwin Locomotive Works). The use of the gage requires the punching of two indentations a fixed distance apart, depending on the gage length, on the structural member prior to the application of the load to the structure. The change in distance between these gage points is then measured accurately after the test by the use of the Whittemore gage. Normally gages are furnished for 2-inch or 10-inch gage lengths, however, other lengths can be obtained. The following indicates the ranges of these gages:

> The Whittemore gage having a 254 mm gage length has a dial indicator, each division of which corresponds to a strain of 0.00001 mm/mm or, expressed as a percentage, to a strain of 0.001 percent. Each rotation of the large indicator (or hand) corresponds to a strain of 0.001 mm/mm or in percent to 0.1 percent.
>
> The Whittemore gage having a 50.8 mm gage length has a dial indicator, each division of which corresponds to a strain of 0.00005 mm/mm or, expressed in percentage, to a strain of 0.005 percent. Each rotation of the large indicator (or hand) corresponds to a strain of 0.005 mm/mm or, in percentage, to 0.5 percent.

The Whittemore strain gage is shown in Figure 19.

Ref: Northrop, Paul A., "Instrumentation for Structures Program," Part I. OPERATION GREENHOUSE, WT-1, 1951.

3.3 SELF-RECORDING DEVICES.

3.3.1 Sandia Self-Recording/Electronic Displacement Gage (USA) (1950).

The Sandia displacement gage is shown in Figure 20. It can be used in either a self-recording or electronic-recording mode.

The gage consists essentially of a paper-supply roller, a take-up roller, and a recording stylus, which for most measurements is directly attached by a tube to the structural member being displaced. The rollers, driven by a DC motor operated by a small dry battery, accommodate waxed paper 12-inches wide upon which the record is made. A centrifugal governor operates a switch controlling the speed of the motor. When the switch is open, some energy is supplied to the motor through a shunting resistance, thus controlling the speed up to $\pm$ 1 percent.

Recording is initiated by a relay. The device permits indication of $\pm$ 6-inch displacement if the stylus is set in the center, or 12-inch displacement if the stylus is set at one end of the shaft. For electronic recording, a 10-turn Helipot is driven by shaft through a rack and pinion

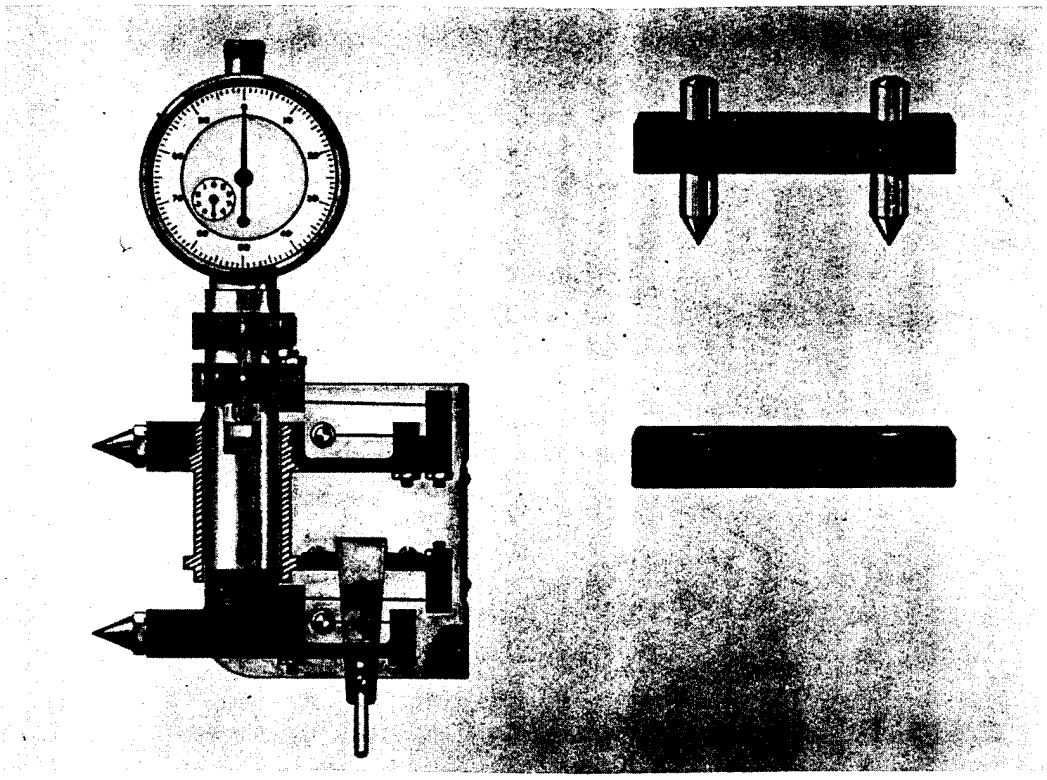

Figure 19. Whittemore strain gage.

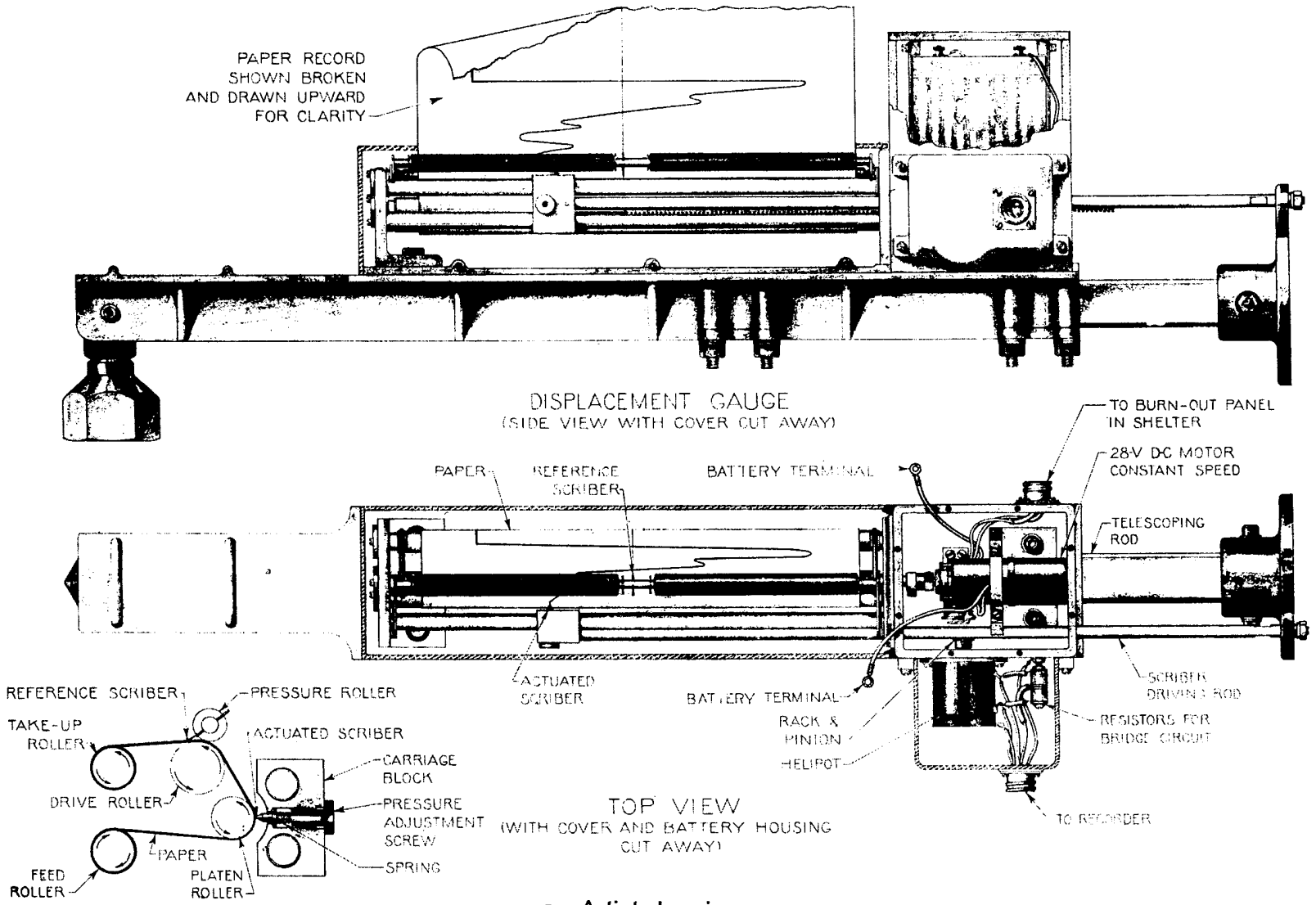

a. Artist drawing.

Figure 20. Sandia 12-inch displacement gage.

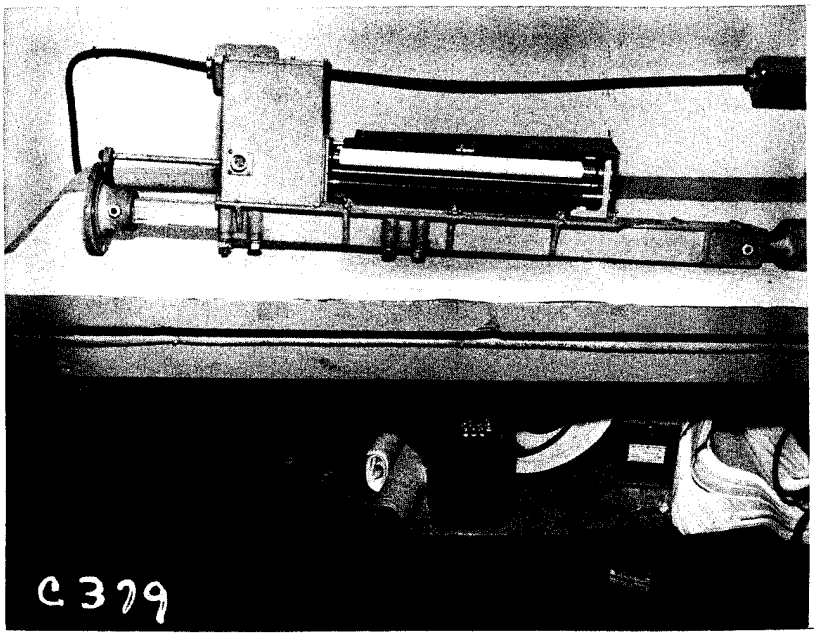

b. Gage photograph.

Figure 20. Sandia 12-inch displacement gage (Continued).

gear. This Helipot is part of a bridge circuit, and control of its resistance value permits the sensitivity of the electronic signal to be adjusted to the magnitude of the expected displacement.

The speed of the driving shaft is about 120 rpm, varying about 5 percent for different motors. For a particular motor, the speed under load is constant within $\pm$ 1 percent. Recording paper speeds between 4 and 7 inches per second are acceptable; the constancy of the speed depending upon that of the motor. Before the blast, the correct paper speed will be determined for each gage.

Some gages can be equipped with a motion-reduction rack and pinion-gear system which has a 5:1 ratio to provide for displacements in excess of 12 inches.

Each gage when deployed in the field is bolted to a pier in the floor of a building and attached by a seamless steel tubing to the structural member under test. A field installation of the gage is shown in Figure 21.

Ref: Northrop, Paul A., "Instrumentation for Structures Program," Part I. Operation GREENHOUSE, WT-1, 1951.

3.3.2 BRL Self-Recording Displacement Gage (USA) (1957).

The BRL self-recording displacement gage uses the same spring-wire mechanism of the BRL electronic gage. To record displacement, the rotary motion of the gage shaft was converted by a machine screw to a small linear motion where it would be scratch-recorded on the rotating glass disk by a stylus. The drive motor, recording table, and recording disk of the type used in BRL self-recording dynamic pressure gages described in Vol I, Section 4.2.8, were housed in an extension of the 4 and 1/2-inch diameter gage case. The gage as deployed in the field adjacent to an electronic gage is shown in Figure 22.

3.3.3 ERA Self-Recording Accelerometer (USA) (1950).

The ERA (Engineering Research Associates) self-recording accelerometer uses a spring-mass system bearing small magnets which erase a pre-recorded signal on a moving magnetic tape. The gage is shown in Figure 23.

Magnetic tape 0.75-inches wide and with an active portion 36-inches long is wound on the supply drum, the speed of which is controlled by an adjustable viscous damper. The tape, after passing around two capstans, is wound on a drum driven by a spring motor. The tape has three channels upon which a 1250-Hz carrier wave is recorded before the tape is installed.

In addition to the two acceleration sensors, a third mass-spring system is positioned to vibrate as a torsional pendulum to provide a time base. The torsional vibrations are initiated when a burn-out wire permits the tape motor to start. The prerecorded 1250-Hz carrier signal on the first 6 inches of tape is left unerased because of the way in which the tape is loaded in the accelerometer. Following this is a section having a constant degree of erasure in the short interval after the burnout before the magnet is accelerated. The rest of the tape is erased to varying degrees depending on the accelerations of the magnet. The unerased

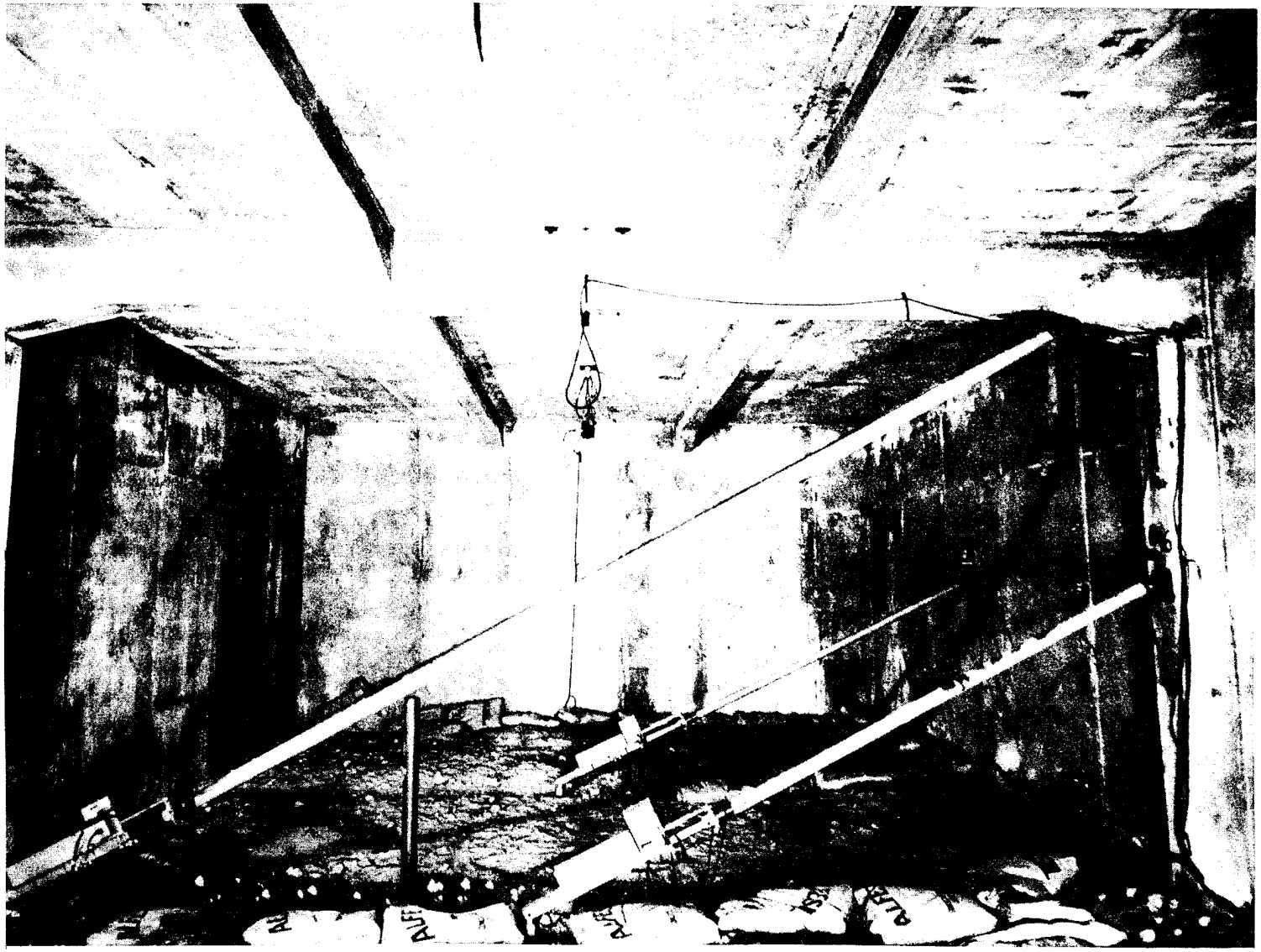

Figure 21. Pre-shot view showing interior of a test structure. Note four displacement gages, one partially concealed, and upright tubing carrying Wiancko air-pressure gage.

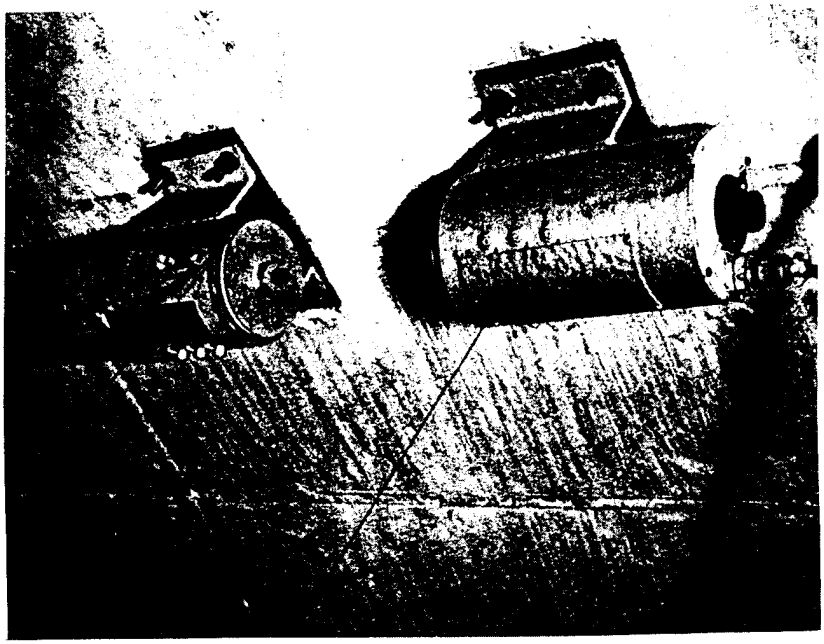

Figure 22. Self-recording displacement gage (left) mounted on inner shell of cylindrical concrete structure.

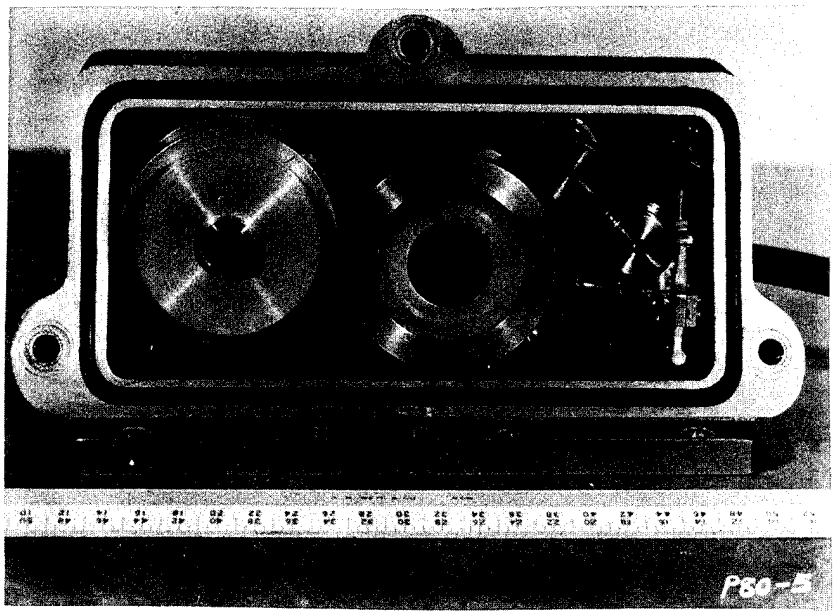

Figure 23. ERA self-recording accelerometer.

portion and the uniformly erased portion are used for calibration. Damping of the seismic elements is controlled by placing a silicone oil between each magnet and a stationary platform just below it.

The playback system, shown in Figure 24, consists of a drum, upon which the 36-inch length of tape is wound in a single layer, and a pickup head, which can be adjusted to any one of the three channels. The output from the pickup is placed as a vertical deflection on a special oscilloscope which has horizontal sweeps of 8, 0.5, 0.2, 0.1, 0.05, and 0.01 seconds. Since the playing time of the tape is 8 seconds, these sweep times permit either the scanning of an entire channel or the magnification of a small portion of the channel. Provision is made for starting the sweep at any point on the tape.

The pickup head is also used for prerecording the 1250-Hz carrier wave and for erasure.

The natural frequency of 10-g elements was 20 Hz. In other ranges, the natural frequency is proportional to the square root of the ratio of the range of the instrument to that of the 10-g element.

Ref: Northrop, Paul A., "Instrumentation for Structures Program," Operation GREENHOUSE, WT-1, 1951.

3.3.4 BRL Self-Recording Accelerometer (USA) (1957).

The BRL self-recording accelerometer was a gage developed on an experimental basis and field tested. The accelerometer sensor element consists of a cantilever beam with a weight attached to its free end. A spring arm attached to the weight holds a stylus and the assembly is attached to the gage chassis so that as the weight oscillates in the plane of the recording disk, the stylus scratches a record of its excursions on the disk. Each beam is shaped to prevent oscillations in any direction except that desired. The gage mechanism is covered by a light sheet metal cup. The accelerometer baffle plate fits the standard pressure-time gage casing so that where high blast pressures are expected and the additional weight of the casing is not detrimental, these casings are used to protect the gage mechanism.

The chassis for the recording turntable assembly is milled from solid-steel stock to produce a more rigid assembly. The motor and disk are mounted in the same manner as that found with the self-recording pressure gage described in Vol I, Section 4.2.8. A BRL self-recording accelerometer, as installed in the field, is shown in Figure 25.

Ref: Bryant, E.J. and Keefer, J.H., "Basic Air-Blast Phenomena," Project 1.1, Operation PLUMBBOB, WT-1401, 1958.

Meszaros, J.J., et al., "Air-Blast Phenomena and Instrumentation of Structures (U)," Project 1.7, WT-1612, 1962. (CONFIDENTIAL-FORMERLY RESTRICTED DATA)

3.3.5 DOFL Self-Recording Accelerometer (USA) (1959).

The Diamond Ordnance Fuze Laboratories (DOFL) accelerometer was designed as a mechanical self-recording, self-contained unit to measure accelerations up to 5000 g's over

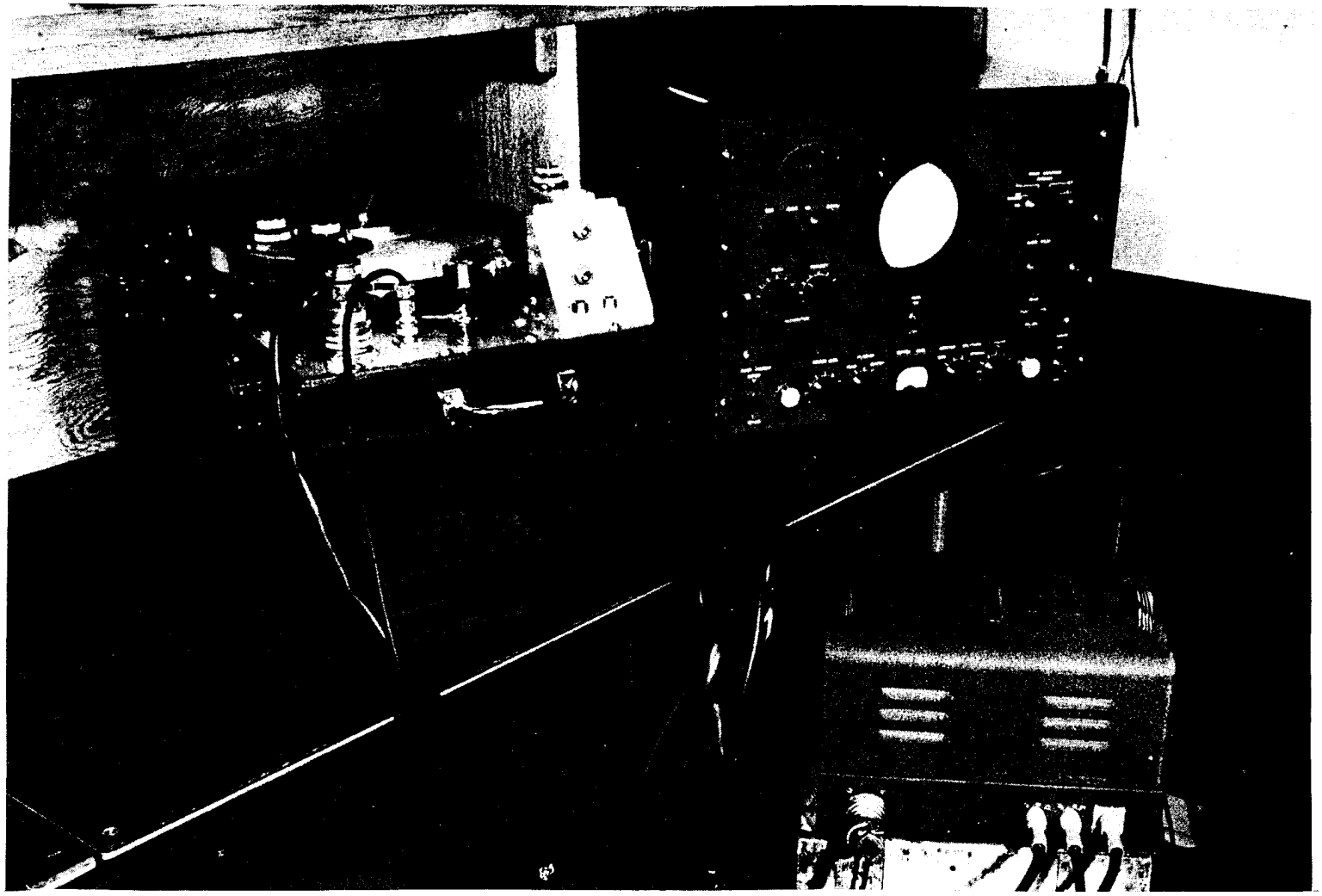

Figure 24. ERA playback.

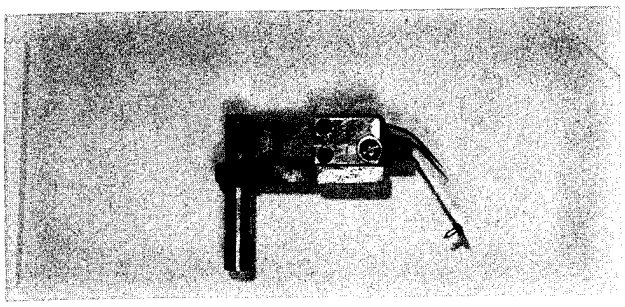

a. Accelerometer sensor.

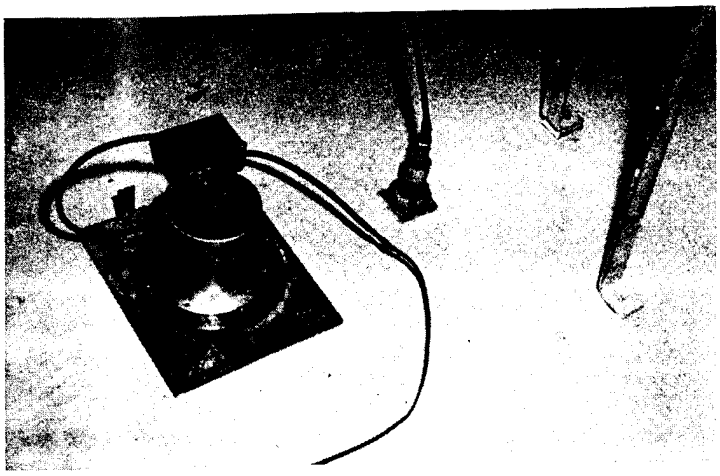

b. Self-recording accelerometer (left) and electronic accelerometer (right) on floor of test structure.

Figure 25. BRL self-recording accelerometer.

periods up to 30 msec. Acceleration versus time is obtained with an estimated accuracy of ± 10 percent.

The sensing element of this accelerometer is a flexible metal reed supported as a cantilever perpendicular to the direction of motion. A mass with a stylus is mounted on the free end of the reed so a record of its deflection can be recorded on a rotating metal disk. The disk is mounted on a torsional spring-driven turntable. The record disk is made of hardened steel and is chromium plated. Machinists' layout fluid is also used to coat the recording surface.

Shown in Figures 26 and 27 are schematics of the DOFL accelerometer. The mechanism is housed in a steel box 1 and 5/8 x 1 and 3/4 x 2 inches where the wall thickness is 1/4-inch thick.

Calibration of both the recorder and the reed are necessary. Interchangeable reed sensors provides for a wide range of acceleration measurements.

Ref: Blagman, George, "A Self-Contained Mechanical Recording Accelerometer," TR-703, Diamond Ordnance Fuze Laboratories, U.S. Army, 1959.

3.3.6 Glenn L. Martin Self-Recording Strain Gage (USA) (1950).

The Glenn L. Martin self-recording strain gage is shown in Figure 28. A chrome-plated steel disc is driven by a spring motor through a flexible shaft. The disc housing is attached to one part of the structural member under test. A diamond stylus bearing on the underside of the disc is attached by an arm to another part of the structural member. The triggering mechanism is solenoid-operated from a 24-volt DC supply. It is possible to record strains of approximately 2-second duration, the time required for one revolution of the disc. In interpreting the record the distance between the scratch made under load and a zero-load circle previously scribed is determined by means of a comparator with which both the angular position of the record line and its linear distance from the zero-load line may be determined. Since the angular velocity of the disc is known, the time at which a given strain occurred can be determined from the angular position.

The velocity of angular rotation has been checked for constancy and repeatability by comparing pulses from a 125-toothed commutator wheel mounted in place of the recording disc, with a 100-Hz signal from an oscillator, both being registered on a Brush pen recorder. Average angular velocity of the third revolution which is the one to be used, was repeatable within 1 percent, but instantaneous values varied by about 10 percent within the revolution.

In tension measurements, the test length is the one-inch distance between two pairs of hardened steel points, one pair on the recording-disc housing and the other on the scriber-point housing. The pairs of points are oriented in parallel lines and penetrate the metal under test about 1/64 inch. The housings themselves are fastened to the specimen by two number 4-40 screws passing through slots in the housing and screwed down lightly. The adjustments permit strain measurements under tension of 0.25 lbs. It is also possible to measure compressional strains up to 0.125 lbs if the mounting points are 1.125 inches apart initially.

The gage is capable of indicating gross deflections from 0.001 to 0.25 inches for each inch of gage span. An accuracy of 5 percent is estimated.

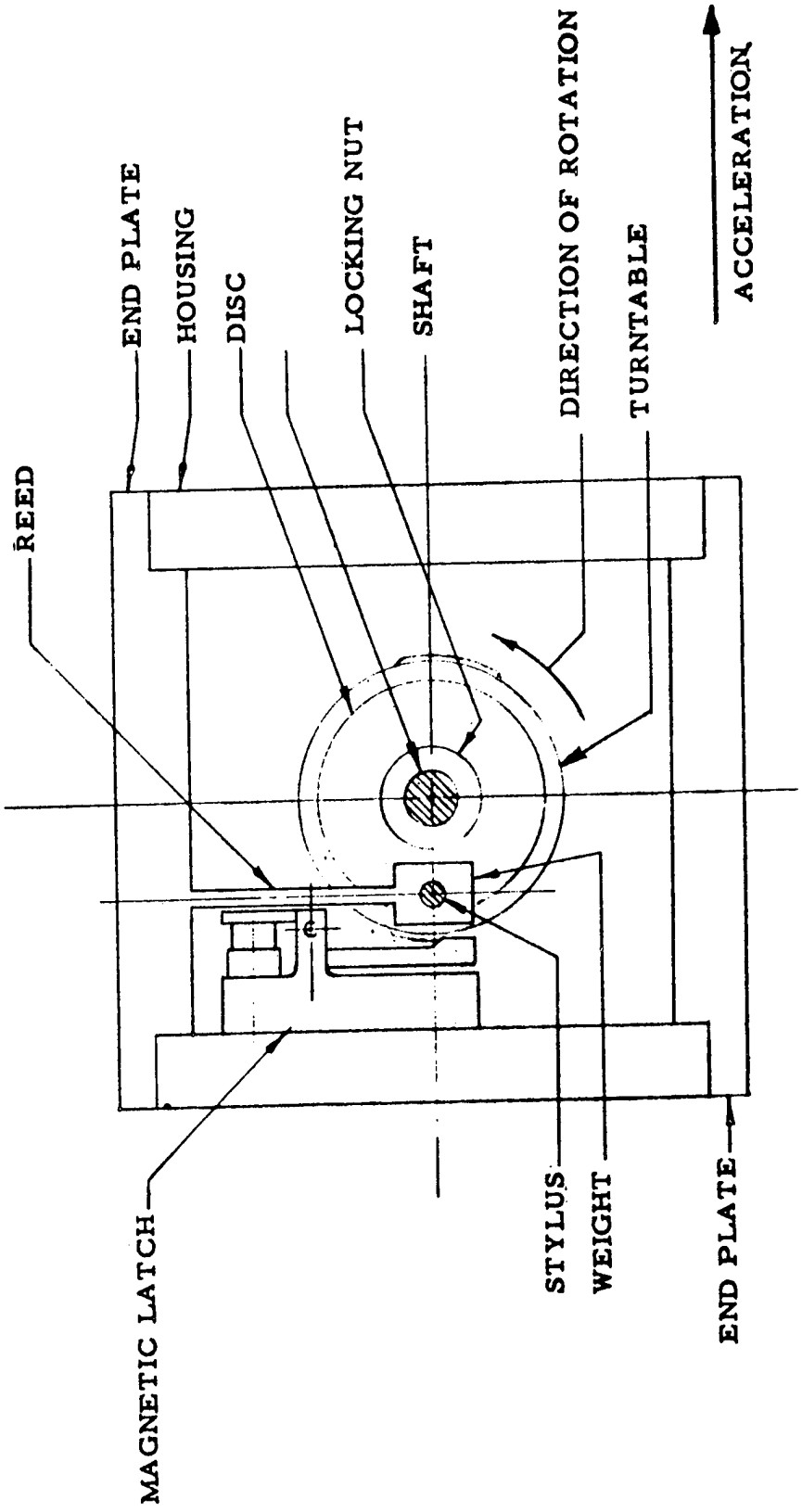

Figure 26. View of DOFL accelerometer with top cover plate removed.

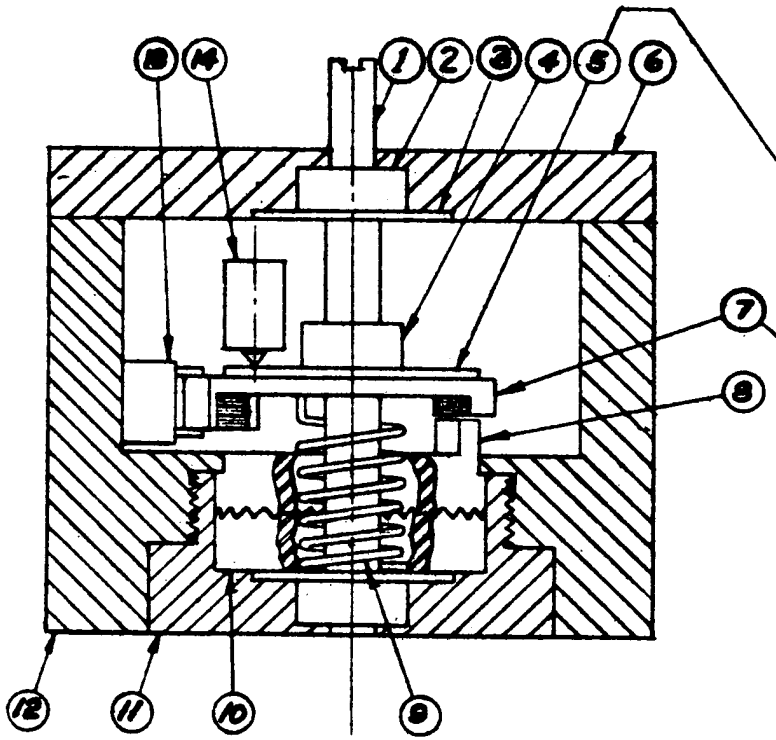

END PLATE REMOVED, WITH CUTAWAY VIEW OF PLUG

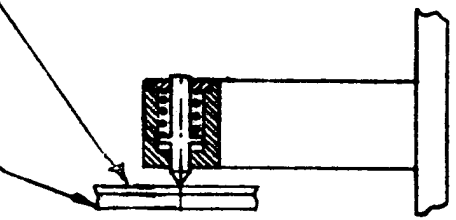

CUTAWAY VIEW OF REED AND STYLUS

1. SHAFT
2. BALL BEARING
3. BALL BEARING KEEPER
4. LOCKING NUT
5. DISC
6. COVER PLATE
7. TURNTABLE
8. TOP SERRATED RING WITH STOP
9. TORSIONAL SPRING
10. BOTTOM SERRATED RING
11. PLUG
12. HOUSING
13. MAGNETIC LATCH, ENGAGED
14. WEIGHT AND STYLUS AT FREE END OF REED

Figure 27. Internal construction of mechanical recording accelerometer.

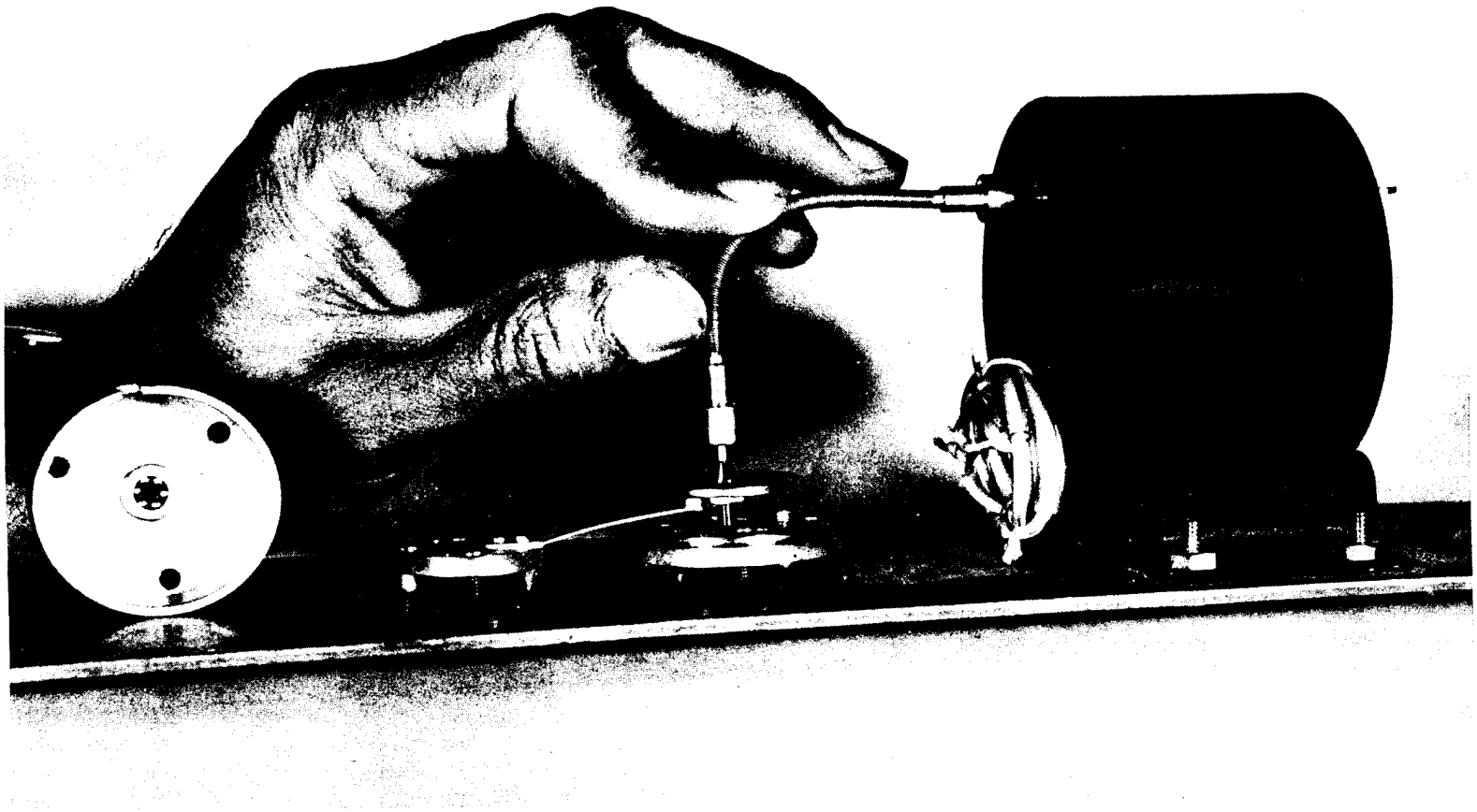

Figure 28. Glenn L. Martin strain gage.

Ref: Northrop, Paul A., "Instrumentation for Structures Program," Part I. Operation GREENHOUSE, WT-1, 1951.

SECTION 4

ELECTRONIC - NUCLEAR TESTING

4.1 DISPLACEMENT.

4.1.1 Sandia Rigid-Rod Displacement Gage (USA) (1950).

The Sandia rigid-rod displacement gage uses a solid 1/2-inch aluminum rod, 10-feet long, anchored at one end to the point of measurement. The opposite end of the rod is attached to the magnetic core of a linear variable differential transformer. The rod is protected by placing it inside a corrugated, flexible 3/4-inch metal tube.

Since the relative earth motions are generally small (0.01 to 0.5 inch in a 10-foot span) and the rod must be free to move, a means had to be provided to zero the unit after it was embedded in the medium by tamping or grouting.

During installation, the rod is clamped in the canister by a pin-and-slot arrangement. After the installation, a motor turns the sleeve containing the slot, thereby freeing the rod to move longitudinally. A second motor then turns three jack screws which hold a cage carrying the LVDT transformer, thereby zeroing the assembly.

Sandia also makes a 3-foot gage. It is similar to the preceding gage in that one end of the rod is terminated in a flat plate and the Schaevitz transformer is in a canister at the opposite end of the rod. The size of the canister is greatly reduced, the locking motor eliminated, and locking of the rod for installation is accomplished by cutting a groove near the end of the rod, in which a bar is placed. When the zeroing motor is operated in either direction, a cam pushes the bar out of the slot and a spring catch holds the bar out of the way. Two motor-driven jack screws move the LVDT transformer back and forth to zero the unit.

In a third model, the LVDT transformer is stationary in the canister. The end of the rod is threaded for several inches and carries an internally threaded cap. Mechanical stops permit the rod to move freely over a limited range, but the rod is not locked as in the previous models. After the gage is embedded in the earth, a motor-and-gear arrangement screws the cap, which carries the LVDT core, back and forth until the unit is zeroed or balanced. In this position, the rod has at least a 50-percent overtravel, the actual amount depending upon the size of the LVDT being used. This unit is smaller in size, is more rigid, and should be simpler to build, adjust, and operate than the previous models. The canister, about 4 inches in diameter, has a 12- to 15-inch diameter anchor plate at one end. The cylindrical portion is covered with a soft sleeve to decouple it from the earth. These features give more precise reference points for gage length. This model may be used with either the 3-foot or the 10-foot rods.

Ref: Northrop, Paul A., "Instrumentation for Structures Program," Part I. Operation GREENHOUSE, WT-1, 1951.

4.1.2 BRL Displacement Gage (USA) (1953).

The BRL displacement gage was designed to measure displacements of structural members with reference to a fixed point. The gage design uses a wire between the fixed point and the sensor and has an optimum range of $\pm$ 0.75 inches to $\pm$ 5.75 inches.

It consists of a helically wound spring made of spring steel SAE1095, Rockwell hardness C49-51, 15-feet long, 3-inches wide, and 0.028-inches thick. The spring is attached to a shaft and wound until the assembly fits into the 4-1/2-inch diameter gage case. A spring clamp on the loose end of the spring locks it to the gage case. The shaft of a 500-ohm potentiometer (Helipot-type 500-GZ) with 360° degrees continuous rotation is connected to the spring shaft. The potentiometer is incorporated in a resistive bridge. For ease of calibration, a dial (100 divisions) is attached to the potentiometer shaft. A grooved pulley with a diameter of either 3.66 inches or 2.5 inches, depending upon the expected displacement, is attached to the spring shaft on the opposite end to the potentiometer. The gage or spring shaft is turned until the spring produces a torque of approximately 100 inch-pounds. A ratchet mounted on the spring shaft prevents the spring from unwinding. High tensile strength piano wire is clamped and wound several times on the grooved pulley. The gage is mounted at one point on the structure and the end of the wire at another point. Tension is placed on the wire by releasing the ratchet. The resistance bridge is balanced to a null point by adjusting the potentiometer and then locked in place. Any displacement between the structural members will turn the shaft, unbalancing the bridge and producing an output proportional to the displacement. The rise time of the gage with a displacement of 5.75 inches as the 100 percent signal using the 3.66-inch pulley is 14.5 msec. For displacements of one inch the rise time is 8.3 msec.

The gage is shown in Figure 29. A drawing of the gage is shown in Figure 30.

Ref: Meszaros, J.J. and Randall, J.I., "Structures Instrumentation," Operation UPSHOT-KNOTHOLE, WT-738, 1955.

4.1.3 LVDT Small Displacement Gage (USA) (1957).

The linear variable differential transformer (LVDT) displacement gage was designed to measure small displacements of 0.001 inches to 0.75 inches. The LVDT element is used as a variable impedance element in conjunction with the BRL wire displacement gage previously described. The hollow cylindrical armature of the LVDT is threaded over the gage wire and clamped in place. The solenoid winding of the transformer, inside which the armature moves axially, is held to the gage case by a rigid frame. Thus, the transducer senses directly the linear motion of displacement and the wire displacement gage mechanism serves only to produce tension in the wire. The coil of the LVDT (manufactured by the Schaevitz Engineering Company) consists of three windings, the middle one of which is the gage input (or primary) winding. The outside pair of windings are connected in series so that the output voltages are in opposition. As the armature is displaced from its balance point (center position) in either direction an output voltage proportional to the motion is produced and recorded.

The gage is shown in Figure 31. A typical record from the gage is shown in Figure 32.

Ref: Meszaros, J.J., et al., "Instrumentation of Structures for Air-Blast and Ground-Shock Effects," WT-1452, 1960.

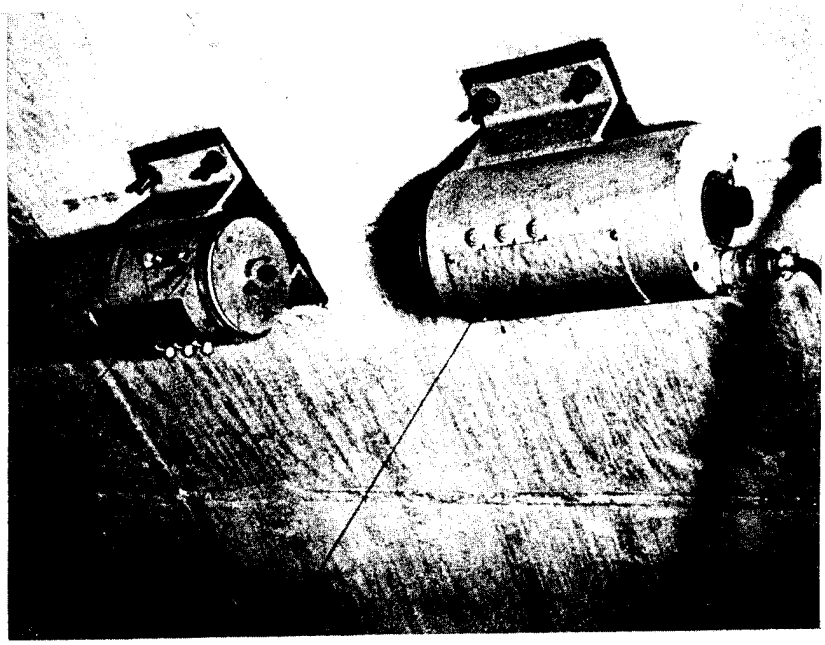

Figure 29. Electronic large-displacement gage (right) mounted on inner shell of cylindrical concrete structure.

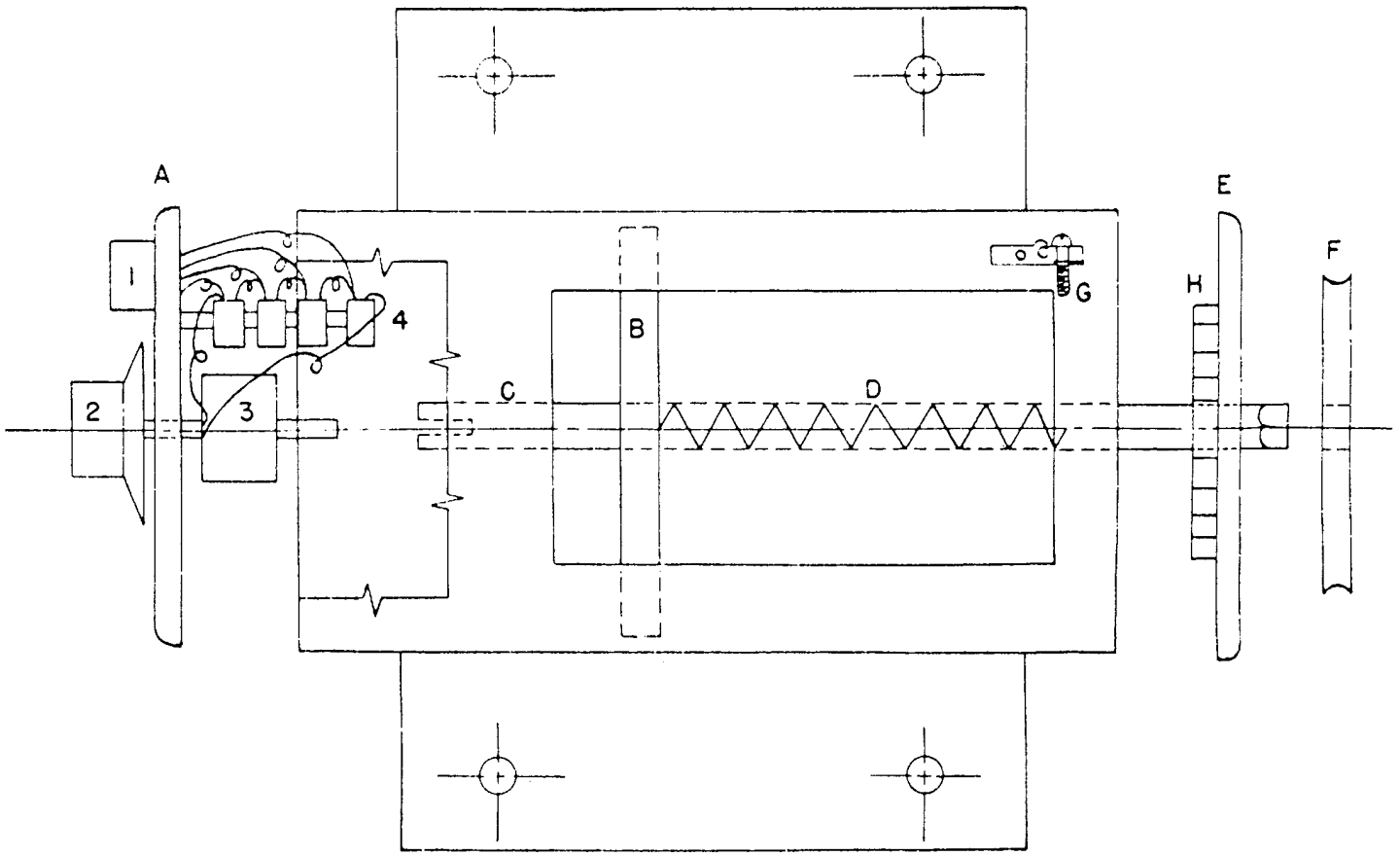

A End Plate
1 Cannon Plug
2 Dial
3 Potentiometer
4 Resistance Bridge
B Bearing Plate
C Shaft
D Helical Wound Spring
E End Plate
F Pulley
G Ratchet Stop
H Ratchet

Figure 30. Mechanical drawing of BRL displacement gage.

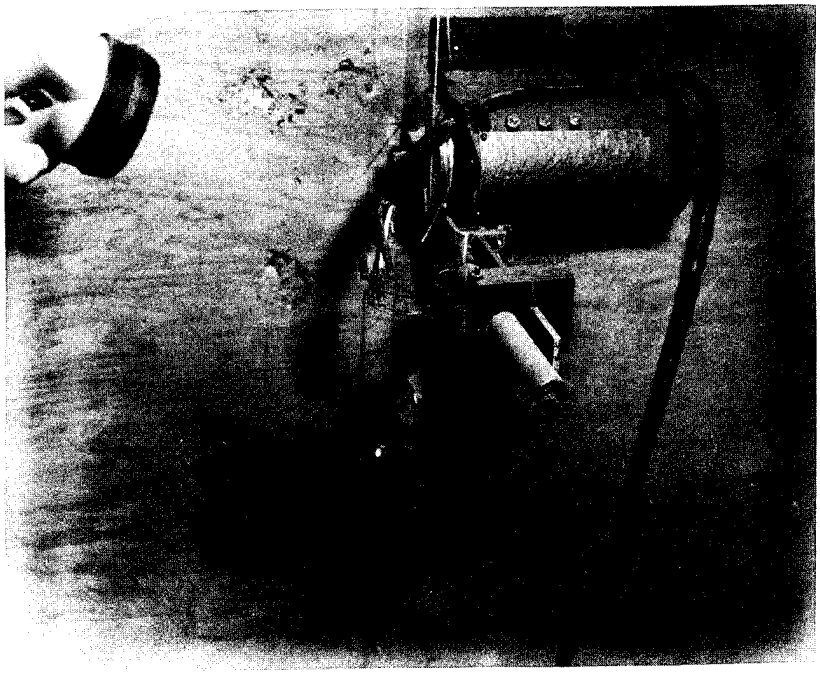

Figure 31. Electronic small-displacement gage mounted on wall of concrete structure.

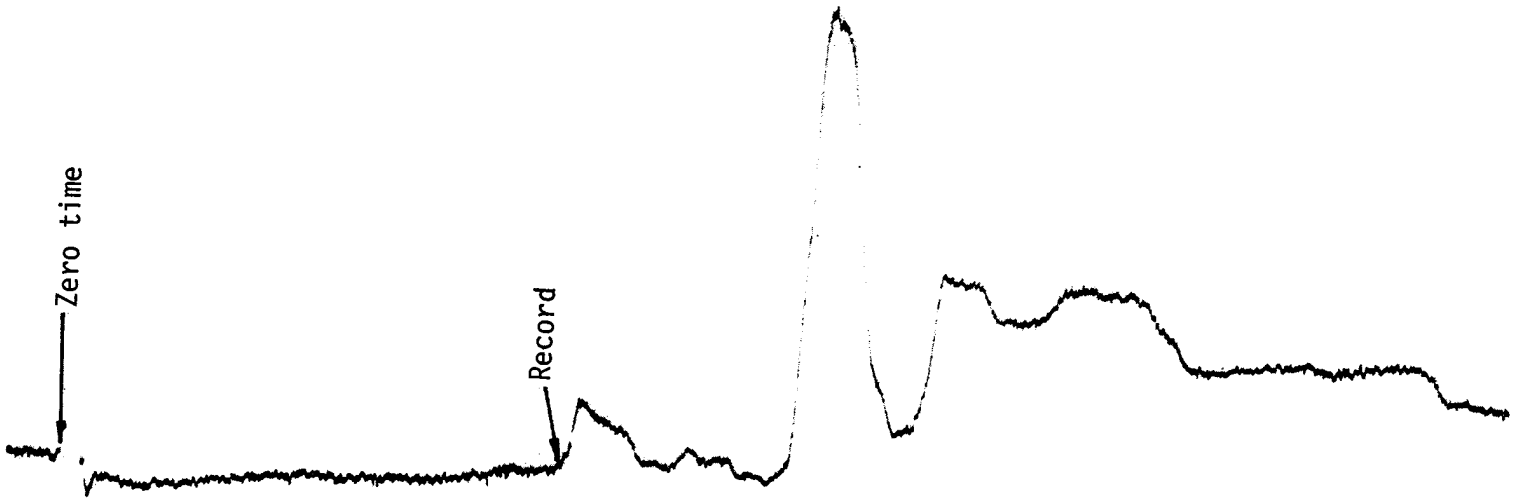

Figure 32. Deflection versus time between roof and column base - LVDT gage.

4.1.4 French Displacement Gage (France) (1957).

The French displacement gage is a potentiometer-type electronic gage designed to measure the displacement of structural members subjected to air blast. A feeler rod is attached to the wiper arm of the potentiometer and to the structural member of interest. Movement of the feeler rod produces a change in resistance in the potentiometer which is sensed by the recording system. The maximum range of the gage is 4 mm.

The displacement gage is shown in Figures 33 and 34.

Ref: Meszaros, J.J. and Schmidt, J.G., "Instrumentation of French Underground Shelters," WT-1535, 1961.

4.1.5 French Seismograph (France) (1957).

Earth movements were measured using a three-directional seismometer. The unit is a mechanical optical-type where the mechanical members which are responsive to the movement are three pendulums, each of which is sensitive to movement in a different plane. The pendulums consist of brass masses attached to flat steel springs secured to steel blocks. The period of the pendulum may be adjusted by moving the masses along the axis of the springs. A vertical, horizontal, and transverse direction of motion is made by the pendulum relative to the direction of ground zero. Recording of the pendulum oscillations are made photographically on oscillograph paper. Each pendulum has a mirror whereby light from a galvanometer lamp striking the mirror reflects onto photographic paper moving past a slit.

Each pendulum has a dashpot containing silicone to provide damping. The vertical pendulum uses fluid with a viscosity of 1000 centistokes, the other dashpots use a fluid of 12,500 centistokes. The natural frequency of the vertical pendulum is 1.39 Hz; the sensitivity is 1.5. (Sensitivity as used here is defined as the ratio of the deflection of the light spot recorded on the photographic paper to the deflection of the pendulum.) The horizontal pendulum has a frequency of 1.85 Hz and a sensitivity of 1.58. The transverse unit has a frequency of 1.78 Hz; a sensitivity of 1.40.

The seismograph was installed securely to the floor of the structure. Figures 35 and 36 show the seismograph.

Ref: Meszaros, J.J. and Schmidt, J.G., "Instrumentation of French Underground Shelters," WT-1535, 1961.

4.2 ACCELERATION.

4.2.1 Wiancko Accelerometer (USA) (1953).

The Wiancko accelerometer is a variable reluctance gage manufactured by the Wiancko Engineering Company. The sensing element consists of an armature banded at its center to the vertex of a "V"-shaped spring member and held in close proximity to an "E" coil as illustrated in Figure 37. A weight, the size of which depends upon the range of the accelerometer, is attached to one end of the armature so that an acceleration in a direction normal to the armature causes it to rotate about the vertex of the spring. The rotation of the

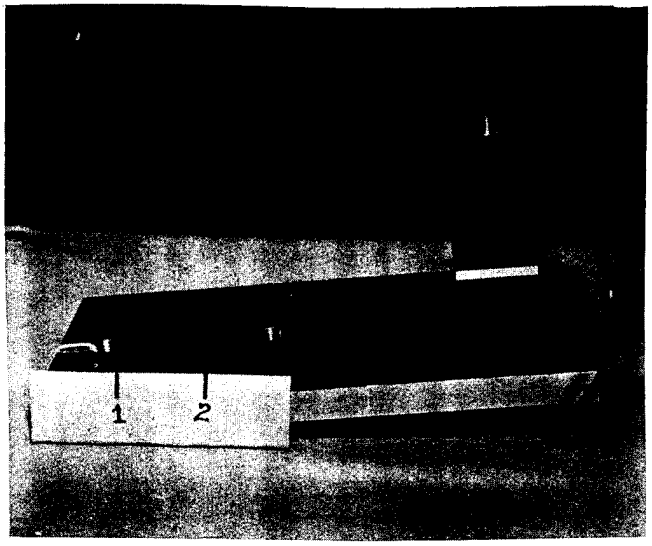

Figure 33. Side view of French displacement gage.

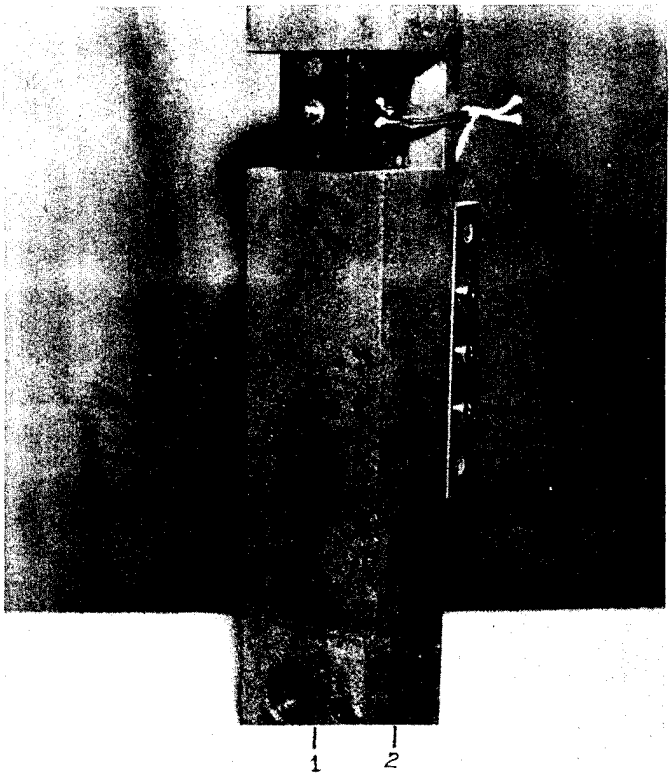

Figure 34. Front view of French displacement gage.

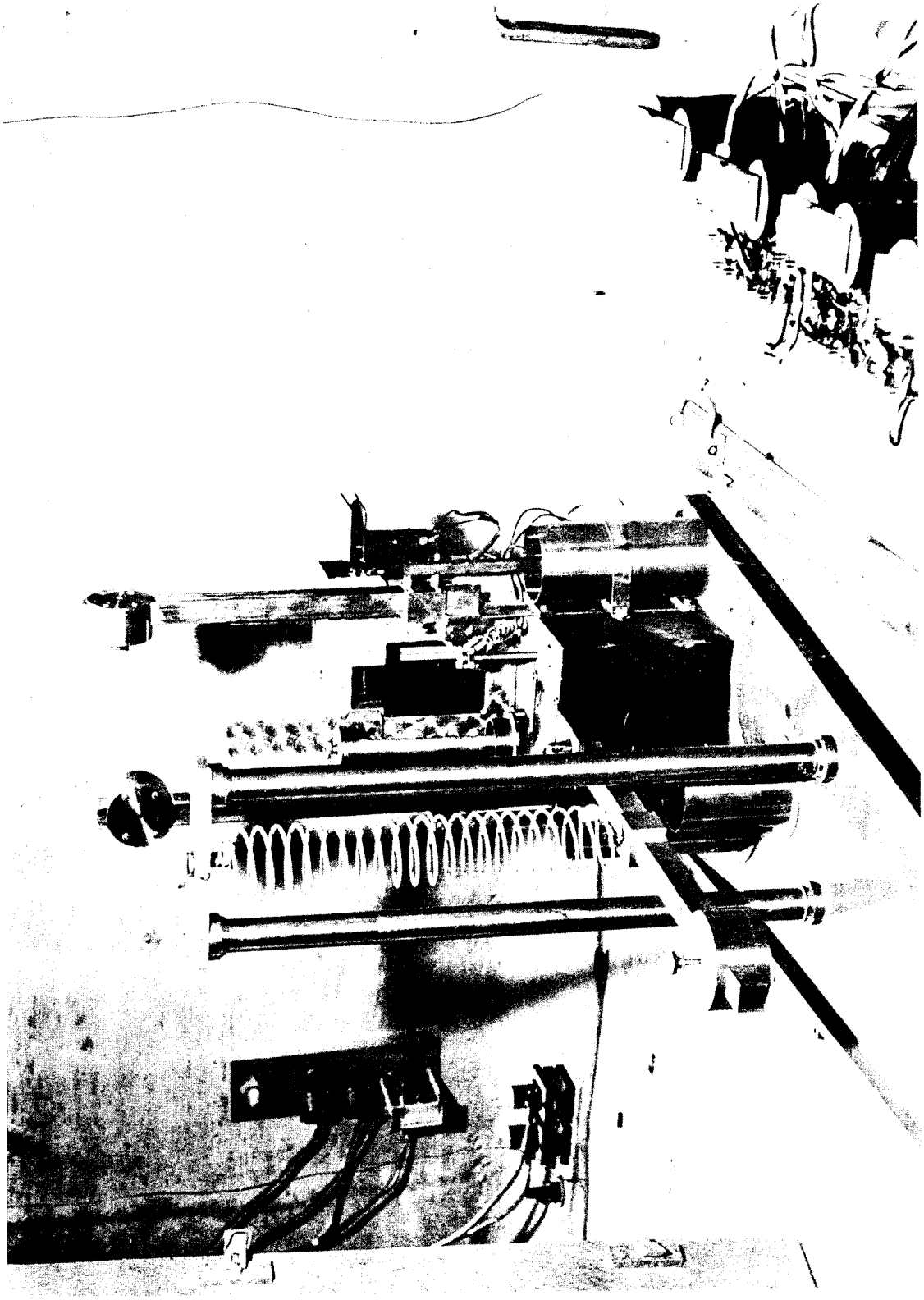

Figure 35. Seismograph installed in a structure.

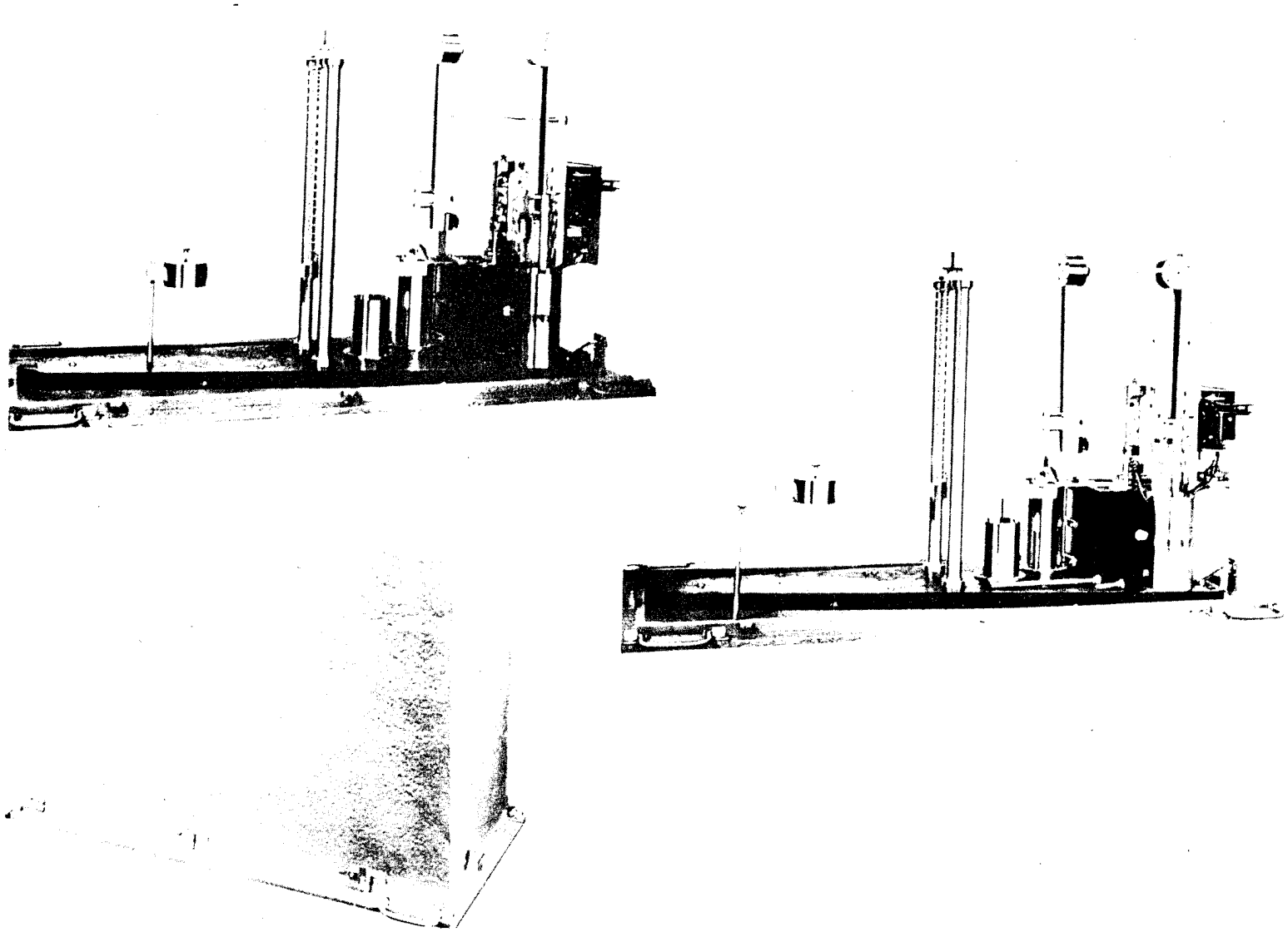

Figure 36. Views of seismograph.

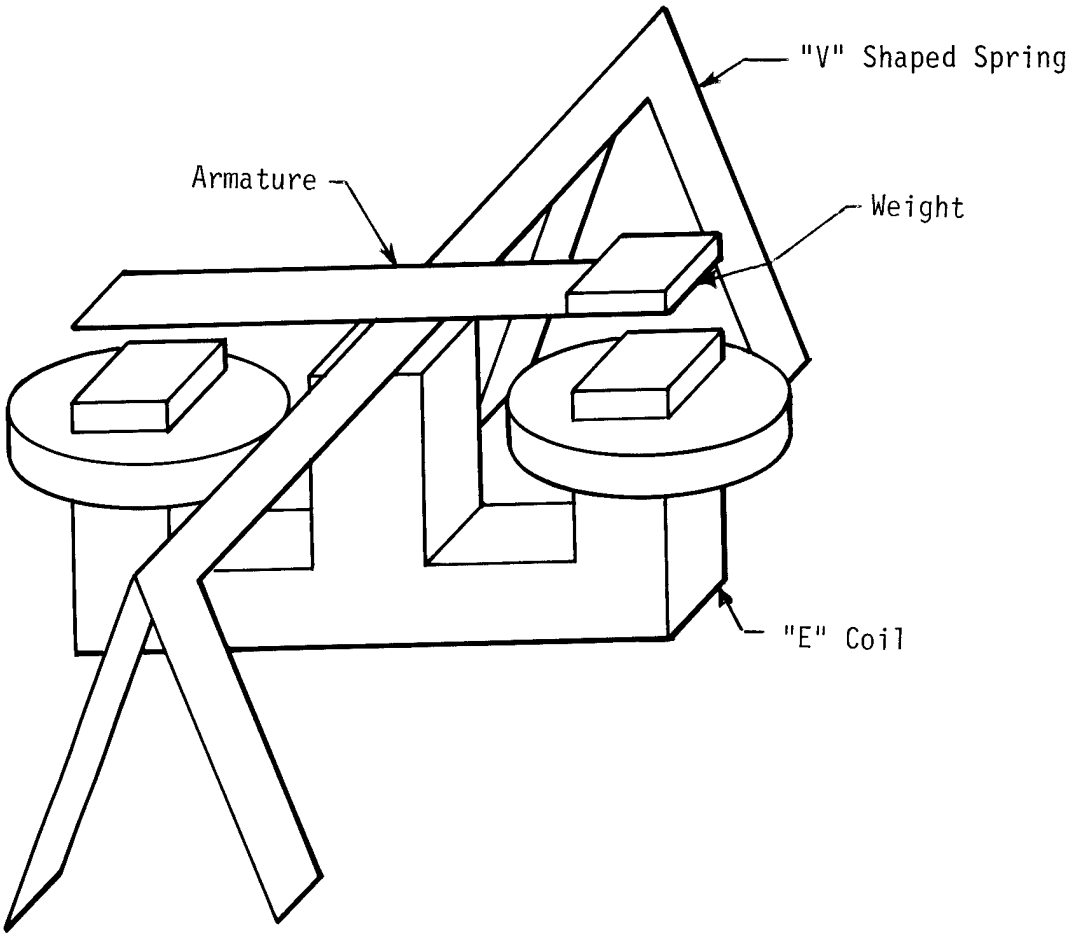

Figure 37. Schematic drawing of accelerometer spring mechanism.

armature causes unbalance in a full impedance bridge of which the windings of the "E" coil are a part. The bridge unbalance is proportional to the acceleration. The natural frequencies vary with range, i.e. a 5-g accelerometer has a natural frequency of 70 kHz; 100-g approximately 400 kHz. The gage system is damped by silicone oil which fills the chamber in which the system is mounted. Normal damping is 0.7 critical at 75°F. An extra-stiff mounting flange is provided, which permits screw-mounting directly on the member in which acceleration is being measured. The gage is mounted with its sensitive axis (the axis of the cylindrical gage case) parallel to the direction of the acceleration being measured.

A typical installation of a Wiancko accelerometer is shown in Figure 38. An acceleration record from a gage is presented in Figure 39.

Ref: Meszaros, J.J., et al., "Instrumentation of Structures for Air-Blast and Ground-Shock Effects," WT-1452, 1960

4.2.2 French Acceleration Gages (France) (1957).

The French acceleration gages of this era used a variable-reluctance sensor. A metallic seismic mass weighing approximately 0.01 oz (0.3 grams) is supported by two flexible silver diaphragms a few hundredths of a millimeter thick. This seismic mass acts as a core in the air gap between two identical transformers. The reluctance of the circuit changes as the movement of the mass causes a change in the relative dimensions of the air gaps in the transformers. This change in reluctance produces variations in the output of the secondary windings of the transformers. The algebraic sum of the voltages induced in the secondary windings is a function of the position of the magnetic core in the air gaps. The output voltage is rectified and fed to the recording system.

Two accelerometers used in an instrument group are shown in Figure 40.

Ref: Meszaros, J.J. and Schmidt, J.G., "Instrumentation of French Underground Shelters," WT-1535, 1961.

4.3 TIME MEASUREMENTS.

4.3.1 Sandia Panel-Time-of-Break (USA) (1950).

A panel-time-of-break was developed to obtain information regarding the order in which parts of a building fail. Its operation may be understood by reference to the schematic shown in Figure 41.

In the diagram, R represents a relay having a response time of 0.1 msec, that is held in a closed position by current from the storage battery in the main recording shelter. This current is caused to flow through conductors mounted on the panel whose time-of-break is to be determined. When the relays are closed, the 100K-ohm resistor constitutes one arm of a bridge, another arm of which is made up of parallel resistors 200K, 400K and 800K. The other two arms of the bridge are made up of the secondary of the power transformer which is center-tapped and across which is shunted a 300-ohm resistor with a 50-ohm potentiometer in series for balance. When a given panel breaks, severing the conductor mounted on it, the closed relay opens and unbalances the circuit by an amount depending

Figure 38. Typical installation of electronic accelerometer.

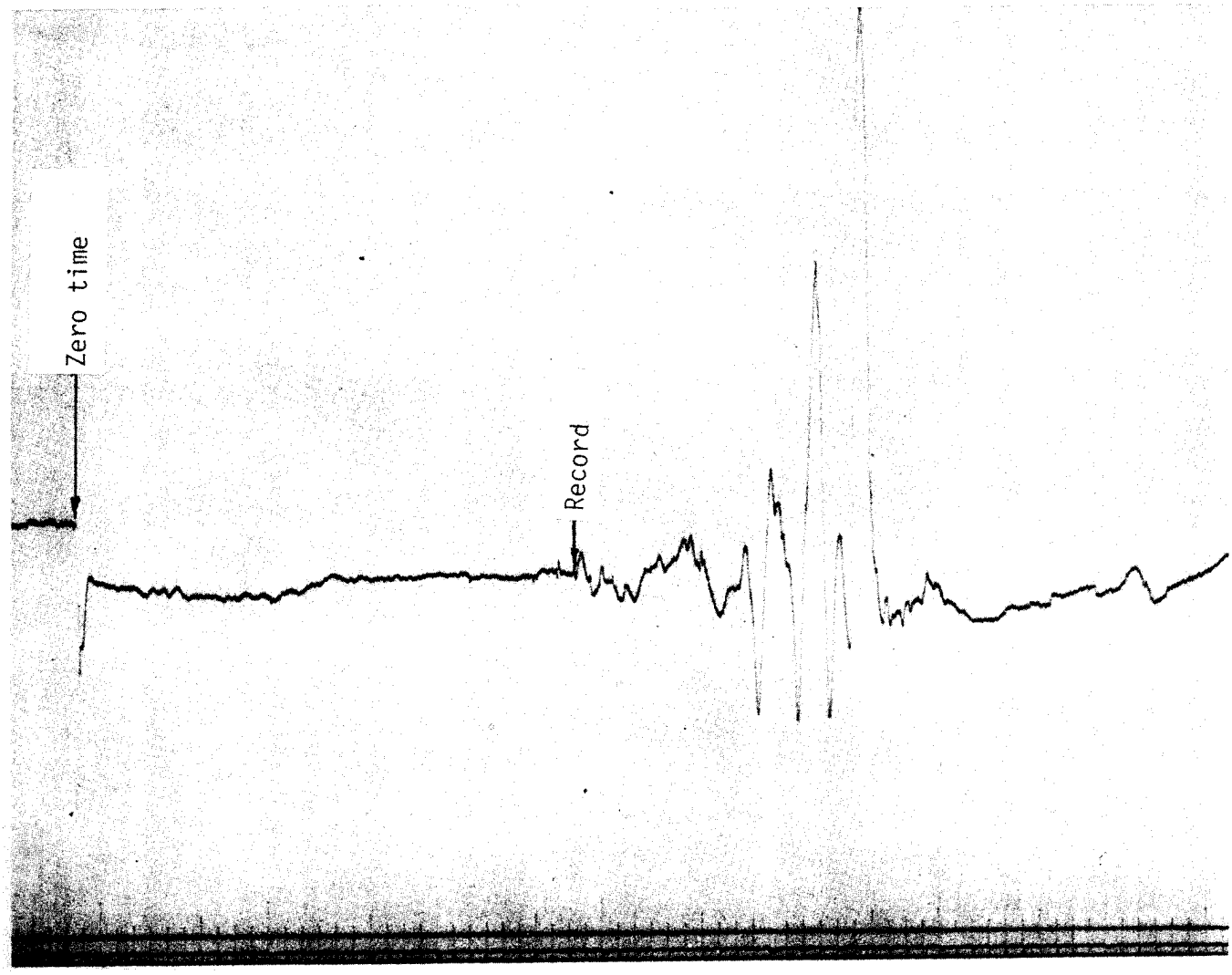

Figure 39. Acceleration versus time on floor of structure - Wiamcko accelerometer.

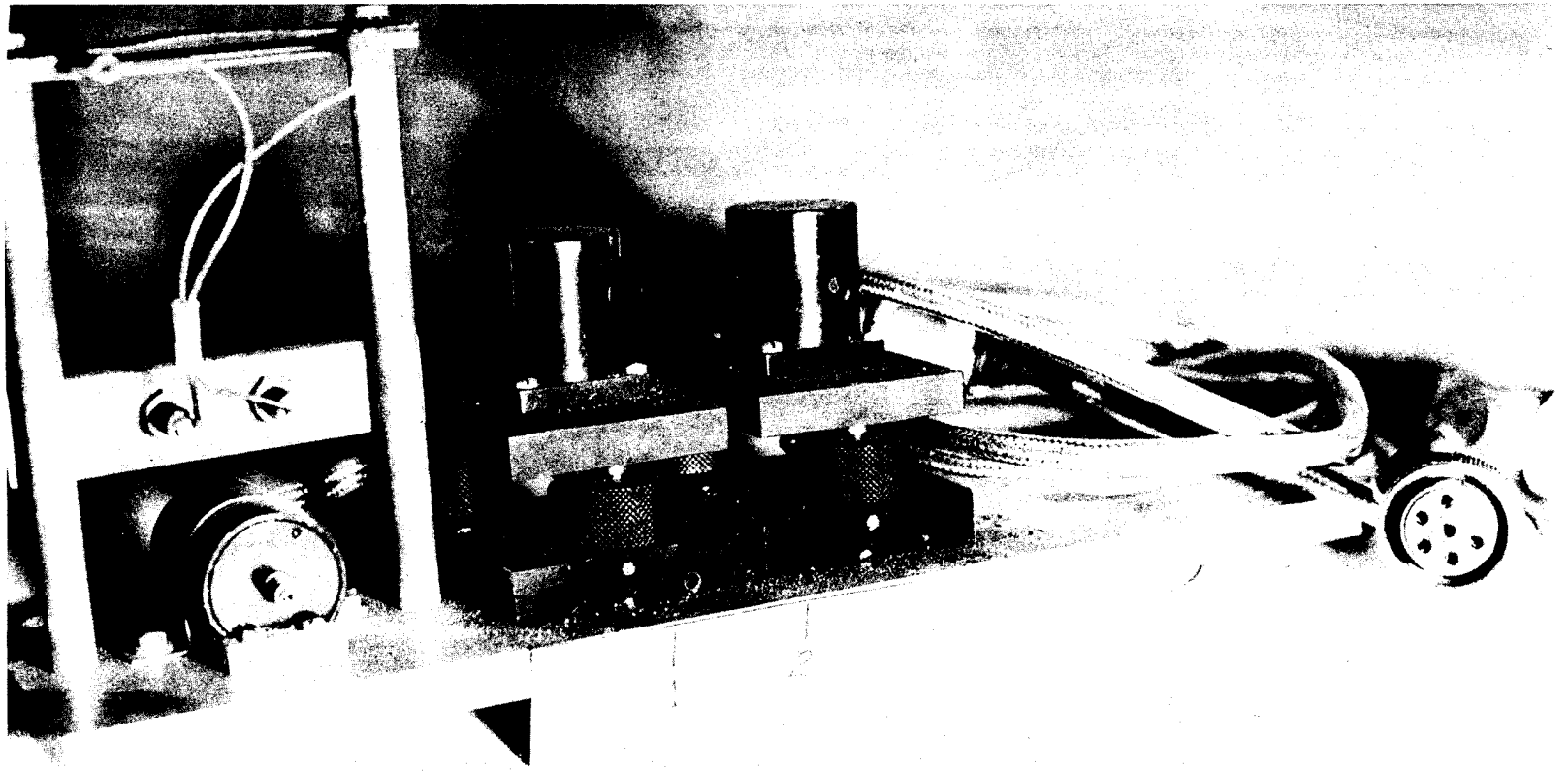

Figure 40. Instrument group consisting of two accelerometers, a resistance thermometer and a low-pressure gage.

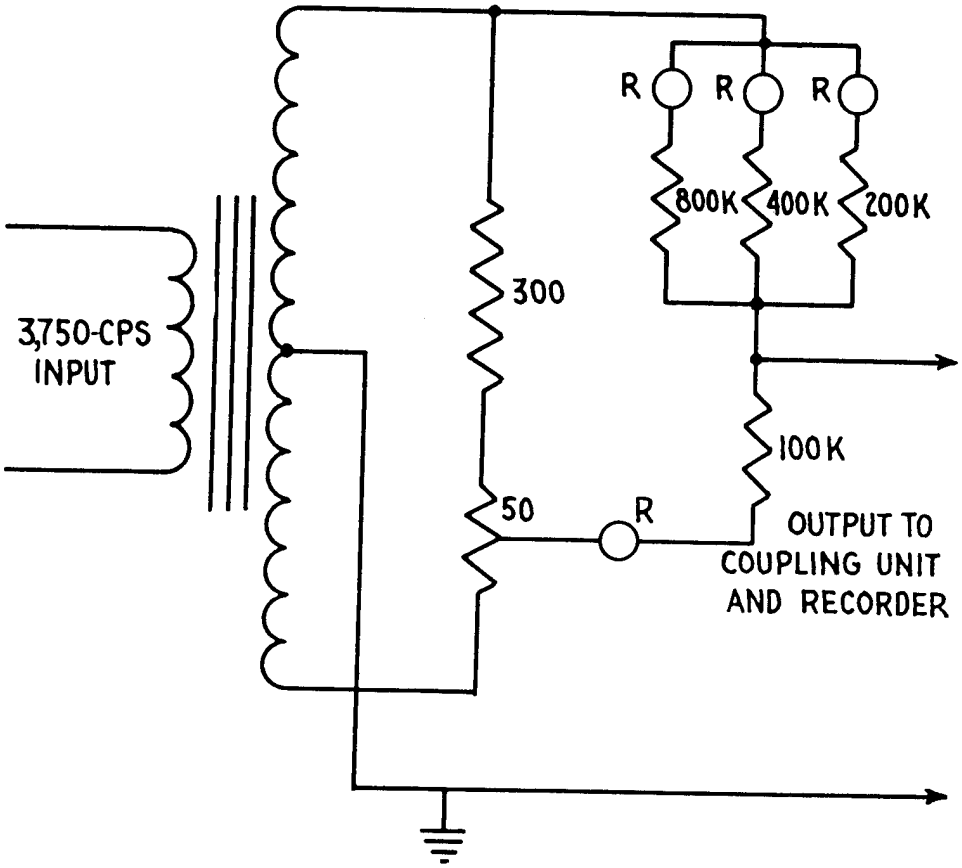

Figure 41. Schematic of panel-time-of-break circuit.

upon which resistor is open-circuited. Successive breaking of panels causes changes in the magnitude of the unbalanced signal which can be related to a particular resistor.

Values of the resistors in the panel-time-of-break equipment are chosen so that taking the signal due to the 800-ohm circuit opening as +1, the 400-ohm circuit upon opening, gives a relative signal of +2; the 200-ohm circuit, +4; and the 100-ohm circuit, +7. The circuits open at any moment can then be determined from the observed signal level. Thus each channel can give information about the behavior of four panels.

A finished panel-time-of-break unit is shown in Figure 42. The small instrument on the top is for testing and calibration. An installation of the panel-time-of-break is shown in Figure 43.

Ref: Northrop, Paul A., "Instrumentation for Structures Program," Part I. Operation GREENHOUSE, WT-1, 1951.

4.3.2 Sandia Stimascope (USA) (1950).

The Sandia Stimascope (Sound Time In Material Scope) was developed to measure the time required for a high-frequency pulse to travel between two points in concrete.

The Stimascope derives trigger pulses for the oscilloscope sweep, the ultrasonic transmitting transducer, and the time base for measuring the pulse transit time from one low-frequency oscillator. The transit time is determined by a blanking pulse which is adjusted to coincide with some part of the ultrasonic oscillations shown on the oscilloscope. The heart of the instrument is a 1000 Hz oscillator having an accuracy of 10 parts in 1,000,000.

A graphic description of the use of the Stimascope is presented in Figure 44. The upper curve shows the blanking pulse adjusted to coincide with the beginning of the received pulse when the transducers are in contact. In the middle curve is the delay during which the pulse is transmitted through a concrete slab. In the lower curve, the measurement of the travel time is shown by delaying the blanking pulse until the blanking pulse again coincides with the beginning of the received pulse. Figure 45 describes the operation of the Stimascope.

The oscillator output is divided in frequency, forming a symmetrical 500-Hz square wave that is used for three purposes: a 250-Hz square wave derived from the 500-Hz wave controls a saw-tooth generator producing the horizontal sweep on an oscilloscope; this 250-Hz square wave, after being delayed in a phantastron circuit, triggers a thyratron that supplies pulses to the transmitting transducer; and either the direct or an inverted 500-Hz square wave from the first frequency divider may be selected to initiate a blanking pulse. The phantastron circuit permits continuous control of the delay of the blanking pulse from zero to 1000 microseconds.

The transmitting transducer, excited by the thyratron pulses, produces recurrent series of damped ultrasonic oscillations having repetition frequencies of 250 series per second. The 4000-microsecond interval between pulses permits each series to fade sufficiently to avoid confusion with the following series. Each transducer uses 45°, x-cut Rochelle salt crystals having a frequency, when mounted, of approximately 100 Hz. The receiver contains four such crystals electrically paralleled; the transmitter has two crystals electrically paralleled. To provide good acoustic coupling between the crystals and the material under test, the

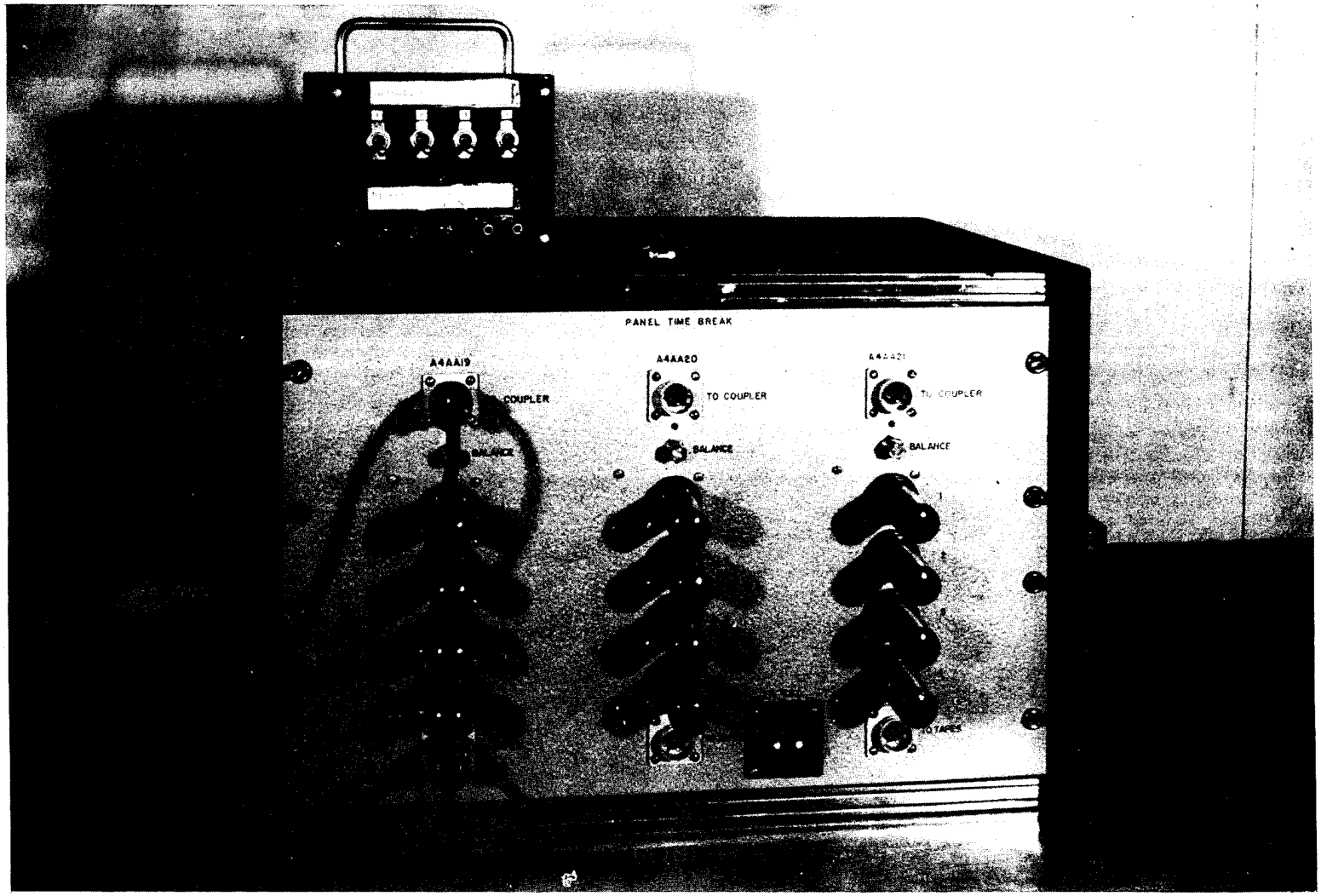

Figure 42. Finished panel-time-of-break unit.

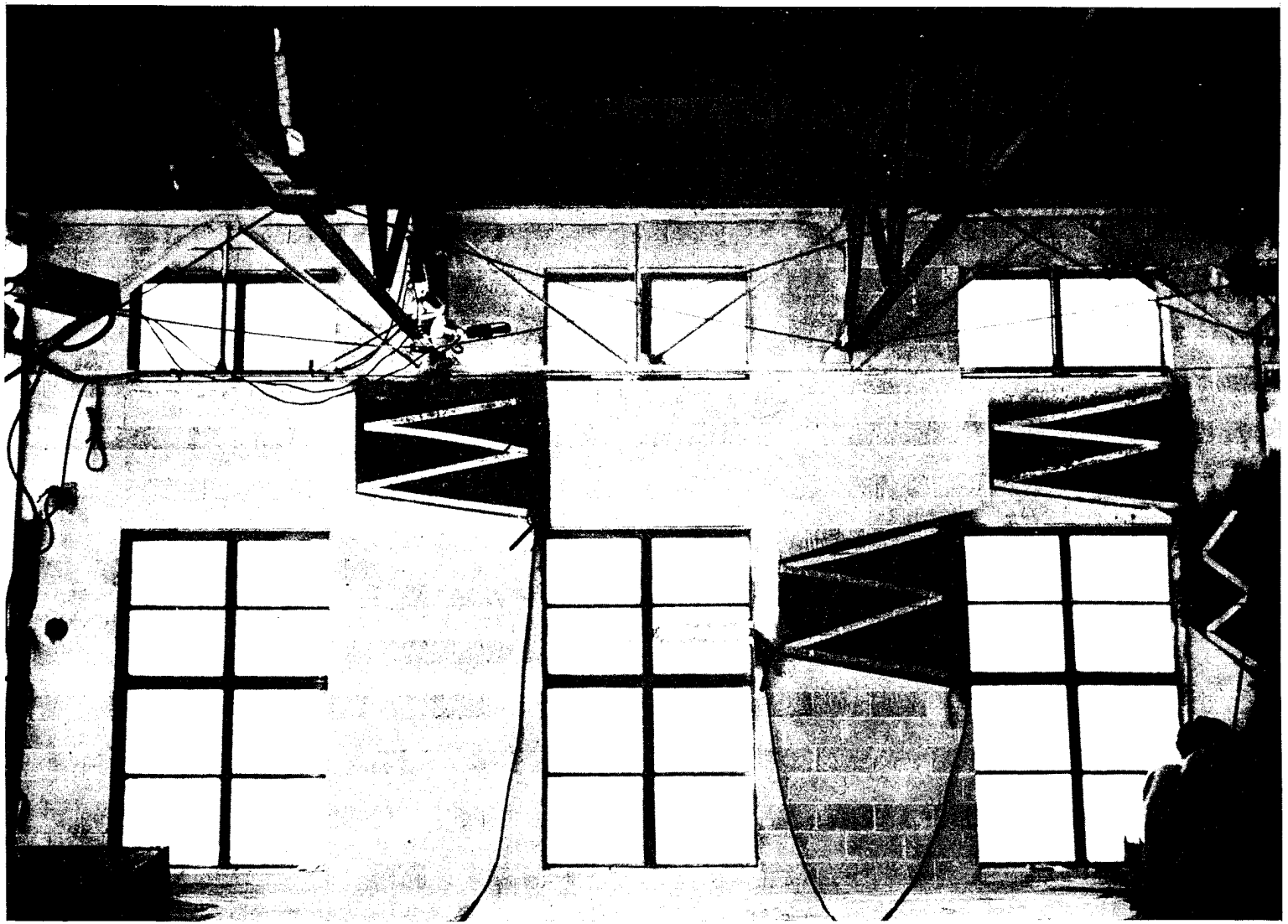

Figure 43. Group of four panel-time-of-break circuits requiring one Webster-Chicago channel for recording.

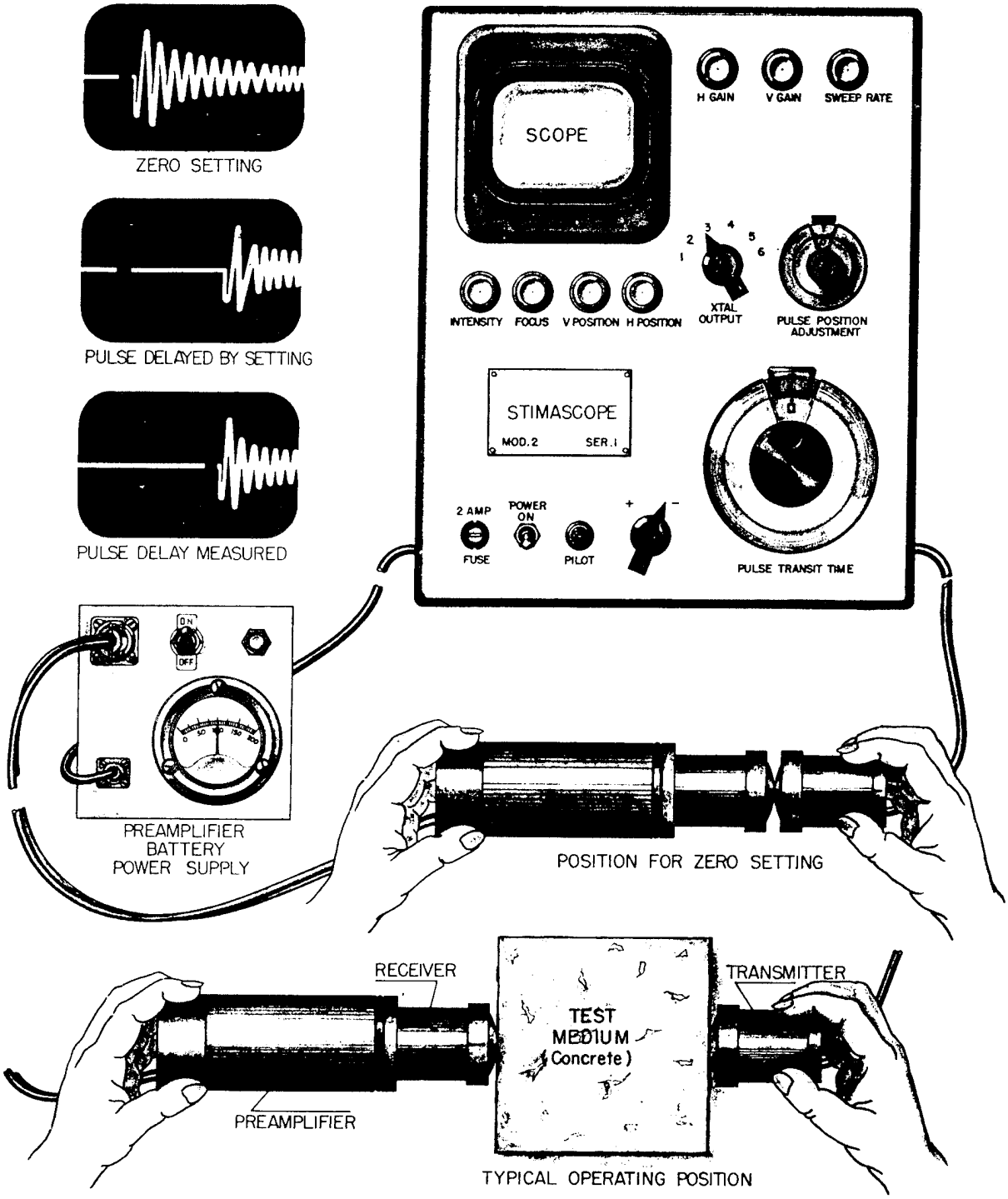

Figure 44. Use of Stimascope.

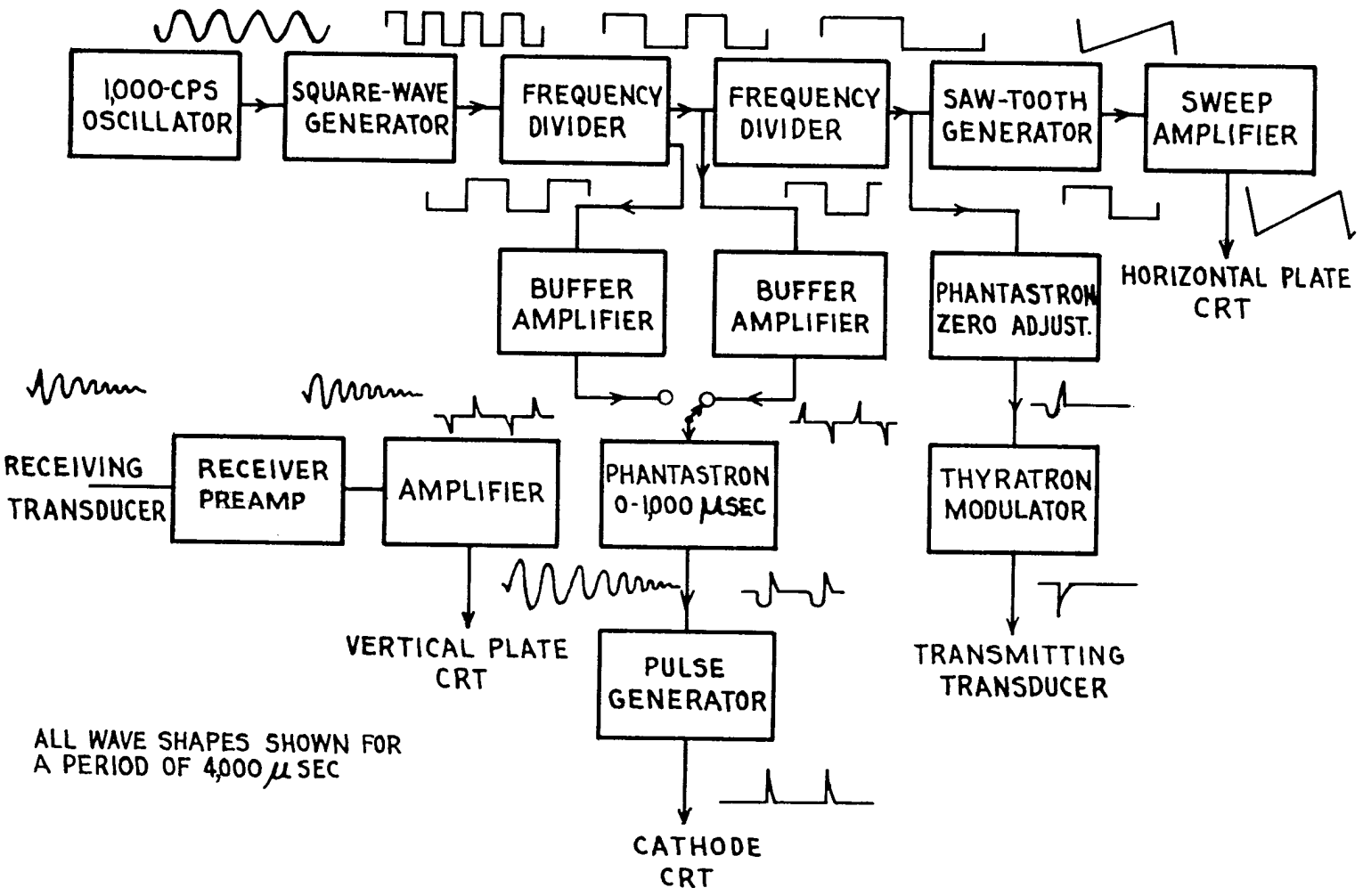

Figure 45. Mode of operation of Stimascope.

transducer is filled with an inert fluid under a low pressure. One end of the transducer is covered by a neoprene diaphragm which, because of the pressure in the transducer bulges outward, ensuring good contact between the transducer and the test surface. The receiver and transmitter are similar, except that a three-stage preamplifier is mounted on the receiver housing so that long cables may be connected from the receiver to the Stimascope.

Experiments indicated a need for some type of surface preparation if the material is porous. In early tests on concrete, water was used. However, water was absorbed into the concrete so rapidly that it was unsatisfactory. Now the surface is coated with any quick-drying liquid cement such as Duco, Walsco radio cement, General Cement Company radio cement, etc. When this has dried, a small amount of oil (castor oil, lubricating oil, etc.) is applied to the surface to couple the transducer diaphragm to the material.

Laboratory tests conducted at MIT to obtain information for interpreting data from the Stimascope show that the velocity of sound in concrete indicates the quality of the concrete.

The Stimascope system is shown in Figure 46.

Ref: Northrop, Paul A., "Instrumentation for Structures Program," Part I. Operation GREENHOUSE, WT-1, 1951.

4.3.3 Pressure Switches (USA) (1958).

Specially designed, normally-open pressure switches were used in a crushing mode to determine shock wave time-of-arrival and velocity data. The switches triggered a pulse generator whose output was presented on an oscilloscope, along with a crystal-controlled time reference signal, and photographed by means of a high-speed camera.

The switches were placed at known distances from the center of the burst and were sequentially crushed. Each switch had its own individual pulse generator which produced a characteristic pulse so that each switch could be identified on the film. The reference gives a complete description of the pulse system and coding used.

The major shortcoming of the pressure switch system was its susceptibility to multiple triggering. This phenomenon usually resulted from the alternate opening and shorting of the switch cables which occurred as the shock wave traveled along their length. In an installation requiring the use of cables several hundred feet in length, the number of extraneous pulses generated could easily be several times as great as the number of useful pulses and thus seriously complicate the analysis of data. A number of different electronic triggering systems have been devised to minimize the extraneous pulses.

Ref: Anderson, D.C. and Porzel, F.B., "Close-In Time-of-Arrival Measurements for Yield of Underground Shot Rainer," WT-1495, AD607,645, 1959.

4.3.4 Sandia Plexiglas Gage (USA) (1962).

Plexiglas was used by Sandia in a gage to measure shock velocity. Plexiglas serves as a matrix in which is embedded small PZT shock detectors, a double PZT ring is also used. The basic gage consists of a pair of PZT wafers 0.125 inches in diameter by 0.020 inches in

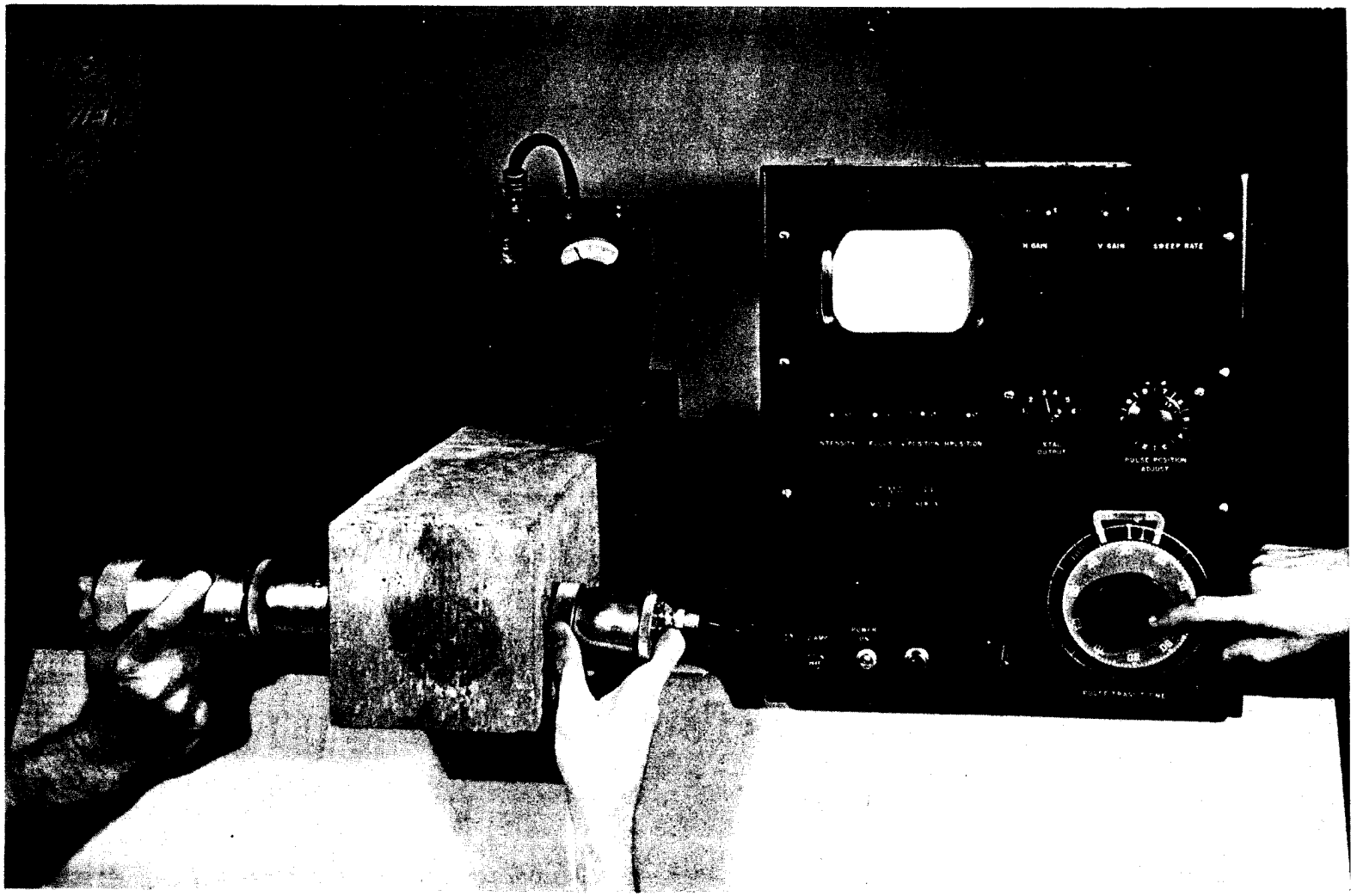

Figure 46. Stimascope system.

length separated by 2.23 inches of plexiglass. The equation-of-state of plexiglass is well known, so the time difference between the PZT signals indicates the shock velocity. They have obtained a pulse of 300 volts from the PZT rings at a pressure level of 150 kb, with a rise time of 1 microsecond. The output from this gage was recorded on a dual-beam oscilloscope (Tektronix 555) using the signal received from the front PZT wafer to trigger the scope sweep.

Ref: Chabai, A.J., "Close-In Phenomena of Buried Explosions," DASA-1382, 1963.

4.4 EARTH PRESSURE STRAIN.

4.4.1 Wiancko-Carlson Earth Pressure Gage (USA) (1953).

The earth pressure gage deployed in the 50s was developed by the Wiancko Engineering Company. This gage is a combination of the Carlson static stress meter and the Wiancko differential-inductor pickup and was known as the Wiancko-Carlson earth pressure gage. The sensing mechanism is formed by two flexible circular plates separated by a spring seal around their edges, see Figure 47. One of the plates is bored concentrically and the hole is covered by a flexible diaphragm flush with the outside surface of the plate. Thus, two adjoining chambers are created; one formed by the volume between the two circular plates and a smaller one formed by the volume of the drilled hole. The chambers are filled with fluid so that when pressure is applied squeezing the two plates together, the flexible diaphragm is bulged outward. This motion is coupled to an armature and causes it to move near an "E" coil of the type shown in Figure 48.

The bored plate is the base of the gage and is placed against the structure. As pressure is applied, the motions of the solid plate and the flexible diaphragm are in the same direction, but the amplitudes of their motions are in inverse proportion to their respective areas. In use, various mounting techniques can be used, but in all cases, provision must be made for allowing a solid flat surface for support of the gage base plate and an even distribution of pressure over the sensitive plate. A typical gage mounting technique used on certain buried structures on one of the tests is described in the following paragraph.

> "A hole the size of the housing for the gage sensing mechanism was cast in the wall of the structure. The gage was then set against the structure, with the sensing mechanism housing fitting into its hole and the base plate resting squarely on the structure surface. A length of pipe, threaded over the gage cable, was screwed into the sensing mechanism housing so that it extended through the hole to the inside of the structure. Over this pipe, in sequence, were placed a washer having a diameter greater than that of the hole through the wall, a helical spring and a nut which screwed on to the end of the pipe to compress the spring. The force produced in the compressed spring, then held the gage firmly against the outside surface of the wall. A fairing of grout was applied around the gage to smooth the contours of the installation. Sieved sand was packed over the face of the gage to give an even pressure distribution."

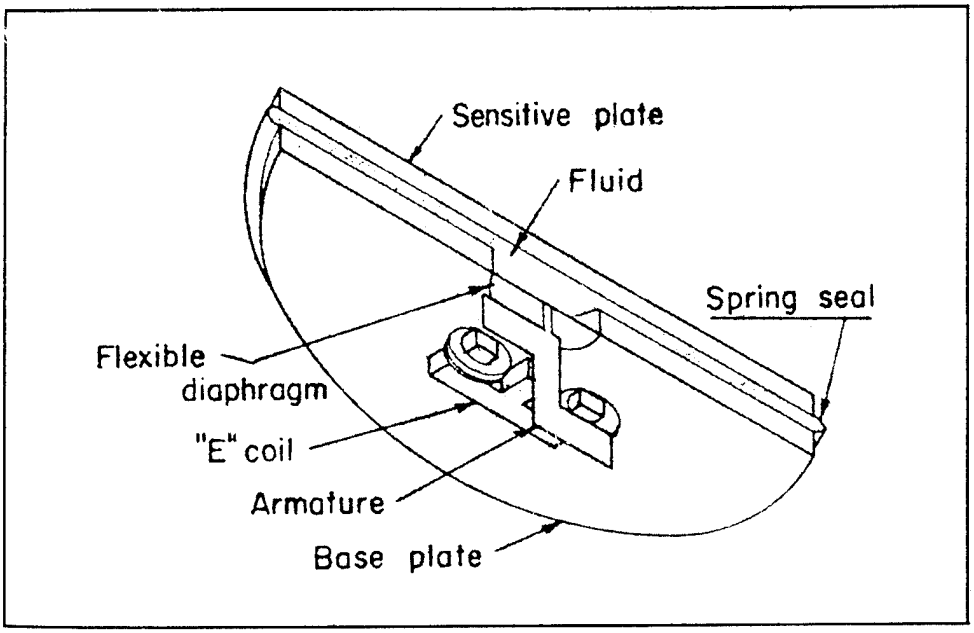

Figure 47. Schematic drawing of earth-pressure gage sensing mechanism.

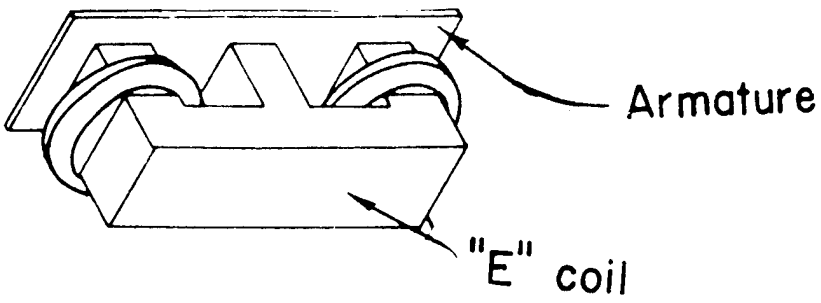

Figure 48. "E" coil for earth pressure gage.

A photograph of the gage is shown in Figure 49. A typical earth pressure record is shown in Figure 50. An accuracy of 10 percent is normally assumed for data obtained with these gages.

This gage was later modified in the 50s to take the Ultradyne diaphragm-type transducer (the Ultradyne pressure gage is described in Vol. I). Since the Ultradyne sensor is smaller in size, the overall gage could be made smaller. The gage was used for pressures above 300 psi.

Ref: Meszaros, J.J., et al., "Instrumentation of Structures for Air-Blast and Ground-Shock Effects," WT-1452, 1960.

4.4.2 French Earth Pressure Gage (France) (1957).

The French earth pressure gage is a potentiometer-type electronic device which uses a piston coupled to the wiper of the potentiometer as the pressure-sensitive element. The action of the piston is opposed by a spring. As the piston responds to pressure a change is recorded by the recording system. As used in 1957, the recording system was a galvanometer-oscillograph.

The earth pressure gage is shown in Figure 51.

Ref: Meszaros, J.J. and Schmidt J.G., "Instrumentation of French Underground Shelters," WT-1535, 1961.

4.4.3 Earth Strain Gage (USA) (1957).

Earth strain gages were designed as shown by the schematic in Figure 52. The gage consisted of a linear differential transformer which was used to measure the change in spacing between two anchors normally separated by 2 to 3 feet. One of the anchors held a light tubular rod which was attached to the movable core of the transformer and the other anchor supported the body of the transformer enclosed in a protective housing. The position of the transformer was adjusted after installation and before back filling. Shown in Figure 53 is the gage unassembled and in Figure 54 the gage installed.

Ref: Swift, L.M., "Ground Acceleration, Stress and Strain at High Incident Overpressures," WT-1404, 1960.

4.5 STRAIN-STRUCTURAL MEMBERS.

4.5.1 Strain Gages (USA) (1953).

In order to properly study the behavior of structures, the experimenter invariably reaches the point where dynamic strain measurements on structural members is essential. Certain requirements govern the choice of the strain gage to be used, these are: (a) reliability of operation; (b) ease of application; (c) ability to resist blast damage; and (d) correct electrical characteristics for the recording system to be used.

In general, the Baldwin SR-4 paper strain gage is the most widely used, and seems to adequately meet the above requirements. Protection is required, usually layers of felt and

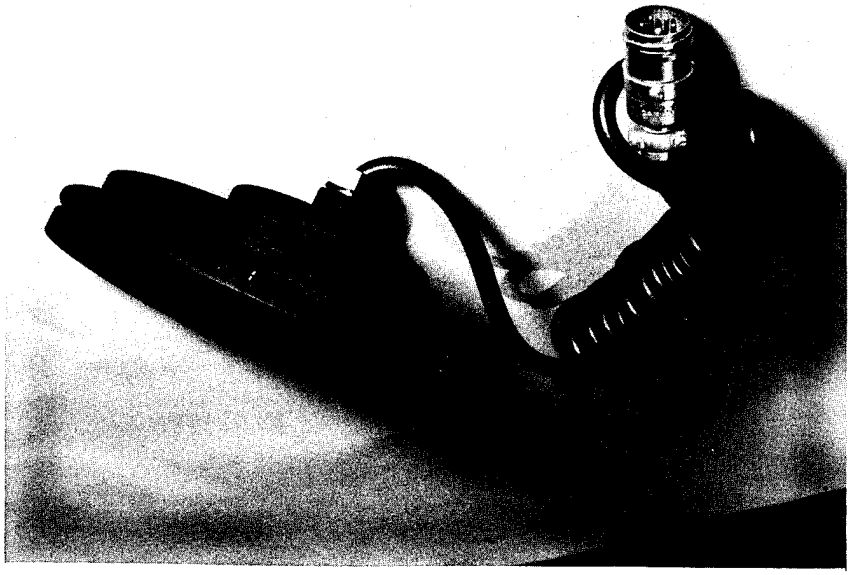

Figure 49. Wiancko-Carlson earth pressure gage.

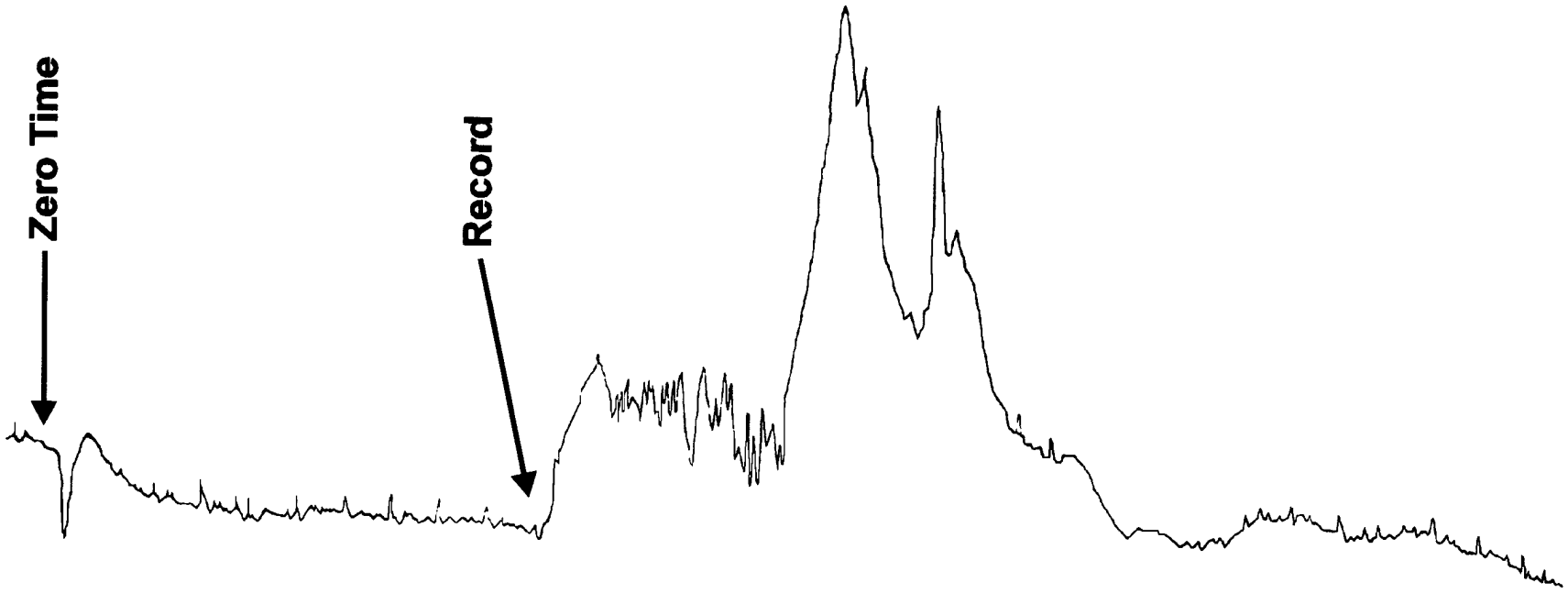

Figure 50. Earth presssure versus time on roof of buried structure.

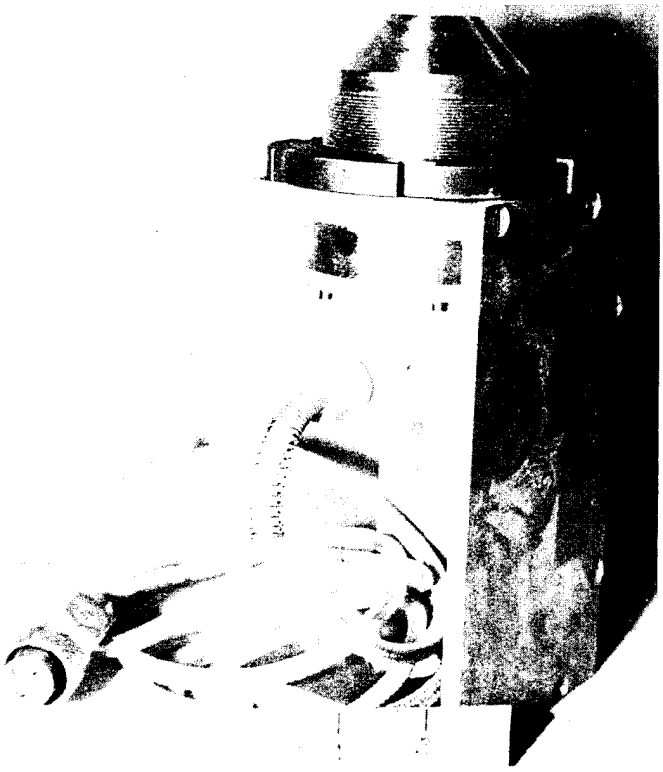

Figure 51. French earth pressure gage.

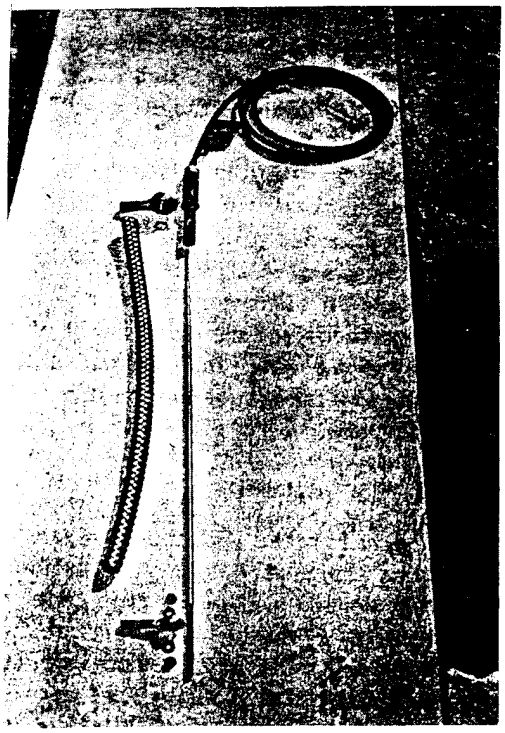

Figure 52. Earth strain gage, unassembled.

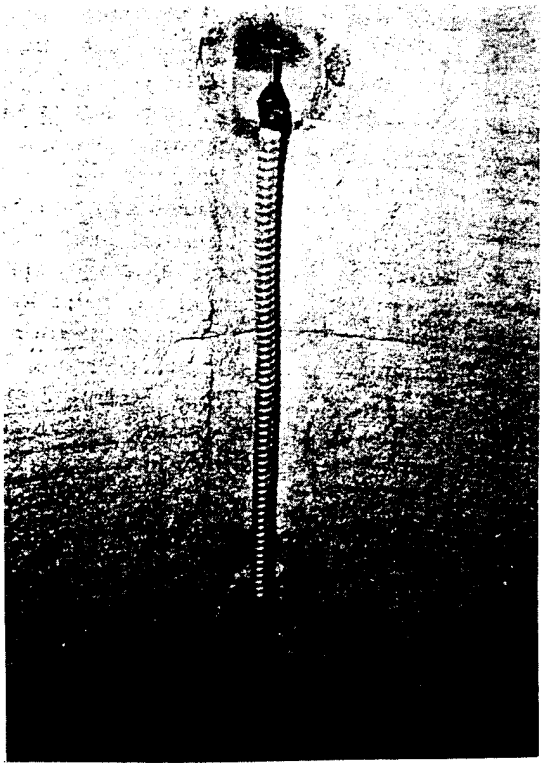

Figure 53. Earth strain gage, installed.

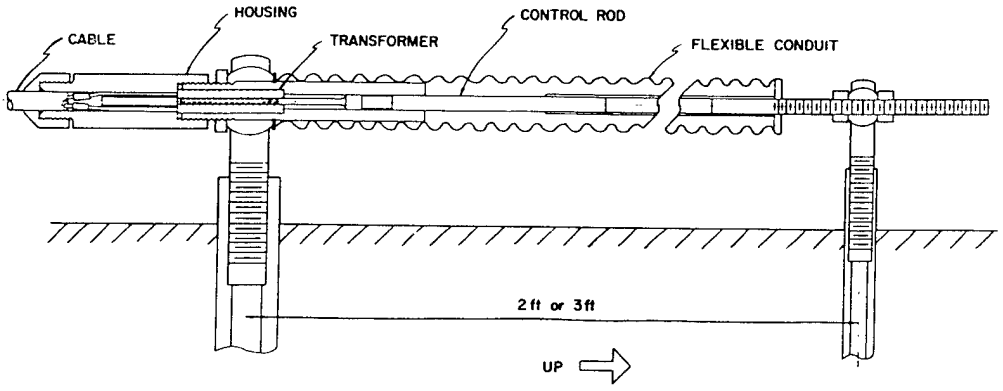

Figure 54. Schematic of earth strain gage.

aluminum foil, on all exposed positions. More than one hundred different types of gages are commercially available and the requirements imposed by any recording system or proposed use can be readily met. A description of the gage itself and its application to structures is not believed necessary. A difficulty in using this gage on nuclear operations is its susceptibility to break down by the large electro-magnetic signals picked up by the gage cable when the detonation takes place. The gages will withstand a voltage pulse of more than 1500 volts, if Armstrong A-1 cement is used. Care taken in grounding and the provision of a protection system will aid in reducing or completely alleviating gage losses. One system consists of using Western Electric spark gaps between the cable shield and ground. Gaps are available that breakdown at about 800 volts. One at each gage position will usually protect the gage from damage. The strain gage can be used as the sensing element for specialized instrumentation. In order to determine the transient drag characteristics of various shapes, actual and ideal, when subjected to air blast loading, the sensing mechanisms were designed for strain gage application.

To determine drag forces on actual structural components, sensors were designed supporting actual beam sections. The strains in the sensors were measured by SR-4 strain gages calibrated to read in terms of total force.

Typical strain gage installations are shown in Figure 55.

Ref: Meszaros, J.J. and Randall, J.I., "Structures Instrumentation, Operation UPSHOT-KNOTHOLE, Project 3.28.1," WT-738, 1955.

4.5.2 Strain Gages (France) (1957).

Strain gages were used to measure strain in steel members and in concrete sections. The gages were of the resistance type. For the steel members the gages had a gage constant K of 2.01 $\pm$ 1 percent and a resistance of 119.1 ($\pm$ 0.22 percent) ohms. The concrete gages had a resistance of 119.8 ohms and a gage constant of K = 2.22. All gages were used in a bridge circuit where the input current is 1000 Hz. The unbalancing of the bridge circuit as a result of the force exerted upon the unit causes modulation of the current. The modulated signal is amplified into a recording unit.

Preparation of the surface of structural elements for the mounting of strain gages is very important. Grinding of steel elements followed by polishing with emory paper prepares the steel for the installation of the gage. Cleaning of the steel with acetone is the final step in the surface preparation. The surface of the concrete to which concrete strain gages are to be attached was ground with an electrical sander, then polished with successively finer grades of sandpaper. The smoothed surface was cleaned with acetone and the gage was cemented with Araldite, a special cement designed for use with concrete strain gages, to the concrete slab. Curing of cemented gages was done with infrared lamps.

Photographs of installed gages are shown in Figures 56 and 57.

Ref: Meszaros, J.J. and Schmidt, J.G., "Instrumentation of French Underground Shelters," WT-1535, 1961.

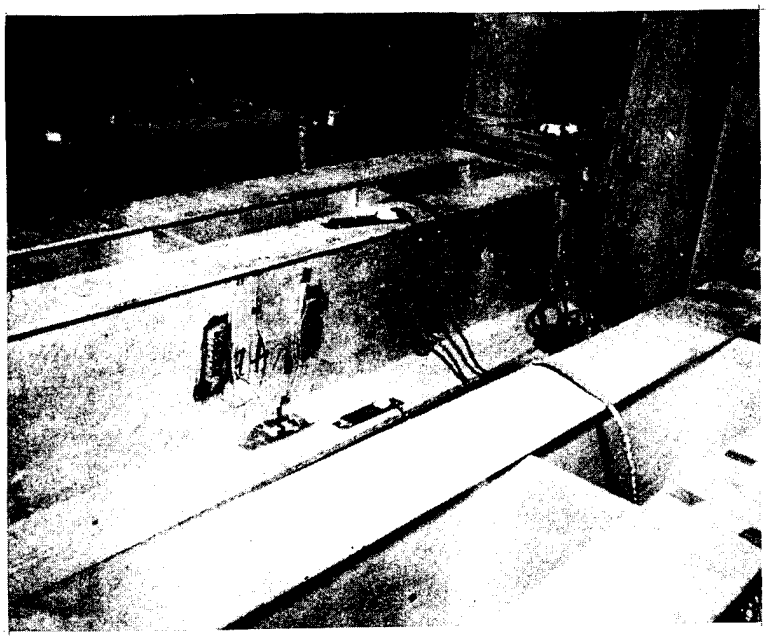

a. Installation on horizontal structure members.

b. Installation on column of test structure.

Figure 55. Strain gage installations.

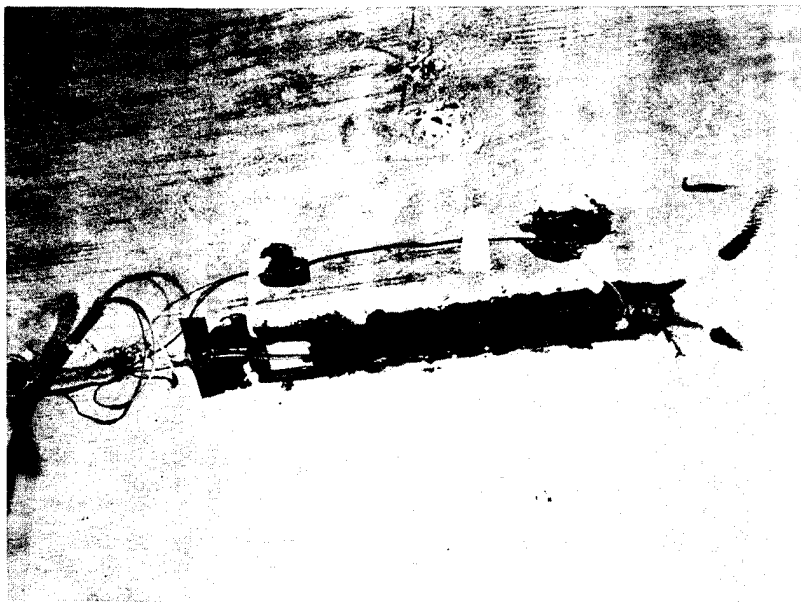

Figure 56. Concrete strain gage installed on ceiling of structure.

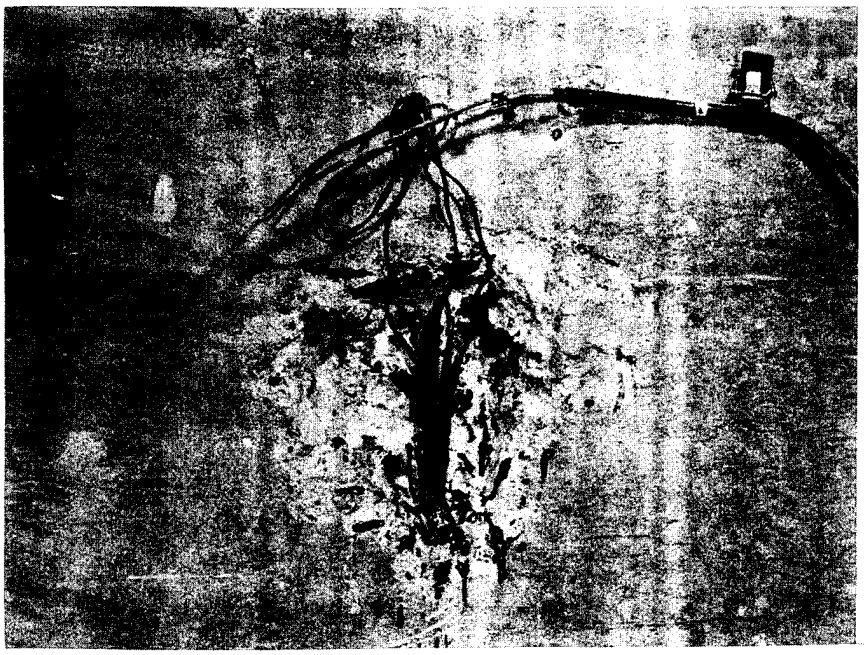

Figure 57. Strain gage installed on vertical reinforcing bar, north wall of structure.

4.6 Recording Systems.

Recording systems used to record the signals from the electronic gages were the same as those used to record from pressure gages in the free field. These systems are described in Sections 4.10, 4.11, and 4.12 of Volume I, "Measurement Techniques and Instrumentation - The Nuclear Era, 1945-1963."

SECTION 5

NON-ELECTRONIC STRUCTURAL - HE TESTING

5.1 DISPLACEMENT-SENSITIVE DEVICES.

5.1.1 Oak Ridge Peak Displacement Gage (USA) (1973).

Oak Ridge National Laboratory improvised a peak beam deflection gage to measure the maximum and the permanent deflections of shelter roofs and of a blast door. A steel base was set up to hold five fixed nails of varying lengths as shown in Figure 58 and nailed to the structural member of interest. A 0.005-inch aluminum foil was epoxied over a 1 x 3 1/2-inch slot cut in the end of a 4-inch diameter can. The can was firmly attached to a firm base independent of the structure, i.e. a post fixed in the ground directly below the nails on a hard rock base. The can-post was located at such a height that before the shot the longest fixed nail was almost touching the aluminum foil.

At blast loading the nails are forced downward and puncture the foil; the maximum and permanent deflection are readily obtained. To determine the maximum deflection, the number of nail holes punched in the foil and the diameter of the hole punched by the shortest nail are noted. Deflections were determined with an accuracy ranging from 1/16 inch to 3/8 inch. Permanent deflections were determined by observing the depth of final penetration of the nails into the foil.

Ref: Kearny, C.H. and Chester, C.V., "Blast Tests of Expedient Shelters," ORNL-4905, Oak Ridge National Laboratory, 1974.

5.1.2 NCEL Deflection Gage (USA) (1963).

Deflection of the inside surface at the mid-length of a cylinder was made with scribes spaced at intervals around the circumference. A round sheet of plastic, mounted on a bicycle wheel, was mounted so that it came into contact with the scribes. A thin coating of machinists blueing was painted on the plastic so that the scribes would etch a visible line whenever they moved in relation to the plastic. A motor turned the bicycle wheel at 3 rps, thereby giving a timed history of the cylinder's deflection.

Ref: Allgood, J.R., "Response of Buried Cylinders in the Near Crater Region," Operation DISTANT PLAIN, DASA 1876-4, 1968.

5.1.3 DRES Spring-Mounted Scratch Gage (Canada) (1969).

The DRES spring-mounted scratch gage was designed to record the deflection of the membrane in a support kit overhead protection (SKOP) trench cover. Shown in Figure 59, it was spring-mounted to record the upward and downward deflection of the membrane at the middle of the cover between the third and fourth support ropes.

Ref: Jones, W.A. and Munro, S., "Field Test of Army SKOP Shelter," Event DIAL PACK Symposium Report, Vol. II, Defence Research Board of Canada, 1971.

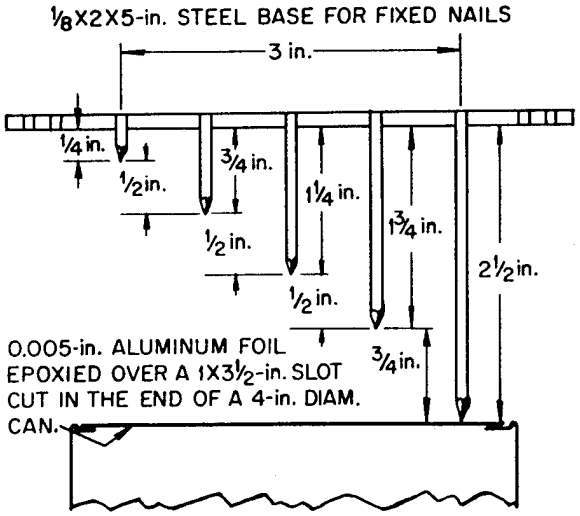

Figure 58. Improvised beam-deflection gage.

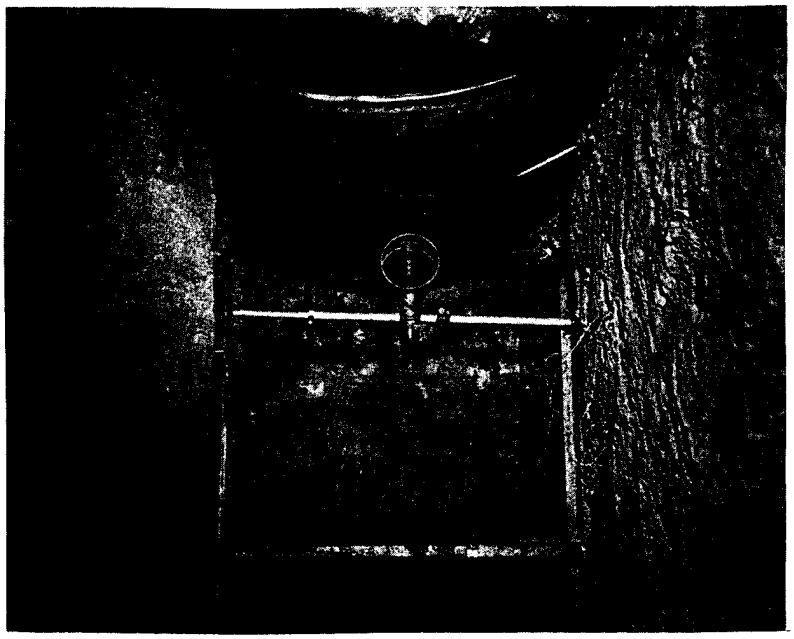

Figure 59. Scratch gage deflection system.

5.1.4 Boeing Differential Motion Scratch Gage (USA) (1969).

The Boeing differential motion scratch gage was designed to measure the relative displacement of the foundation of a hardened antenna structure and the soil media. The gage incorporated a spring-loaded pointer installed in the structures foundation and a scratch plate which was designed to move with the soil. The gage is illustrated and shown in Figure 60. The purpose of the measurement was to determine relative structural motion.

Ref. Averill, R.L., et al., "Hardened Radar Antenna Structural Response Investigation," Event DIAL PACK Symposium Report, Vol. II, Defence Research Board of Canada, 1971.

5.1.5 Swedish Passive Deflection Gage (Sweden) (1991).

The Swedish passive deflection gage consisted of a small-diameter telescoping rod with a small rubber grommet which responds to displacement. The gage was used to measure permanent deflections of the front wall, the side walls, and the roof. From the displacement of the rubber piece, the maximum displacement can be obtained. A post-test view of the gage is shown in Figure 61.

Ref: Vretblad, Bengt E., "Ground Shock Test of SST4 Shelters," DISTANT IMAGE Symposium Report, POR7379-4, 1992.

5.1.6 Slope Indicator (USA) (1964).

A slope indicator, called a mouse, which consists of a simple pendulum with electrical contacts for determining the pendulum position, is lowered into the casing to define the slope of various sections of the cased hole both before and after the blast. The casing is constructed in such a manner that each 2-foot section can partially telescope to offset the effects of the ground motion.

Ref: Rowland, R.H., "Blast and Shock Measurement State-of-the-Art Review," DASA-1986, 1967.

5.1.7 Scratch and Contact Gages (USA) (1964).

A tube coated with machinists' bluing is placed inside the casing and anchored to the bottom of the hole. A scribe on the casing responds to the ground motion, marking the inner tube. After the test, the inner tube is rotated, so as not to obscure the scribe marks of the transient motion, and removed to expose the record of peak transient displacement. The method is relatively cheap and reliable but poor in accuracy, and of course, gives no time histories. The tube must survive the ground motion.

A similar gage in principle was used in Army shelters as illustrated in Figure 62a. It shows a rod scratch gage attached to the wall and reference frame. The gage consists of a 3/4-inch (19-mm) diameter aluminum rod, painted with machinists' bluing, which is attached to the wall by a pin coupling. The rod passes through a guide hole in a small aluminum bar attached to the reference frame. Double-toothed spring metal scribes ride on opposite sides of the rod,

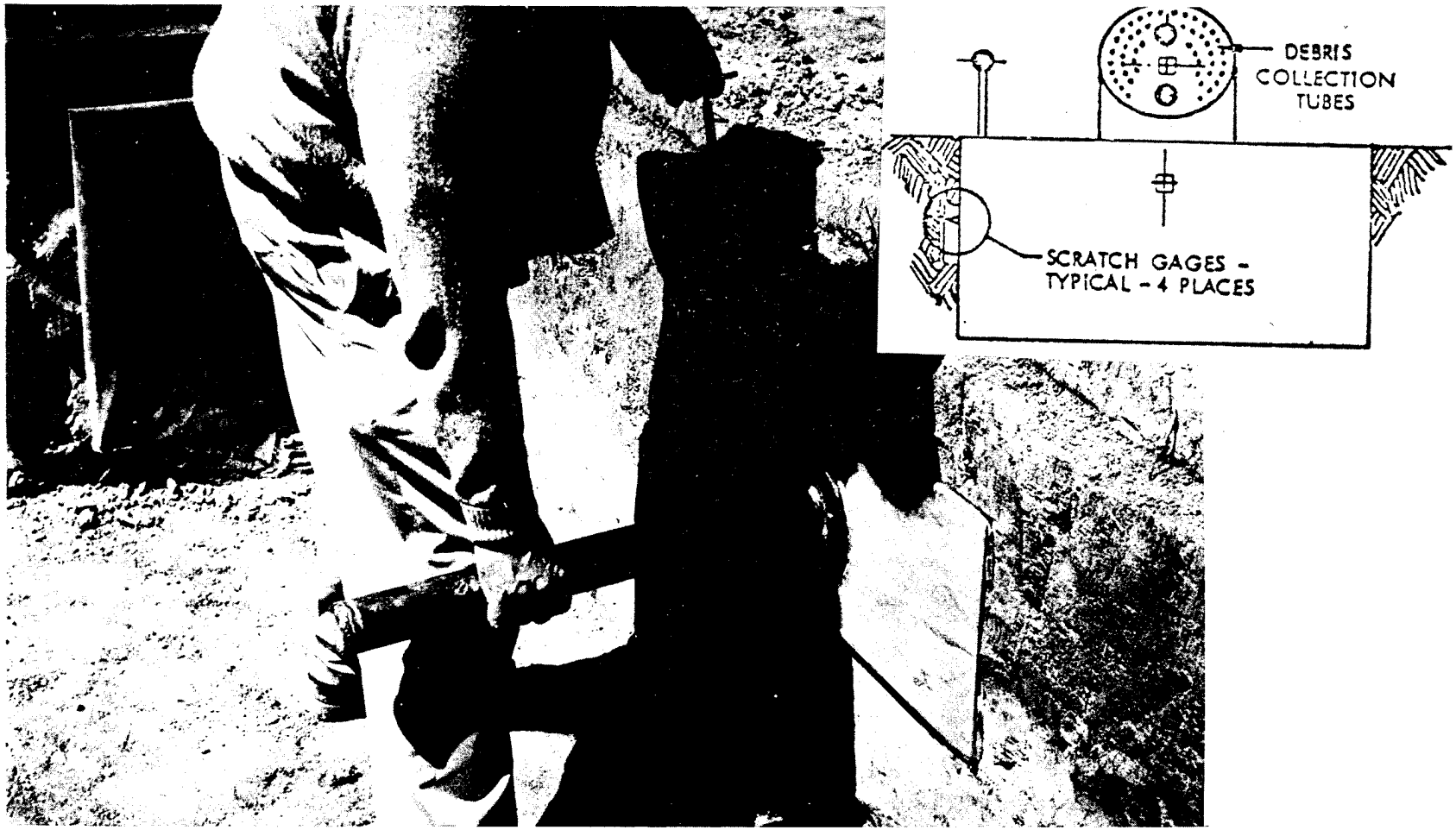

Figure 60. Differential motion scratch gage prior to installation in structure.

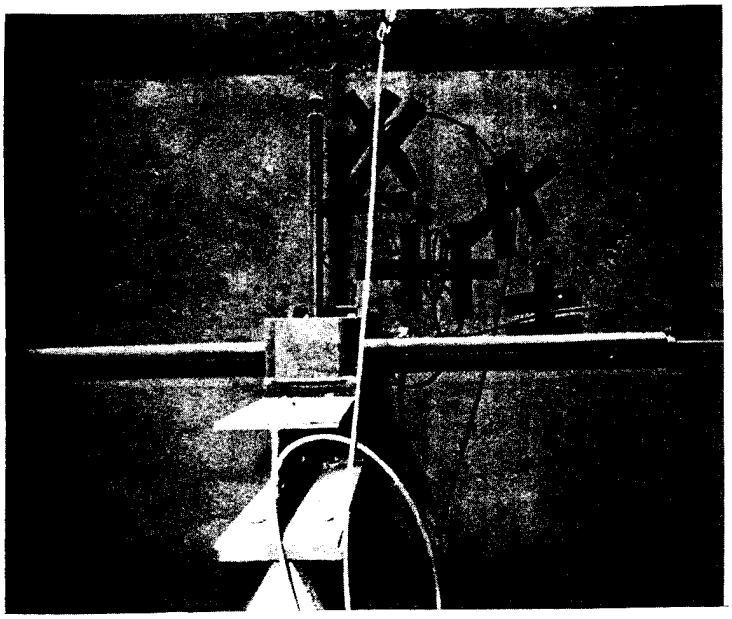

Figure 61. Passive deflection gage.

a. Rod scratch recording peak displacement gage.

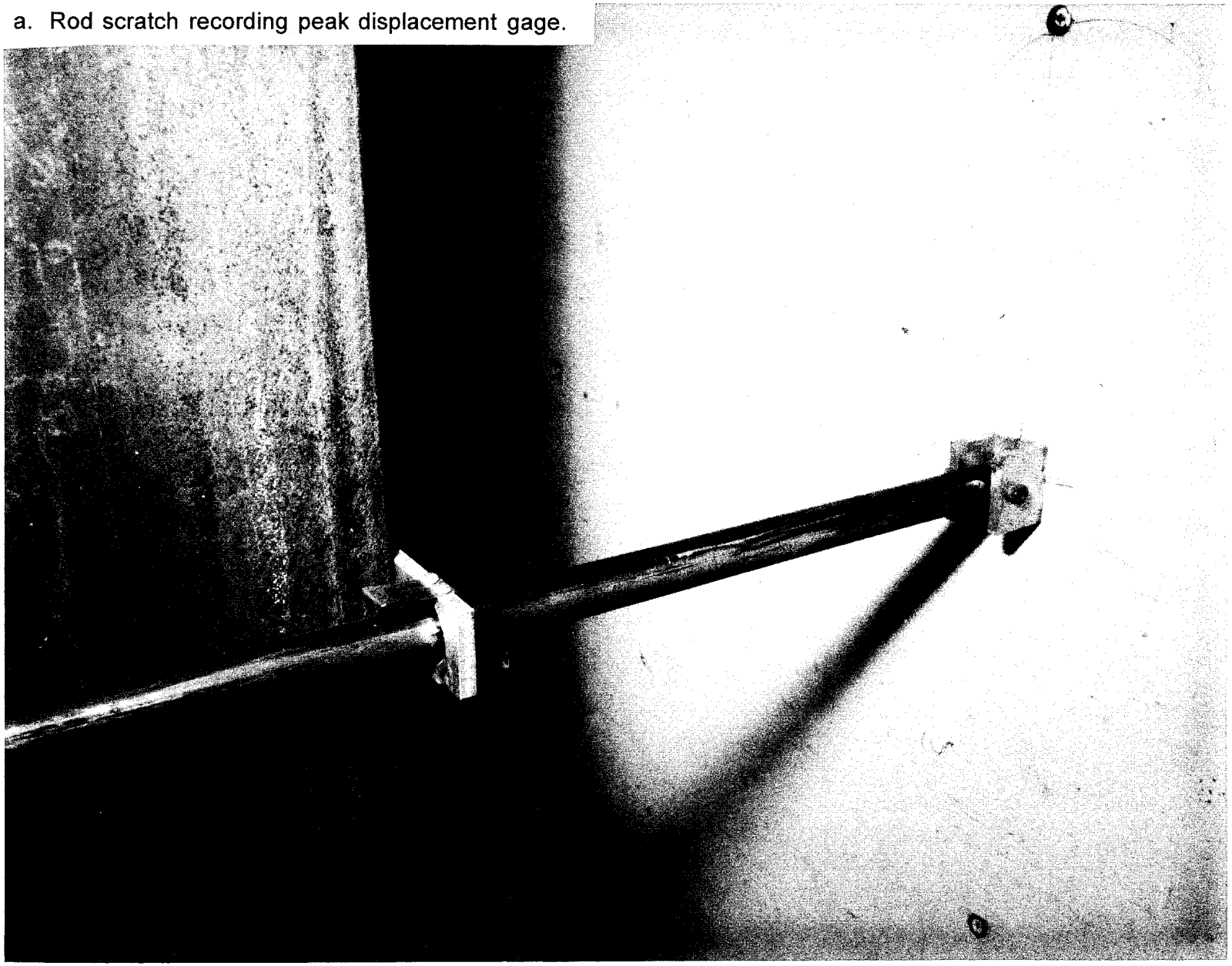

Figure 62. Passive displacement gages used in shelters.

and mark maximum inward and maximum outward movement of the rod through the guide hole. The gage provides readings of rod movement with an error of 1/32 inches (0.8 mm).

Arrays of contact registration displacement gages as well as rod scratch gages were deployed on tests with Army vans. Gages of both types are shown in Figure 62b. The contact registration displacement gages were made of thin strips of sheet balsa wood of lengths differing by 0.5 inches (12.7 mm). The strips were glued alternately to each side of a length of wood with a cross-section of 1/2 inch by 3/4 inch (12.7 mm by 19 mm). In case a strip should bend and not break when struck by a panel, each strip was tipped with a red marking material configured to indicate if contact occurred, and to mark the contacting surface. Lipstick was used as the marking material.

The manufacture of the gages was simple but tedious. The gages were fastened to the channel iron gage mount with glass fiber tape. The distance of the base of each gage array from the roof or wall was measured. The location of the perpendicular projection of each tip to the roof or wall was marked so that any displacement of the surface at the time of contact could be noted. With length increments of 0.5 inches (12.7 mm), peak displacements were measured with an error of $\pm$ 0.25 inches (6.4 mm).

Ref: Seknicka, A.J., "Measurement of Permanent Horizontal and Vertical Ground Motion," Operation SNOWBALL Symposium Proceedings, Vol. I, DASA-1642-1, 1965.

Ethridge, N.H., et al., "Blast Response of Electronic Van Semi-Trailers (M348A2)," Proceedings of the MILL RACE Preliminary Results Symposium, Vol III, POR 7073-3, 1982.

5.1.8 TRW Reed Gage (USA) (1965).

The TRW reed gage is a peak-reading shock spectra gage. The gage has a number of masses on cantilever springs or reeds mounted on a rigid base. The masses and spring constants of the reeds are such that their natural frequencies cover the range 2 to 300 Hz. For higher levels of shock, the gage uses ten nominal reed frequencies of 3, 10, 20, 40, 80, 120, 160, 200, 250, and 300 Hz. For lower levels, the gage uses eight nominal frequencies of 2, 3, 5, 10, 20, 40, 80, and 120 Hz.

The masses have scribers which are in contact with a polished record plate coated with lamp black. When the gage base is subjected to shock, the displacement of the reed is recorded on the record plate. Following the test, the measurements are converted to mass displacements by use of calibration factors.

The TRW reed gage is shown in Figure 63. The gage may be positioned in such a manner as to record either vertical or horizontal motion.

Ref: Rowland, R.H., "Blast and Shock Measurement State-of-the-Art Review," DASA 1986, 1967.

Pieper, F.A. and Galbraith, F.W., "Ground Shock Spectrum Measurements," WT-4054, 1966.

b. Contact registration displacement gages.

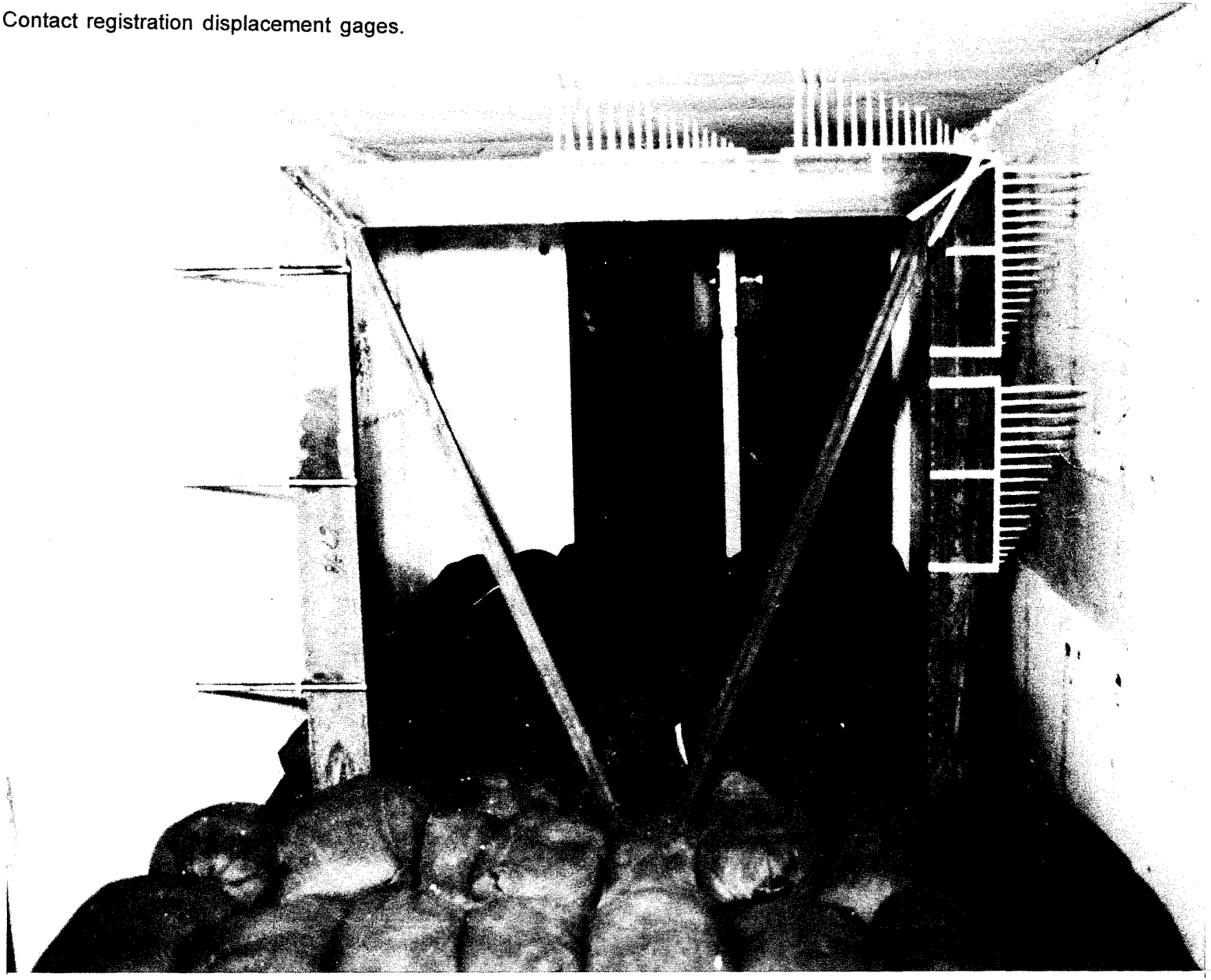

Figure 62. Passive displacement gages used in shelters (Continued).

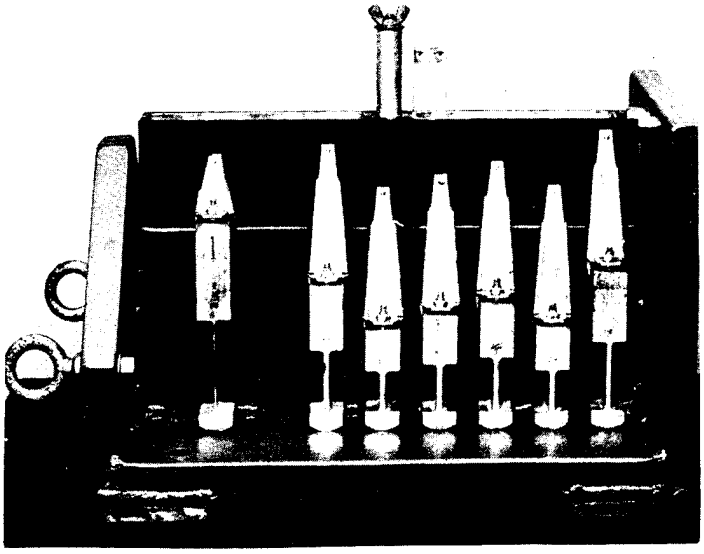

Figure 63. TRW reed gage.

5.1.9 Boeing Passive Soil Stress Gage (USA) (1968).

The Boeing soil stress gage consisted of crushable foam blocks designed to give an estimate of free-field stress. The blocks are shown in Figure 64. The strength of each block was selected to crush if soil pressures exceeded a certain level. Relative displacements were also measured with wires connected to each block and slip gages designed in the block.

Ref: Averill, R.L., et al., "Hardened Radar Antenna Structural Response Investigation," Event DIAL PACK Symposium Report, Vol. II, Defence Research Board of Canada, 1971.

5.2 PRESSURE SENSITIVE DEVICES.

5.2.1 UCRL Pin Gage (USA) (1965).

UCRL has modified a pin gage, originally designed for laboratory measurements, to obtain field data. Small electrical contactors, or pins, are placed at accurately measured positions within and near the upper surface of an aluminum block located at the bottom of the gage and oriented toward the direction of shock propagation, see Figure 65. The time sequence of pin closures is recorded, yielding both shock and free-surface velocities. Since it has been shown that to a good approximation the free surface velocity is just twice the particle velocity, the peak pressure in the aluminum may be calculated. If the shock compression curve of the medium is known, graphical mismatch calculations can be used to calculate a medium pressure. It should be noted that the free-surface information is actually not required since the relation between shock and particle velocity is well known for aluminum. This redundancy is nevertheless desirable in a field instrument. Peak pressures from nuclear detonations in granite and volcanic tuff have been successfully measured with this gage.

Variations of this gage exist where the aluminum is replaced by salt, the medium being measured, in order to reduce the complexity of the calculations. (The gage must be adequately coupled to the medium.)

Ref: Holzer, F., "Measurements and Calculations of Peak Shock Wave Parameters from Underground Nuclear Detonations," Journal of Geophysics Research, 70, 4, 893, 1965.

5.2.2 UCRL Peak-Pressure Plastic Gage (USA) (1965).

The UCRL peak-pressure plastic gage is shown schematically in Figure 66. A 30-mil thick Lucite shell is coated on both sides with a conducting silver paint, which also forms the ground connection to the cable shield. The Lucite globe is filled with epoxy for increased mechanical strength. When a stress front traverses the thin wall of the gage, a current whose amplitude is proportional to the peak stress flows through a load resistor connected to the inner and outer surface. It is postulated that, since the lighter components of a molecule have higher mobilities, the passage of a shock will preferentially align the molecules in the direction of the shock travel. For materials whose molecules have a permanent dipole moment, the charge liberated varies linearly with the peak stress over a region bounded by a threshold pressure and a saturation value. It is linear over the stress range, which is 50

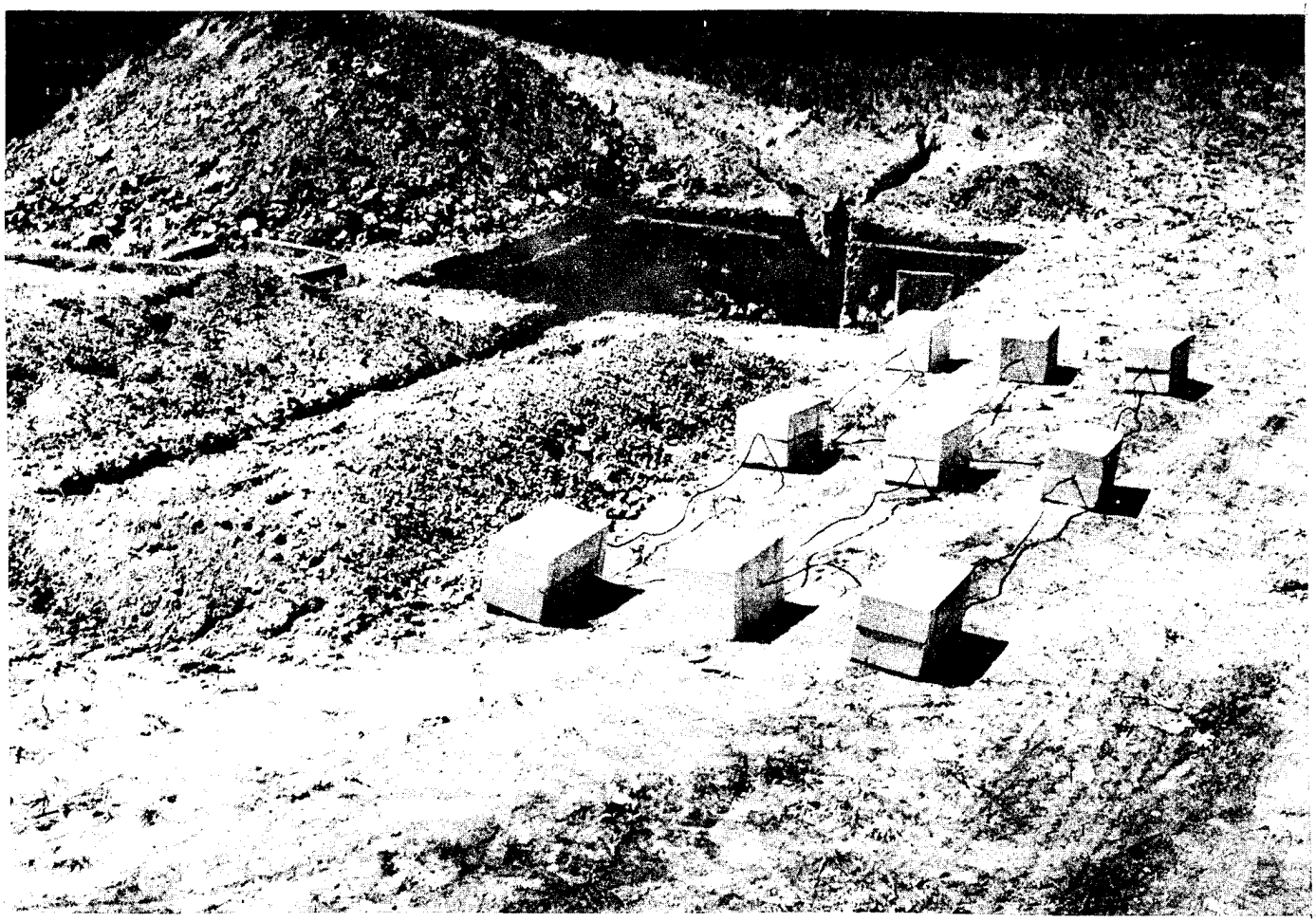

Figure 64. Free-field foam crush blocks designed to give an estimate of free-field stress (prior to installation).

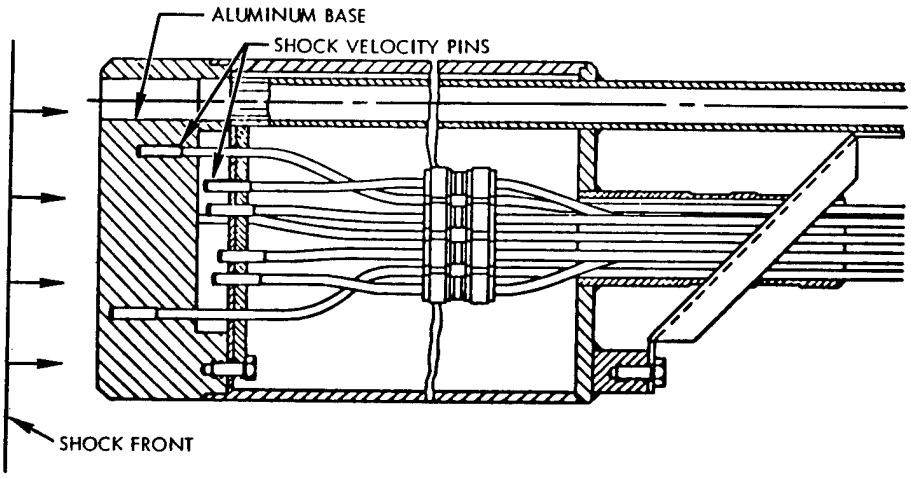

Figure 65. UCRL pin gage.

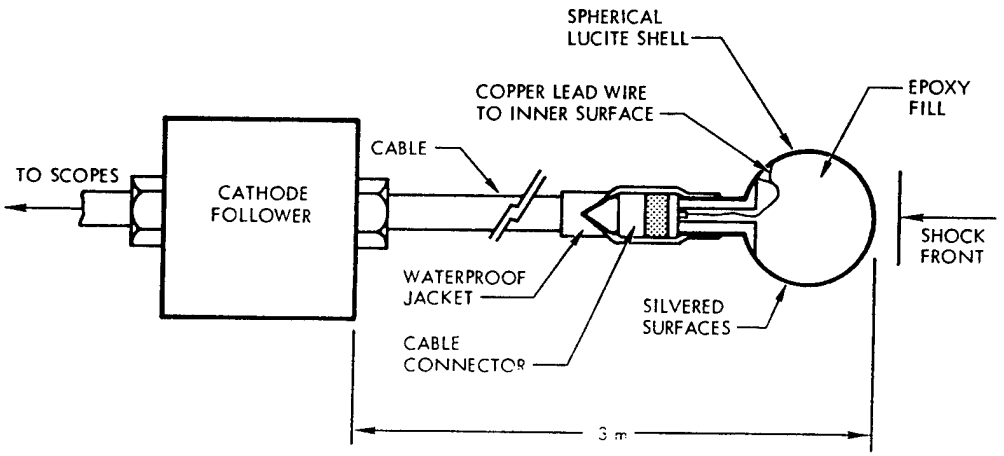

Figure 66. UCRL peak-pressure plastic gage.

to 180 kilobars in Lucite. The corresponding range in the detonation medium depends on the impedance mismatch between it and Lucite.

Ref: Holzer, F., "Measurements and Calculations of Peak Shock Wave Parameters from Underground Nuclear Detonations," Journal of Geophysics Research, 70, 4, 893, 1965.

5.3 SELF-RECORDING DEVICES.

5.3.1 WES Self-Recording Displacement Gage (USA) (1963).

The WES self-recording displacement gage was designed to measure time histories of relative displacements on the order of 1 inch to 1 foot of structural members subjected to the blast. The WES self-recording gage was composed of four major components: (a) drum assembly, (b) motor and transmission, (c) spline assembly, and (d) stylus. Completely assembled, the gage weighs almost 20 pounds and may vary in length from 3 feet to 4 feet and 3 inches.

A schematic of the gage is shown in Figure 67 and the assembled gage in Figure 68.

The drum assembly originally consisted of a machined Lucite recording drum and two split ball bearings with retaining rings. It was realized that the relatively soft, irregular surface of the Lucite was undesirable, and that a writing surface of metal, such as brass or stainless steel, would permit the use of a comparatively rigid stylus with less danger of gouging or chipping. However, a transparent material was chosen for the drum to allow inspection of the record without having to split the drum open. The drum is 16 inches long and 1 and 1/4 inch in inside diameter, and rotates in its bearings at speeds up to about 140 rpm. Because the drum speed determines the abscissa or time axis of the record, it is important that the speed remain constant during a test.

A later modification was made whereby a recording drum of steel replaced the Lucite one so a spark gap timing circuit could be used. With this arrangement any change in the drum speed would show up in the spacing of the marks. The wiring diagram for the timing device is shown in Figure 69. The revised gage is shown in Figure 70.

A peak displacement can be obtained by a linear scratch of the stylus on the inside of a polished brass cylinder which does not rotate. The motor and transmission assembly are therefore eliminated from the gage, making it lighter and less expensive. The stylus is mounted in a Teflon bushing and is designed to be in contact with its writing surface at all times, and thus no solenoid is required. The brass cylinder is split open and laid flat to read the record. A peak displacement on the order of several inches can be measured with this gage. See Figure 71 for a schematic of the WES peak displacement gage.

Ref: "Evaluation of WES Self-Recording Displacement Gage," Miscellaneous papers, No. 1-644, U.S. Army Engineer Waterways Experiment Station, Corps of Engineers, Vicksburg, MS, 1964.

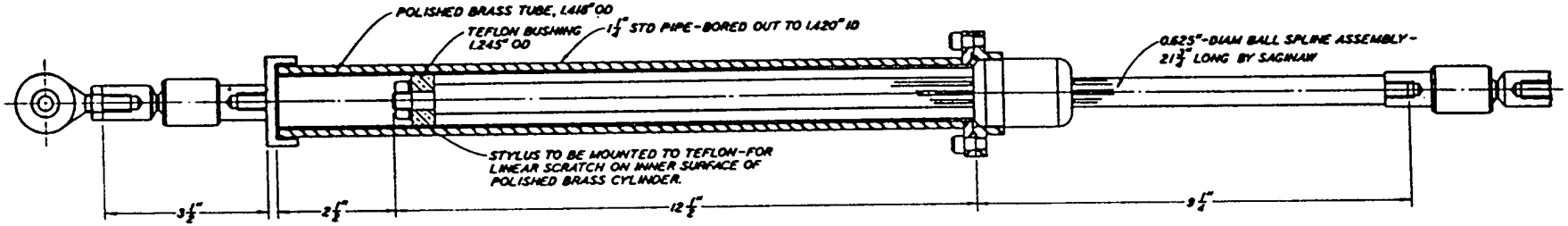

Figure 67. WES peak displacement gage.

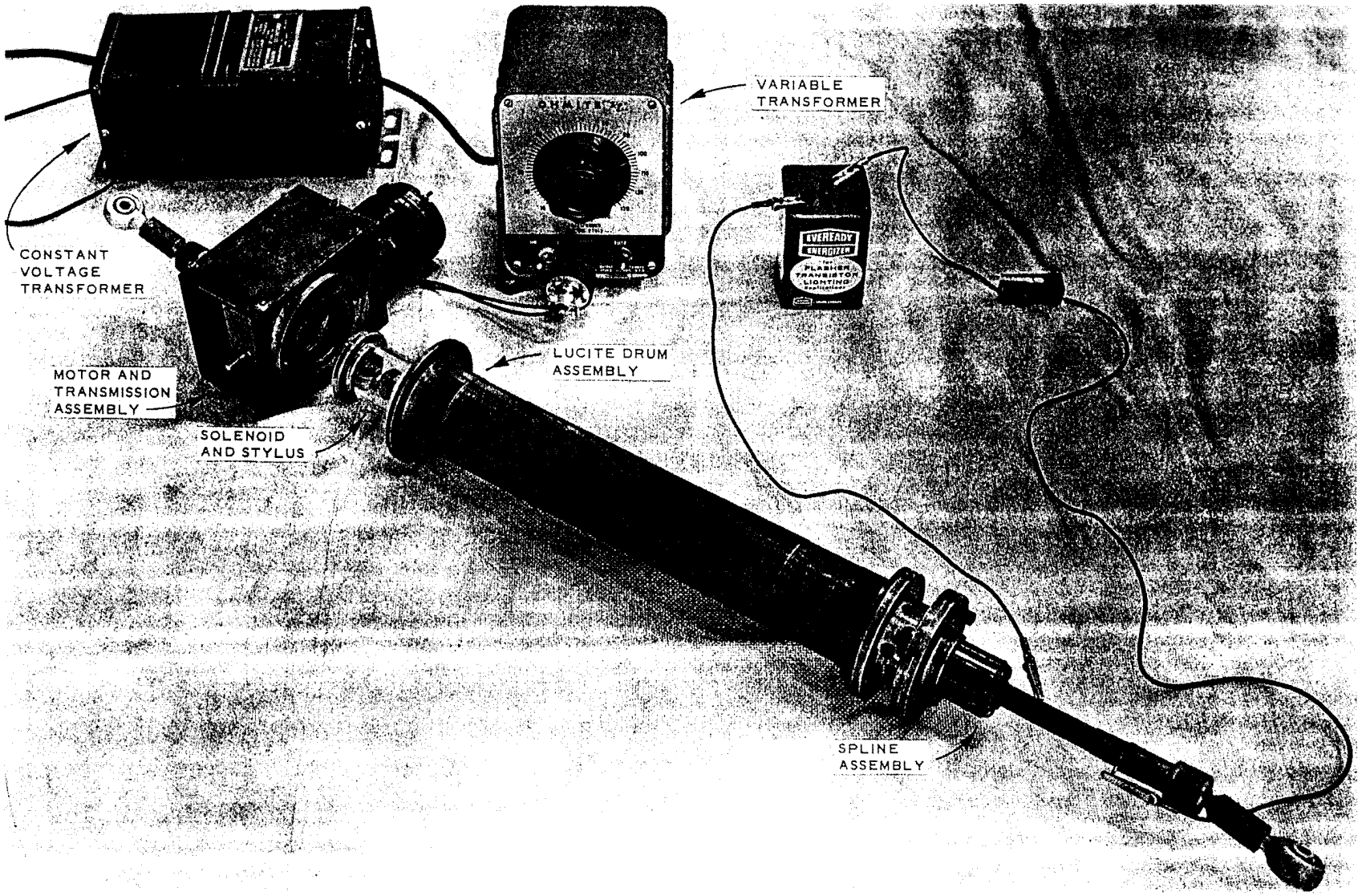

Figure 68. WES self-recording displacement gage.

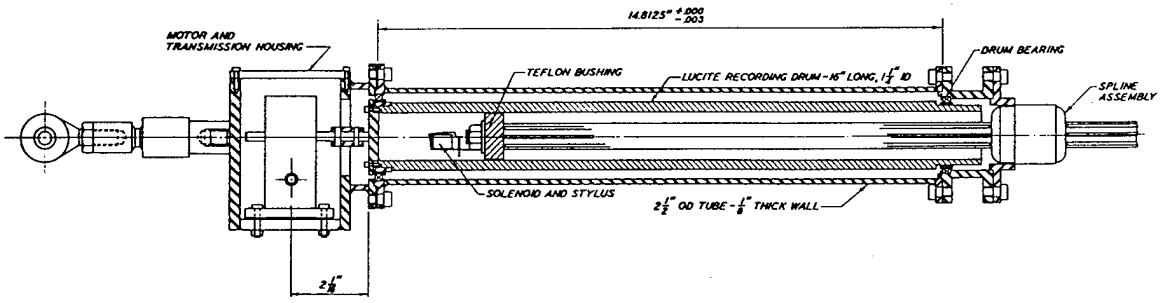

Figure 69. Details of WES self-recording displacement gage.

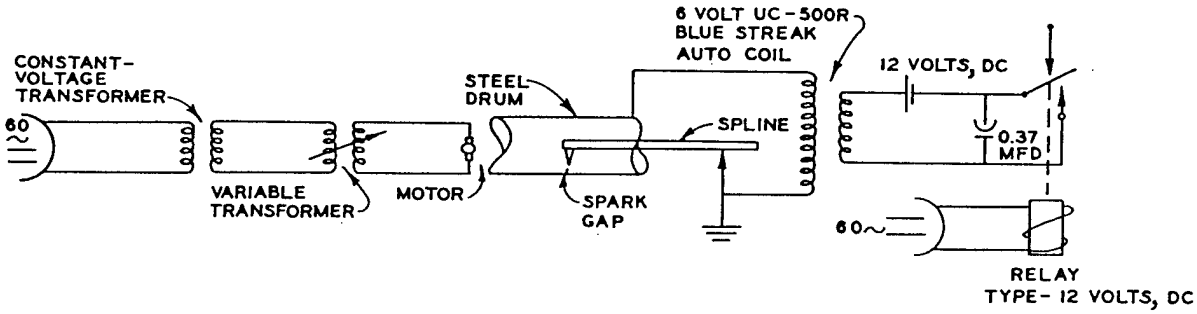

Figure 70. Wiring diagram for revised mechanical gage with timing device.

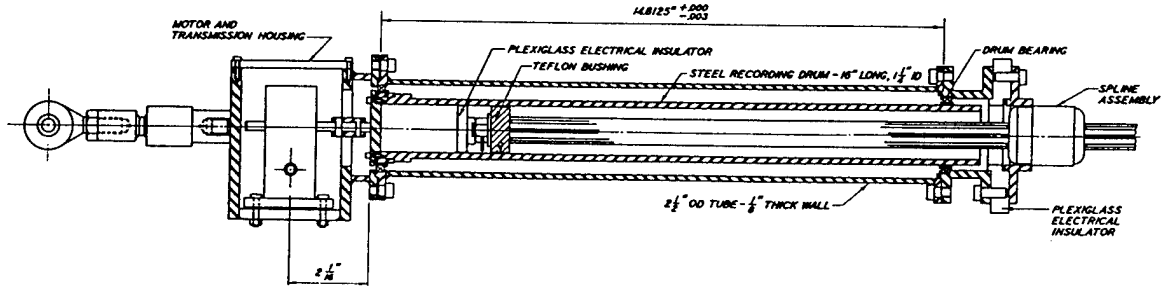

Figure 71. Revised WES mechanical displacement gage.

5.3.2 UED Peak Load Self-Recording Stress Gage (USA) (1963).

The United Electrodynamics Corporation (UED) peak load self-recording stress gage is a peak-only device employing a pre-recorded magnetic tape which is modulated by a permanent magnet on the sensing element. A diaphragm, which moves in accordance with soil pressure, controls the reluctance of an air gap. The amount of erasure is a measure of the peak stress load.

The heart of the gage is the magnetic circuit which consists of 10 small chrome steel magnets, Armco iron pole pieces, and two series gaps. One gap is fixed and magnetic tape is inserted to sense the change in flux. The second gap is variable and is used to control the flux in the magnetic circuit. The diaphragm which completes the circuit deflects predominately at the center and with very little at the edges. It was found that induction values in chrome steel magnets do not approach the curve values in the literature until the magnets have a length-to-area ratio of 10 or more, thus the reason for 10 magnets.

The gage is shown in Figure 72. Shown in Figure 73 is a calibration oscillogram which shows the modulation of the pre-record magnetic tape. The diaphragm is designed to deflect 0.0005 inches for 200 psi. The initial control gap is 0.0007 inches.

The gage was found to respond to one millisecond rise-time pulses with an accuracy of $\pm$ 15 percent. Some problem areas were uncovered during the testing phase. These were:

1. response to acceleration along transverse and longitudinal axes,
2. sensitivity to high temperatures,
3. tape routing and handling allowing severe noise-obscuring results, and
4. mechanical noise in the readout systems.

Ref: "A Peak Load, Self-Recording on Structure Stress Gage," WL-TDR-64-11, Air Force Weapons Laboratory, Kirtland AFB, NM, 1964.

5.3.3 DRES Mechanical Deflection Gage (Canada) (1967).

The DRES mechanical deflection-time gage was designed especially for measuring the radial motion of the sandwich hemispheres of a radome relative to a bridge in the center. The assembly is shown in Figure 74. A light aluminum arm hinged at both ends was attached to the inner shell surface at each location. Radial motion of the arm was recorded by a pen trace on paper tape. The paper tape was driven by a motor operating at a speed of 3.6-feet per second. A 120 Hz timing signal was applied to the recording paper as a time reference.

Ref: Walkinshaw, D.S. and Laidlaw, B.G., "Blast Response of M22 Radome," Event DIAL PACK Symposium Report, Vol. I, Defence Research Board of Canada, 1971.

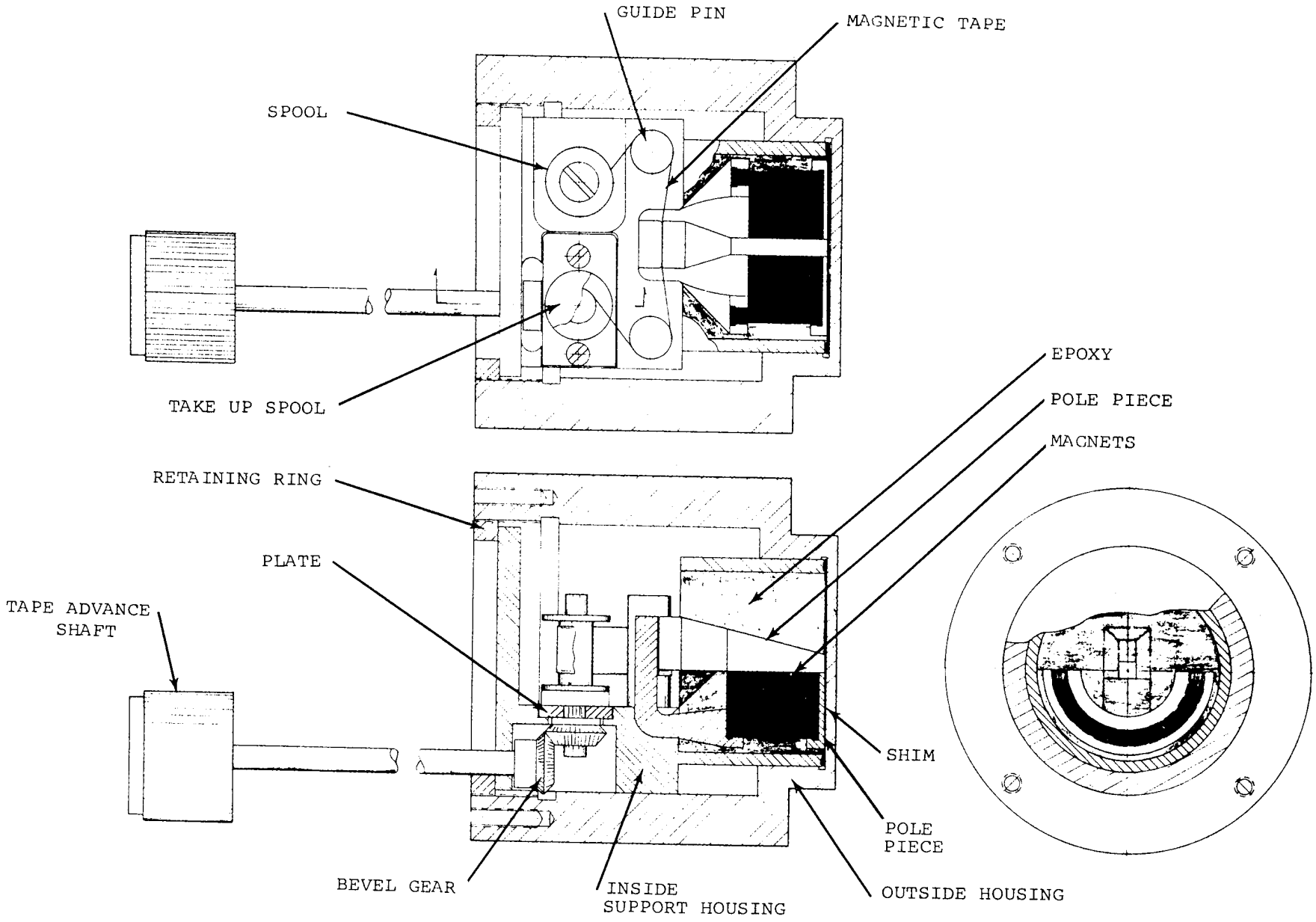

Figure 72. Self-recording magnetic peak load stress gage.

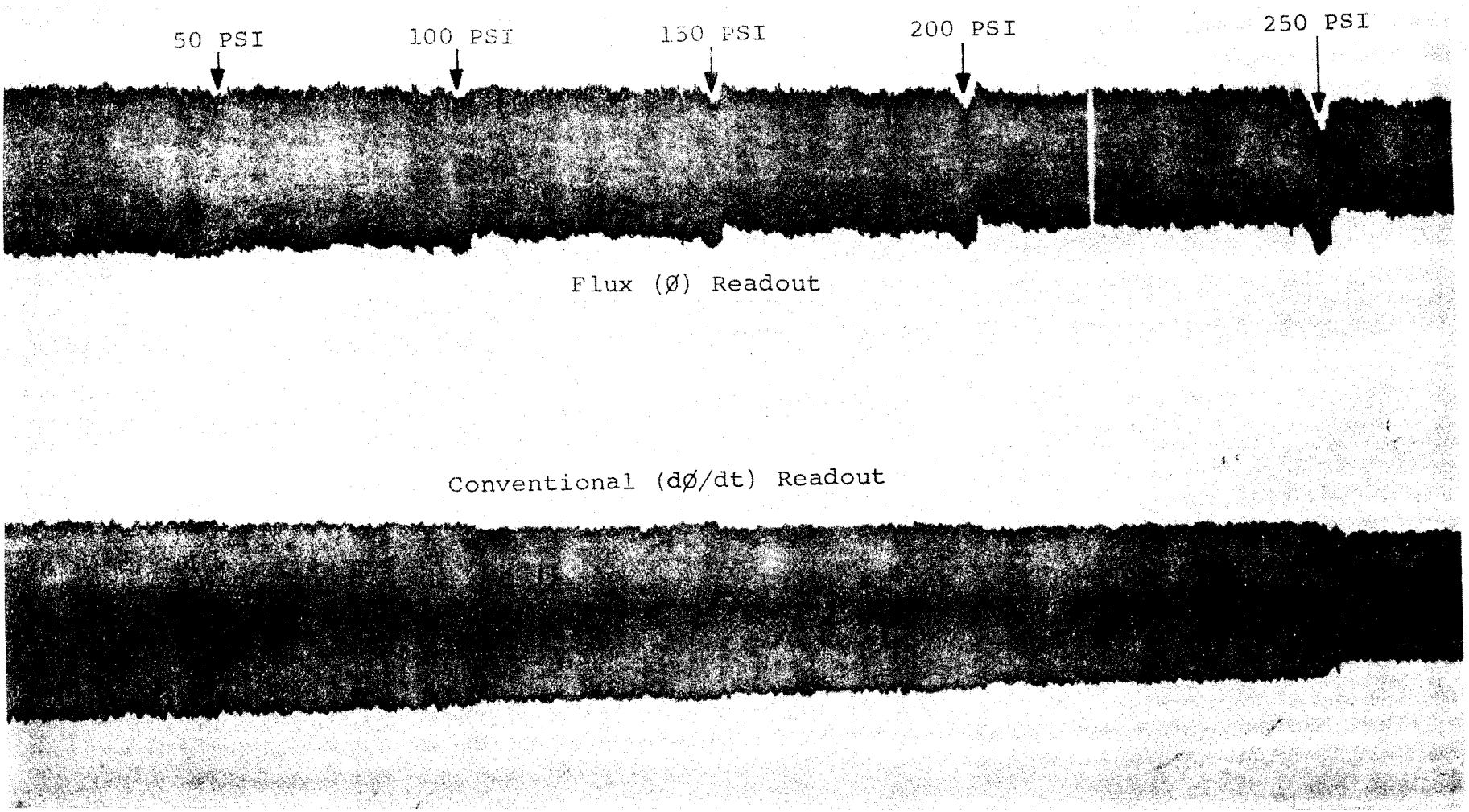

Figure 73. Typical calibration oscillogram; outputs from Hall head and conventional head recorded simultaneously.

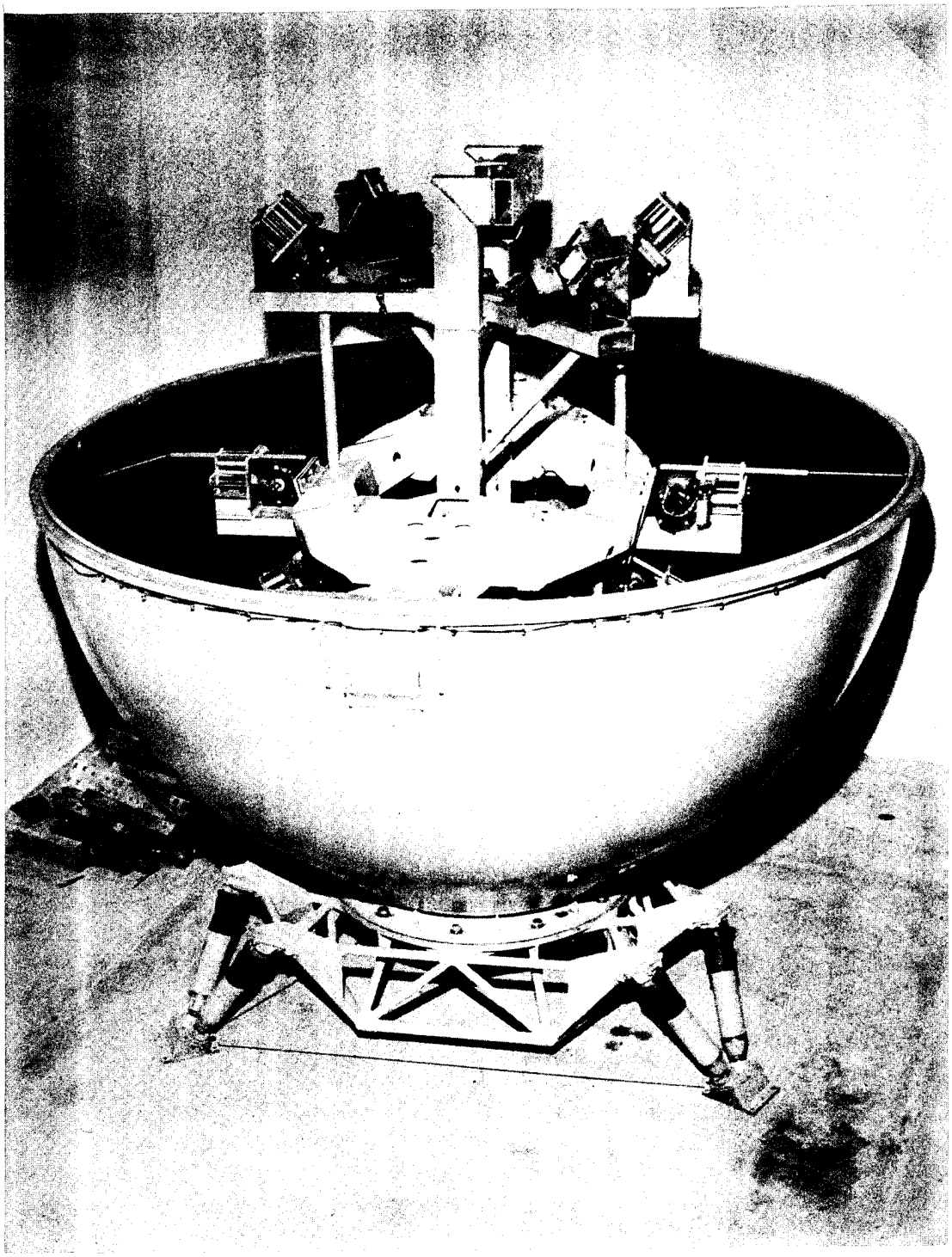

Figure 74. Mechanical deflection gage assembly.

SECTION 6

ELECTRONIC STRUCTURAL - HE TESTING

6.1 DISPLACEMENT.

6.1.1 WES Electronic Displacement Gage (USA) (1963).

The WES displacement gage uses the same type of housing, spline, and universals as the WES self-recording displacement gage described in Section 5.3.1. The basic difference between the two gages is that, instead of driving a stylus which draws the record on a drum, the spline on the electrical gage drives the wiper arm of a linear potentiometer mounted on the instrument. The record is obtained on a cathode-ray oscilloscope or other suitable recorder. The potentiometer used was a Bourns Model 108 with a 6-inch travel.

The gage is shown in schematic form in Figure 75 and presented as a unit in Figure 76.

Ref: "Evaluation of WES Self-Recording Displacement Gage," Miscellaneous Papers, No. 1-644, U.S. Army Engineer Waterways Experiment Station, Corps of Engineers, Vicksburg, MS, 1964.

6.1.2 Differential Displacement (USA) (1960s).

6.1.2.1 Spool Gage (USA) (1964). The AFWL spool gage consists of two semi-rigid thin discs, connected by a thin, sliding, hollow stem. The sensing element is either a linear variable differential transformer or a linear potentiometer. Relative movement between the discs is measured directly.

A study of the methods involved in relative displacement measurements in soil concluded that for accurate measurement a spool gage should incorporate the following features:

1. The ratio of the area of the end plate to the cross-sectional area of the coupling shaft should be at least 60.

2. The shaft should be in a segmented configuration to carry no load and allow freedom of motion.

3. The lateral surface of the shaft should have a low coefficient of friction and less than 5 percent of flexible material.

4. The gage should be quite short compared to the length of an input pulse.

5. Data within increments of time smaller than those required to assume a nearly uniform strain state between end plates are not valid.

6. End plates should be rigid, as thin as possible, and of low mass.

The major problem with spool gages is their placement within the soil mass in such a manner as to minimize arching effects and impedance mismatch caused by the gage and by possible

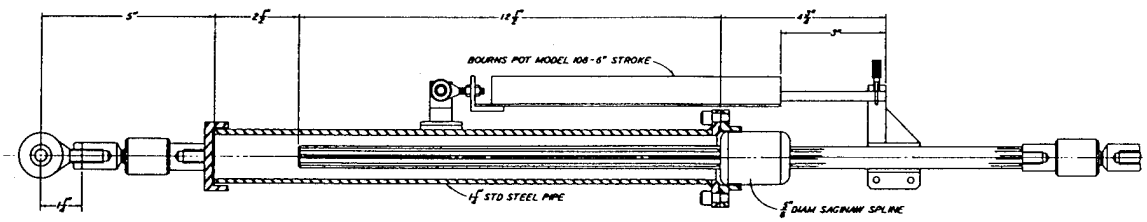

Figure 75. Details of WES electrical displacement gage.

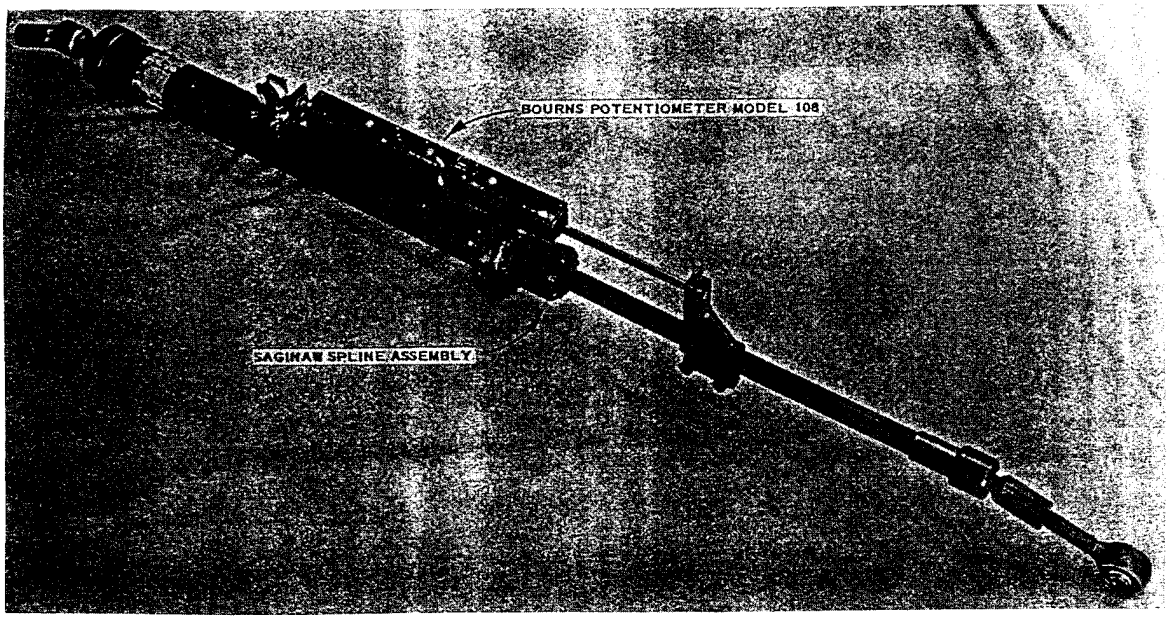

Figure 76. WES electrical displacement gage.

voids in the backfill. In general, spool gages have poor accuracy and poor resolution. It is almost impossible to construct one that is waterproof.

Ref: Baker, W.E. and Lynch, R.E., "A Study of Parameters and Methods Involved in Relative Displacement Measurements in Soil," AFWL-TR-65-75, 1965.

6.1.2.2 IITRI Coil Gage (USA) (1965). The IITRI (Illinois Institute of Technology Research Institute) coil gage measures differential displacement between two points which are not mechanically coupled, see Figure 77. The gage points are wire coils encapsulated in 3/4-inch diameter by 1/16-inch thick discs embedded in soil, oriented to be parallel and concentric. A second set of coils is positioned at a convenient location. The principle of operation is that of an air core differential transformer with a null balancing system to permit accurate measurements of small strains.

In operation, the drive-coil circuit is composed of a 50-kHz oscillator and drive-coil power amplifier. The pickup coils are connected to an amplifier, which in turn is connected to a synchronous detector, filter, and meter. When the spacing of the two coil sets is different, a small differential voltage appears at the input of the amplifier. Once amplified, the signal is the envelope of this high-frequency carrier. The synchronous detector (a conventional ring demodulator) separates the envelope from the high-frequency carrier. The demodulator output is zero when the carrier input is zero or nulled, and is either positive or negative in polarity when the two pickup coil voltages are not equal. The polarity depends on which coil has the larger voltage, thereby indicating whether the coils embedded in the sample have moved closer together or farther apart. The response time of the gage, defined as the time from 10 percent to 90 percent of peak output, was determined experimentally to be approximately 0.01 millisecond.

There are no mechanical coupling effects, as in the spool gage, but the output is to some degree sensitive to lateral and rotational misalignment.

IITRI has used coils up to 6 inches in diameter which allow gage lengths up to 18 inches, and hence are less sensitive to local discontinuities in large soil samples. The system consists of two sets of coils with a driver coil and a pickup coil in each set. A 10-Hz oscillator is used to power the driver coils. The pickup coils from each set are combined in two arms of a balanced reactance bridge. The relative displacement between two coils of one set serves to unbalance the bridge. The amplitude-modulated signal is then demodulated to obtain a DC signal proportional to the relative displacement between the two embedded coils. A full-scale output of 0.3 volts (at maximum sensitivity) can represent 1.4 percent strain in the 18-inch gage span. The cross-talk between adjacent sets of coils near each other is limited to 1 percent when a common oscillator is used and a separation of nine coil diameters is maintained between coil sets.

Ref: Truesdale, W.B. and Schwab, R.B., "Soil Strain Gage Instrumentation," AFWL-TR-65-207, 1966.

6.1.2.3 SRI Soil Strain Gage (USA) (1960). The SRI-designed soil strain gage consists of a long tube whose ends are securely fastened to the medium. The relative displacement of the ends is sensed by an LVDT attached to one end piece. The plunger, an armature, is extended by a rod which varies in length, depending on the strain range for which the gage

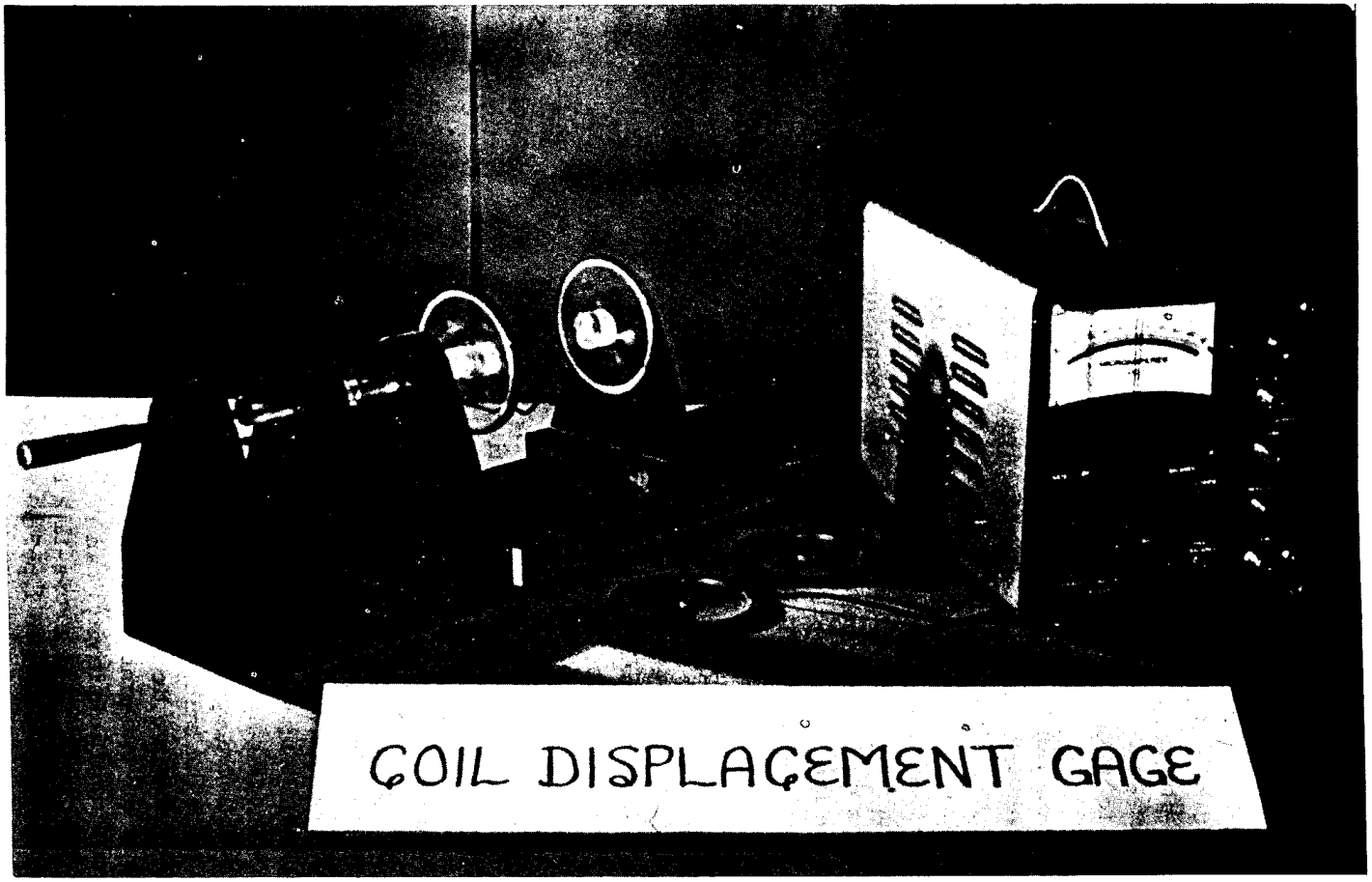

Figure 77. IITRI soil displacement gage shown in laboratory.

was designed. The LVDT displacement range was ± 0.25 cm, and strains of 0.8 to 4 ppk could be realized with gage lengths of 60 to 300 cm.

The gage is presented in schematic form in Figure 78.

Ref: Swift, L.M., "Development of Soil Displacement and Strain Gages," DASA-1267, 1961.

6.1.2.4 Sandia Rack and Pinion Inertial Displacement Gage (USA) (1962). In the Sandia rack and pinion gage a moving rack is fastened to a mass carried on a ball bushing which rolls on a splined shaft. The signal output is generated by a rotary differential transformer. The maximum displacement measured is about 4 feet; the rise time of the gage is about 0.5 seconds, and the sensitivity of the gage is 0.04 g.

Ref: Chabai, A.J., "Close-In Phenomena of Buried Explosions," DASA 1382, 1963.

6.1.2.5 SRI Inertial Displacement Gage (USA) (1960).

The gage is housed in a 6-inch diameter sphere. A DC motor and solenoid are included in the case to permit calibration and leveling of the inner cage after grouting.

The SRI gage measures either horizontal or vertical soil displacements of up to 36 inches for time periods of 2 seconds, with an accuracy of about 1 inch. Angular deflection of a geared pendulum is sensed by an E-shaped Wiancko variable reluctance sensor fastened to the gage case. The effective length of the pendulum, and therefore its natural period, is substantially increased by gearing it to a flywheel. The flywheel rotates through an angle of 15.6 degrees for 1 degree of rotation of the pendulum, resulting in small pendulum motions for large earth motions. This arrangement results in the instrument having a long natural period, i.e., 3 to 5 seconds. A steel vane attached to the pendulum shaft passes over the Wiancko core and balances the inductances when the pendulum is in its neutral position. The vane may be adjusted so that the electrical unbalance of the coil varies linearly with pendulum angle. In the vertical component gage, the pendulum is held in a horizontal position by a weak spring.

Ref: Swift, L.M., "Development of Soil Displacement and Strain Gages," DASA 1267, 1961.

6.1.3 French Displacement Gage (France) (1985).

France deployed a linear potentiometer displacement gage as depicted in Figure 79 in the field on a test of anti-blast valves and doors.

Ref: Malavergne, J., et al., "Tests of Anti-Blast Valves and Doors," Proceedings of the MINOR SCALE Symposium, POR 7158-4, 1986.

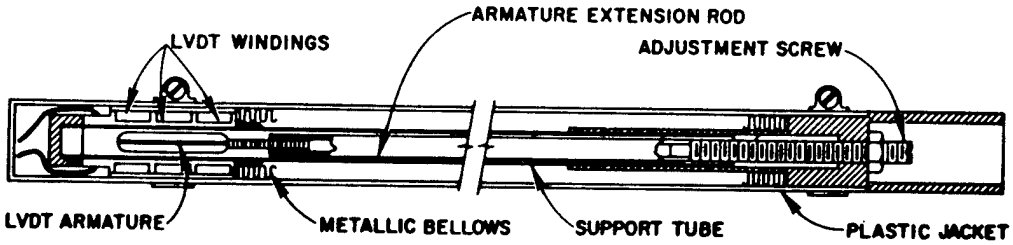

Figure 78. SRI soil/strain displacement gage.

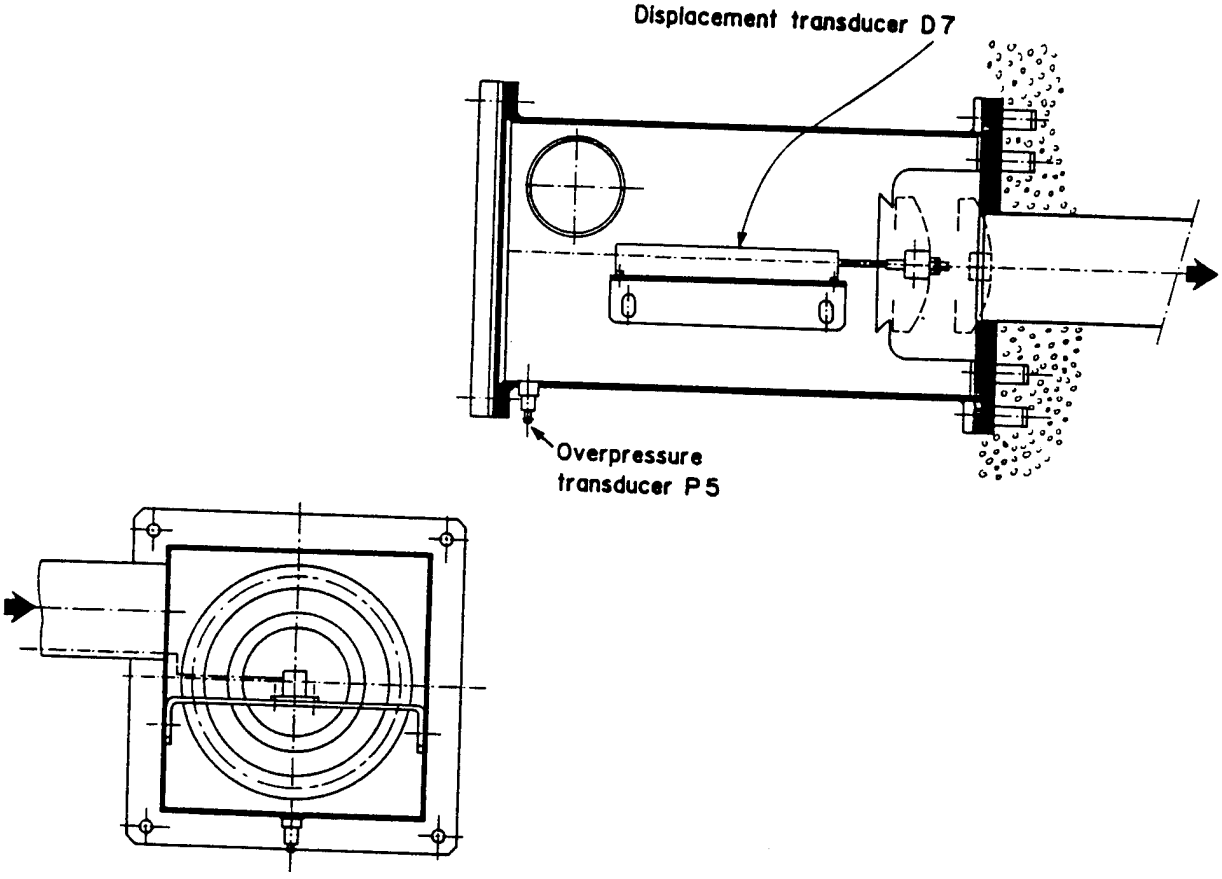

Figure 79. French linear potentiometer displacement gage.

6.1.4 Commercially-Available Gages.

60s	Bourns Type 108 Linear Potentiometer
80s	Longfellow LFS 12/300-OA5 Linear Potentiometer Manufactured by Waters Manufacturing Corporation
80s	SWEMA RLP4104/10 (Sweden)

Users: Canada, Norway, Sweden, USA, and France

6.2 ACCELERATION INSTRUMENTATION - HYDRODYNAMIC ZONE.

6.2.1 Endevco Accelerometer (USA) (1964).

A lead-zirconate-titanate piezoelectric gage manufactured by the Endevco Corporation was calibrated to 15,000 g. These gages are nearly undamped resonant systems with natural frequencies to about 80 kHz. The gage, amplifier, and an active calibration unit were incorporated in a single canister. Mechanical protection for the electronics was provided by flow-coating them with hard epoxy and potting them in the canister with a resilient silicone rubber.

Ref: Rowland, R.H., "Blast and Shock Measurement State-of-the-Art Review," DASA-1986, 1967.

6.2.2 SRI-FMX Accelerometer (USA) (1964).

The SRI-FMX accelerometer is a variable-reluctance diaphragm-type gage. Acceleration orifices deflect a stainless steel diaphragm supported between two coils as seen in Figure 80. As the diaphragm and its associated ferrite discs (used to achieve a high frequency response) change position relative to the coils, the change in inductance changes the frequency of each of two FMX oscillator circuits.

The ultimate range of this accelerometer is stated to be dependent only on the material of the gage body, which at about 125,000 g begins to yield under its own inertia. The range of the gage is set by varying the diaphragm thickness. Since these gages are essentially undamped resonant systems, and are expected to ring and overshoot if excited at frequencies near their natural resonance, every effort is made to make the natural frequency as high as possible.

EMP effects seriously affected the gage in field tests.

Ref: Rowland, R.H., "Blast and Shock Measurement State-of-the-Art Review," DASA 1986, 1967.

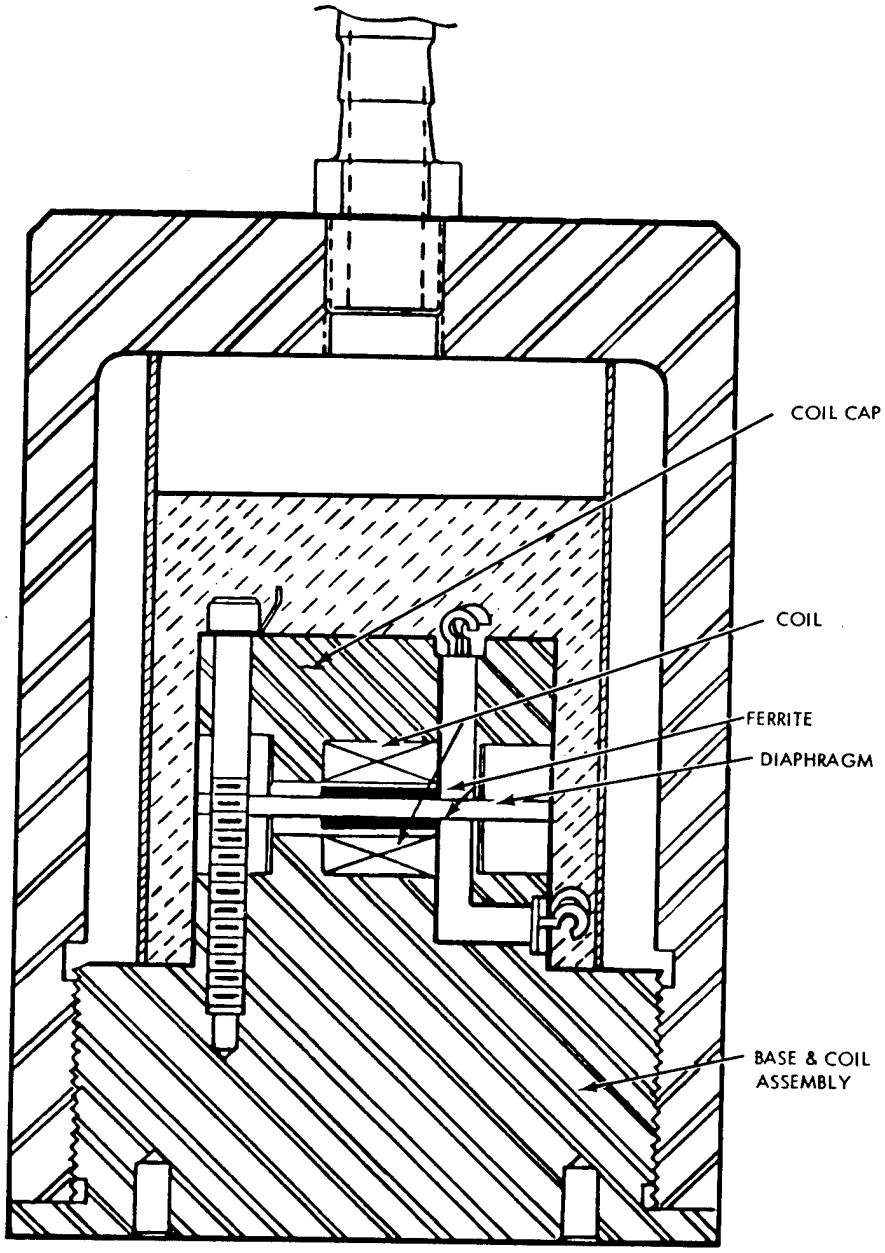

Figure 80. Cross-section of a typical SRI-FMX accelerometer.

6.2.3 Commercially-Available Gages.

60s	Cubit Corporation Model 2225, Piezo Endevco Model 2619, Piezo Endevco Tri-Axial Model 2223C, Piezo Statham Model 4-202, Strain Sunstrand Models QA-900, QA-1000, Strain Endevco Models 2264 AMI, 2260, 2261, Piezoresistive Sensor Products Type A1, Piezoresistive Kulite Model GB-625-250, Piezoresistive
80s	Endevco Models 2264, 2262, 7270, 7255 Piezoresistive

Users: Canada, Norway, Sweden, USA, France, and Great Britain

6.3 EARTH STRESS/STRAIN.

6.3.1 SRI-FMX Strain Gage (USA) (1963).

The SRI-FMX strain gage shown in Figure 81 was constructed of a 3-inch long piece of 1 and 1/2-inch diameter stainless steel tubing capped with stainless steel reference-point caps at each end. The tubing is the strain element in the gage.

Inside the tubing were two coils assembled so as to face each other, on the longitudinal axis of the gage, 1/4- to 1/2-inch apart. The coils were mechanically fixed relative to each other and one reference flange. A ferrite-disc, steel-disc, ferrite-disc assembly was placed between the coils and was mounted on a steel shaft which slid through center holes in each coil assembly; the shaft was fixed to the other reference flange.

Compression or extension of the strain element due to forces on the caps caused the disc assembly to move relative to the two fixed coils. Movement of the disc assembly relative to each coil changed the inductance of each coil, which in turn changed the frequency of each of the two FMX oscillator circuits. For calibration, the shaft on which the disc assembly was mounted was made a threaded connection to the flange to permit disc-to-coil relative motion. The shaft was fixed in position and waterproofed upon completion of the calibration sweep.

The steel strain element tubing was designed to give the same strain for a given force as did the grout slug which was displaced.

The gage was subject to EMP effects.

Ref: Sauer, F.M. and Vincent, C.T., "Close-In Earth Motion Studies/Pressure Measurements in the Hydrodynamic Region (U)," POIR 3016, 1966. (CONFIDENTIAL-RESTRICTED DATA)

6.3.2 Sandia Thick Quartz Earth Pressure Gages (USA) (1965).

The Sandia thick quartz gage is fabricated from synthetic-grown material supplied, cut, and polished to very close tolerances. The x-cut crystals have a diameter which varies from 2 to

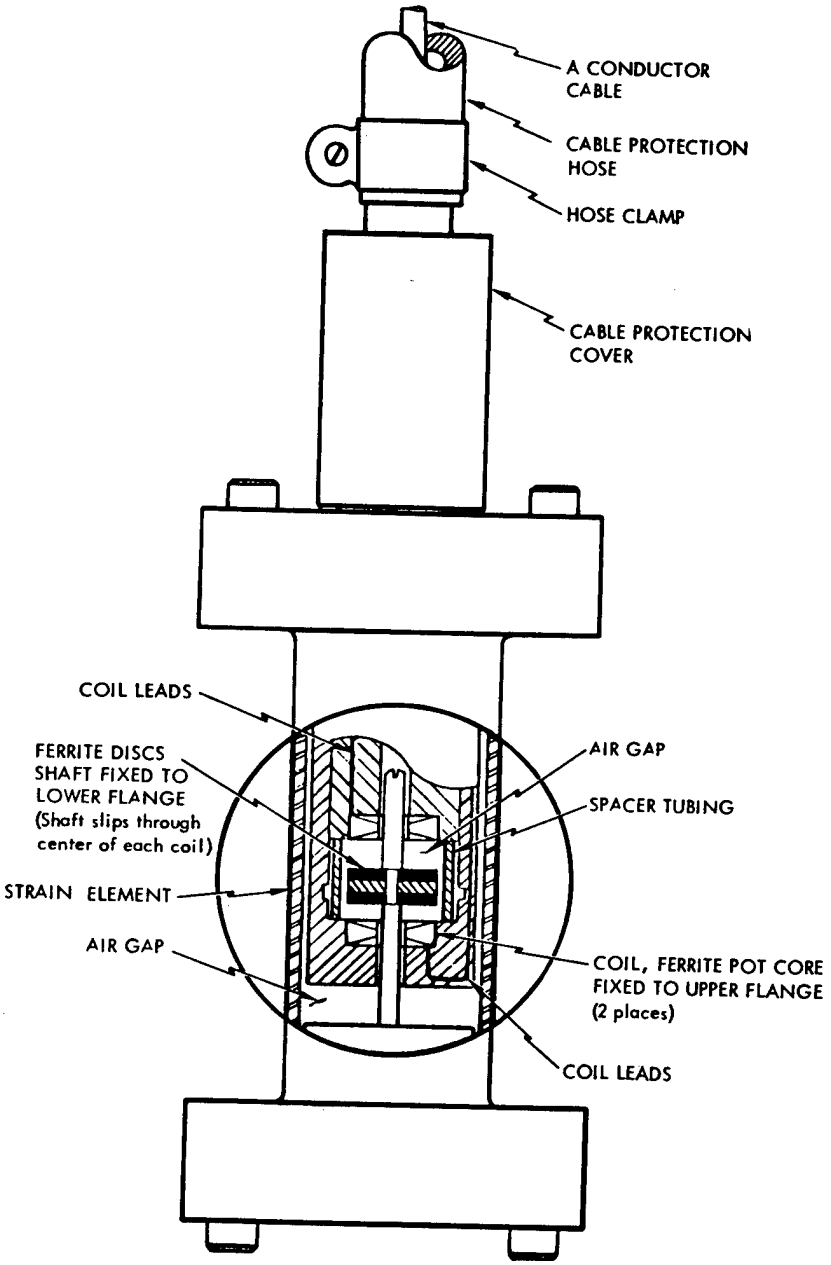

Figure 81. Cross-section of SRI-FMX strain gage.

4 inches and a thickness of 0.5 to 1 inch. Since the speed of shock propagation in quartz is about 0.23 inches per microsecond (or 4.4 microseconds for a 1-inch gage) the thinner gages produce shorter usable records before the signal is obscured by reflections from the back face of the crystal due to impedance-mismatch effects.

The latest model gages are 4 inches in diameter and 1-inch thick. The ratio of diameter to thickness is important in determining the accuracy of the gage because of shock reflections from the side surface of the disc. A ratio of 4:1 results in an accuracy of about 1 percent.

The polished crystals have metallic electrodes vapor-deposited on the front and back faces as thin (100 microinches) films. The most common electrode material is silver over a sublayer of chrome. A guard ring or groove 0.003- to 0.004-inches wide is cut through the back surface electrode. The diameter of the circle formed by the ring is 1 and 1/2 times the thickness of the gage. The guard ring is electrically connected to the front surface electrode through a low value bleed resistance (50 to 100 ohms) to match the electrical impedance of the center, or active, electrode. The active electrode is attached to the center conductor of a coaxial cable. The outer shield of the cable is connected to the junction of the front surface and the bleed resistor. The gage is pressure-bonded to the sample under test with a thin layer of epoxy.

A high output signal level is realized whose magnitude is a function of the area of the center electrode. As an example, a 3/4-inch electrode will produce an output of approximately 50 to 60 volts for a pressure of 15 kb. Consequently, the gage can be used to produce a signal which can be transmitted over long wires directly, without need of amplifiers. Signals can be sent through over 2,000 feet of cable in this manner. Some form of equalizer is employed at the end of long cables to reshape the pulse before driving the scope or recorder. This technique has been used very successfully in reading out quartz data, although the signal strength may be reduced by approximately an order of magnitude in the pulse-forming network.

Ref: Bass, R.C. and Hawk, H.L., "Close-In Shock Studies, FERRIS WHEEL Series, FLAT TOP I Event," POR 3005, 1965.

Chabai, A.J., "Close-In Phenomena of Buried Explosions," DASA 1382, AD423422, 1963.

6.3.3 UED Spool Stress Gage (USA) (1960).

The UED (United Electrodynamics Corporation) spool gage was designed to measure pressures up to 5000 psi. Each section consists of a thin circular disc, 4 inches in diameter, attached to an aluminum tube or stem. The stem of one section fits inside the other section, sliding freely on ground and lapped cylindrical surfaces. The sensing element in the latest version is either a Micro Systems or Schaevitz-Bytrex semiconductor strain gage; however, gages using both variable capacitance and LVDT sensors have been constructed.

The gage is installed in soil with the stem along the axis of stress to be measured; a pressure applied to one of the discs strains the central aluminum column. The sensors on the column produce an output proportional to the strain. The gage is installed with the sliding stems

extended, and soil from the gage location is replaced at its original compaction between the end plates.

The gage has an output of 100 millivolts full scale. It is very stiff and has an aspect (height/diameter) ratio of about 1.5:1; thus there is an effect due to shock transit time over the gage which stresses the soil and the gage differently, and perhaps some effect due to shock focusing. The density of the gage is about that of aluminum, or twice the density of sand. AFWL has determined that, in dry sand, the gage over-registers the pressure by factors of 1.1 to 1.2 for static loads and 1.3 to 1.4 for dynamic loads.

The placement of the gage is a major problem, especially when it comes to backfilling between the discs to attain original soil density.

Ref: Winston, T., "Research Studies on Free Field Instrumentation," AFSWC-TR-60-55, 1960.

Stegner, J.K. and Obenchain, R., "Research Studies on Free Field Instrumentation," AFSWC-TR-63-45, 1963.

6.3.4 UED Sand Dollar Pancake Gage (USA) (1963).

The UED (United Electrodynamics Corporation) sand dollar pancake gage design was a very thin disc which incorporated a capacitance-type of sensor.

The gage attempts to minimize the effect of mismatching the modules of deformations between the soil and the gage by reducing the thickness of the gage. The differential strain between the gage and soil is a function of their respective moduli of deformation and the aspect ratio of the gage. As the aspect ratio is made to approach zero, the differential strain also approaches zero although the relation between the moduli of deformation remains unchanged.

Although developed in the laboratory, the gage was never used in a field test.

Ref: Stegner, J.K. and Obenchain, R., "Research Studies on Free Field Instrumentation," AFSWC-TR-63-45, 1963.

6.3.5 BRL Pancake Gage (USA) (1964).

The BRL pancake gage uses a 4-arm bonded strain gage as a sensor. Its range is from 0 to 60 psi with a 30-mv output at full scale and a frequency response of 0 to about 200 Hz. The gage is 3 inches in diameter and 0.4 inches thick, with an aspect ratio of about 0.13:1. The total weight is 115 grams with a density of 3 grams per cc. The sensitive part of the gage consists of a single diaphragm which takes up the central 65 percent of the total area of one side. The diaphragm thickness controls the flexibility or stiffness of the gage. Since the outer edge of the gage is insensitive to pressure, arching effects concentrating near the rim should be minimized. BRL has constructed a somewhat smaller gage, a type J-2, 2 inches in diameter which measures soil stress to 90 psi.

Ref: Baker, W.E. and Lynch, R.E., "A Study of Parameters and Methods Involved in Relative Displacement Measurements in Soil," AFWL-TR-65-75, 1965.

6.3.6 WES-SE Pancake Gage (USA) (1964).

The WES-SE gage is a double-diaphragm gage which uses a semi-conductor strain element as the sensor. The gage is shown in Figure 82; it was designed to record pressures up to 1000 psi. The design is based on the principle of a deflecting, rigidly clamped, circular diaphragm. The gage is wafer-shaped with an active diaphragm in both the top and the bottom surfaces. The semiconductor strain-gage sensors (Micro Systems Inc., PEI-16-350, P type) are bonded to the diaphragms. The aspect ratio of the gage is about 0.1:1 but is adjustable by the addition of an epoxy ring or baffle around the outer edge of the disc. Table 5 lists the main gage characteristics. The Air Force has found the SE to be a rugged, dependable and repeatable instrument; however, they doubt its value at zero depth of burial because of the difference in stress distributions in air and soil, i.e., a uniform distribution in air and a non-uniform distribution in soil. The over-registration factor was determined to be 1.1 static and 0.85 dynamic in dry sand.

Ref: Rowland, R.H., "Blast and Shock Measurement State-of-the-Art Review," DASA-1986, 1967.

6.3.7 IITRI Pancake Gage (USA) (1964).

The IITRI (Illinois Institute of Technology Research Institute) developed a gage very similar to the WES-SE gage. This gage uses a 2-arm bridge semi-conductor strain gage as a sensor. Since there is but one diaphragm, the gage records the stress at zero depth of burial. AFWL reports a tentative over-registration factor 0.9 static and 1.1 dynamic; these values are based on few data, however, and may change. The present gage records pressure from 0 to 500 psi.

Ref: Truesdale, W.B. and Schwab, R.B., "Soil Strain Gage Instrumentation," AFWL-TR-63-207, 1965.

6.3.8 Filpip Gage (USA) (1960).

The filpip gage is a thin wafer-shaped variable capacitance gage developed by the Spitz Laboratories, Inc. It is used primarily to measure soil pressure in laboratory work. Two ranges are available: -10 to +10 psi and -10 to +100 psi. The gage is constructed of Saran plastic with stainless steel plates and mica dielectric. The diameter is 1 inch, and the thickness is 0.035 inches. Static tests show the gage to be linear with applied pressure and a static over-registration factor of about 1.1 to 1.2. The variable capacitance sensor is probably not the best available for a nuclear environment but the gage might find use in HE field tests.

Ref: Rowland, R.H., "Blast and Shock Measurement State-of-the-Art Review," DASA-1986, 1967.

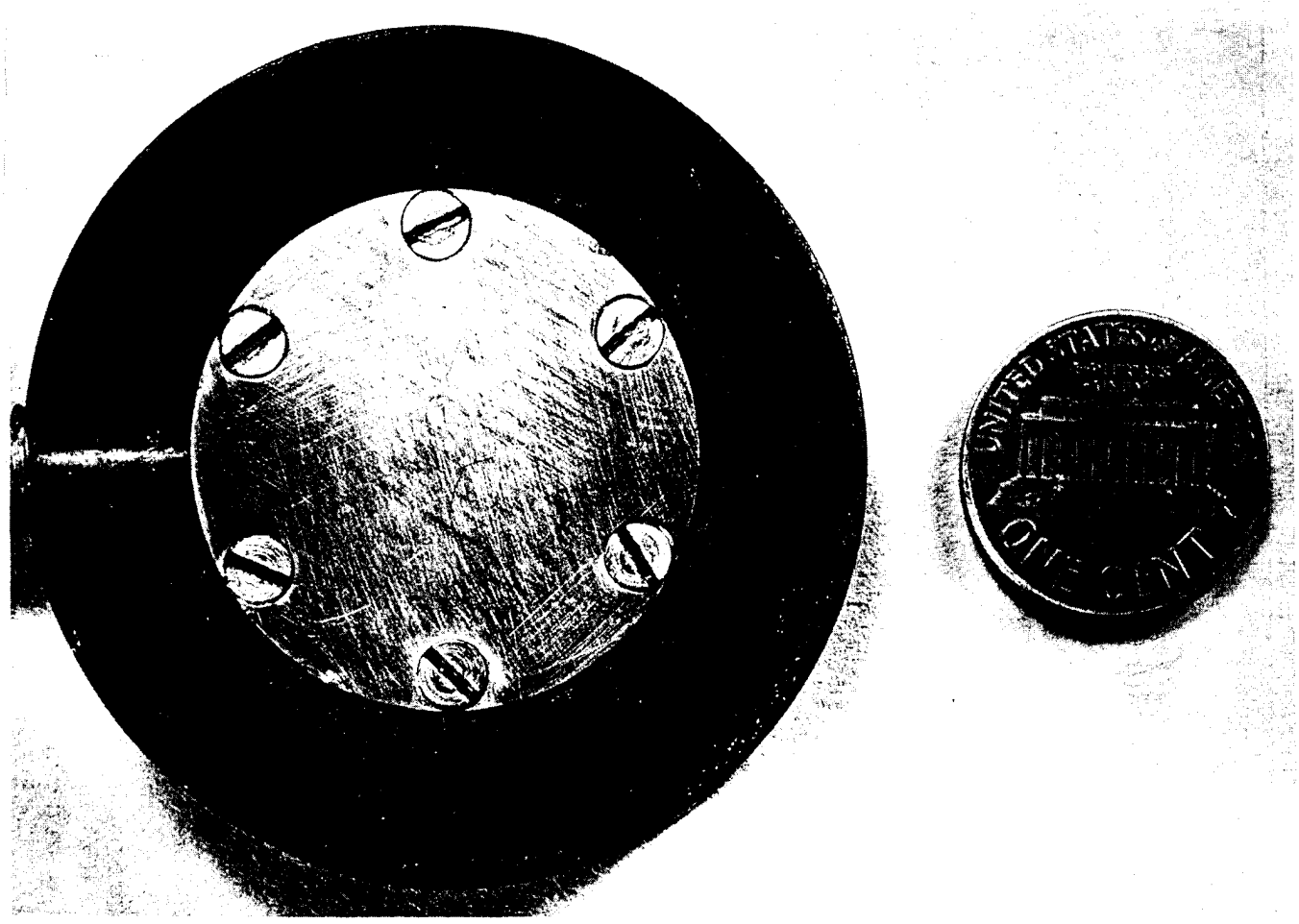

Figure 82. WES-SE soil stress gage.

Table 5. Characteristics of the WES-SE soil stress gage.

Overall Dimensions: Diameter Thickness	 2 inches 0.226 inches
Diaphragm Dimensions: Diameter Thickness	 0.75 inches 0.075 inches
Linear Range (Approximate)	0 - 2000 psig
Output	0.017 microvolts/v/psi
Linearity	0.4 percent full scale
Hysteresis	1.6 percent full scale
Temperature Range	Below 30° to 150°F
Recommended Excitation	10 volts
Maximum Excitation	21 volts
Acceleration Sensitivity Normal to Diaphragm	0.04 psi/g
Apparent Strain Sensitivity	20 to 30 microinches/in/psi
Thermal Sensitivity	1 psi/°F
Natural Frequency	>40 kHz
Response Time (to a step input)	<6 x 1 10^{-6} sec

6.3.9 SRI Surface Shear Gage (USA) (1961).

The SRI surface shear gage was constructed to measure airblast-induced surface shear forces in the 0 to 200 psi overpressure region. The gage is shown in Figure 83 and consists of a flat plate, 1-foot square, supported on two octagonal half-rings similar to the moving ring used in the SRI total-drag probe. The strain rings in turn are fastened to steel mounting plates which are attached securely to a massive concrete base. The top surface of the gage is covered with ordinary stair tread material providing a sandpaper-like finish in contact with the soil.

Two strain-gage bridges are used in the shear gage to obtain independent measurements of normal and shear forces. Each leg of the bridges contains two strain gages in series, one mounted at each end of the strain-sensing element. Damping is obtained by filling the gage enclosure with polybutene-20 which has a viscosity of about 6,500 centistokes at 90°F.

Ref: Swift, L.M., "Development of Soil Displacement and Strain Gages," DASA-1267, 1961.

6.3.10 Rensselaer Tri-Axial Gage (USA) (1964).

The Rensselaer Polytechnic Institute, Troy, NY, has constructed for NCEL a tri-axial soil pressure gage to measure 0 to 100 psi with a 1-millisecond rise time. The shape of the gage is spherical, which makes it independent of both the directions of the soil properties and the directions of the stress field in the soil. The shell of the gage, 3 inches in diameter, is divided into 8 equal segments obtained by one equatorial and two longitudinal planes of intersection at right angles to each other. These segments are made sufficiently rigid to act as curved beams, each triangular segment being supported at 3 points. Six strain-gaged spokes extend from the center of the sphere to the points of intersection of the covering segments. The system of measurement is based on the requirement that the 3 space components at each point of intersection can be measured separately. In total, 18 force components are required to establish the magnitude and direction on the force acting on the gage in space.

A placement technique has been developed to minimize the effects of the presence of the gage in the soil. Placement is accomplished by surrounding the gage with a flexible elastic medium. The diameter of this elastic medium is sufficiently large to exclude the possibility that the stress concentration effects, due to the rigid inclusion of the spherical gage, will prevent significant displacement at its boundary. Transfer of stresses acting on the outer boundary of the elastic medium then occurs through the intermediary of a material with known properties and dimensions.

The prototype gage exhibited undesirable characteristics of non-linearity and hysteresis which were attributed to imperfect bonding between the gage and the elastic medium. It is unknown whether developmental work is continuing on this gage.

Ref: Rowland, R.H., "Blast and Shock Measurement State-of-the-Art Review," DASA-1986, 1967.

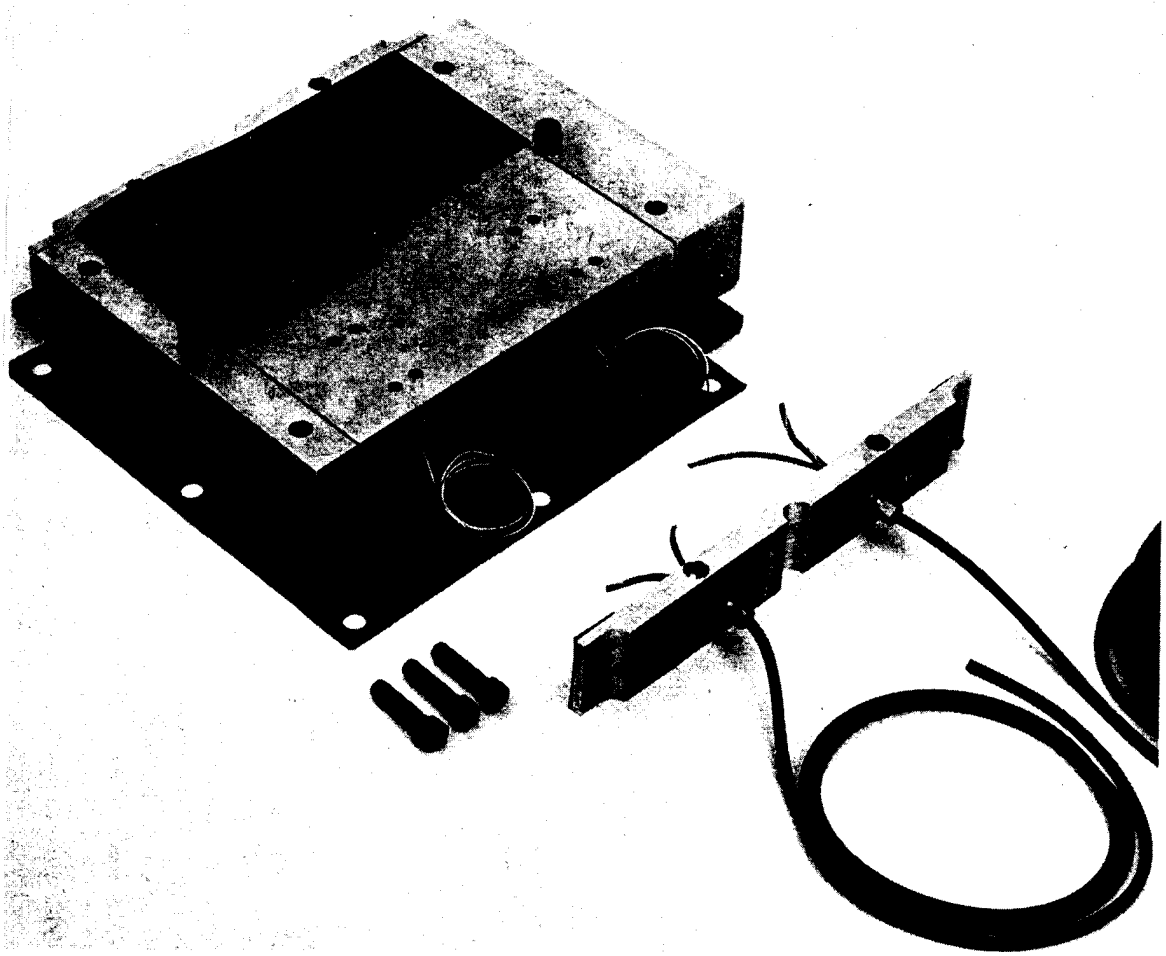

Figure 83. SRI surface shear gage.

6.3.11 Commercially-Available Gages.

Structural Strain

60s	BLH Strain Gages, 21BLH Type FAE-50-1256, FA-100-6 Micro Measurements Type EA-06-250B6-120 Derifoil Strain Gage
80s	Micro Measurements CEA-06-250-ON-350

Soil Stress/Strain

80s	Kulite Model Q080 Kulite Model VM-750 (Interface Pressure)

Users: Canada, Norway, Sweden, France, USA, Great Britain, and Switzerland

The structural strain gage is shown in Figure 84.

6.4 PRESSURE (HYDRODYNAMIC REGION).

6.4.1 Manganin Gages (USA) (1963).

Manganin gages to measure pressures of 20 to 450 kilobars (kb) have been produced by a number of organization, i.e., Harry Diamond Laboratories (HDL), Stanford Research Institute (SRI), Sandia Corporation (SC), and the Illinois Institute of Technology Research Institute (IITRI).

A typical pressure gage is fabricated from 3-mil (0.003-inch) diameter manganin wire which undergoes piezo-resistive changes when subjected to pressure. To bias the gage, a constant-current supply is triggered by an external sensor, located in the area of measurement, just prior to the production of the pressure pulse to be measured. The power supply delivers from 0.2 to approximately 2 amperes of current in a pulse about 50 microseconds wide (or longer if greater recording time is feasible). The actual change in resistance of the manganin due to the pressure pulse is detected as a change in voltage occurring between two voltage probes. The timing of triggering the constant current supply is obviously critical since it must coincide with the arrival of the pressure pulse.

To give some feel for the sensitivity of the manganin gage, a 30-percent change in resistance might be expected for a peak pressure of 100 kb. The gage is linear between about 25 and 400 kb. Up to 50 microseconds of write time can be obtained with the manganin wire gage. Rise times of 5 shakes (5×10^{-8} seconds) are possible with 3-mil wire and some work has been accomplished using 1-mil wire, or ribbon, with a somewhat faster response time. The gage is considered to be very good for peak pressure measurements, although long pressure tails might be somewhat difficult to measure accurately.

Manganin gages respond to the pressure in the medium in which they are embedded. Thus, if the embedding material replicates the properties of the earth (or rock) in which shock propagation is being studied, the gage output is proportional to the earth pressure. However, when the gage is embedded in a medium different from the surrounding earth, the gage output must be corrected for impedance mismatch between the embedding material and the

STRAIN GAGES

Measured Parameter: Structural strains

Range: 0-10%

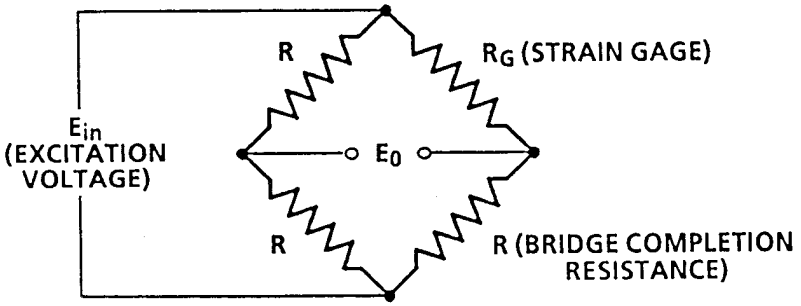

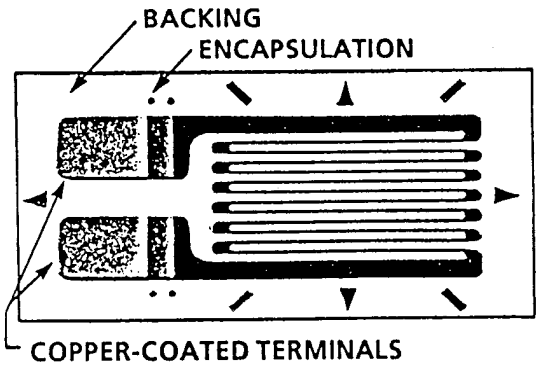

Principle: Gage resistance changes in direct proportion to change in length. Wheatstone bridge circuit is used to accurately measure small resistance changes.

Figure 84. Structural strain gage.

earth. The correction can be calculated if the equation-of-state of both the soil and the embedding material is known.

When used as a pressure gage, the wire is embedded close to the surface of an insulating material and the gage placed in contact with the surface to be sensed. As long as the wire is insulated properly, a variety of materials may be used to mount the gage. For example, the wire may be attached with an epoxy directly to a granite core. The gage may be used to sense pressure in curved surfaces.

The lower limit of usefulness of the manganin wire pressure-time gage is generally considered to be approximately 20 kb. However, examination of static pressure data seems to indicate that, with some further development effort, the range of the gage might be extended to as low as 1 kb.

A. **HDL and IITRI Manganin Gages**. Both the HDL and the IITRI gages use a manganin spiral about 3/8 inch in diameter, embedded in either plexiglass or epoxy insulator, and oriented so that the plane of the spiral is parallel to the shock front. The manganin measures the shock profile existing in the insulator. The corresponding peak pressure in the adjacent medium depends on the shock impedance and the equation-of-state of the two media.

The HDL gage, designed for material response studies, uses three coplanar spirals embedded so that their centers lie along radii 120 degrees apart and 1 inch from the center of the gage. By determining the arrival time at each spiral, the obliquity of the shock front may be determined. Sandia uses a similar technique with their impedance-mismatch gage.

B. **SRI Manganin Gage**. The SRI manganin gage, shown in Figure 85, uses a grid of 3-mil wire embedded in a C-7 epoxy insulator. The manganin wire is an active resistive element of an electrical four-arm bridge circuit. Up to at least 150 kb, the C-7 behaves ideally, i.e., as a fluid of low electrical conductivity. The initial goal of the gage design was a 0.1-microsecond rise time, >50-microsecond recording time, and a $\pm$ 10 percent-accuracy in the range from 10 to 500 kb. These goals are gradually being met. Durations of about 30 microseconds at pressures of about 30 kb, and 20 microseconds at 100 kb, have been achieved with a gage 4-inches thick and 6 inches in diameter. Pressures have been recorded at temperatures up to the melting point of manganin, 1020°C.

In addition to the C-7 epoxy, SRI has successfully constructed manganin gages using aluminum, granite, limestone, and highly-compacted tuff as the embedding medium. Studies are now being performed to determine methods of embedding the sensor in playa (earth) material which has the same density and water content as the soil where the measurement is to be made.

C. **Sandia Manganin Gage**. The Sandia manganin gage, similar to the SRI gage, uses both a grid of wire and the C-7 epoxy insulator. The gage is larger, 6-inches thick and 8 inches in diameter, and has achieved a recording time of 50 to 60 microseconds before the gage fails and the wire breaks.

Other materials besides quartz and manganin are used in high pressure gages. BRL has constructed a gage which depends on the change in electrical conductivity of sulphur subjected to pressure; SRI uses the piezoresistive properties of calcium; an IITRI gage

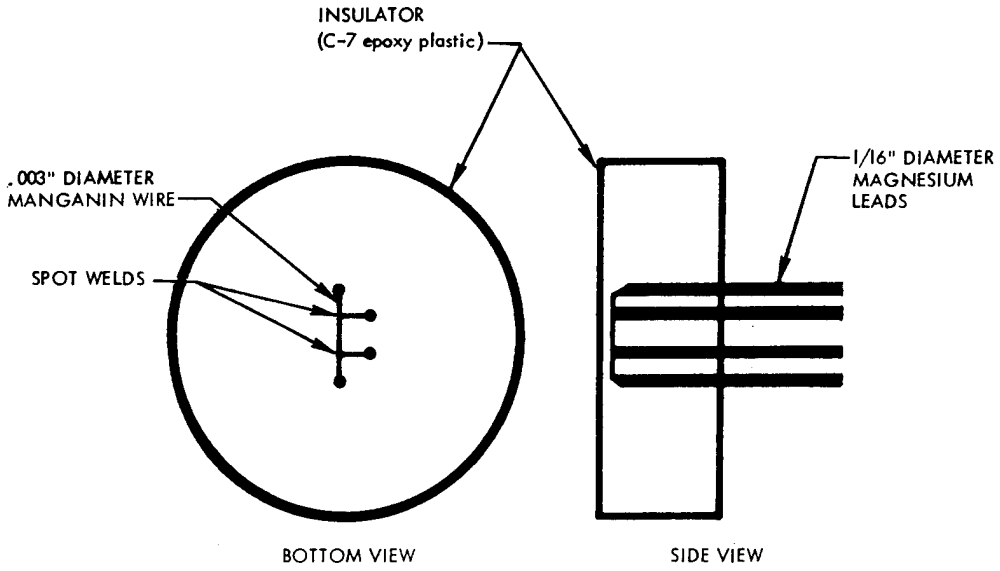

a. Configuration of gage in C-7 epoxy gage.

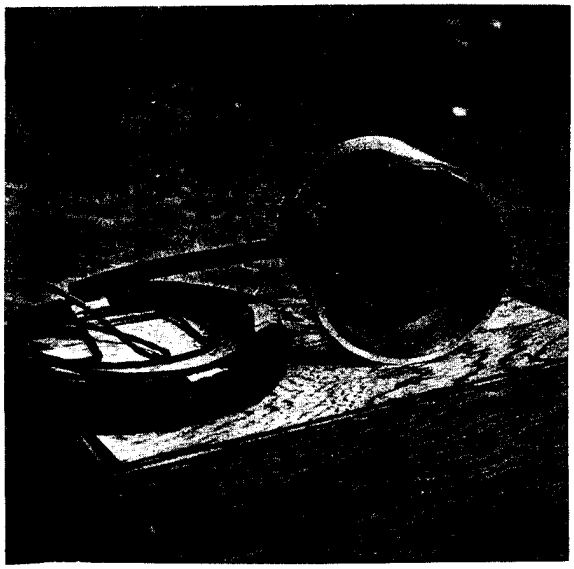

b. Gage shown with cables attached.

Figure 85. SRI manganin pressure gage.

depends on electrolytic properties of solutions; and the UCRL plastic gage depends upon the depolarization of a solid.

Ref: Chabai, A.J., "Close-In Phenomena of Buried Explosions," DASA 1382, AD423422, 1963.

Keough, D.H., "Pressure Transducer for Measuring Shock Wave Profiles, Phase IX: Additional Gage Development," DASA 1414-1, AD459058, 1964.

Bass, R.C. and Hawk, H.L., "Close-In Shock Studies, FERRIS WHEEL Series, FLAT TOP I Event," POR 3005, 1965.

Vincent, C.T., "Hydrodynamic Earth Pressure Measurements," Operation DISTANT PLAIN Preliminary Report, DASA 1876-4, 1968.

6.4.2 Sandia Impedance Mismatch Gage (USA) (1963).

Sandia developed an impedance mismatch gage to measure pressures up to 1000 kb, with rise times of less than 1 microsecond. The gage measures shock transit times in samples of known Hugoniot. When a strong shock wave propagates through a medium whose equation of state is unknown and then meets two or more materials whose Hugoniots are known, these materials acquire, from the shock, a pressure-particle velocity which can be determined by measuring the transit time of the shock. By applying the conservation equations to the system of waves resulting after the shock passes the interface, the pressure and particle velocities in the reflected wave (which must lie on the reflection Hugoniot - or mirror image of the Hugoniot - of the medium) may be calculated.

In the field use, a core sample from the emplacement hole is cut into a flat disc about 8 inches in diameter and 1-to 2-inches thick. On this disc are mounted three smaller discs, 1 and 1/2 inches in diameter and 0.394-inches thick. Two of these smaller discs are mismatch material and one is of the rock medium. Centers of these discs lie at 120-degree intervals on a circle of 1 and 1/2-inch radius. A shock detector is positioned on each disc and three more are placed in a circle of 3/4-inch radius inside the small discs. The shock detectors are small wafers of PZT (Clevite Corporation, Cleveland, Ohio), 0.120 inches in diameter and 0.020-inches thick, sandwiched into a small brass housing to which a standard Microdot coaxial cable is connected. The signal from the detectors is fed into a delay-time coding mixer circuit which can identify the direction of shock propagation.

Ref: Chabai, A.J., "Close-In Phenomena of Buried Explosions," DASA 1382, 1963.

6.4.3 IITRI Electrolytic Cell Gage (USA) (1964).

The IITRI electrolytic cell, shown in Figure 86, utilizes a piezoresistive liquid. Two platinum spheres act as electrodes in an electrolyte, whose composition varies according to the pressure to be measured. The cell constant, ion concentration, and ion mobility of the electrolytic cell each undergo reproducible changes during shock loading. The net result of these changes is a change in the electrical resistance of the cell. The gages are calibrated in an explosively loaded water column. Three solutions are presently used to provide three pressure ranges:

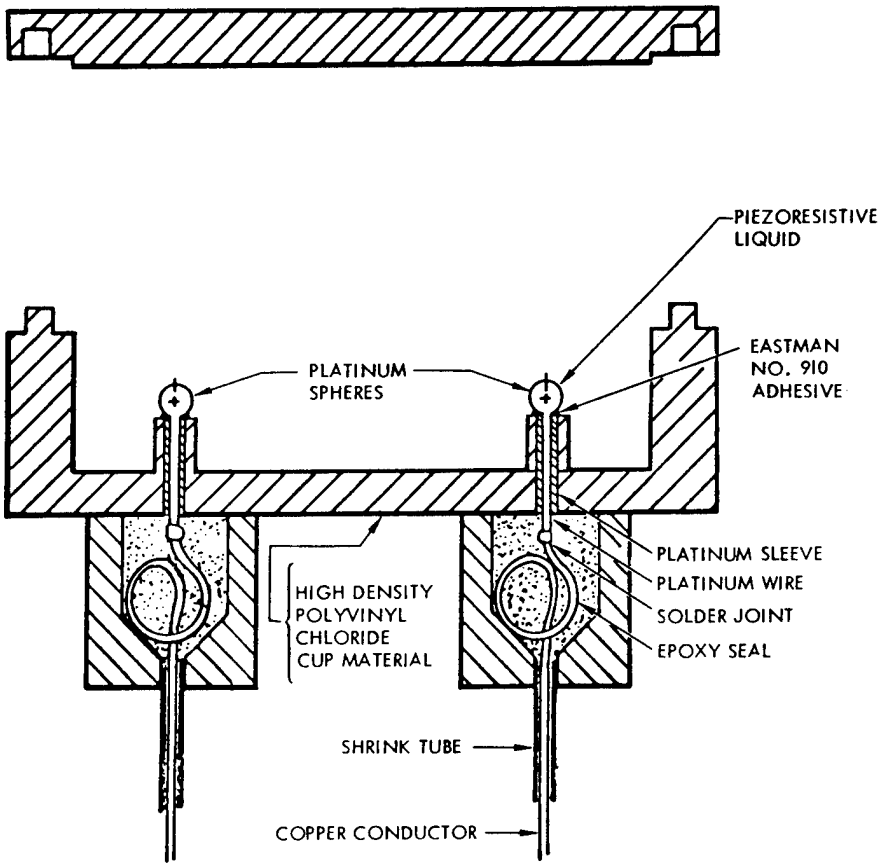

Figure 86. IITRI high-pressure electrolytic cell shock pressure gage.

1.	Carbon tetrachloride	150 to 350 kb
2.	Paraffin	50 to 150 kb
3.	Ammonia	5 to 50 kb

Recording times of from 5 to 200 microseconds have been achieved, depending on the peak pressure level and the distance from the burst.

Like the manganin gages, the IITRI cell is subject to the triggering problem for oscilloscope recording, but this purely electronic problem can be solved with the present level of technology. There is the possibility that the EM pulse and initial radiation in a nuclear burst will produce changes in the cell that will result in a false determination of pressure. The developers of the gage at IITRI felt that this was not the case and tested the gage in simulated nuclear environments.

Ref: Rowland, R.H., "Blast and Shock Measurement State-of-the-Art Review, DASA 1986, 1967.

6.4.4 SRI Calcium Gage (USA) (1964).

The SRI calcium gage is designed for measurements in the 5- to 25-kb range. A thin film of piezoresistive calcium is vacuum-vapor deposited on an optically flat substrate. The general configuration of the sensor is shown in Figure 87. The piezoresistive element is located within the insulating medium and lies in a plane which is parallel to the shock front. It is in the form of a four-terminal network which permits resistance measurement of only its central portion, thus avoiding effects due to contact resistance between the leads and the element. Electrical connections to the piezoresistive element are by means of four leads embedded in the insulator and oriented perpendicular to the plane of the shock front. When the shock crosses the element, it produces simultaneous compression and acceleration. The result is a fast transducer response with preservation of electrical continuity. A rise time of 20 nanoseconds and a 10-microsecond recording time have been achieved.

Ref: Williams, R.F., "Pressure Transducer for Measuring Shock Wave Profiles, Phase X: Measurement of Law-Pressure Shock Wave Profiles," DASA 1653, 1965.

6.4.5 BRL Sulphur Gage (USA) (1961).

In the BRL sulphur gage, shown in Figure 88, the main body of the gage is made of Teflon, which was selected because it is non-polar and does not generate spurious signals when shocked, does not conduct at pressures below several hundred kilobars, and is a close match to the shock impedance of sulphur. The gage is prepared by machining a shallow cavity in the Teflon base. The Teflon is drilled and copper electrodes are pressed into place. Gold foil, 0.001-inch thick, connects the copper electrodes to the cavity region where the sulphur is placed. Vacuum-melted sulphur is cast into the cavity. After it solidifies, the excess is ground away, leaving a thin layer of sulphur, 0.007-inch thick, to bridge the gap between the gold foils. The 0.007-inch sulphur thickness permits adequate time resolution for most measurements. Teflon front-insulation, usually 0.010-inch thick, it bonded to the surface with an epoxy matched to the density of Teflon by the addition of inert filler. The 0.010-inch

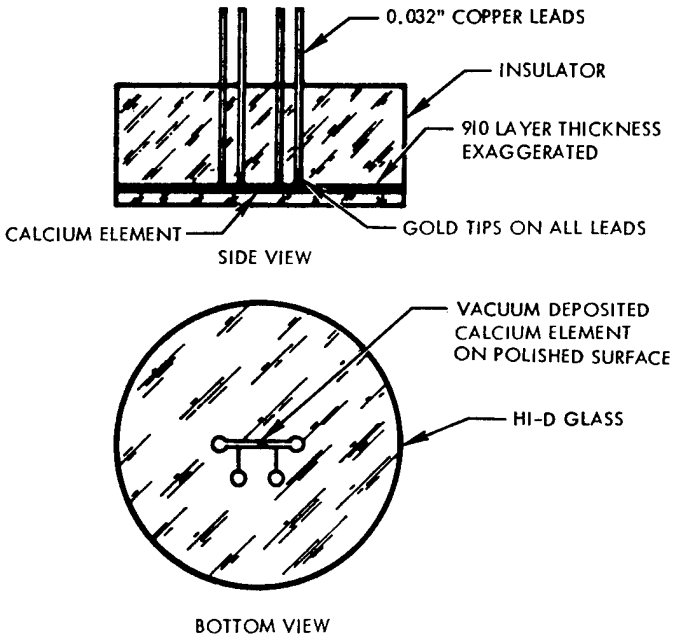

Figure 87. SRI calcium pressure gage.

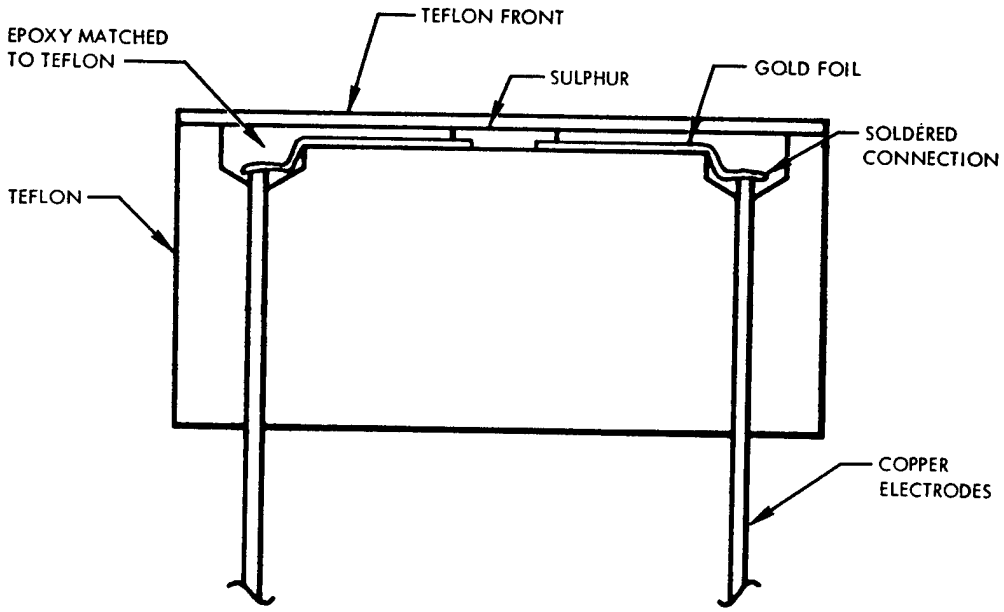

Figure 88. BRL sulphur gage.

thickness of the Teflon front permits the sulphur to be close to the point where the measurement is desired and minimizes attenuation.

While some degree of success has been achieved using this gage in the laboratory, no attempt has yet been made to use it in field tests. Some possible shortcomings should be pointed out. First, the influence of temperature on conductivity has been neglected, in that the compression-temperature relationships associated with the shock jumps used for calibration have been assumed to be the same as the compression-temperature relationships existing under conditions of the pressure profile measurements. Second, although compressed sulphur is assumed to be an intrinsic semiconductor, impurities may influence the conductivity and could introduce reproducibility problems. Both of these shortcomings were considered in further investigations.

Ref: Hauver, G.E. and Netherwood, P.H., "Pressure Profiles of Detonating Baratol Measured with Sulphur Gauges," BRL Technical Note 1452, 1962.

6.4.6 Sandia Thin Quartz Gage (USA) (1965).

The Sandia thin quartz shock pressure gage uses one or two x-cut synthetic quartz discs, 0.5 inches in diameter and 0.05-inches thick, mechanically coupled to the surrounding medium (invariably rock) with a matching grout. Figure 89 shows the two types of gages.

Unidirectional stress along the x-axis produces a piezoelectric charge proportional to the area of the quartz, the stress level, and the piezoelectric constant of quartz. This charge is integrated by accumulation on a capacitor, and a voltage-controlled oscillator located near the transducer is used to provide an amplified signal for recording.

The quartz delivers a net positive charge; thus, should a negative charge from some other source be stored in the capacitor, the voltage out of the emitter follower could indicate a stress lower than the actual stress because a portion of the positive charge from the quartz would be required to destroy the negative charge stored on the capacitor.

In one application in HE simulation, the presence of an EM-like disturbance triggered the recording oscilloscopes and the data were either obscured in the disturbance or arrived following the oscilloscope sweeptime. Fortunately, the data were also being recorded on FM tape so the pressure records were not lost. If nothing else, this experience should indicate the value of dual recording and show that even in chemical explosions, precautions must be taken to avoid the bias of recorded data from electrical disturbances resulting from the detonation.

Ref: Bass, R.C. and Hawk, H.L., "Close-In Shock Studies, FERRIS WHEEL Series, FLAT TOP I Event," POR 3005, 1965.

Chabai, A.J., "Close-In Phenomena of Buried Explosions," DASA 1382, AD423422, 1963.

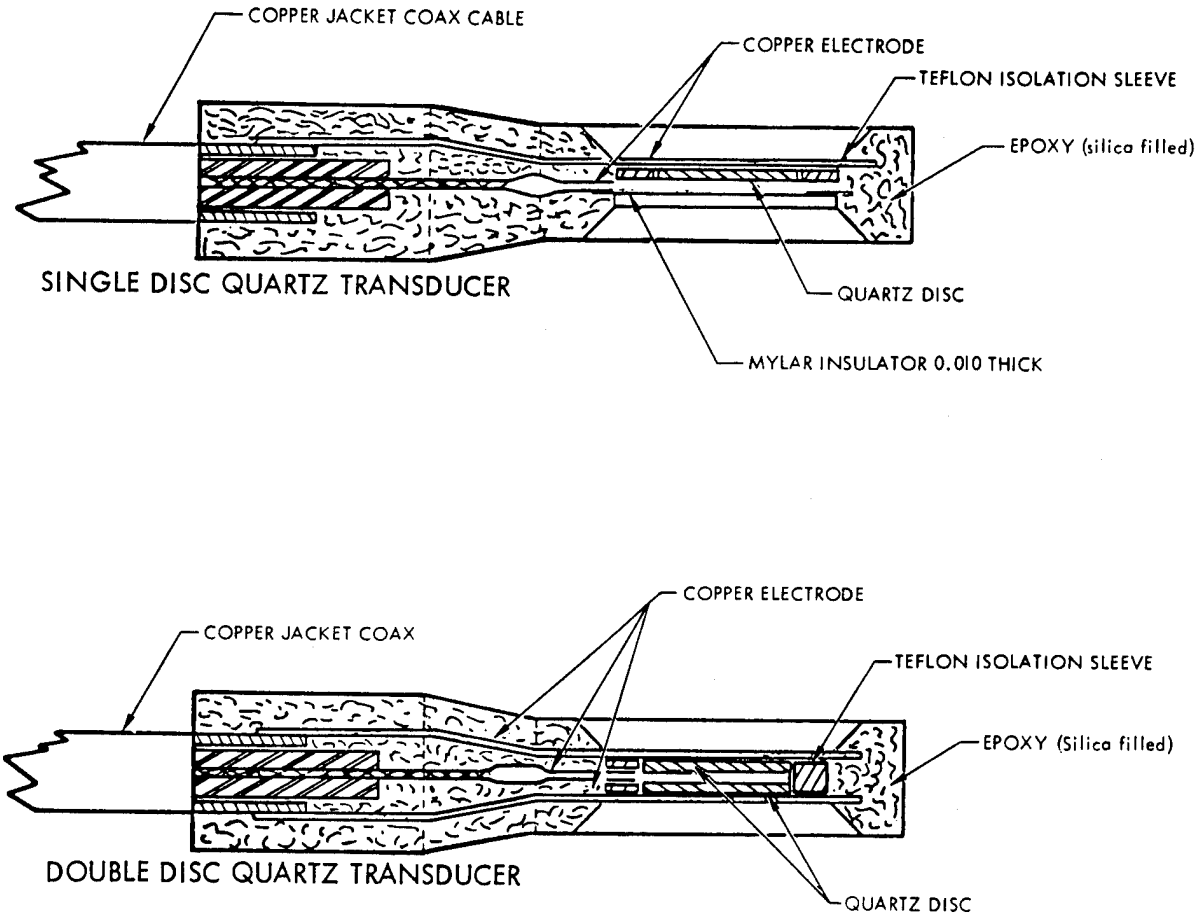

Figure 89. Sandia thin quartz pressure gages.

6.4.7 Commercially-Available Gages.

Air Pressure

80s	Endevco Model 8530B, piezoresistive Kulite XT-190, piezoresistive Kulite HSK-11-375, piezoresistive

Users: All.

6.5 RATE GYRO.

6.5.1 Angular Velocity Rate Gyro (USA) (50s, 90s).

The rate gyro was used on a limited basis on both high explosives and nuclear test programs to determine the rate of overturning of vehicles. The early instrument was a catalogue item with the Giannini Company, manufactured to determine the rate of overturning of masses which have been subjected to linear and angular accelerations.

Essentially, the Giannini gyro is a pneumatically damped unit which varies the resistance of a potentiometer as a function of angular velocity. The potentiometer was arranged in a conventional bridge circuit, the output of which was coupled to the recording system by means of a slightly modified Wiancko coupling unit. The recording system was non-linear.

The DC voltage required to drive the rotor of the rate gyro was obtained from the battery of the vehicle on which the gyro was mounted, and was applied at -30 minutes using the timing signal applied to the instrument shelter. It was found in the 50s that the Giannini gyro needed a recording system with a linear response and with added circuitry to eliminate undersireable effects.

In the 90s, Humprey Model FG40-0101-1 gyroscope was used. These were spring-driven free gyros mounted on 0.25-inch (6.4-mm) Sorbothane. They used an output potentiometer configured as a two-arm active Wheatstone bridge.

The Giannini and Humprey gyros are shown in Figure 90.

Ref: Meszaros, J.J. and Randall, J.I., "Structures Instrumentation, Operation UPSHOT-KNOTHOLE, WT-738, 1955.

Raley, R.J., et al., "Truck/Shelter Test, DISTANT IMAGE," DISTANT IMAGE Symposium Report, Vol III, POR 7379-3, 1992.

6.6 TIME MEASUREMENTS.

6.6.1 SLIFER Cable (USA) (1960).

A continuous measure of shock front position was obtained by the effect of the shock crushing a cable. The SLIFER (Shorted Location Indicator by Frequency of Electrical Resonance) gage is an electrical transmission line which is embedded in the earth so that the stress wave will move along the length of the cable. The cable is physically weak in comparison with the stress produced by the shock front and will thus be shorted at the shock front by crushing. This short will move with the local shock velocity in the medium.

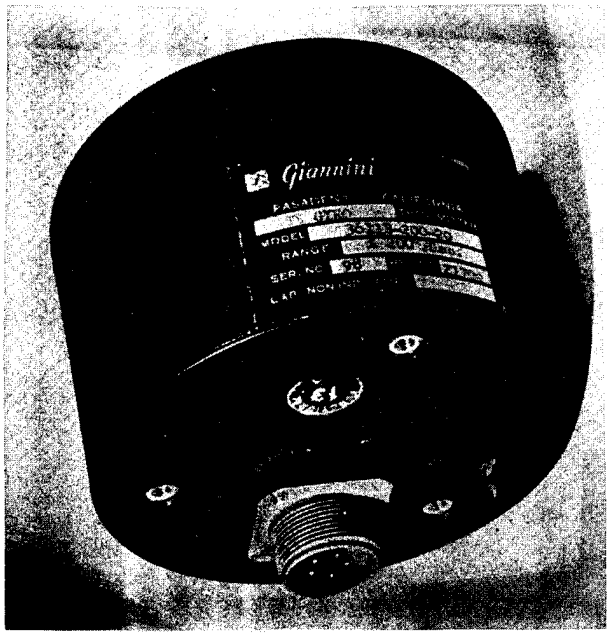

a. Giannini gyro.

Figure 90. Rate gyros.

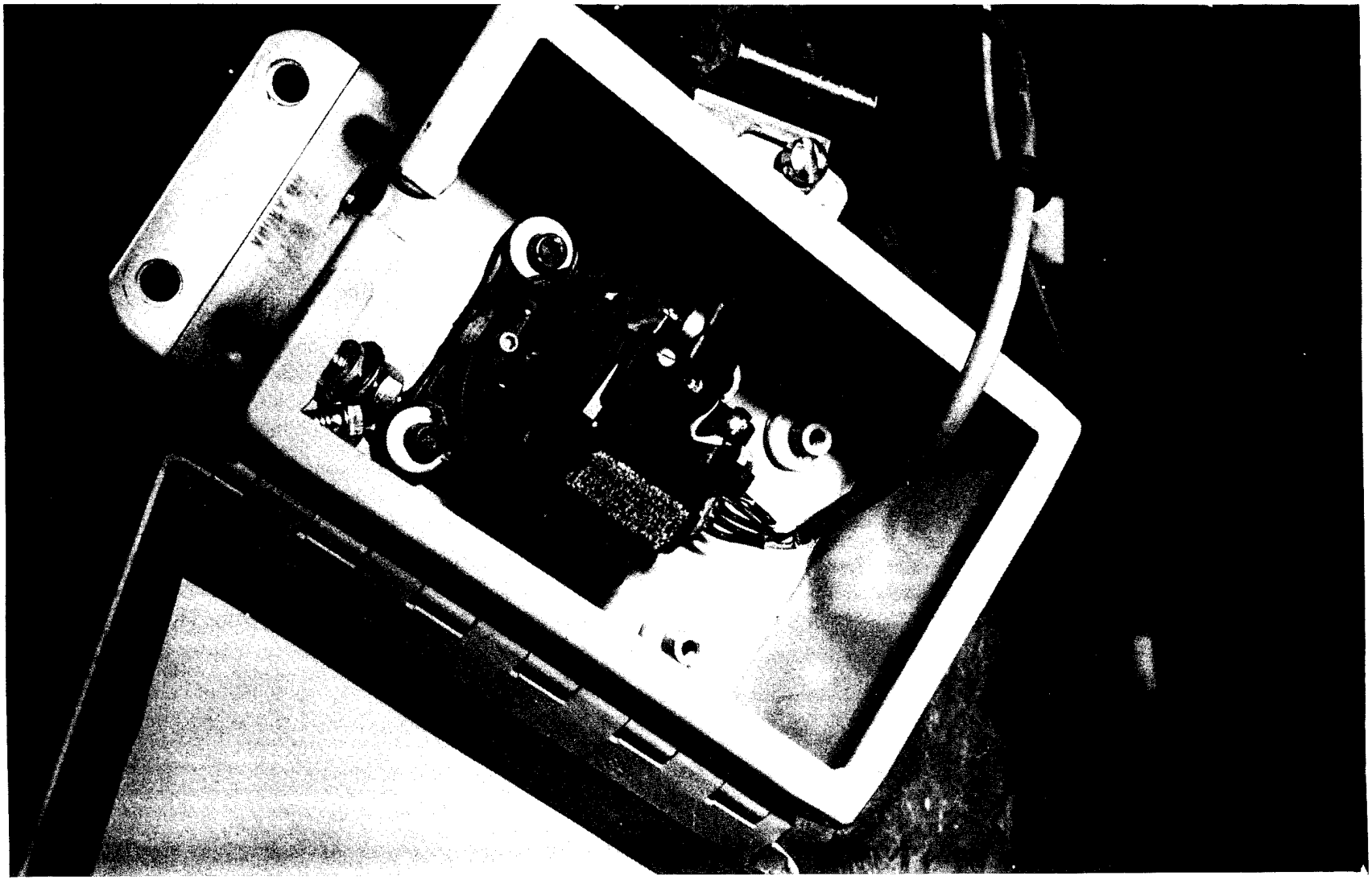

b. Humphrey gyro.

Figure 90. Rate gyros (Continued).

The transmission cable constitutes an inductive impedance in a tuned circuit of a Colpitts oscillator, its inductance being related to the cable length. As the shock front continuously shortens the buried cable, the frequency of the oscillator is increased in direct relation to the shock front position along the line. The output of the Colpitts oscillator is heterodyned with a crystal oscillator and the difference frequency recorded on magnetic tape.

The derivative of the relation of the shock front position versus time provides a measure of shock velocity versus distance. If the equation-of-state of the shocked medium is known, the shock pressure versus distance can be inferred.

In field operations, 1/2-inch air-dielectric coaxial Telcon cables are installed radially from ground zero at various depths, and attached to the oscillator. The Telcon cable has been found to crush at pressures above 1 kb. A solid-dielectric coaxial cable, RG-8, has been used when it was necessary to guard against the possibility of water penetration into the Telcon, or where there was danger of damage by the backfill operation. The RG-8 crushes at pressures above 10 kb.

After-the-detonation retrieval of the cable and a measurement of the distance of crushing serves as a check on the SLIFER technique since the distance to a pressure level of 1 kb (or 10 kb) can be directly measured.

Calibration of a resonance cable requires two measurements of the oscillator frequency, one with the cable shorted at its extreme end and the other with the cable shorted at the oscillator. For a cable 100 feet long, typical frequencies will vary from about 500 kHz at full length to 700 kHz at zero length. The frequency can be adjusted by changing lumped values of capacitance and inductance in the oscillator circuit.

Errors in shock position using this technique, arising from the measurement method and from the survey of initial cable placement, are believed to be no greater than about 6 inches. The accuracy of the pressure calculated from these positions is determined by how well the backfill matches the impedance of the undisturbed medium. In HE field tests it is common to position the cable three to six months in advance of the test to allow for natural settling and compaction.

Ref: Rowland, R.H., "Blast and Shock Measurement State-of-the-Art Review," DASA 1986, 1967.

6.6.2 AFWL Time-of-Stress-Arrival System (USA) (1965).

The AFWL time-of-stress-arrival system is a 100 channel inertial time-of-arrival system which was developed to measure stress arrival time in soils and rock.

In field operation a shock pulse associated with the dilatational and distortional waves triggers a buried omnidirectional inertia-switch sensor and a pulse is sent through high-level transmission lines. The switch closure is converted to a unidirectional standard pulse by a monostable single-shot multivibrator. This pulse energizes a neon glow tube on a display console. The total optical display consists of a matrix of glow-tubes having a geometrical relation to the sensor locations. The glow tube output is photographed by a high-speed

framing camera. Timing is obtained by Beckman type 605A decade counting units on the console.

A group of these sensors, distributed throughout the depth of vertical holes, yields the time history of the waves at a given distance from ground zero. By combining the data from a number of vertical arrays, a two-dimensional time history of the waves may be found.

The sensors from each vertical array are connected to a transmission cable through a junction box containing an EM pulse overvoltage protection device. The system junction combines the two functions by utilizing a printed-circuit spark gap for both the connection of the sensor leads to the transmission cable and overvoltage protection. The electronic input circuitry requires only the overvoltage be held to 50 to 100 volts. Thus, the printed-circuit gap and a conventional NE-2 neon glow lamp across the input of the electronics are sufficient.

The sensor consists of a heavy mass in the form of a ball suspended on springs inside a light fluid-filled spherical shell. Changes in velocity or acceleration of the shell result in relative displacements between the mass and the shell. When the relative displacement equals the clearance between the ball and the shell, contact is made, a circuit is closed and the signal generated. Preliminary laboratory tests have indicated sensor closure rise times were less than one microsecond.

The response threshold of the sensor can be varied by changing the springs which support the mass, or by changing the viscosity of the damping oil, or both. Thresholds as low as 0.5 g and as high as 20 g may be obtained; thus, the system can record times of arrival of pulses of different magnitudes.

The system may also record the arrival of different waves since the recovery time of the system is about 1 microsecond (somewhat higher for the stiffer gages). The indicator on the optical display is lighted for one multivibrator period each time the sensor is activated, but a complete open-close-open cycle must be exhibited by the sensor or no further multivibrator action will occur. High-frequency ringing of the sensor will not result in more than one operation of the multivibrator since the oscillations will occur during the dead time of the one-shot multivibrator (i.e., the time during which the glow-tube is lit). A low-frequency ringing may be identified by the repetitive pulse train and can be accounted for during data analysis.

By using a quasi-digital display and high-level transmission lines, susceptibility to electromagnetic disturbances such as the EM pulse is materially reduced. Converting the data to pulses gives more freedom from background and permits data gathering under conditions impossible for conventional analog systems. Since the time-of-arrival sensor operates as a switch sending a 12- or 24-volt signal to the system, the signal level is sufficiently high to overcome the background noise which normally results in almost total signal obscuration in the case of the conventional analog systems operating at millivolt levels.

It was reported that only one difficulty occurred using the system. In one test the sensors were pressure-grouted within deep emplacement holes. The grout, under pressure, displaced the oil between the shell and the ball mass and immobilized the ball.

Ref: Robinson, M.G., "Multichannel Time-of-Arrival Instrumentation System," AFWL-TR-65-191, 1966.

6.6.3 Sandia Shock Wave Detector (USA) (1965).

Sandia Corporation had developed a shock wave detector which is a modification of the pressure-switch. Two lead-zirconate-titanate piezoelectric rings detect the stress wave arrival as shown in Figure 91. The local shock velocity can be calculated from the time difference in triggering the two elements if the emplacement geometry of the gage is accurately known.

Ref: Holzer, F., "Measurements and Calculations of Peak Shock Wave Parameters from Underground Nuclear Detonations," Journal of Geophysics Research, 70, 4, 893.

6.7 SOIL PARTICLE VELOCITY.

6.7.1 SRI Mark I (USA) (1960).

The SRI Mark I vertical particle velocity gage uses a linear differential transformer as the sensing element. The gage is shown in Figure 92.

A solenoid in the gage holds the transformer core in a raised position. The core is released and allowed to fall under the influence of gravity in a highly viscous oil. The motion of the core mass is opposed by flow of the oil around the moving core. The core attains an approximately constant velocity for a fall time of about 2 seconds with a total travel of 0.3 inches. The flowing oil exerts a force on the core that is proportional to the velocity of the mass relative to the case of the gage. This force is equal and opposite to the inertial force on the moving mass. The gages have a finite bandwidth over which displacement of the transducer in its case is proportional to the particle velocity. The core release is synchronized so that the ground shock (hopefully) arrives at the gage while the core is falling at a uniform velocity and while sufficient fall time remains to measure the velocity. The response of the gage is within 5 percent from 0.2 to about 200 Hz. The maximum range is about 64 fps. This range can be increased by using a more viscous oil; however, this would decrease the gage sensitivity.

The basic Mark I gage measures 1.2 inches in diameter and is 3.3-inches long (3.0 x 8.2 cm). Normally, a mounting flange 2.5 inches in diameter is attached to one end of the gage.

Ref: Rowland, R.H., "Blast and Shock Measurement, State-of-the-Art Review," DASA 1986, 1967.

6.7.2 SRI Horizontal Gage (USA) (1960).

The SRI horizontal gage employs the concept of an overdamped, low natural frequency, pendulum accelerometer. This is shown in Figure 93a. The maximum range of measurement is about 100 fps. The sensor is the coil assembly of a Wiancko variable reluctance element and a cantilevered mass in the form of a pendulum. The pendulum is flat in cross-section and is surrounded with a heavy silicone oil to allow extreme damping. With the pendulum hanging vertically, the undamped natural frequency is about 5 Hz (this varies somewhat between individual gages). When the pendulum is oil-damped, the frequency is lower due to the mass of the oil which moves with the pendulum.

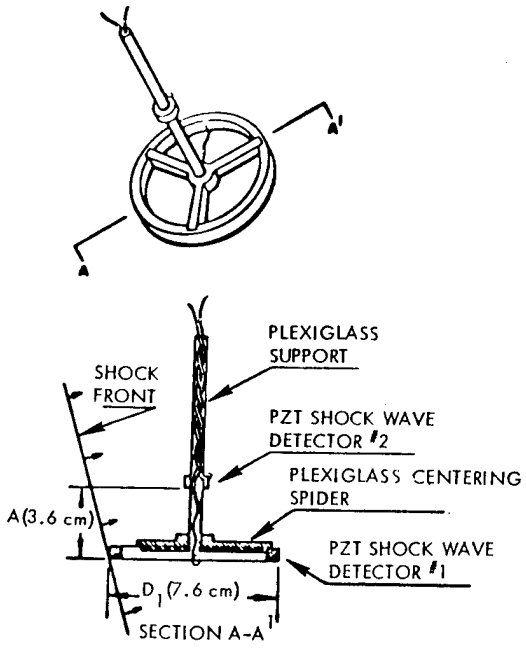

Figure 91. Sandia shock-wave detector.

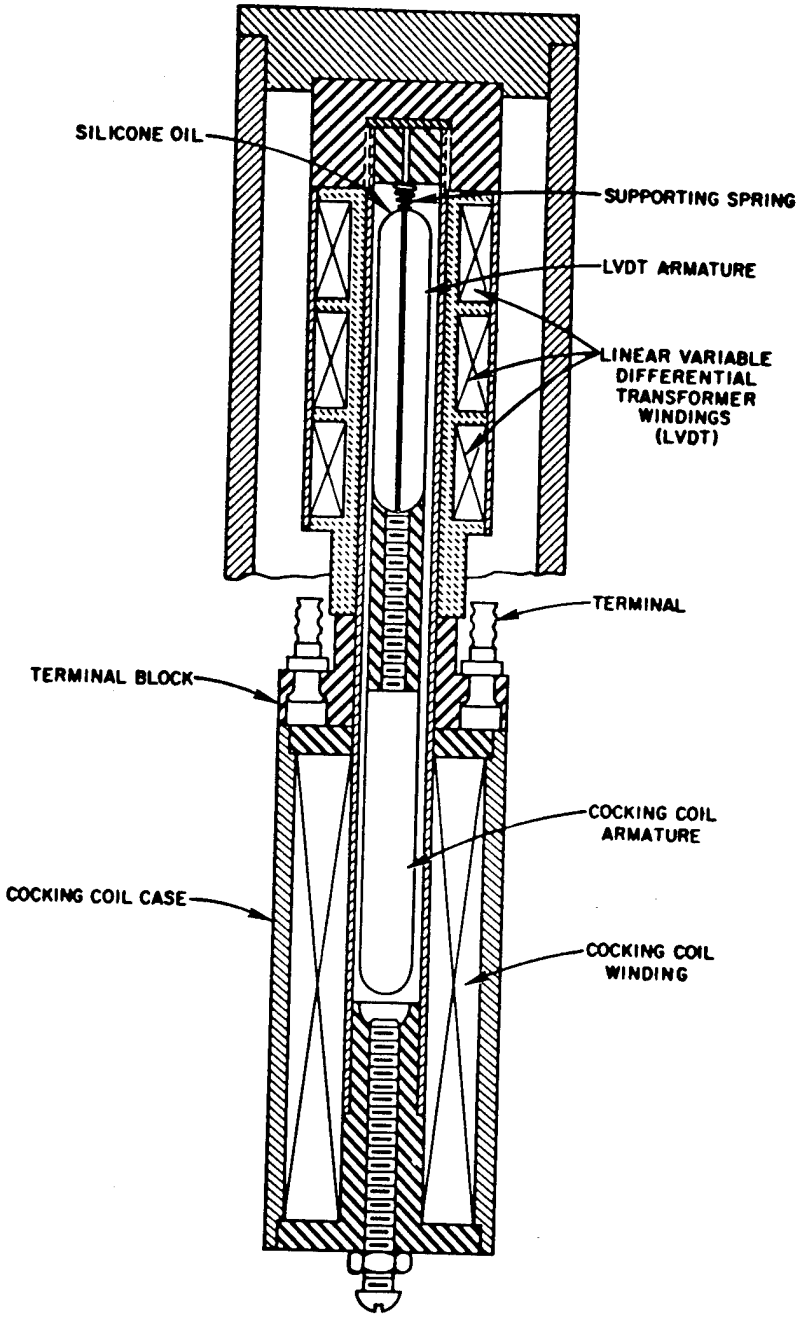

Figure 92. SRI Mark I velocity gage.

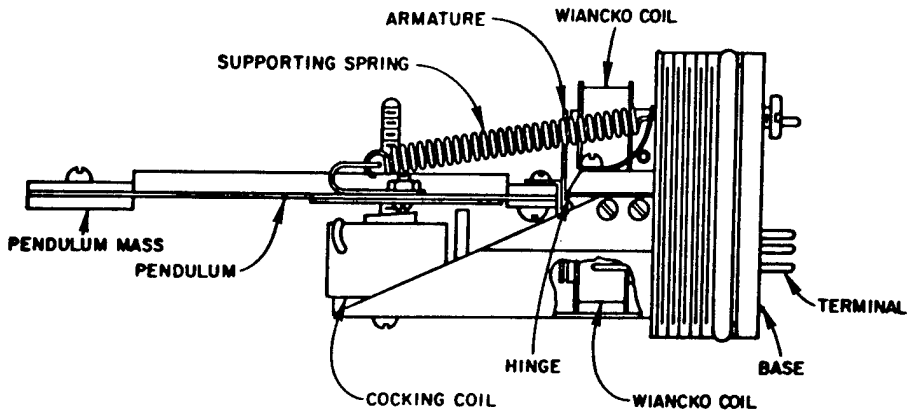

(a) Layout for horizontal measurement.

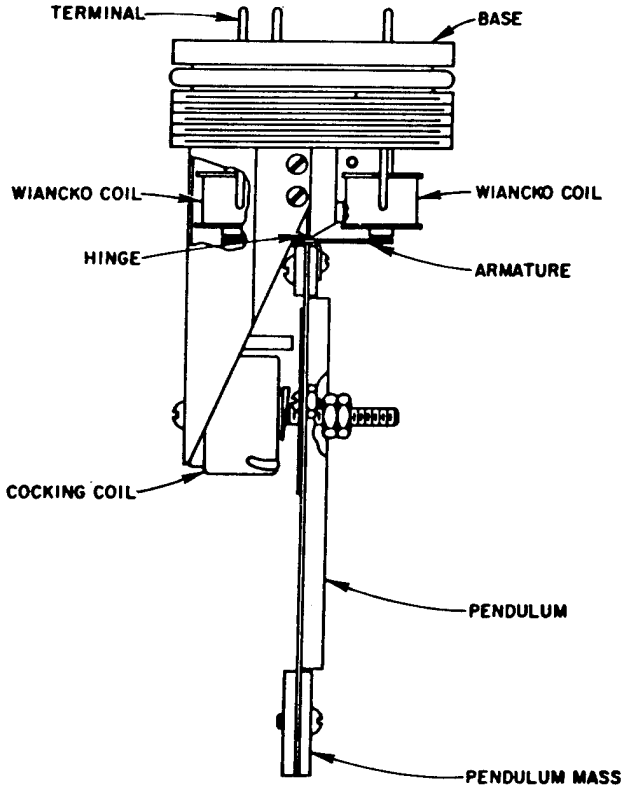

(b) Layout for vertical measurement.

Figure 93. Horizontal and vertical Mark II velocity gage.

The deflecting coil assembly, which (when energized) pulls the moving elements off-scale to one side, serves several purposes. When the gage is mounted for true horizontal measurement, energizing and then releasing this coil provides a record from which the low-frequency time constants may be directly derived. When it is necessary to measure at some angle other than horizontal (up to 30 degrees from the horizontal), this coil serves to trigger the release of the moving element in a fashion similar to that of the vertical gage. Finally, for field calibration, the coil is energized, the gage is turned on its side, and a record is taken as the coil is released.

The horizontal gage was modified for the vertical position by the addition of a weak spring which supports the pendulum in a neutral position. This gage, called the Mark II, is shown in Figure 93b.

Ref: Swift, L.M., "Development of an Earth Velocity Gage," DASA-1191, 1960.

6.7.3 SRI Mark III Gage (USA) (1960).

The SRI Mark III vertical velocity gage was developed for an HE test in limestone to meet the need for a gage with an increased frequency response. The gage is shown in Figure 94.

The plunger in Mark III is the armature in the LVDT, instead of being a separate part coupled to the transducer as in Mark I. This reduces the mass of the moving parts of the gage. At the same time clearances are smaller than in the similar Mark I gage to increase the viscous force, and the length and oil volume are reduced to minimize false response to acceleration by compression of the oil. The gage is aperiodic, that is, no spring is provided to maintain it in the null position. A cocking coil is provided to lift the plunger to the top of its travel before the shot. Gage response is from 0 to >3000 Hz and measures velocities of 110 feet/second.

Like the Mark I, provision was made to release the plunger at a predetermined time before the shot so that the plunger would be falling during arrival of the signal. This feature produced much difficulty. The precise timing of the release was a matter of considerable importance. Since the rate of fall of the plunger is a function of the viscosity of the oil, which is temperature-dependent, release times had to be adjusted after the gages were in place and had come to thermal equilibrium with the surrounding rock.

Ref: Swift, L.M., "Development of Soil Displacement and Strain Gages," DASA 1267, 1961.

6.7.4 Sandia DX Gage (USA) (1964).

The Sandia DX is a modification of the SRI design. The DX is specifically designed to extend the range of particle velocity measurements into the 300 fps region and to withstand shock loads in excess of 1200 g. Sandia redesigned the pendulum suspension, the pendulum and the armature assembly. They designed a system for filling the gages with damping fluid (DC 200 silicone oil) under vacuum to eliminate the possibility of air mixing with the damping fluid and causing changes to the damping ratio, and they used a flexible bellows to accommodate temperature expansion of the damping fluid. Two models of the gage are produced. One with a brass pendulum, is designed to measure velocities in the 0.1- to 25-fps range, while the other, with an aluminum pendulum, is for the range of 10 to 300 fps.

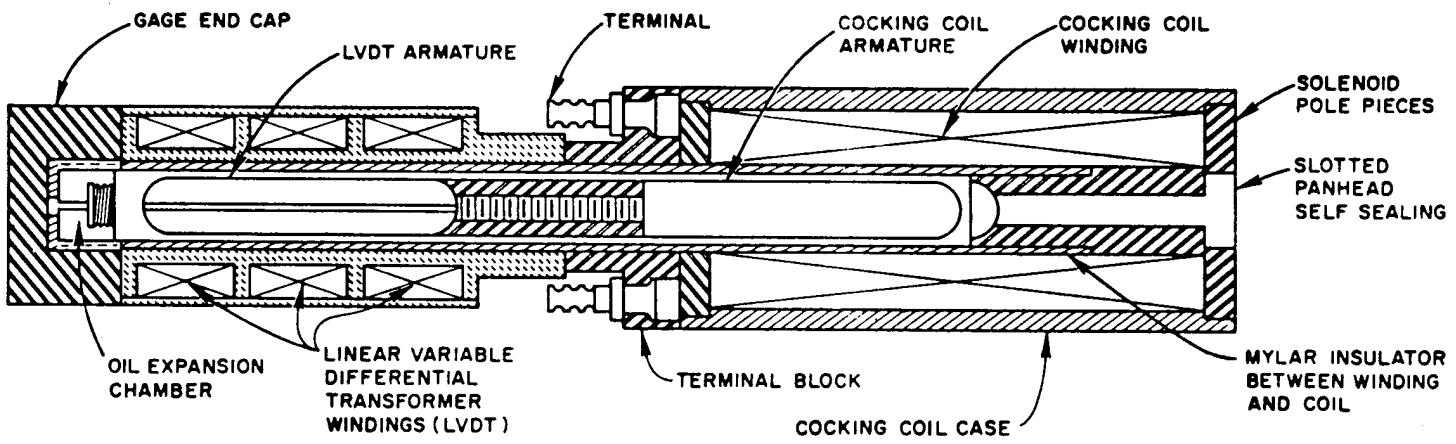

Figure 94. SRI Mark III velocity gage.

However, there are problems with the DX gage:

1. With a 3-kHz carrier, the maximum frequency response is less than 600 kHz,

2. The variable reluctance element can only be energized by an AC system (AFWL considers this to be a disadvantage - Sandia does not),

3. The mounting arrangement is poor, and a special housing is required, which increases the size and weight of the gage system, and

4. Any oil-damped gage is temperature sensitive.

Even with these limitations, AFWL reports that the DX is the best available field gage. It is very rugged and has produced reliable results from field tests.

Ref: Morse, T.B., "Instrumentation Accessories for Earth Motion Measurements," Sandia Corporation M-65-330, 1965.

6.7.5 SRI-AFWL Miniature Velocity Gage (USA) (1966).

The SRI-AFWL miniature velocity gage is a redesigned version of the Mark I gage. The Mark I gage was decreased in its size and weight and increased in its frequency response. The gage measures velocity transients from less than 2 cm/sec to above 600 cm/sec over a frequency range from 1 to 500 Hz. It senses velocity along one axis only and is not affected by crosswise accelerations up to at lease 30 g. The sensitive axis may be horizontal or vertical or inclined, provided a small external adjustment is made to counteract gravity. The gage is nearly a cube of about 5-cm edge length and weighs 375 gm.

The gage works on the principle of a highly overdamped spring-mass system with its undamped natural frequency at the geometric mean of its range. The relative displacement between mass and instrument case is a direct measure of the velocity of the case.

In the present model the mass consists of a thin rod suspended between two parallel cantilevered leaf springs, as well as a damping cup and the core of a LVDT which are rigidly attached to the rod. The cup slides with a radial clearance of about 0.04 mm over a stationary piston and provides viscous damping by shearing a viscous oil film between cup and piston. The LVDT, whose coils are embedded in the stationary piston, records the relative motion between the piston and cup.

The gage has been vibration-tested at frequencies from 0.25 to 1000 Hz and appears to be flat in the range 1 to 500 Hz, to within 5 percent. The smallest velocity it will sense is below 2 cm/sec, and the maximum velocity is above 600 cm/sec. An over range of about 50 percent is tolerated before the gage hits rigid stops, but the gage is nonlinear in the over-range region. The gage appears to be unharmed by accelerations as high as 40 g and perhaps more, but its acceleration tolerance has not been determined.

Gage sensitivity is affected by temperature changes by about 1 percent per °F. The gage shows a tilt signal which, for a horizontal gage, is about 1.5 percent of full scale per degree

of tilt. The gage is not affected by loads of up to 1000 pounds on the case. It will withstand shocks of approximately 4000 g along the sensitive axis and 1000 g along the cross axis.

Tests of the gage in soil indicate that its presence disturbed the motion field to the extent that the measured velocities may have been considerably in error; however, this same problem undoubtedly exists with all other velocity gages used in soil. The results of these tests indicate the gage measures the input velocity of shock-loaded soils to within about 10 percent.

This version of the SRI velocity gage is probably easier to use in the field than any of its predecessors. The square case may be more easily mounted on a surface than could the older round, pendulum-type gages.

SRI calculations indicate that it may be possible to raise the upper limit of the frequency range to 2000 or 3000 Hz without extensive redesign. At the same time, the maximum velocity allowed would be increased from 600 to about 3000 cm/sec, but with a corresponding drop in sensitivity. Conversely, an increase in sensitivity may be achieved by weakening the springs. This could increase the sensitivity by as much as a factor of four and lower the effective frequency range.

Ref: Chilton, E.G., et al., "The Development and Evaluation of a Miniature Velocity Gage," AFWL-TR-65-46, 1967.

6.7.6 EPCO Velocimeter (USA) (1964).

The EPCO (Engineering Physics Company) velocimeter employed the effect of mutual induction to measure particle velocity. An electrical conductor moving in a magnetic field will have an electronic potential developed across its terminals. Specifically, if a wire conductor is buried in the soil near an explosion, in the presence of a magnetic field, a voltage will be generated at its terminals when it is caused to move through the magnetic field by the impinging shock wave.

Ref: Danek, W.L. and Dargis, A.A., "Particle Velocimeter for use Close-In to Underground Explosions," DASA 1431-1, 1964 and DASA 1431-2, 1965.

6.7.7 EPCO Faraday Gage (USA) (1964).

The EPCO Faraday gage employs the principle of the deformation of a wire by a shock wave in the presence of the earth's magnetic field which gives rise to a measured voltage. The faraday gage is presented in Figure 95.

Ref: Danek, W.L. and Dargis, A.A., "Particle Velocimeter for use Close-In to Underground Explosions," DASA 1431-1, 1964 and DASA 1431-2, 1965.

6.7.8 EPCO Self-Inductance Gage (USA) (1964).

In the self-inductance gage, a strong magnetic field is established by passing a large current through a parallel wire system. The gage is shown schematically in Figure 96.

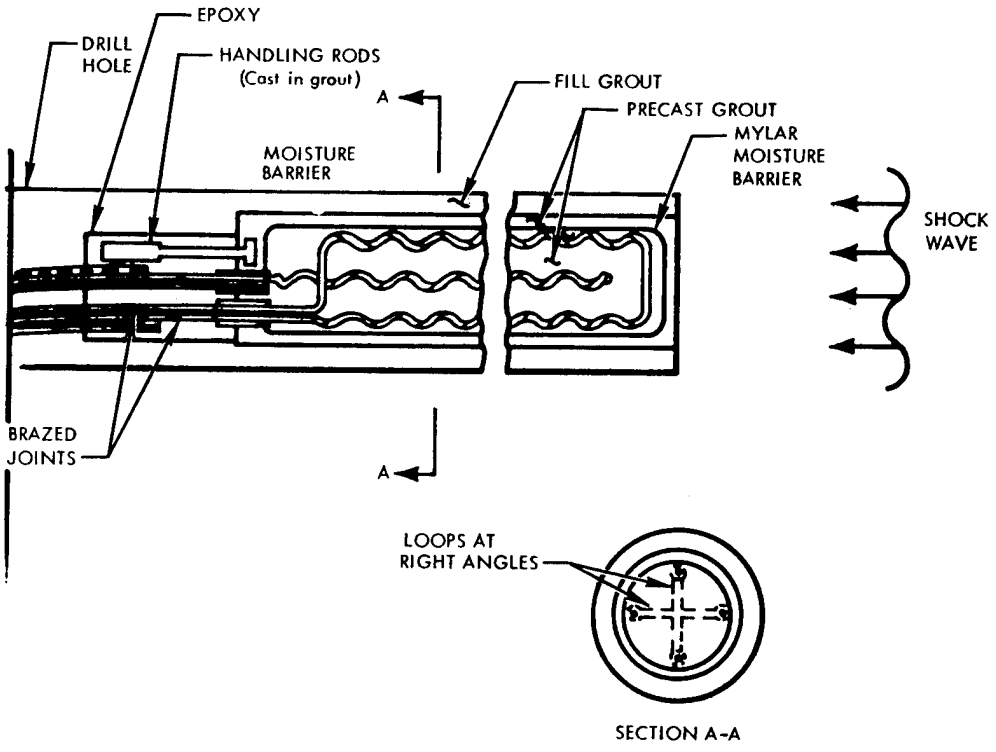

Figure 95. EPCO Faraday induction velocimeter.

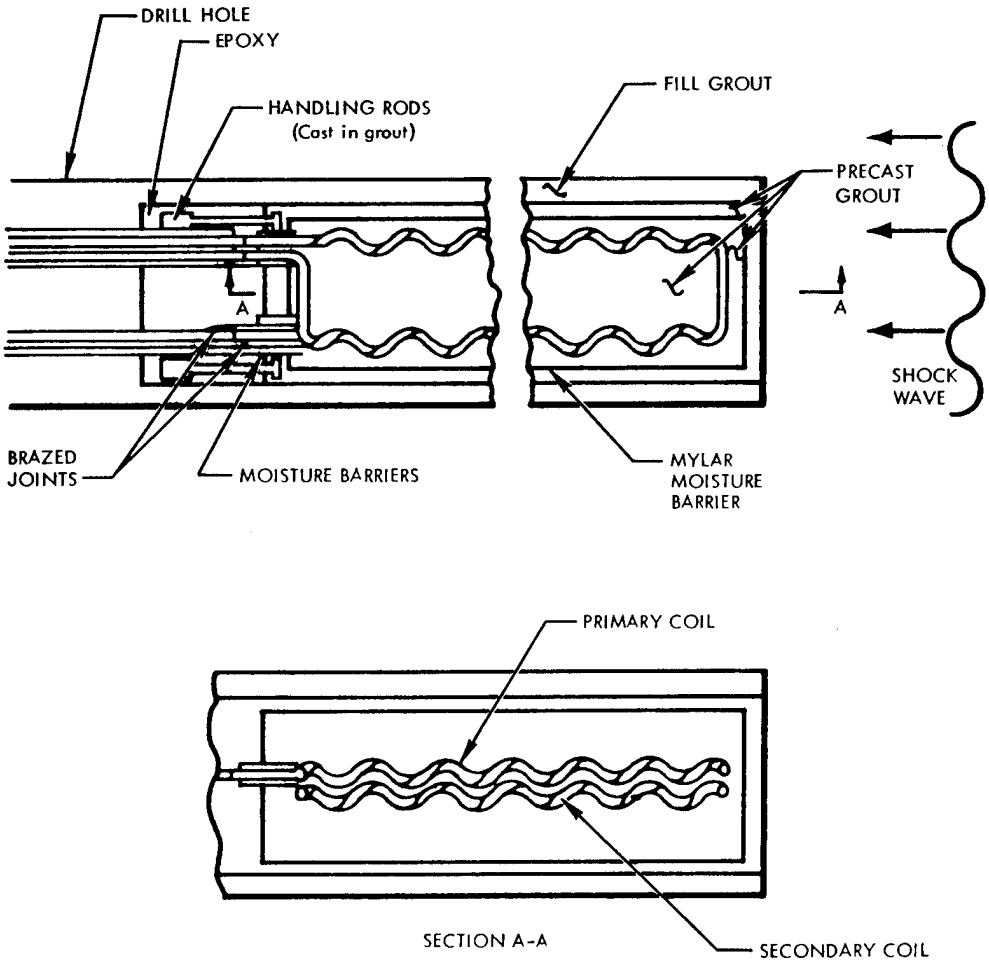

Figure 96. EPCO self-inductance particle velocimeter.

As this electrical configuration is deformed by the shock wave, the voltage generated is used to measure particle velocity. The mutual inductance per unit length between the two circuits is measured as the shock front shortens the circuits along the x-axis. The device was designed to measure velocities as high as 1000 ft/sec. The limiting factor in recording time is the technical problem of keeping the conductor in one piece in the presence of the shock wave, as times of up to 100 microseconds are anticipated.

Since the EPCO analysis of methods of particle velocity measurement was made, laser technology has undergone a tremendous advancement. It is probably technically possible, using a vacuum light pipe or perhaps fiber optics, to determine the particle velocity. The advantages of a laser technique would be considerable in that EMP would be less of a problem.

Ref: Danek, W.L. and Dargis, A.A., "Particle Velocimeter for use Close-In to Underground Explosions," DASA 1431-1, 1964 and DASA 1431-2, 1965.

6.7.9 CEC Velocity Pickup (USA) (1964).

The CEC velocity pickup is a spring magnet device with a total travel of 0.5 inches, Consolidated Electrodynamics Corporation Model 4-106H. The standard gage was modified by rewinding the coil with a larger wire and fewer turns to produce a voltage in the 500-ohm load of about 40 mv per inch per second of velocity. If subjected to a velocity of about 500 inches/second, the peak signal would be a very respectable 20 volts. The low-frequency response limit is set by the natural frequency of 5 Hz which permits satisfactory operation at 10 Hz and above. The gage was tested on a shake table and found to be operative at 4000 g.

Ref: Rowland, R.H., "Blast and Shock Measurement, State-of-the-Art Review," DASA 1986, 1967.

6.7.10 Crescent Velocity Pickup (USA) (1965).

The Crescent Manufacturing Company velocity gage is self-generating and consists of a solenoid and a magnetized plunger. The solenoid is composed of two coils mounted end-to-end within a nonmagnetic tube. Motion of the magnetized plunger induces a voltage in each winding proportional to the particle velocity. The gage is arranged as a closed cylinder with the magnetic plunger resting at the lower end. Earth motion causes the cylinder to move relative to the plunger, creating an electrical output. Motion of the plunger compresses the air, which damps the motion of the plunger relative to its case. Output of the VE-200 series was determined by SRI to be 100 mv/in/sec with the two windings connected in series adding.

Ref: Sauer, F.M. and Vincent, C.T., "Close-In Earth Motion Studies/Pressure Measurements in the Hydrodynamic Region (U)," POIR 3016, 1966. (CONFIDENTIAL-RESTRICTED DATA)

6.7.11 DRES Velocity Transducers (Canada) (1970).

For studying the drag on cylinders produced by a blast wave, the cylinders were mounted so that they were free to move when struck by the blast wave. Velocity transducers for

measuring directly the velocity of each cylinder (horizontally mounted, 3.5 - 12 inches in diameter) as a function of time were based on the principle that a permanent magnet travelling through a coil produces a voltage which is directly proportional to the velocity of the magnet within the coil. A pair of transducers connected in parallel was used on each cylinder so that the voltage output was proportional to the average velocity of the two ends of the cylinder. The transducers used at all locations other than that at the lowest pressure level were Hewlett-Packard Model LV syn 6LV4 with a four-inch nominal working range. The cylinder had Model 6LV2 transducers installed which used only a 2-inch nominal stroke. The magnetic rod in each transducer coil was extended by a brass rod fastened to an aluminum eyelet which passed over the shaft on each end of the cylinder.

The output of the transducers was sufficiently high that no amplification was necessary. The output of the transducer pair was simply fed through a potential divider consisting of two resistors mounted on the outside of the base plate into a strain gage cable passing underground to the recording bunker. The strain gage cable was connected to a magnetic tape recorder and the voltage-time output recorded.

Ref: Mellsen, S.B., "Drag Measurements on Cylinders by the Free-Flight Method," Event DIAL PACK Symposium Report, Vol 1, Defence Research Board, Canada, 1971.

6.7.12 Commercially-Available Gages.

60s	Sparton Southwest Inc. 601 Hewlett-Packard Model LV SYN 6LV4, 2

Users: Canada

6.8 Flexible Measuring Devices (USA) (1955).

Flexible measuring devices were designed to determine the influence of structural flexibility on the perpendicular loads generated against a structure by earth propagated pulses. Each device consisted of a forward mass, 30 inches square, connected by torque tubes to a relatively heavy rear supporting mass. Normal loads resulting from the pressure pulse acting against the front face of the forward mass could be measured.

There were groups of three flexible measuring devices; within each group of three devices one of the four parameters assumed to be of greatest importance in influencing dynamic structural flexibility was varied so as to study the influence of this particular parameter. The four parameters were: (1) the static structural flexibility as indicated by deflection under static loads, of the loaded structural element, that is the forward mass as supported by the torque tubes; (2) the mass of the loaded structural element; (3) the mass of the structure supporting the loaded structural element; and (4) the length of the structure in the direction of pulse travel.

Shown in Table 6 is the various combinations of length, stiffness, and mass used for the different flexible structures and the instrumentation used on them. Each flexible measuring device consisted of a loaded structural element of mass M. This was supported by four torque tubes, with some stiffness K, mounted on a relatively heavy main structure of mass

Table 6. Instrumentation of flexible measuring devices.

X indicates presence of a measuring channel.

Device[1]	L (ft)	M (lb)	K in/psi	S[2] (lb)	Pressure	Acceleration	Strain
FMD1	10 L2	483 M2	0.001 K4	8933 S2	X -	X -	X -
FMD2	10 L2	483 M2	0.03 K3	8933 S2	X -	X -	X -
FMD3[3]	10 L2	483 M2	0.06 K2	8933 S2	X -	X -	X -
FMD4	10 L2	483 M2	0.09 K1	8933 S2	X -	X -	X -
FMD5	10 L2	263 M1	0.06 K2	8933 S2	X -	- -	- -
FMD6	10 L2	993 M3	0.06 K2	8933 S2	X -	- -	- -
FMD7	10 L2	1503 M4	0.06 K2	8933 S2	X -	- -	- -
FMD8[3]	10 L2	483 M2	0.06 K2	8933 S2	X -	X -	X -
FMD9	20 L3	483 M2	0.06 K2	8955 S2	X -	- -	- -
FMD10	5 L1	483 M2	0.06 K2	8727 S2	X -	- -	- -
FMD11	30 L4	483 M2	0.06 K2	8786 S2	X -	- -	X -
FMD12	10 L2	483 M2	0.06 K2	16,803 S1	X -	- -	X -
FMD13[3]	10 L2	483 M2	0.06 K2	8933 S2	X -	X -	X -
FMD14	10 L2	483 M2	0.06 K2	6254 S3	X -	- -	- -
FMD15	10 L2	483 M2	0.06 K2	3577 S4	X -	- -	X -

[1] In addition, two pressure gages, FFG-1 and FFG-2 were located in the medium at the same distance as the devices to determine free-field pressure.
[2] Actual weights of "S" devices furnished by Mason & Hanger-Silas Mason, Las Vegas, Nevada.
[3] FMD3, FMD8, and FMD13 are standard comparison instruments.

S. Each loaded structural element was of uniform flexibility over the entire loading surface. The various flexibilities of the loaded elements were arbitrarily expressed as the deflections resulting from a static pressure of 1 psi on the 30 inch square front face. The deflections for four different stiffnesses were K1 = 0.09 inches, K2 = 0.06 inches, K3 = 0.03 inches, and K4 = 0.001 inches. These devices are shown in Figures 97, 98, and 99.

The loaded structural element consisted of a 3/4-inch steel plate, 30-inches square, mounted on torque tubes and stiffened with a 3 and 3/4-inch thick reinforced concrete plate also 30-inches square. The entire combination weighed 483 pounds. The mass of the supporting structures for all devices except three varied between 8727 and 8955 pounds. As seen in the table, the others were 16,803 pounds, 6254 pounds, and 3577 pounds.

Figures 100 through 105 show the devices in various stages of preparation and final installation. Only certain devices were instrumented with pressure, acceleration, and strain sensors.

Ref: Dohrenwend, C.O., et al., "Flexible Measuring Devices and Inspection of Operation JANGLE Structures," WT-1125, 1958.

6.9 Recording Systems.

Recording systems used to record the signals from the electronic gages were the same as those used to record from pressure gages in the free field. These systems are described in Section 4.9 of Volume II, "Measurement Techniques and Instrumentation - The High Explosive Era, 1959-1992."

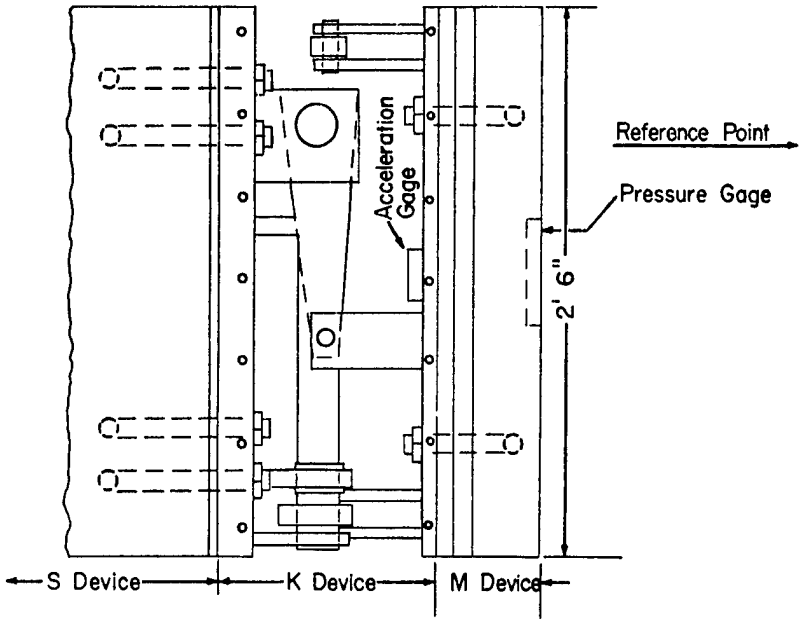

Figure 97. Elevation of assembled S, K, and M devices.

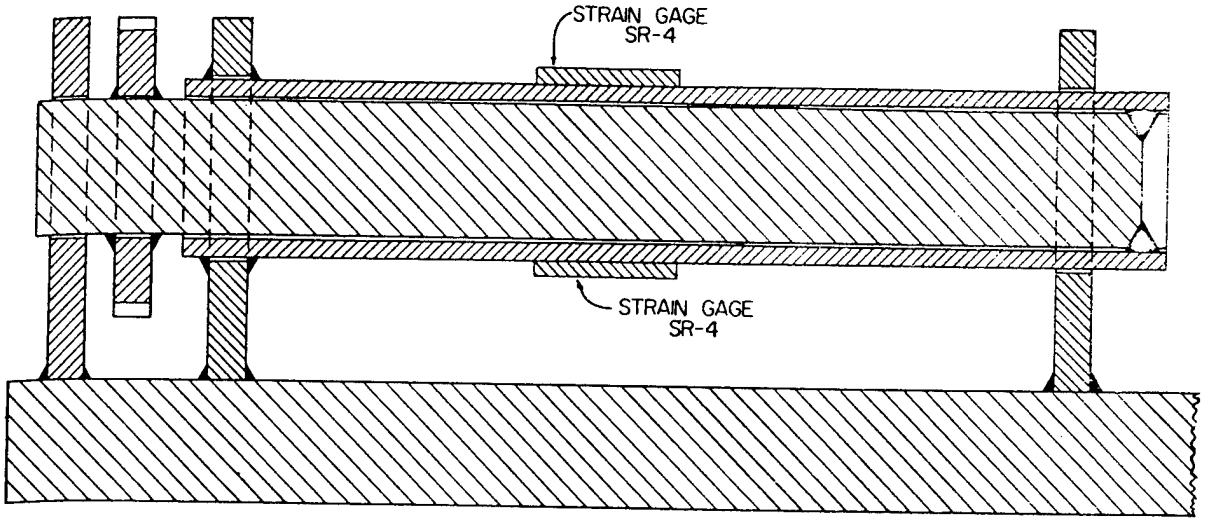

Figure 98. Torque tube for K1 and K2 devices.

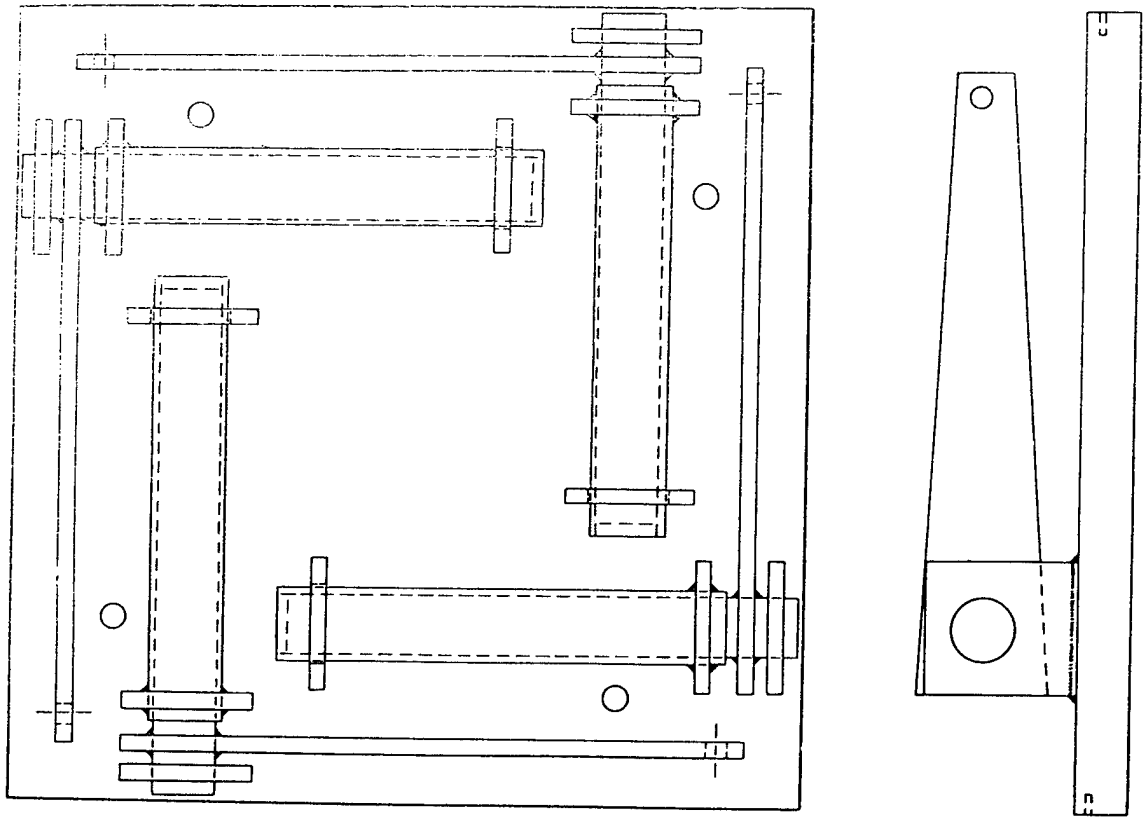

Figure 99. Typical torque layout.

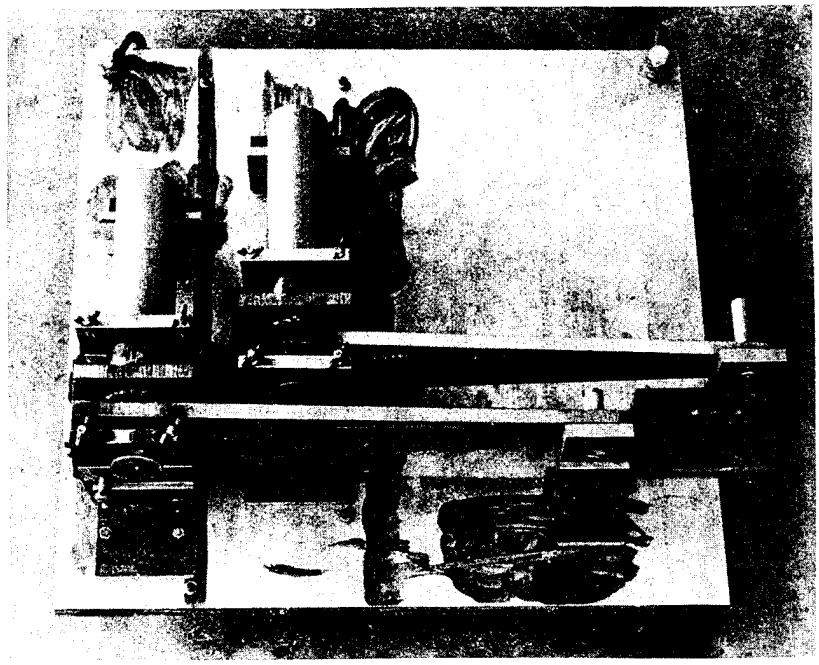

Figure 100. Jig for positioning torque tube support.

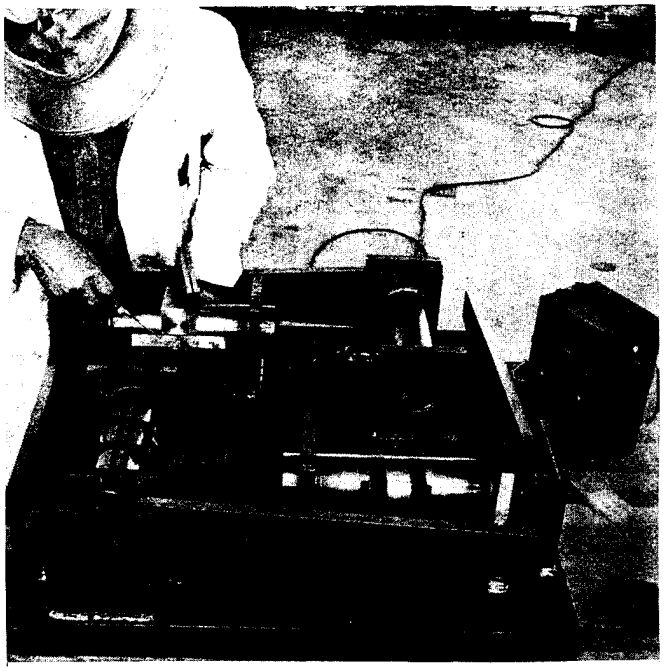

Figure 101. Strain gage application.

Figure 102. M and K devices at site.

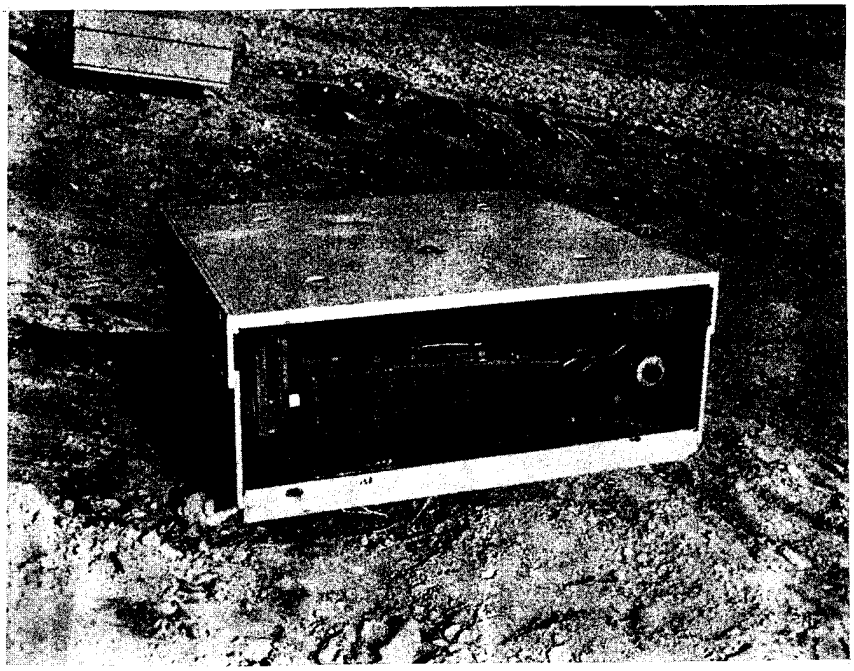

Figure 103. Flexible device K4.

Figure 104. Installation of K device.

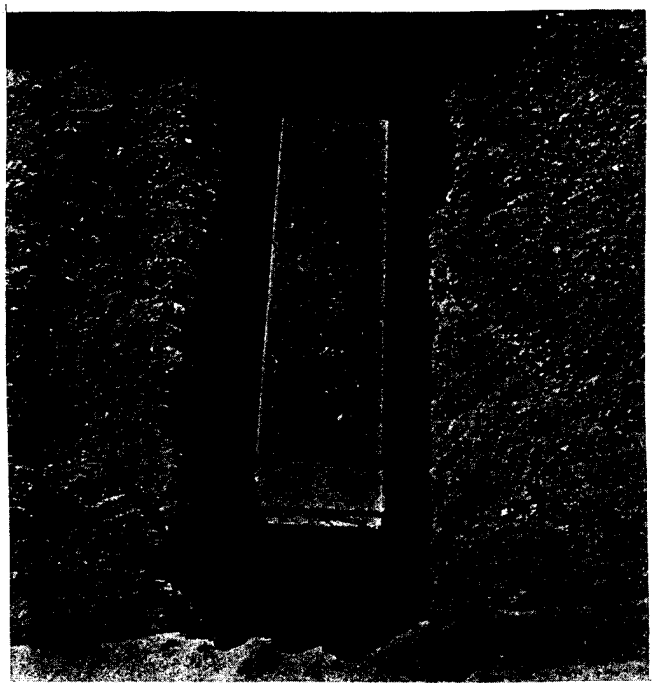

Figure 105. Complete assembly.

SECTION 7

GAGE CALIBRATION TECHNIQUES

The American Society of Mechanical Engineers in the 70s produced A Guide for the Dynamic Calibration of Pressure Transducers. The guide was originally published as American National Standard ANSIB88.1-1972. Currently the document number is ANSIMC88.1-1972. In this document, calibration is defined as "a test during which known values of measurand are applied to a transducer and corresponding output readings are recorded." Others would say that calibration is a process of comparison of the output of an instrument to the output of a validated transfer standard.

What is a transfer standard? A transfer standard is explained via the following example. The clock used in the validation of the speedometer was calibrated by comparing its output to the one at the National Institute of Standards and Technology (NIST). The clock at NIST is validated by relating its output to a fundamental atomic vibrational frequency. The NIST clock becomes a transfer. Since one can seldom compare an instrument to the primary transfer standard, intermediate (secondary) transfer standards are used, sometimes several in a chain. An instrument which has been calibrated by comparing it to one of the secondary transfer standards is then said to be traceable to NIST.

Validation is another word often used and is defined as a process by which one can determine the instrument output for a known input function. A known input is often difficult to get. In order that the input function be known, fundamental quantities must be traceable to first principles. A speedometer for instance can be validated by measuring the distance traveled and the time of travel.

A static and dynamic calibration is a very necessary and desirable part of any testing procedure. The dynamic calibration is needed for the selection of blast wave transducers intended for use in large-scale field tests. The transducer's natural frequency, rise time, possible deviations from static calibration, and other such characteristics may be observed during the dynamic calibration of the transducer.

Calibration devices take many forms; each is designed to calibrate gages over a specified range of the measurand, to determine frequency response, and to determine response to temperature and acceleration.

Calibration generally requires a measurement system with known accuracy and a test unit which is certified against this system. In most cases, a transducer which has been calibrated is used as a "secondary standard" to transfer accuracy to other items. The accuracy of a calibration is dependent upon a reference which may be another piece of hardware, a physical phenomena, or a process. In the U.S., the National Institute of Standards and Technology is the organization to which all measurements, except time, are legally referenced. Other countries have a similar organization. Because direct NIST traceability does not exist, each calibration system depends upon indirect means and calculations for estimating system accuracy. Stated accuracies can often be neither independently verified nor disproved.

Blast measurements are always measurements of rapid pulses. In many applications, the pressure pulse is accompanied by a dynamic temperature pulse, electromagnetic pulses, detonation products, and powerful mechanical shocks and vibrations exist. To physically protect the gage from these processes, various means such as screens, grease, or some other material or method is employed.

Because the process being measured is a major strain on the gage, users frequently calibrate the gage not only before the test but after the test as well to detect any drastic performance changes which may have taken place during the measurement process.

Blast gages can exhibit hystersis, nonlinearity, nonrepeatability, zero shift, resonances, and sudden, catastrophic failure. Their output is affected by strain on the cables, thermal transients and shocks, mechanical vibrations, electrical effects (ground loops, lead resistances, etc.), ambient conditions, photo flash, and warm-up time. Many of these deleterious effects, if they exist, will be determined through calibration; those which cannot are minimized through mounting and installation procedures.

A listing of parameter information desired of a calibration process is given in Table 7.

In the discussion to follow, calibration systems have been divided into three groups; static systems, pressure-pulse systems, and dynamic systems. Pressure gages will be the primary subject of discussion.

Ref: Secretariat, A Guide for the Dynamic Calibration of Pressure Transducers, ANSIB88.1-1972, The American Society of Mechanical Engineers.

7.1 Static Systems.

"In a static state a gage is characterized by its sensitivity. The sensitivity is practically constant within the range of the gage and is defined as the ratio of the variation of the output over the variation of the input" (Damion, J.P., 1991).

The simplest system for conducting a static calibration of pressure gages is a portable one which can be taken to the installed site of the gage. It is very important to conduct an in-place calibration of a gage for in so doing all the components of a data acquisition system which can influence the accuracy of the data are included. These components are the cabling system, the signal conditioning equipment, the amplifier, and the recorder. A calibration system used in the 50s which incorporated dial pressure gages as secondary standards is shown in Figure 106. A calibration record of this era is shown in Figure 107. It will be observed that calibration steps of 25 percent were used to cover non-linearity effects generally common to the systems of the day. Improvements in transducers and recording systems were soon made and non-linearity problems were essentially eliminated.

A calibration unit employing digital pressure gages as secondary standards was introduced in the 80s and is shown in Figure 108. Apparatus employed to carryout the calibration of other types of gages is shown in Figures 109 and 110. Figure 109 shows the calibration of a small displacement, and Figure 110 shows the calibration of an earth pressure gage.

Table 7. Desired calibration information.

PARAMETER	UNIT
Full Scale Output at 10 Volts (FSO)	mV
Zero Offset	% FSO
Nonlinearity	% FSO
Hysteresis	% FSO
Nonrepeatability	% FSO
Comined Effect of Linearity, Repeatability, and Hysteresis	% FSO, RSS
Zero Shift after 2.5X Overpressure	% FSO
Input Resistance	ohm
Output Resistance	ohm
Zero Error Due to Temperature -18° to 65°C -54° to 74°C	 % FSO % FSO
Diaphragm Resonant Frequency (At Specified Measurand Levels)	kHz
Flat Frequency Response of Transducer	kHz
Warmup Time (1% Accuracy)	mS
Acceleration Sensitivity	% FSO/g
Zero Shift with Mounting Torque	% FSO
Nonlinearity at 2X Range	% 2X FSO
Insulation Resistance at 50 Vdc	Megohm
Noise (DC to 50,000 Hz)	microvolts rms
Rise Time	microseconds

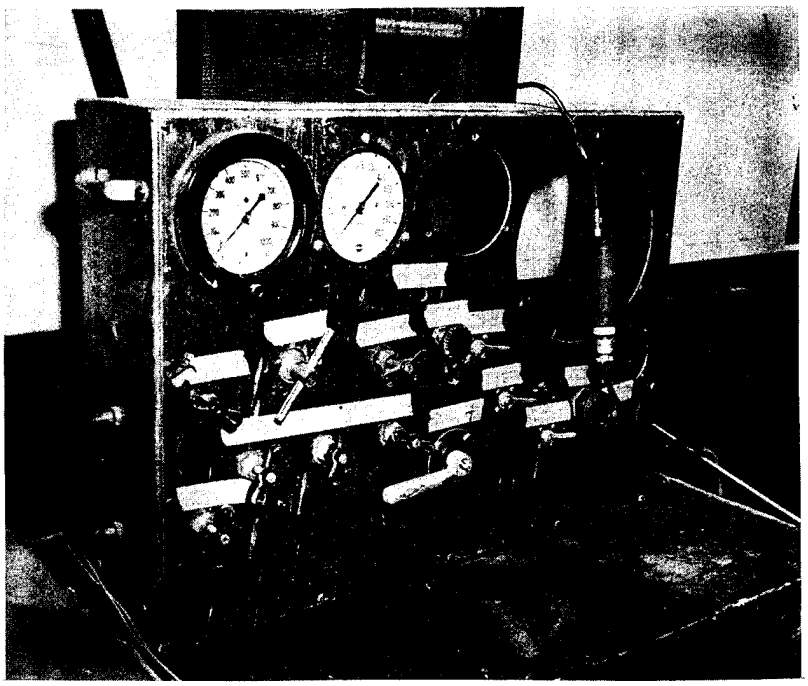

Figure 106. Typical calibration of Wiancko pressure gages.

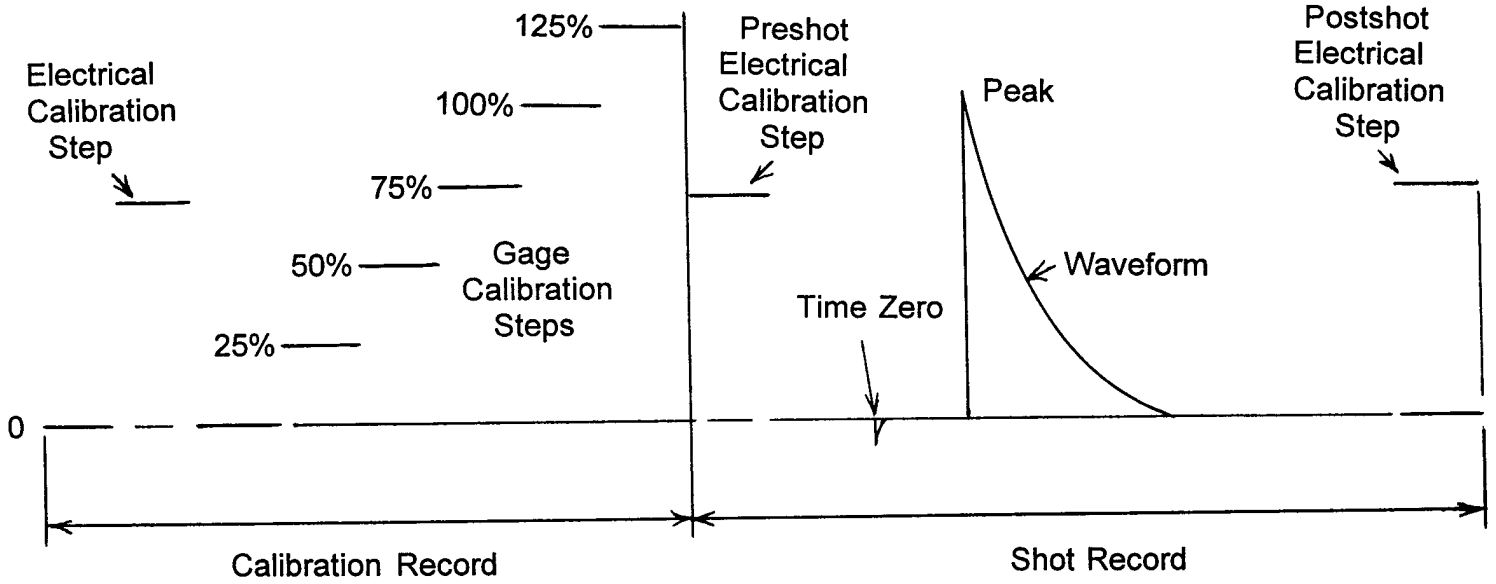

Figure 107. Calibration record from the 50s.

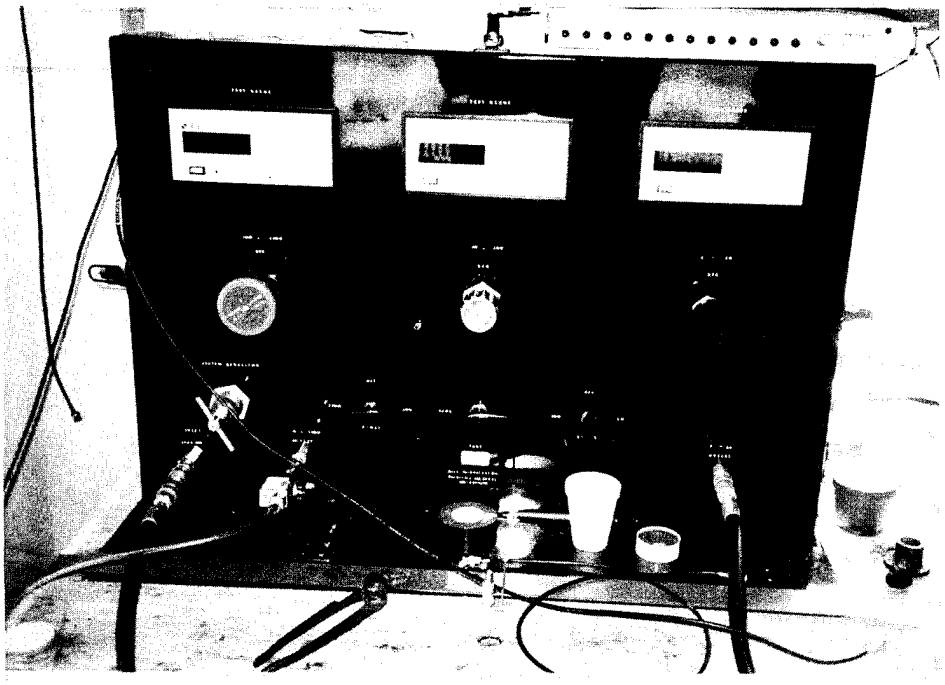

Figure 108. Calibration unit employing digital pressure gages.

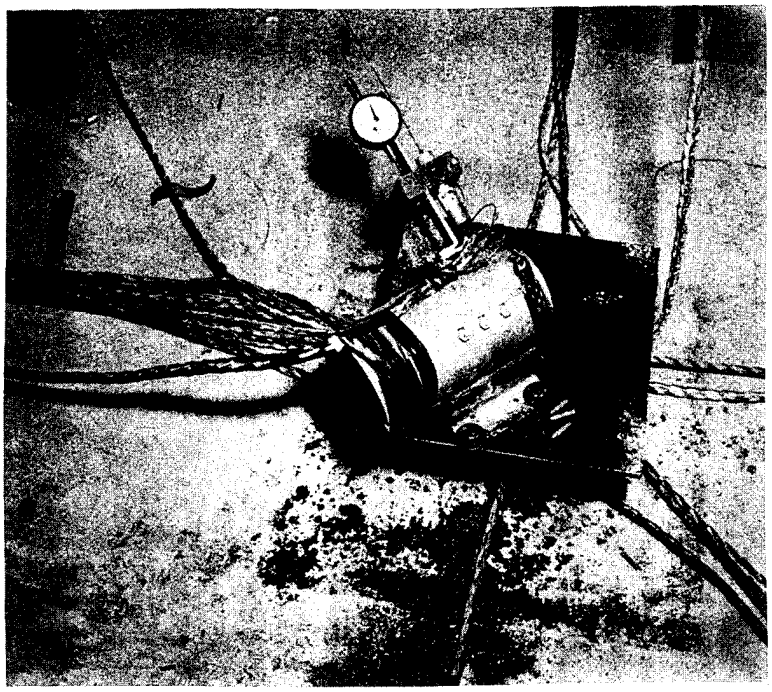

Figure 109. Small-displacement gage calibration.

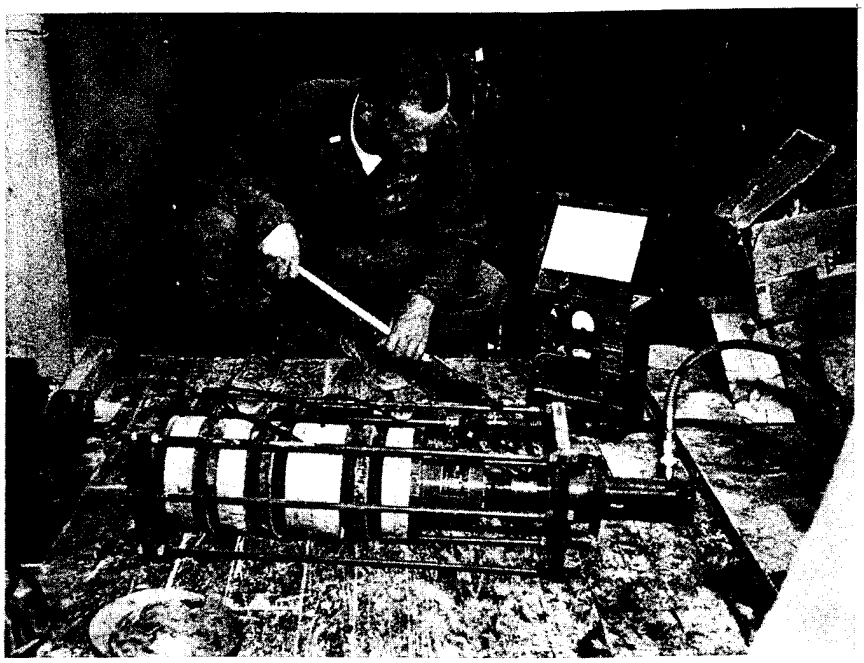

Figure 110. Calibration of earth-pressure gage.

A spin table was taken to the field site to provide the means to calibrate an accelerometer. This is shown in Figure 111.

Bottled nitrogen was used as the pressure source for calibrating pressure gages up to 2000 psi. Ranges beyond 2000 psi were cared for by other means.

A system designed and most commonly used with DC-type pressure gages, such as piezoresistive, strain, and the like, with long discharge constants is the dead-weight tester. Two versions of this system are shown in Figure 112. A precise pressure head is generated and applied to the transducer. A valve placed in the system, as seen in the lower figure, releases the pressure quickly to the gage. A response time of 60 msec is obtained.

Another device uses a piston in a cylinder, shown in Figure 113, to generate an impulse by dropping an anvil on the piston. Force applied is calculated from anvil weight and height dropped.

Still another drop-test calibrator for pressure gages is shown in Figure 114. This unit is capable of providing pressures up to about 25,000 psig. A larger version is designed for a maximum of 50,000 psig. This tester consists of a rigid aluminum channel frame made of 1 and 3/8-inch x 3-inch stock bolted together to hold the vented brass guide tube of 1 and 3/4-inch OD. Steel or tungsten weights (4, 8, and 10 pounds) are dropped down the 4-foot long guide tube onto a 5/16-inch diameter piston. This piston is coupled by a thin silicone oil in the calibrator head, to the test and reference transducers. The cross-section view in the figure shows additional details of the piston and calibrator head. A small rubber pad is used on top of the piston to damp unwanted oscillations on the traces. The interior calibrator head volume is kept small in order to couple most efficiently the force to the transducer. An accurately calibrated and very linear tourmaline hydraulic transducer is used as a reference to compare with the test transducer when a weight is dropped to give a calibration pulse. The rise time is about 3 msec and the pulse duration is 6 msec. A more modern version is shown in Figure 115.

Drop testers in the 90s have a capacity up to 100,000 psi.

Ref: Ball, John M., "Army Dynamic Pressure Measurements," Proceedings, Workshop on the Measurement of Transient Pressure and Temperature. National Institute of Standards Technology NISTIR-4828, Vern E. Bean and Gregory J. Rosasco, editors, 23-24 April 1991.

Damion, J.P., "Means of Dynamic Calibration for Pressure Transducers," Proceedings, Workshop on the Measurement of Transient Pressure and Temperature. National Institute of Standards Technology NISTIR-4828, Vern E. Bean and Gregory J. Rosasco, editors, 23-24 April 1991.

Coulter, George A., "Dynamic Calibration of Pressure Transducers at the BRL Shock Tube Facility," BRL-MR-1843, 1967.

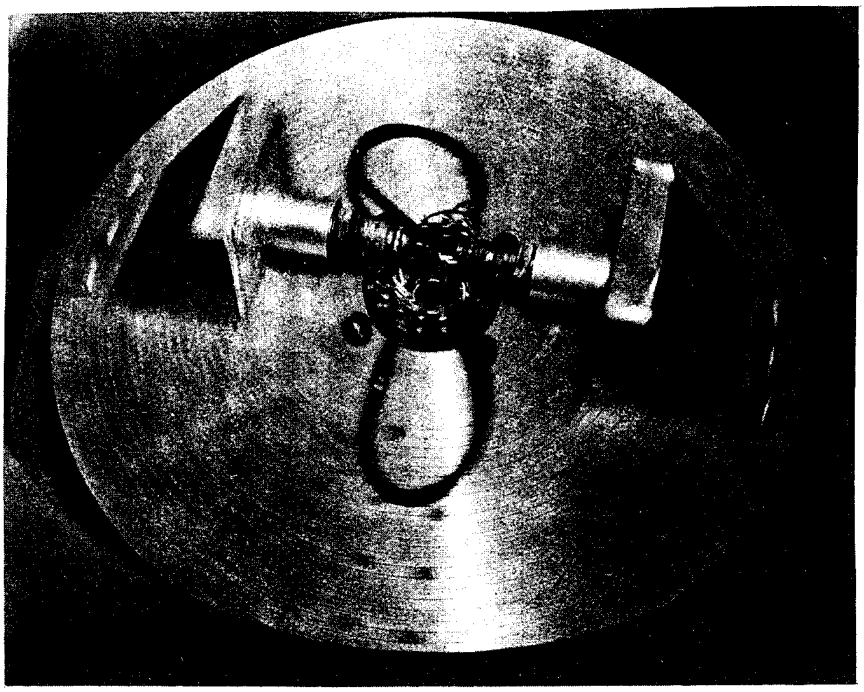

Figure 111. Calibration of accelerometer.

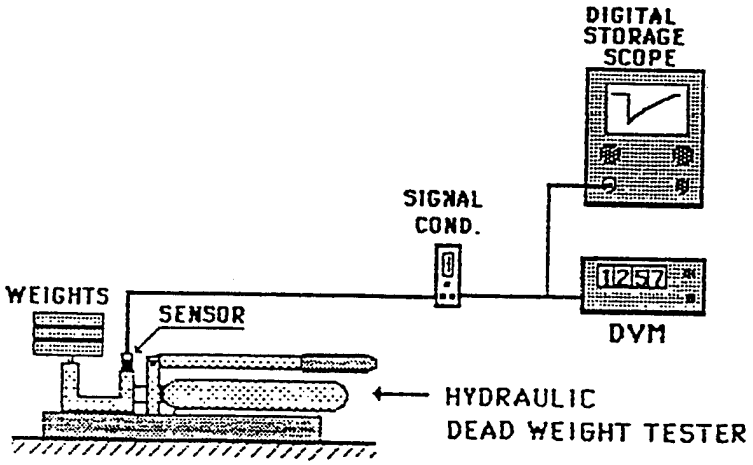

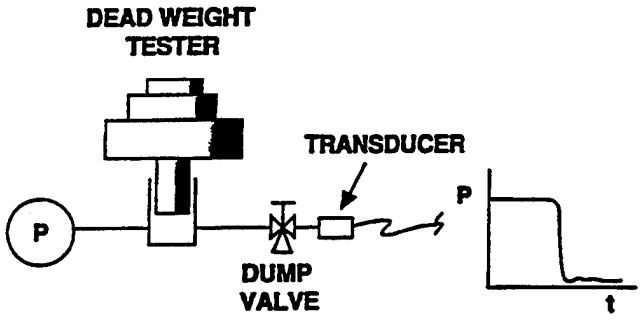

HYDRAULIC DEAD WEIGHT CALIBRATOR

Figure 112. Calibration systems most commonly used with DC-type pressure gages.

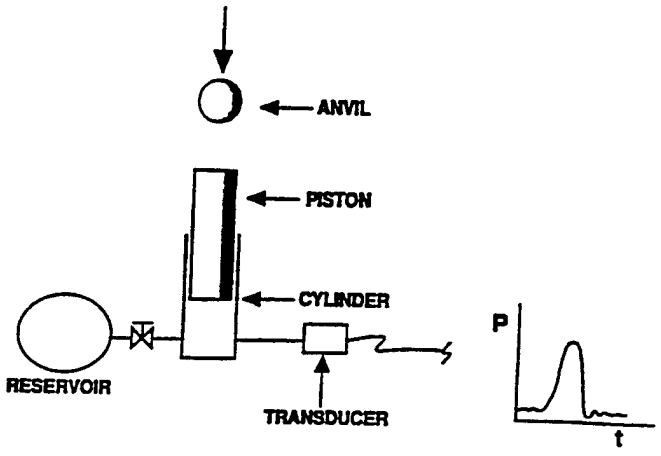

Figure 113. Drop ball impulse calibrator.

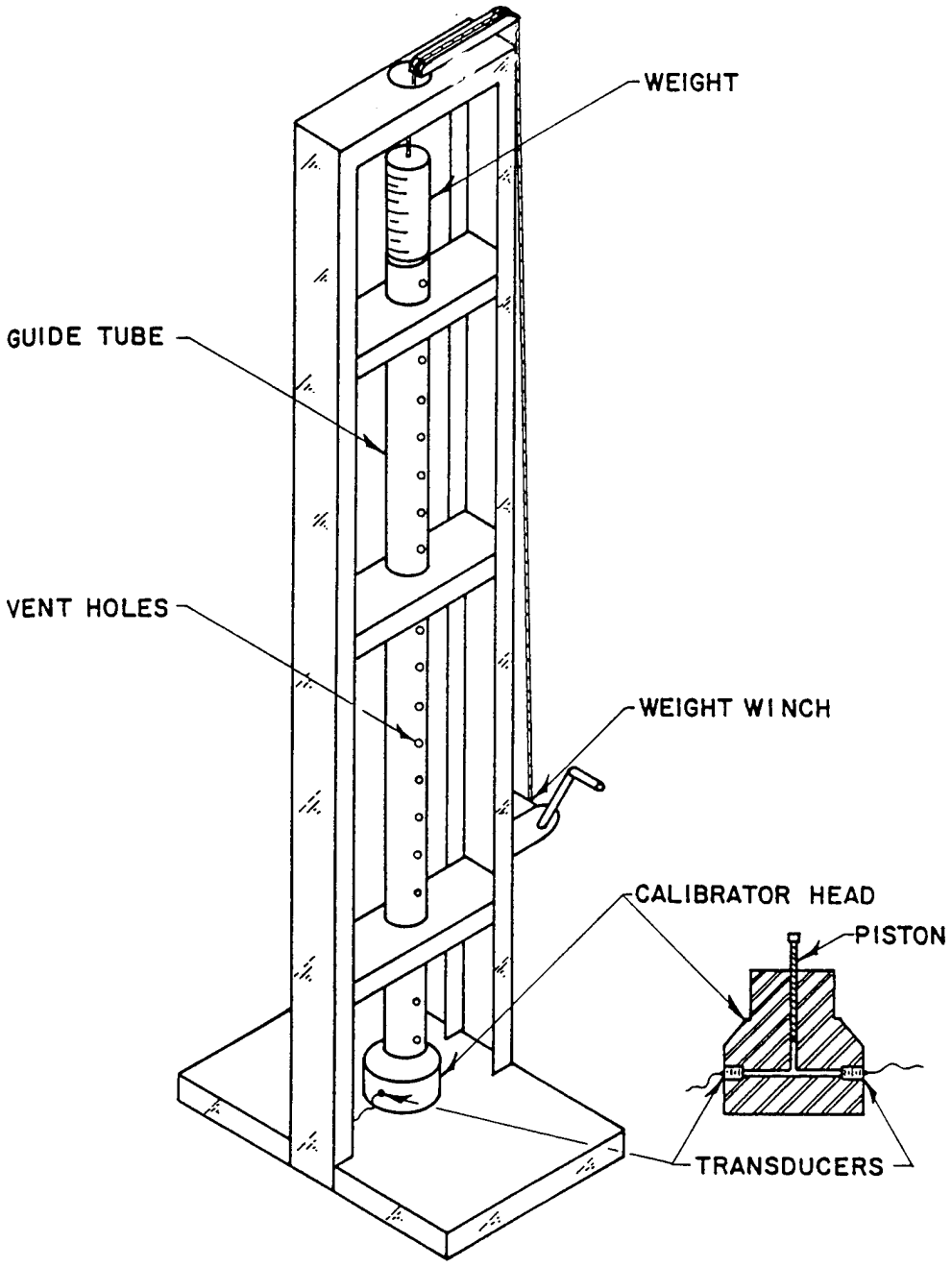

Figure 114. Drop test calibrator.

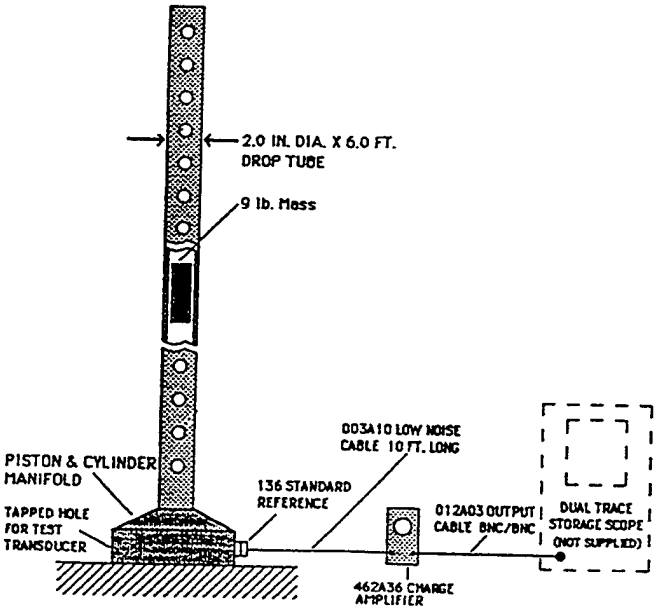

Figure 115. Modern drop-test calibrator.

7.2 Pressure Pulse Systems.

Those calibration systems which generate a pressure pulse with a known rise time and a limited duration are considered herein as quasi-static systems.

An air pulse calibrator is illustrated in Figure 116. Basically the calibrator consists of an air reservoir, a manual or solenoid valve, and a dial monitor or digital pressure gage to set an accurate static reference pressure. The air reservoir tank volume is very large (20,000:1) compared to the interior of the solenoid valve or manual valve so the control pressure gage may be read and assumed to give the magnitude of the pressure pulse applied to the transducer. The fast opening device is illustrated in Figure 117. A two way solenoid valve was modified with a manual release valve. A Teflon o-ring seal was substituted after a standard rubber o-ring did not release properly. The system produces a rise time of 5 msec.

A liquid-based system built around a very fast acting valve is illustrated in Figure 118. The chamber is pressurized and the static pressure measured. The valve releases exposing the test gage to a sudden pressure step.

Another air pulse calibrator is illustrated in Figure 119. This device uses a uniquely actuated very vast poppet valve to generate a step pressure pulse. It has proven useful for generating accurately known repeatable performance with steps to 2000 psi.

An AVL calibrator generates a pressure pulse by converting the kinetic energy from an impact mass into the compression energy of a fluid inside a hydraulic high pressure chamber. The impact mass strikes a piston in the measuring head, the piston immerses into a pressure chamber and compresses the fluid. The system is illustrated in Figure 120. Two gages, one a reference gage, receive a pressure pulse. A range of 14.5 - 116 kpsi is achievable. Comparison of the test gage results when the reference gage makes it easy to check the quality of transducers. Figure 121 shows a version of the basic system with a PC.

Another device was designed to incorporate the capabilities of several of the special- purpose calibrators into one device. Designated the "Aronson" shockless pressure step generator, its capabilities include the use of high-accuracy digital reference pressure standards and fast-acting poppet-type valves to produce positive or negative step pressures with rise times approaching those of shock tubes. A diagram of the Aronson calibrator is shown in Figure 122.

"The concept and operation of the Aronson step pressure generator is quite fundamental. It simply involves applying to the transducer an accurately known static pressure very quickly. This is accomplished by pressurizing the main reservoir "A" with an accurately measured static pressure and then exposing the transducer to the reference pressure by releasing the quick-opening poppet valve. The pressure drop in the main reservoir due to the added volume between the transducer diaphragm and poppet valve is negligible with flush diaphragm pressure sensors. Any pressure drop would be indicated by the digital pressure gage which monitors pressure in the reservoir.

The Aronson step pressure generator has two separate pressure reservoirs (A & B) in which the pressure is controlled by accurate static digital pressure gages. In addition to the main pressure reservoir "A," pressure between the poppet valve and the diaphragm of the transducer (reservoir "B") can be pressurized with a known static pressure. Having control of a known pressure in each reservoir offers unique capability to compare static versus

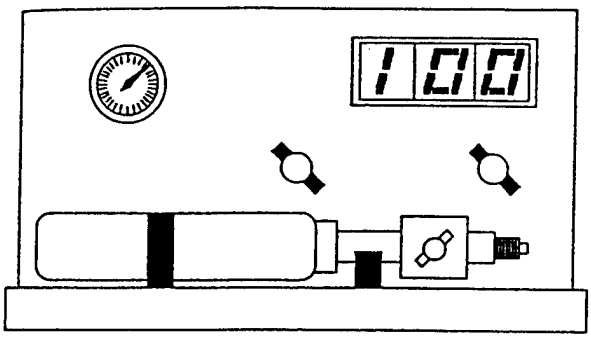

Figure 116. Air pulse calibrator.

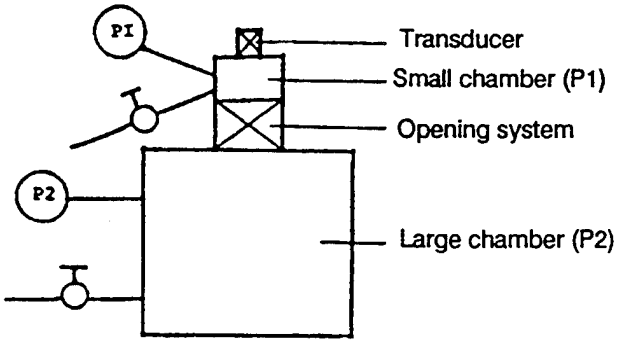

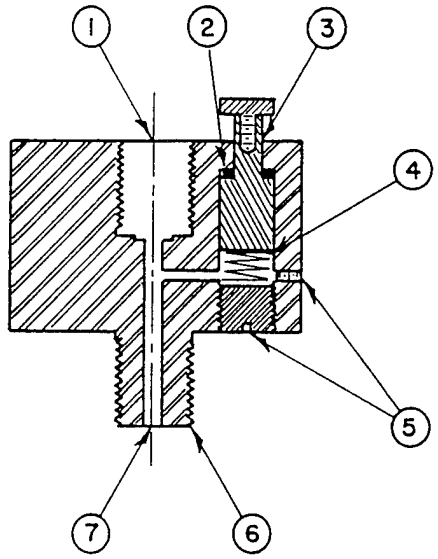

1. TRANSDUCER PORT – 1/2-20 NF
2. TEFLON O-RING
3. RELEASE VALVE
4. SPRING
5. PLUGS
6. 1/4 – 18 PIPE THREAD
7. AIR INLET FROM TWO-WAY SOLENOID VALVE

Figure 117. Fast opening device.

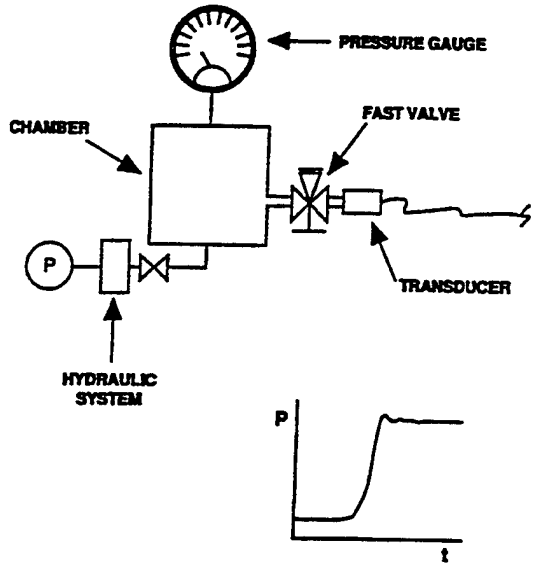

Figure 118. High-pressure hydraulic step function calibrator.

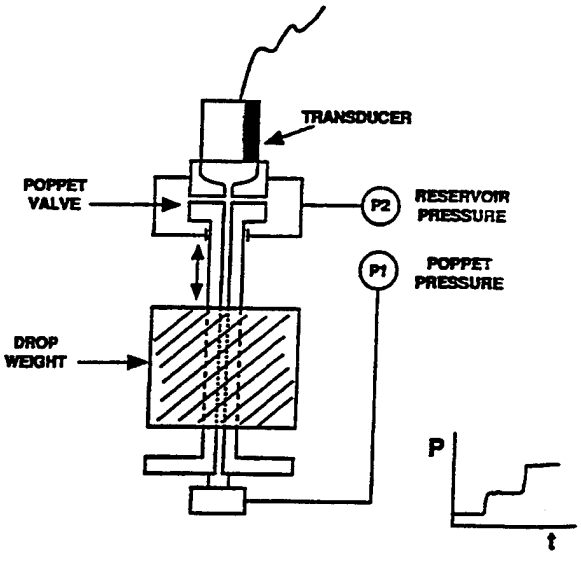

Figure 119. Pneumatic step generator.

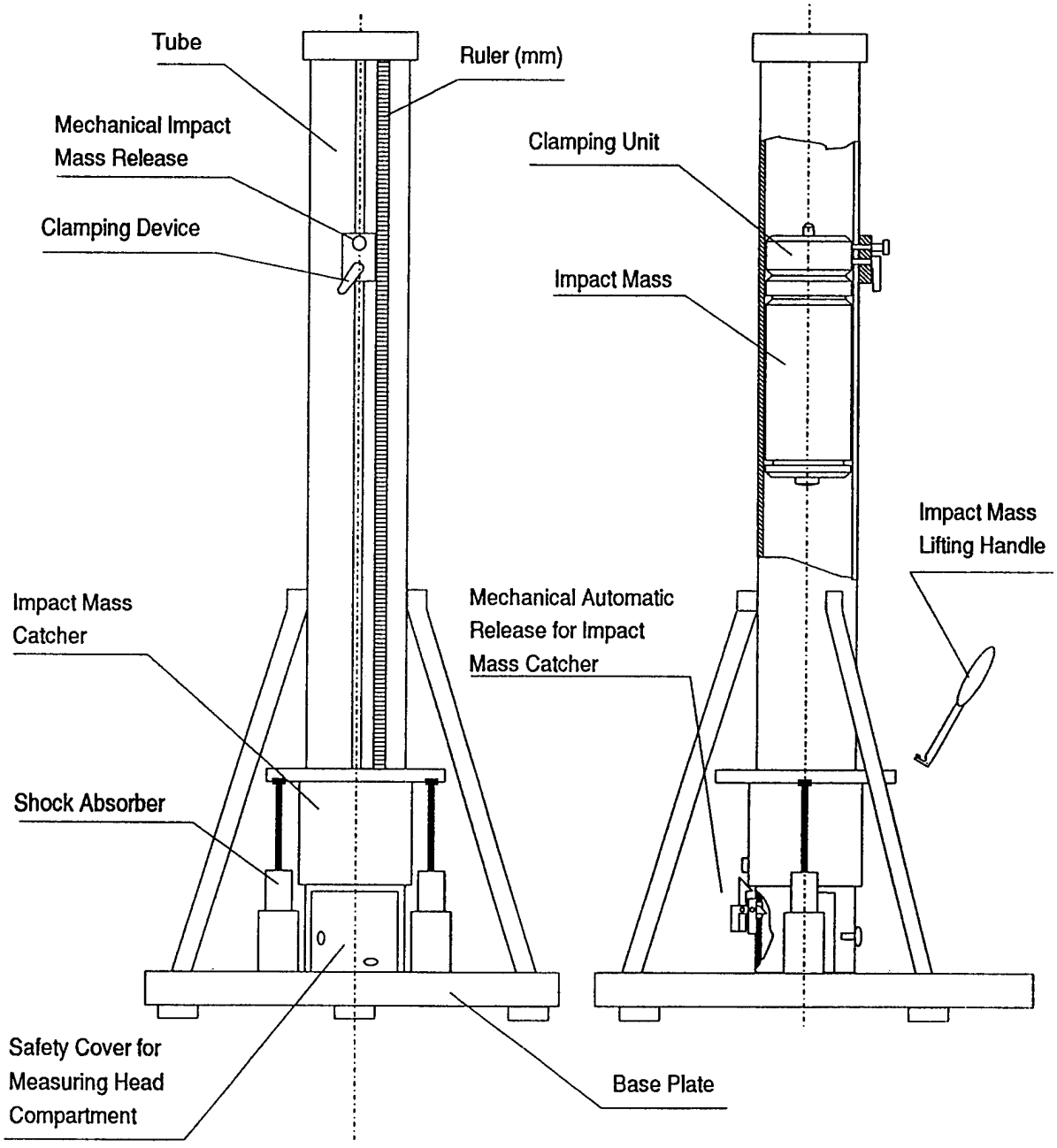

Figure 120. AVL calibrator.

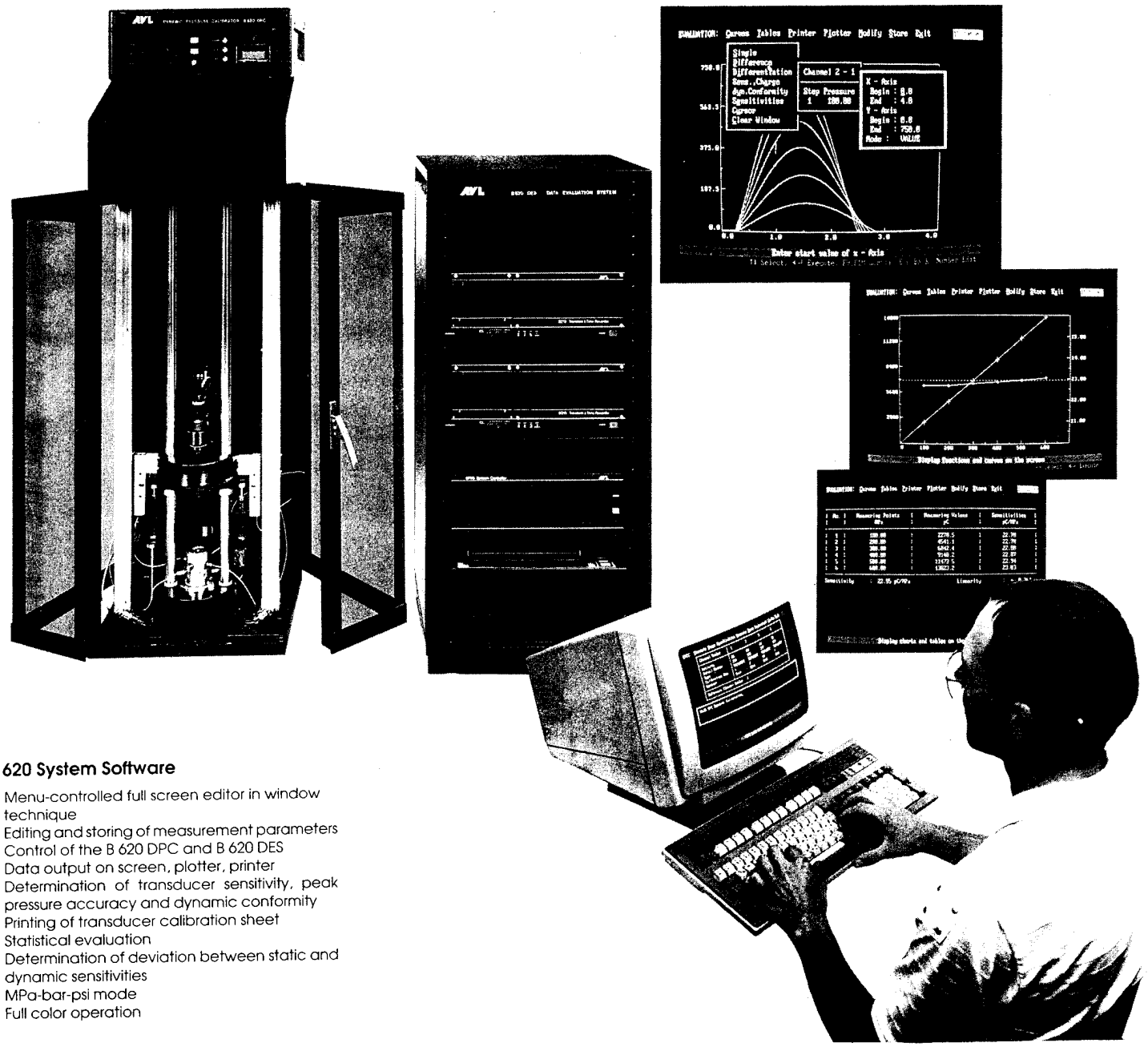

B 620 System Software

- Menu-controlled full screen editor in window technique
- Editing and storing of measurement parameters
- Control of the B 620 DPC and B 620 DES
- Data output on screen, plotter, printer
- Determination of transducer sensitivity, peak pressure accuracy and dynamic conformity
- Printing of transducer calibration sheet
- Statistical evaluation
- Determination of deviation between static and dynamic sensitivities
- MPa-bar-psi mode
- Full color operation

Figure 121. Basic AVL system with a PC.

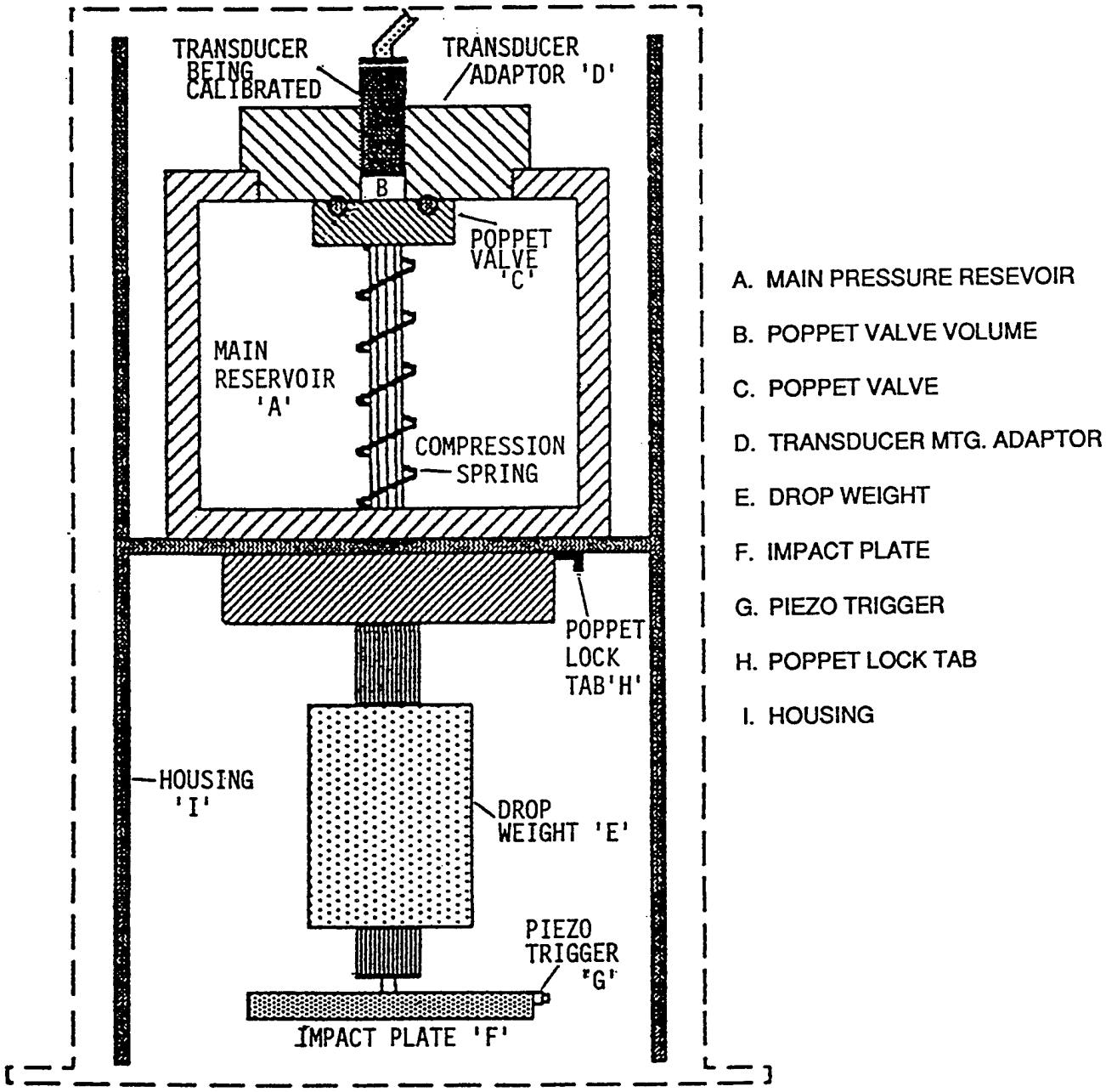

Figure 122. Mechanical system diagram of Aronson shockless pressure-step generator.

dynamic response, and provide small incremental pressure steps at higher static levels" (Lally, 1991).

Rise time of a step pressure depends on: (1) type of gas used (helium recommended for fastest rise time); (2) diameter of poppet valve; (3) initial pressure difference across the poppet valve; and (4) design of transducer diaphragm (flush or recess).

Traceability to NIST is through calibration of accurate DC reference gages used to set the known static level to which the transducer under calibration is being rapidly switched.

Ref: Lally, James F., "Dynamic Step-Pressure Calibration," Proceedings, Workshop in the Measurement of Transient Pressure and Temperature. National Institute of Standards and Technology NISTIR-4828, Vern E. Bean and Gregory J. Rosasco, editors, 23-24 April 1991.

AVL Company Brochure, "Static & Dynamic Calibration of Piezoelectric High-Pressure Transducers," 1993.

7.3 Dynamic Systems.

Dynamic calibration systems may be characterized as those which provide a history of the time variation of the calibration pulse. The systems described earlier are both simple and accurate but are somewhat limited by the rise time. This is a disadvantage in that a gage may function during a slow rise air-pulse calibration but may have a different output or fail during the air shock loading. A transducer when shock loaded may be stimulated to vibrate or ring at its natural frequency and may break. To check this possibility, shock tube calibrations are used in a calibration program.

There are several shock tubes of varying sizes used in calibration. A 2-inch shock tube is small and simple to operate. It operates from a cold-gas driver and is of constant area throughout. Instead of air, compressed bottled helium or nitrogen is used as the driver gas. The pressurized gas causes pre-selected diaphragms to break and create the shock waves. Close repeatability of shock pressure is obtained without scoring of the diaphragm. A tube is shown in schematic form in Figure 123. A photograph of a 2-inch tube is shown in Figure 124.

A velocity system is used to determine peak pressure. A short 6-inch baseline between counter trigger pickups is used to minimize any shock front attenuation that may occur. In order to adjust the counter triggers for equal rise time and amplitude, considerable care must be used, otherwise a velocity error will cause an incorrect value for the calibration shock pressure.

The shock tube has test ports both side-on in the test section and face-on in the closed-end flange for a reflected pressure calibration. Expected pressures for the tube are given in Table 8.

A portable device for in-situ calibration of pressure gages was developed to generate pressures up to 200 psi with rise times of less than 25 microseconds with an accuracy of one percent or less. This system is shown in Figures 125 and 126.

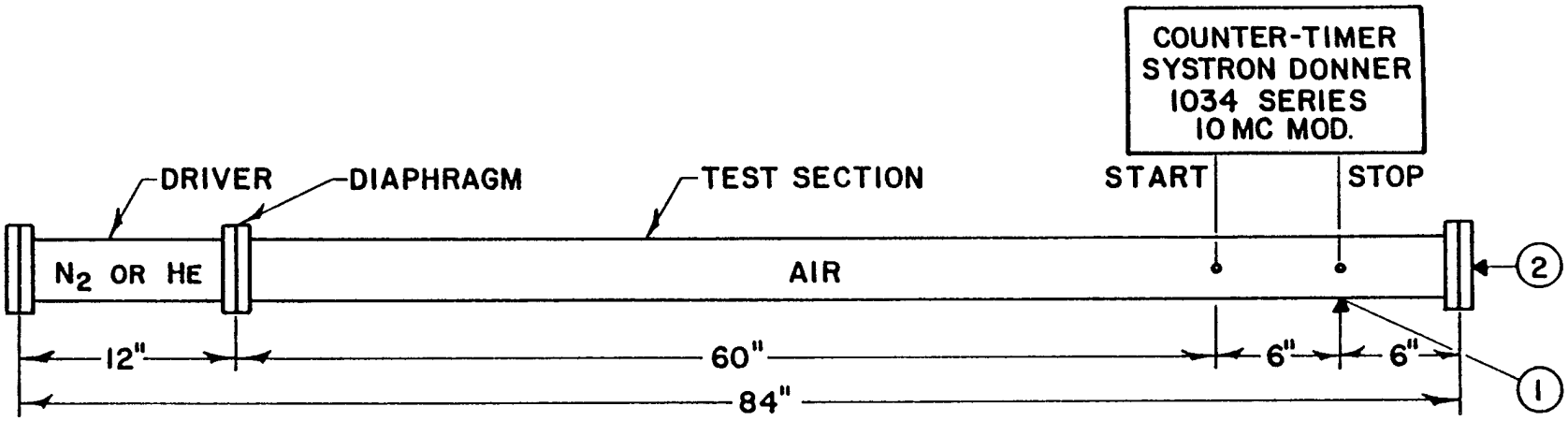

(1) SIDE-ON PRESSURE TRANSDUCER

(2) REFLECTED PRESSURE TRANSDUCER

Figure 123. Schematic of a two-inch calibration shock tube.

Figure 124. Photograph of a two-inch calibration shock tube.

Table 8. Shock pressure as a function of diaphragm type and driver pressure - 2-inch shock tube.

Shock Overpressure, psi	Reflected Overpressure, psi	Diaphragm Material	Driver Gas	Driver Pressure, psig
		11-00-0 Aluminum		
180	1050	0.064"	Helium	1400
144	790	0.040		880
130	690	0.032		760
90	435	0.020		423
58	245	0.032	Nitrogen	760
		Mylar		
32	110	0.010"	Nitrogen	225

NOTE: Fill driver slowly to obtain pressures listed.

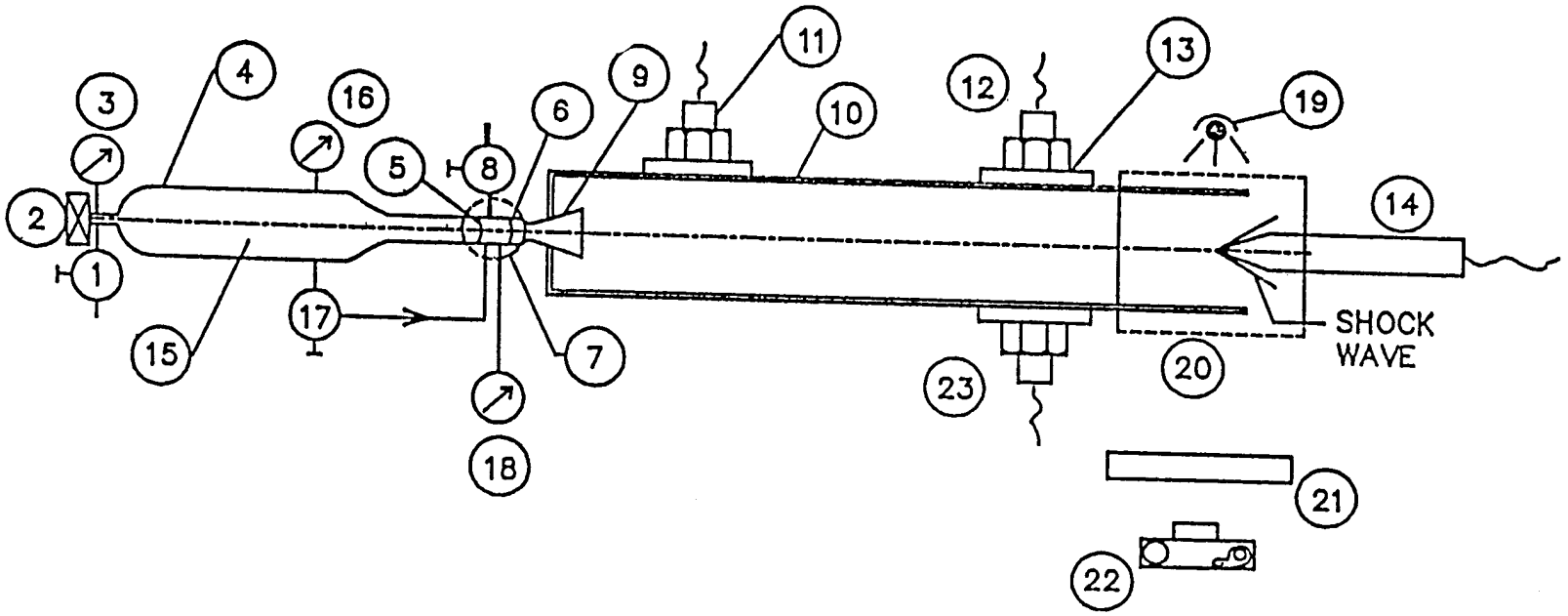

1. BLEED VALVE
2. FILL VALVE
3. PRESSURE GAGE
4. PRESSURE RESERVOIR
5. UPSTREAM DIAPHRAGM
6. DOWNSTREAM DIAPHRAGM
7. DIAPHRAGM BLOCK
8. BLEED VALVE
9. EXPANSION NOZZLE
10. DRIVEN CHAMBER
11. STANDARD TRANSDUCER
12. STANDARD TRANSDUCER
13. ADAPTER BLOCK
14. PITOT TYPE TEST TRANSDUCER
15. HELIUM
* 16. TEMPERATURE GAGE
17. REDUCER VALVE
18. DIAPHRAGM PRESSURE GAGE
* 19. POINT LIGHT SOURCE
* 20. TRANSPARENT TEST SECTION
* 21. FROSTED SCREEN
* 22. CAMERA
* 23. FIELD TEST TRANSDUCER

* PHASE II

Figure 125. Schematic of blast gage calibrator.

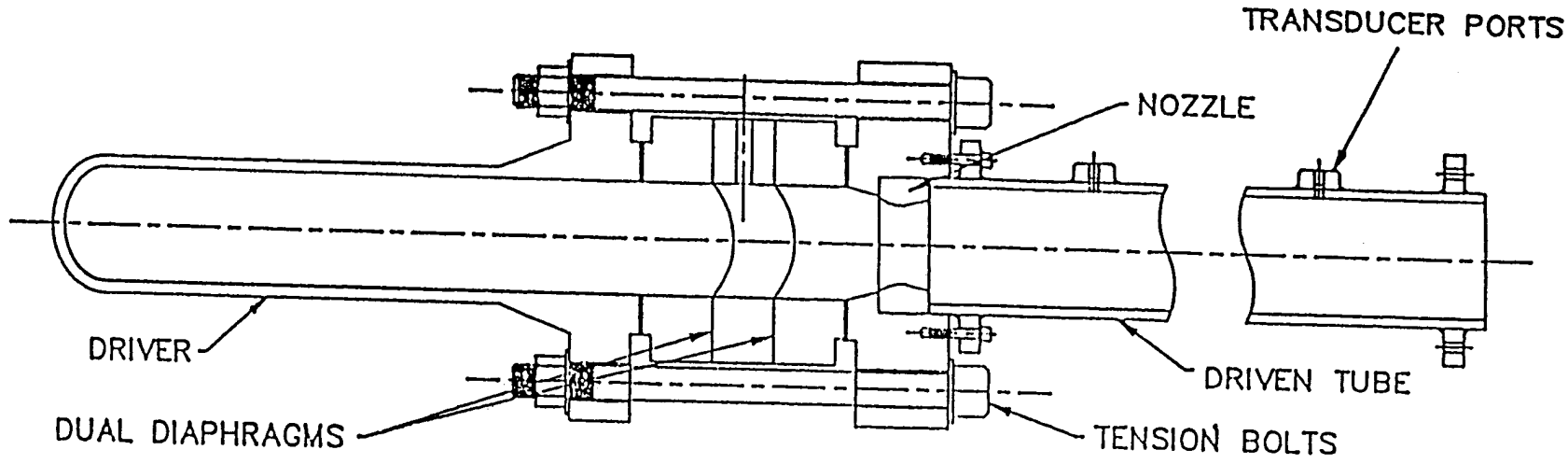

Figure 126. Schematic of portable shock tube calibrator.

A portable shock tube was designed as a practical way to pulse a gage and system. Shown in Figure 127, the unit is used primarily for pressures under 100 psi. The driving unit is a commercially-available dummy launcher designed for use by hunters. The launcher directs the gases from the cartridge at an angle to the axis. Cartridges are those designed for and used with ramsetting tools. The driving unit and aluminum expansion tube are machined so that they fit together and can be held together with set screws. A rubber cap is used at the end of the tube to provide a flexible surface to seal the end of the shock tube against a plate containing the test gage.

A compact reusable air-blast calibration facility was developed to calibrate high pressure gages. The goal of this system is to provide a flat uniform shock front up to 6.5 kbars. The system is driven by dilute explosive tiles arranged and initiated such that a planar shock front is produced. This system is useful for large sized gages such as bar gages. Based on test results it yields a 15 percent variation in peak pressures and an 8 percent variation in late time impulse. The system is illustrated in Figure 128.

Ref: Coulter, George A., "Dynamic Calibration of Pressure Transducers at the BRL Shock Tube Facility," BRL-MR-1843, 1967.

Sanai, M., "Simulation and Instrumentation Development, Vol I: Use of New Foam Dilute Explosive Tiles in SRI CRABS Facility for Evaluation of Airblast Gages," Technical Report DNA-TR-88-249-V1, 1988.

Winiary, M.L., "Nuclear Effects Blast and Shock Instrumentation," DNA-TR-88-2, 1988.

Osofsky, Irving B., et al., "Portable High-Explosive Pressure Transducer Calibrator," Proceedings of the Fifth State-of-the-Art Blast Measurementation Meeting, Defense Nuclear Agency, 1988.

Ethridge, Noel H., Personal Communications.

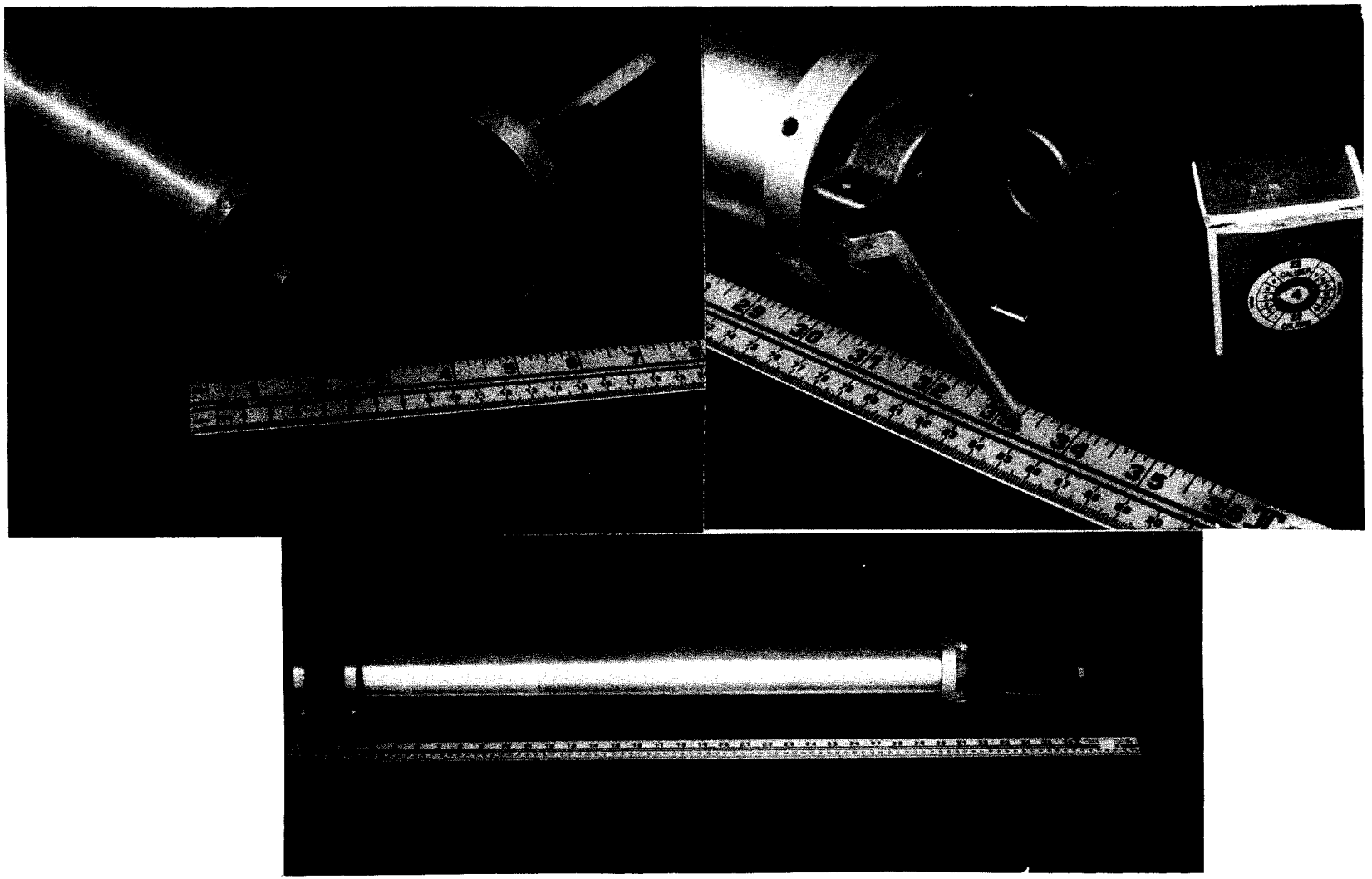

Figure 127. Portable shock tube gage pulsing system.

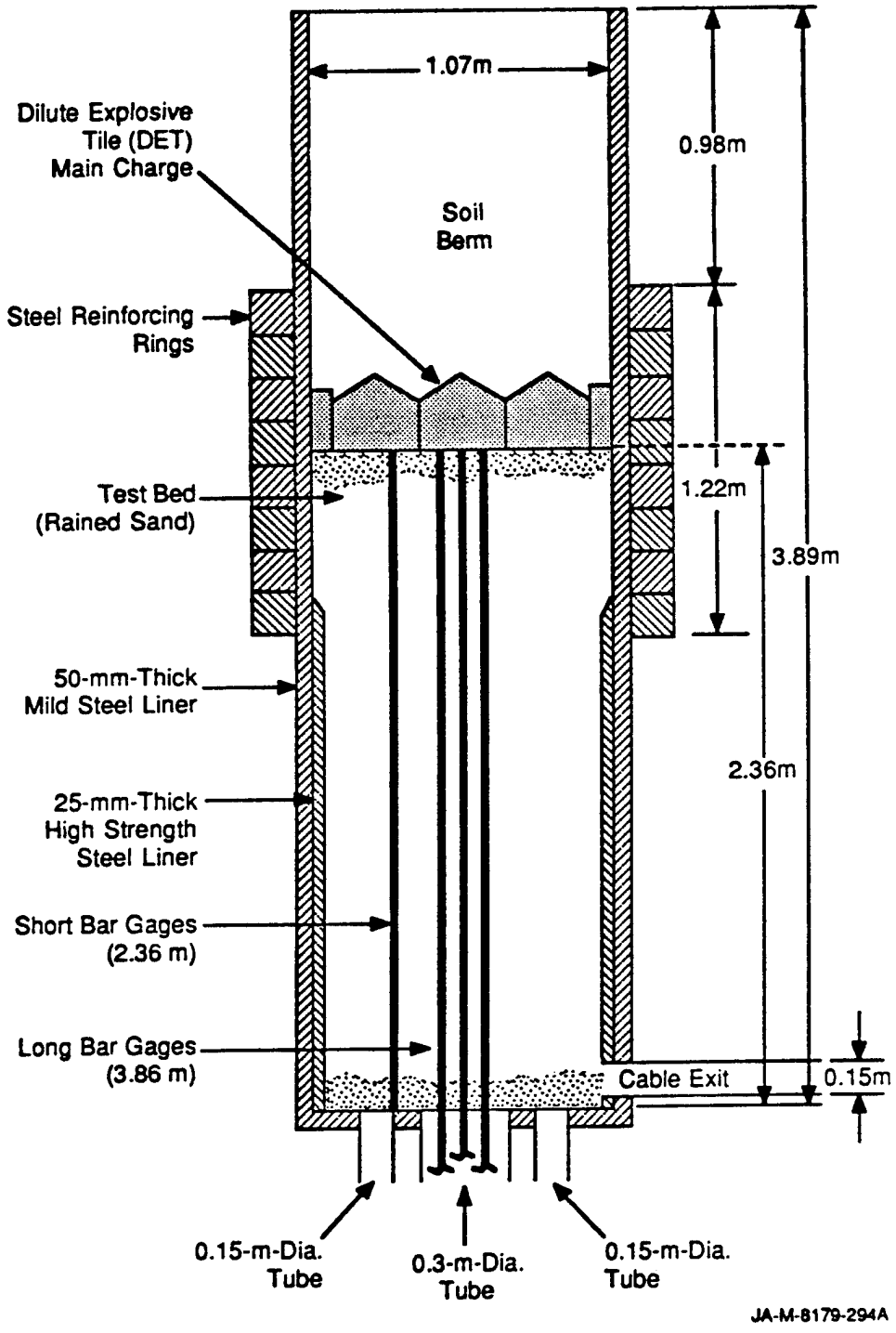

Figure 128. Schematic of compact reusable airblast simulator (CRABS) facility at SRI.

SECTION 8

CONCLUSION

Instrumentation of structures and military equipment exposed to nuclear explosions began on a large scale soon after the successful detonation of the A-bomb. The U.S. Navy was interested in the blast effects of nuclear weapons on their ships and exposed a number of them at the Bikini Atoll . Land-based structures and military equipment were soon included in the testing plans and the first extensive program of this type was carried out in 1951. Subsequent tests included civil defense structures and equipment.

In the early days of testing, large numbers of all conceivable types of electronic and non-electronic devices that gave any evidence of successfully yielding information were deployed. Some of the devices used were discarded, however, most were updated and used on successive tests. The instrumentation was utilized to measure the loading and response of targets so that effects could be analyzed, design techniques developed and verified, and hardened structures and equipment evaluated.

With the establishment of the moratorium on atmospheric nuclear testing an intensive testing period came to an end. Research and development activities concerning nuclear explosion effects on structures and equipment generated the need for continued testing. In 1964 Canada, the United Kingdom, and the United States collaborated on a large-scale structural testing program carried out using high-explosives to simulate nuclear airblast. Test programs of this nature continued on a periodic basis through the past decades. The development of large blast simulators have reduced the need for the large-scale HE tests, but the need for appropriate instrumentation continues.

As the reader passes through these pages which describe the instrumentation, he will gain a sense of the advances made since the beginning of testing. Gages have become smaller in physical size with a higher natural frequency. Gages utilizing new principles and new technology have been developed so that all the parameters of interest can be measured. Extensive use of commercially available gages has been made by all countries in the pursuit of knowledge about the response of structures and equipment to blast. Further progress can be expected as new technologies are applied in the field of instrumentation.

SECTION 9

REFERENCES

"A Peak Load, Self-Recording on Structure Stress Gage," WL-TDR-64-11, Air Force Weapons Laboratory, Kirtland AFB, NM, 1964.

Allgood, J.R., "Response of Buried Cylinders in the Near Crater Region," Operation DISTANT PLAIN, DASA 1876-4, 1968.

Anderson, D.C. and Porzel, F.B., "Close-In Time-of-Arrival Measurements for Yield of Underground Shot Rainer," WT-1495, AD607,645, 1959.

Averill, R.L., et al., "Hardened Radar Antenna Structural Response Investigation," Event DIAL PACK Symposium Report, Vol. II, Defence Research Board of Canada, 1971.

AVL Company Brochure, "Static & Dynamic Calibration of Piezoelectric High-Pressure Transducers," 1993.

Baker, W.E. and Lynch, R.E., "A Study of Parameters and Methods Involved in Relative Displacement Measurements in Soil," AFWL-TR-65-75, 1965.

Ball, John M., "Army Dynamic Pressure Measurements," Proceedings, Workshop on the Measurement of Transient Pressure and Temperature. National Institute of Standards Technology NISTIR-4828, Vern E. Bean and Gregory J. Rosasco, editors, 23-24 April 1991.

Bass, R.C. and Hawk, H.L., "Close-In Shock Studies, FERRIS WHEEL Series, FLAT TOP I Event," POR 3005, 1965.

Blagman, George, "A Self-Contained Mechanical Recording Accelerometer," TR-703, Diamond Ordnance Fuze Laboratories, U.S. Army, 1959.

Bryant, E.J. and Keefer, J.H., "Basic Air-Blast Phenomena," Project 1.1, Operation PLUMBBOB, WT-1401, 1958.

Chabai, A.J., "Close-In Phenomena of Buried Explosions," DASA-1382, 1963.

Chilton, E.G., et al., "The Development and Evaluation of a Miniature Velocity Gage," AFWL-TR-65-46, 1967.

Coulter, George A., "Dynamic Calibration of Pressure Transducers at the BRL Shock Tube Facility," BRL-MR-1843, 1967.

Damion, J.P., "Means of Dynamic Calibration for Pressure Transducers," Proceedings, Workshop on the Measurement of Transient Pressure and Temperature. National Institute of Standards Technology NISTIR-4828, Vern E. Bean and Gregory J. Rosasco, editors, 23-24 April 1991.

Danek, W.L. and Dargis, A.A., "Particle Velocimeter for use Close-In to Underground Explosions," DASA 1431-1, 1964 and DASA 1431-2, 1965.

Dohrenwend, C.O., et al., "Flexible Measuring Devices and Inspection of Operation JANGLE Structures," WT-1125, 1958.

Ethridge, N.H., et al., "Blast Response of Electronic Van Semi-Trailers (M348A2)," Proceedings of the MILL RACE Preliminary Results Symposium, Vol III, POR 7073-3, 1982.

"Evaluation of WES Self-Recording Displacement Gage," Miscellaneous papers, No. 1-644, U.S. Army Engineer Waterways Experiment Station, Corps of Engineers, Vicksburg, MS, 1964.

Hauver, G.E. and Netherwood, P.H., "Pressure Profiles of Detonating Baratol Measured with Sulphur Gauges," BRL Technical Note 1452, 1962.

Holzer, F., "Measurements and Calculations of Peak Shock Wave Parameters from Underground Nuclear Detonations," Journal of Geophysics Research, 70, 4, 893, 1965.

Jones, W.A. and Munro, S., "Field Test of Army SKOP Shelter," Event DIAL PACK Symposium Report, Vol. II, Defence Research Board of Canada, 1971.

Kearny, C.H. and Chester, C.V., "Blast Tests of Expedient Shelters," ORNL-4905, Oak Ridge National Laboratory, 1974.

Keough, D.H., "Pressure Transducer for Measuring Shock Wave Profiles, Phase IX: Additional Gage Development," DASA 1414-1, AD459058, 1964.

Lally, James F., "Dynamic Step-Pressure Calibration," Proceedings, Workshop in the Measurement of Transient Pressure and Temperature. National Institute of Standards and Technology NISTIR-4828, Vern E. Bean and Gregory J. Rosasco, editors, 23-24 April 1991.

Malavergne, J., et al., "Tests of Anti-Blast Valves and Doors," Proceedings of the MINOR SCALE Symposium, POR 7158-4, 1986.

Mellsen, S.B., "Drag Measurements on Cylinders by the Free-Flight Method," Event DIAL PACK Symposium Report, Vol 1, Defence Research Board, Canada, 1971.

Meszaros, J.J., et al., "Air-Blast Phenomena and Instrumentation of Structures (U)," Project 1.7, WT-1612, 1962. (CONFIDENTIAL-FORMERLY RESTRICTED DATA)

Meszaros, J.J. and Schmidt, J.G., "Instrumentation of French Underground Shelters," WT-1535, 1961.

Meszaros, J.J., et al., "Instrumentation of Structures for Air-Blast and Ground-Shock Effects," Project 30.5, WT-1452, 1960.

Meszaros, J.J., et al., "Instrumentation of Structures for Air-Blast and Ground-Shock Effects," Project 3.7, WT-1426, 1959.

Meszaros, J.J. and Randall, J.I., "Structures Instrumentation," Operation UPSHOT-KNOTHOLE, WT-738, 1955.

Morse, T.B., "Instrumentation Accessories for Earth Motion Measurements," Sandia Corporation M-65-330, 1965.

Northrop, Paul A., "Instrumentation for Structures Program," Part I. OPERATION GREENHOUSE, WT-1, 1951.

Osofsky, Irving B., et al., "Portable High-Explosive Pressure Transducer Calibrator," Proceedings of the Fifth State-of-the-Art Blast Instrumentation Meeting, DNA, 1988.

Pieper, F.A. and Galbraith, F.W., "Ground Shock Spectrum Measurements," WT-4054, 1966.

Raley, R.J., et al., "Truck/Shelter Test, DISTANT IMAGE," DISTANT IMAGE Symposium Report, Vol III, POR 7379-3, 1992.

Robinson, M.G., "Multichannel Time-of-Arrival Instrumentation System," AFWL-TR-65-191, 1966.

Rowland, R.H., "Blast and Shock Measurement State-of-the-Art Review," DASA-1986, 1967.

Sanai, M., "Simulation and Instrumentation Development, Vol I: Use of New Foam Dilute Explosive Tiles in SRI CRABS Facility for Evaluation of Airblast Gages," Technical Report DNA-TR-88-249-V1, 1988.

Sauer, F.M. and Vincent. C.T., "Close-In Earth Motion Studies/Pressure Measurements in the Hydrodynamic Region, "Unpublished".

Secretariat, A Guide for the Dynamic Calibration of Pressure Transducers, ANSIB88.1-1972, The American Society of Mechanical Engineers.

Seknicka, A.J., "Measurement of Permanent Horizontal and Vertical Ground Motion," Operation SNOWBALL Symposium Proceedings, Vol. I, DASA-1642-1, 1965.

Shelton, F.H., Reflections of a Nuclear Weaponeer, Shelton Enterprises, Inc., 1988.

Stegner, J.K. and Obenchain, R., "Research Studies on Free Field Instrumentation," AFSWC-TR-63-45, 1963.

Swift, L.M., "Development of Soil Displacement and Strain Gages," DASA-1267, 1961.

Swift, L.M., "Ground Acceleration, Stress and Strain at High Incident Overpressures," WT-1404, 1960.

Swift, L.M., "Development of an Earth Velocity Gage," DASA-1191, 1960.

Truesdale, W.B. and Schwab, R.B., "Soil Strain Gage Instrumentation," AFWL-TR-65-207, 1966.

Vincent, C.T., "Hydrodynamic Earth Pressure Measurements," Operation DISTANT PLAIN Preliminary Report, DASA 1876-4, 1968.

Vretblad, Bengt E., "Ground Shock Test of SST4 Shelters," DISTANT IMAGE Symposium Report, POR7379-4, 1992.

Walkinshaw, D.S. and Laidlaw, B.G., "Blast Response of M22 Radome," Event DIAL PACK Symposium Report, Vol. I, Defence Research Board of Canada, 1971.

Williams, R.F., "Pressure Transducer for Measuring Shock Wave Profiles, Phase X: Measurement of Law-Pressure Shock Wave Profiles," DASA 1653, 1965.

Winiary, M.L., "Nuclear Effects Blast and Shock Instrumentation," DNA-TR-88-2, 1988.

Winston, T., "Research Studies on Free Field Instrumentation," AFSWC-TR-60-55, 1960.

DISTRIBUTION LIST

MABS V3

DEPARTMENT OF DEFENSE

DEFENSE INTELLIGENCE AGENCY
ATTN: DIW-4

DEFENSE NUCLEAR AGENCY
ATTN: SPSD D PYLE
ATTN: SPSD P SENSENY
ATTN: SPWE
ATTN: SPWE E TREMBA
ATTN: SPWE K PETERSEN
2 CY ATTN: SSTL
ATTN: TDTR

DEFENSE TECHNICAL INFORMATION CENTER
2 CY ATTN: DTIC/OC

FIELD COMMAND DEFENSE NUCLEAR AGENCY
ATTN: FCTI G S LU
ATTN: FCTO
ATTN: FCTT-T E RINEHART
ATTN: FCTT DR BALADI
ATTN: FCTTS G GOODFELLOW
ATTN: FCTTS P RANDLES

DEPARTMENT OF THE ARMY

U S ARMY COLD REGION RES & ENG LAB
ATTN: CECRL-MAILROOM

U S ARMY ENGR WATERWAYS EXPER STATION
ATTN: C WELCH CEWES-SD-R
5 CY ATTN: CEWES-SD-R HOWARD WHITE
ATTN: RESEARCH LIBRARY

U S ARMY NUCLEAR & CHEMICAL AGENCY
ATTN: MONA-NU DR D BASH

U S ARMY RESEARCH LAB
ATTN: SLCBR-SS-T

DEPARTMENT OF THE NAVY

DAVID TAYLOR RESEARCH CENTER
ATTN: CODE 1770

DEPARTMENT OF THE AIR FORCE

AIR FORCE ARMAMENT LABORATORY
ATTN: A BRINSON
ATTN: D WATTS

AIR UNIVERSITY LIBRARY
ATTN: AUL-LSE

HQ 497 IG/INOT
ATTN: INT

DEPARTMENT OF ENERGY

LAWRENCE LIVERMORE NATIONAL LAB
ATTN: ALLEN KUHL

LOS ALAMOS NATIONAL LABORATORY
ATTN: J OGLE

SANDIA NATIONAL LABORATORIES
ATTN: TECH LIB 3141

OTHER GOVERNMENT

CENTRAL INTELLIGENCE AGENCY
ATTN: OSWR/NED 5S09 NHB

DEPARTMENT OF THE INTERIOR
ATTN: D RODDY

FEDERAL EMERGENCY MANAGEMENT AGENCY
ATTN: OFC OF CIVIL DEFENSE

DEPARTMENT OF DEFENSE CONTRACTORS

AEROSPACE CORP
ATTN: LIBRARY ACQUISITION

AEROTHERM CORP
ATTN: J SAPERSTEIN

APPLIED RESEARCH ASSOCIATES
ATTN: R FLORY

APPLIED RESEARCH ASSOCIATES, INC
2 CY ATTN: J KEEFER
2 CY ATTN: N ETHRIDGE
2 CY ATTN: RALPH REISLER

APPLIED RESEARCH ASSOCIATES, INC
ATTN: C J HIGGINS
ATTN: F E SEUSY
ATTN: N BAUM

APPLIED RESEARCH ASSOCIATES, INC
ATTN: J SHINN

APPLIED RESEARCH ASSOCIATES, INC
ATTN: R FRANK

APPLIED RESEARCH ASSOCIATES, INC
ATTN: J L DRAKE

BDM FEDERAL INC
ATTN: E DORCHAK

BOEING TECHNICAL & MANAGEMENT SVCS, INC
ATTN: ROBERT M SCHMIDT

CARPENTER RESEARCH CORP
ATTN: H J CARPENTER

FLUID PHYSICS IND
ATTN: R TRACI

GEO CENTERS, INC
ATTN: B NELSON

IIT RESEARCH INSTITUTE
ATTN: DOCUMENTS LIBRARY

JAYCOR
ATTN: J STUHMILLER

JAYCOR
ATTN: CYRUS P KNOWLES

MABS V3 (DL CONTINUED)

KAMAN SCIENCES CORP
ATTN: D BRYCE
ATTN: J CHANG

KAMAN SCIENCES CORP
ATTN: DASIAC

KAMAN SCIENCES CORPORATION
ATTN: DASIAC

LOGICON R & D ASSOCIATES
ATTN: C K B LEE
ATTN: D SIMONS
ATTN: LIBRARY

LOGICON R & D ASSOCIATES
ATTN: D CARLSON

LOGICON R & D ASSOCIATES
ATTN: G GANONG
ATTN: J RENICK
ATTN: J WALTON

MAXWELL LABORATORIES INC
ATTN: C PETERSEN
ATTN: K D PYATT JR
ATTN: MARK GROETHE
ATTN: P COLEMAN
ATTN: S PEYTON

MAXWELL LABORATORIES INC
ATTN: S HIKIDA

PACIFIC-SIERRA RESEARCH CORP
ATTN: H BRODE

SCIENCE APPLICATIONS INTL CORP
ATTN: C HSIAO
ATTN: G EGGUM
ATTN: H WILSON
ATTN: TECHNICAL REPORT SYSTEM

SCIENCE APPLICATIONS INTL CORP
ATTN: W LAYSON

SCIENCE APPLICATIONS INTL CORP
ATTN: G BINNINGER

SRI INTERNATIONAL
ATTN: A FLORENCE
ATTN: DR JIM GRAN
ATTN: J GIOVANOLA
ATTN: J SIMONS
ATTN: M SANAI
ATTN: P DE CARLI

SUNBURST RECOVERY INC
ATTN: C YOUNG

TECH REPS, INC
ATTN: F MCMULLAN

TITAN CORPORATION
ATTN: J ROCCO
ATTN: J THOMSEN
ATTN: S BABCOCK

TITAN CORPORATION (THE)
ATTN: R ENGLAND

TRW INC
ATTN: TIC

TRW SPACE & DEFENSE SECTOR
ATTN: W WAMPLER

WASHINGTON STATE UNIVERSITY
2 CY ATTN: PROF Y GUPTA

WEIDLINGER ASSOC, INC
ATTN: H LEVINE

WEIDLINGER ASSOCIATES, INC
ATTN: T DEEVY

WEIDLINGER ASSOCIATES, INC
ATTN: M BARON

FOREIGN

ATOMIC WEAPONS ESTABLISHMENT
20 CY ATTN: MICHAEL T GERMAN

DEFENCE CONSTRUCTION SERVICE
20 CY ATTN: ARNFINN JENSSEN

DEFENCE RESEARCH ESTABLISHMENT SUFFIELD
ATTN: DAVID V RITZEL

DEFENCE TECHNOLOGY & PROCUREMENT AGENCY
20 CY ATTN: BERNARD H ANET

ERNST MACH INSTITUT
20 CY ATTN: WERNER HEILIG

FOA
ATTN: HAKAN AXELSSON

FORT F
20 CY ATTN: BENGT VRETBLAD

MINISTERE DE LA DEFENSE
20 CY ATTN: SOLANGE GRATIAS

TNO - PRINS MAURITS LABORATORY
20 CY ATTN: JAAP WEERHEIJM

UNIVERSITY OF VICTORIA
20 CY ATTN: JOHN M DEWEY